UNIVERSITY OF **Hull**

The Synthesis and Evaluation of Ferroelectric Liquid crystal Host Materials

Thesis submitted for Degree of Doctor of Philosophy by

Srinivas Reddy Komandla

(Under the supervision of Dr. Robert A Lewis)

8/11/2015

This thesis is dedicated to my Grand Parents Late.Sri.MallaReddy, VenkatammaKomandla and my Parents, Sri. Damodhar Reddy, Savitha Komandla for their support and encouragement all the time throughout my life.

Abstract

This research is based on the synthesis and evaluation of liquid crystalline host materials for use in ferroelectric liquid crystal devices. The liquid crystal materials are synthesised by incorporating silane bulky end groups linked by an alkoxy spacer to a fluoroterphenyl molecular core.

The main aim of the research is to improve the alignment quality with the ultimate aim of bookshelf alignment. Almost as important is the target of wide temperature range, high tilt, and low melting SmC phase materials, but maintaining the low rotational viscosity of the fluoroterphenyl core.

The syntheses are reported of a series of silane compounds with bulky terminal groups attached to mono-, di-, and tri-fluoroterphenyl cores. The initial targets contain a pentamethyldisilane end group, but the route was unsuccessful so simpler targets with a butyldimethylsilane bulky end groups were prepared. The key part of the synthesis involves hydrosilylation, low temperature directed lithiation and Suzuki-Miyaura coupling reactions. The report discusses the syntheses and transition temperatures obtained from DSC and thermal polarising optical microscopy. The trends in the transition temperatures, and tilt angles of derived FLC materials, values are discussed and compared to literature compounds.

An exemplar is the addition of a chiral dopant (BE8OF2N) to butyl(6-((4"-((10-(butyldimethylsilyl)decyl)oxy)-2',3'-difluoro-[1,1':4',1"-terphenyl]-4-yl)oxy)hexyl)dimethyl-silane **30a** produces a high SmC* tilt angle of around 45° which varies little with temperature and there is a step in Ps data. This example **30a** is mixed in percentages up to 50% with a model difluoroterphenyl **KC1020** substituted in the middle ring. The bulky end group suppresses the N and SmA phase when compared to the dialkyl mesogen. A marked reduction in crystallisation temperature shows eutectic behaviour which is promising for ferroelectric mixture formulation. The same example **30a** mixed with **KC1019**, fluorinated on the end ring, has similar behaviour, but with more support of the SmC phase. Other silane materials are mixed with **KC1020** only, and their phase behaviour is discussed. Selected 50% mixtures of **30a**+**KC1019**, **30a**+**KC1020**, and an end ring monofluoroterphenyl-butyldimethylsilane **39**+**KC1020** are doped with 7% w/w of standard dopant BE8OF2N(-*S*) aimed at the ideal phase sequence I-N*-SmA*-SmC*-C. The SmC* tilt angles are close to the ideal value of 22.5° at room temperature but Ps values vary.

Acknowledgements

I would like to thank my supervisor Dr. Robert A Lewis for my introduction to the world of liquid crystals and ferroelectric host materials and for their continued support, guidance and encouragement throughout the course of this work. I am very grateful for his patience and advice in the preparation of this thesis. I could not have imagined having a better advisor and mentor for my PhD study. I express my deepest gratitude to my second supervisor Dr. Mike Hird for boosting my morale throughout the course of research. He has always been caring, a source of wisdom and motivation.

Special thanks go to Dr. Rob.Mc Donald for his great support, useful discussions, suggestions and evaluation of the compounds throughout my time spent in the lab. It is my pleasure to acknowledge all my current and previous colleagues, especially Dr. Viswanath Reddy, Dr. Andy, Dr, Chris, Dr. Ana, David Allan, Zia, Rami, Alex Forster, Amos and James Hussey for their enormous support and providing a good atmosphere in the lab and Liquid crystal research group. I will always be grateful to them for helping me to develop the scientific approach and attitude. I would like to thank Kingston Chemicals and the University of Hull for funding my research.

Thanks must also go to the technical staff for the analysis of intermediates and final products synthesised during the period of research, especially, Dr. Kevin J. Welham (MS) and Mrs Carol Kennedy (Elemental analysis). I wish to thank my friend Dr. Muralidhar Reddy Billa for introducing the Hull University.

I can't imagine my current position without their love and support from my family. I would like to pay high regards to my grandparents Late Mallareddy, Venkatamma, my parents Damodhar Reddy, Savitha Komandla, my younger brother Prakash Reddy, my aunt Aruna Devi Komandla and all my family members, who have been a constant source of love and encouragement throughout my life.

Last, but not least, I would like to pay high regards to my wife Neelima (Laxmi sri) Komandla for her sincere encouragement and support throughout my research work and thesis write up.

Srinivas Reddy Komandla
August- 2015.

1Contents

List of Figures:

List of tables:

List of Abbreviations

Abbreviations that are commonly known and used in this thesis are listed below:

Ac	-	Acetyl
aq	-	Aqueous
Bu	-	Butyl
Crys	-	Crystal
n-BuLi	-	n-Butyllithium
DSC	-	Differential scanning calorimetry
DCM	-	Dichloromethane
DMSO	-	Dimethylsulfoxide
Et	-	Ethyl
EtOAc	-	Ethyl acetate
EtOH	-	Ethanol
FLC	-	Ferroelectric liquid crystal
I	-	Isotropic liquid
EL	-	Electroluminescence
EtOH	-	Ethanol
FT-IR	-	Fourier transform-infrared
GC	-	Gas chromatography
IR	-	Infrared spectroscopy
J	-	Coupling constant
Lit	-	Literature
LC	-	Liquid crystal
LCD	-	Liquid crystal display
MBBA	-	N-(4-Methoxybenzylidene)-4-butylaniline

MeOH	-	Methanol
MS	-	Mass spectrometry
min	-	Minutes
MP	-	Melting point
N	-	Nematic
N^*	-	Chiral nematic
n	-	Director
NMR	-	Nuclear magnetic resonance
OMP	-	Optical polarising microscopy
P	-	Helical pitch
P	-	Planar conformer
P_0	-	Reduced polarisation
Ph	-	Phenyl
ppm	-	Parts per million
Ps	-	Spontaneous polarisation
RT	-	Room temperature
Sat	-	Saturated
Sm	-	Smectic phase
SmA	-	Smectic A
SmA*	-	Chiral smectic A
SmC	-	Smectic C
SmC*	-	Chiral smectic C
SSFLC	-	Surface-stabilised ferroelectric liquid crystal
T	-	Temperature
THF	-	Tetrahydrofuran
TLC	-	Thin layer chromatography

T_g	-	Glass transition temperature
UV-vis	-	Ultraviolet-visible
δ	-	Chemical shift
θ	-	Tilt angle
λ	-	Wavelength

Risk assessment

All experiments were carried out in accordance with the University of Hull's Health and Safety guidelines. A full COSHH and risk assessment was carried out for each new experiment, signed by the undertaking student, supervisor (Dr R.A. Lewis) and the departmental safety officer (Dr T. McCreedy) before any practical work started.

1. Introduction to liquid crystals:

1.1 Liquid crystals:

Liquid crystals have characteristic properties and uses. Research in the field continues as new applications are developed and liquid crystals continue to play a dynamic role in modern technology.

Liquid crystals are a state of matter in between the disordered, isotropic liquid and that of the amorphous or crystalline solid. Compounds that form the liquid crystalline state possess an anisotropic structure. They have many of the mechanical properties of liquids, like high fluidity, merging and formation of droplets, and at the same time they are similar to crystals, in that they show anisotropy in their electrical,mechanical, optical, and magnetic properties.[1]

The unique features of LC's are the presence of long-range orientational order in the packing of constituent molecules and sometimes one or two-dimensional quasi long-range translational or positional order. Liquid crystals exhibit a variety of sub-phases, which differ one from another by their physical and structural properties. Although liquid crystal mesophases combine the properties of a solid and an isotropic liquid, they exhibit very specific electro-optical phenomena, which have no equivalents in crystalline solids or in isotropic liquids.[2]

The molecules in a crystalline solid have long-range positional and orientational order. When heated the molecular interactions between the molecules begin to breakdown. If all intermolecular interactions breakdown simultaneously *e.g.*, for a molecule with a symmetrical shape, then an isotropic liquid is formed. However, if the interactions breakdown in several stages, *i.e.*, side to side or end to end, then intermediate states of matter so-called liquid mesophases are formed. As in all phases of matter, the one that exists at a particular temperature and pressure is determined by achieving the minumum free energy *i.e*.; the combination of energy arising from forces of attraction (enthalpy) and from the freedom to move (entropy). This is summarised in the Gibbs equation (Figure **1**) Mesophases are characterised by an orientation order, defined by the director **n**; the molecules themselves possess little or no positional order. The degree of order within a mesophase is defined by the order parameter, S.[3]

$$\Delta G = \Delta H - T\Delta S$$

Figure **1**: *Gibbs equation.*

Liquid crystal materials present both in technological applications and in the natural world. Almost all modern electronic displays are liquid crystal material based displays. Lyotropic liquid-crystalline phases are abundant in living systems; for example in cell membranes and many proteins are liquid crystals.

1.2 History of liquid crystals:

The research of liquid crystals began in 1888, when an Austrian botanistFriedrich Reinitzer observed two distinct melting points in cholesteryl benzoate (**1**) while working at the Charles University in Prague. In his experiments, he increased the temperature of a solid sample and observed the crystal change into a hazy liquid with some unusual colour behaviour, when he increased the temperature, the material changed again into a clear liquid. Because of his early work, Reinitzer is often credited with discovering a new phase of matter *i.e.,* the liquid crystal phase.[57]
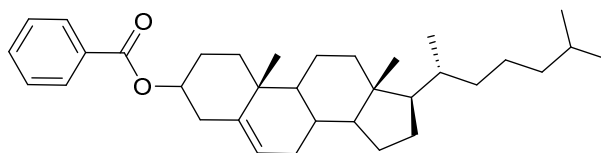
1

Figure **2:** *Structure of cholesteryl benzoate.*

The initial melting to a cloudy liquidoccurred at 145.5 °C, and became a transparent, clear liquid at 178.5 °C. This phenomenon was reversible on cooling. Reinitzer described three important features of cholesteryl benzoate *i.e.,* the existence of two melting points, the ability to rotate the polarisation direction of light and the reflection of circularly polarised light.[2, 5, 57]

After this discovery, Reinitzer discontinued research on liquid crystals but it was taken on by Lehmann and he realized that he had encountered a new phenomenon. In his postdoctoral years he became expert in microscopy and crystallography and started a systematic study, first on cholesteryl benzoate **1**, and related compounds which have the double-melting phenomenon. He observed these materials under polarised light, with a microscope which

was equipped with a hot stage enabling high temperature observations; with this equipment he observed that the intermediate phase as cloudy and it is clearly sustained flow particularly under a microscope, convinced that he was dealing with a solid. In August 1889, he had published his results in Zeitschrift fur Physikalische Chemie.[2]

The German chemist Daniel Vorländer, from the beginning of 20th century until his retirement in 1935, continued and significantly expanded Lehmann's work and he synthesised many novel liquid crystals. However, the topic was unfashionable and the materials remained a pure scientific curiosity for about 80 years.[4] In 1969, Hans Kelker synthesised a substance that had a nematic phase at room temperature, MBBA ((4-methoxybenzylidene)-4-butylaniline) **2**, still a commonly cited compound in liquid crystal research.[6]
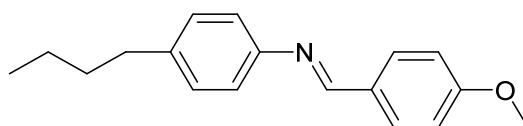
2

Figure **3:** *Structure of MBBA ((4-methoxybenzylidene)-4-butylaniline)*

The next step to commercialisation of liquid crystal displays was the synthesis of further chemically stable substances *i.e.,* cyanobiphenyls with low melting temperatures by George Gray.[7] This work with Ken Harrison and the UK MOD (RSRE Malvern), in 1973, led to Hull University and BDH Chemicals being able to manufacture materials that soon led to the rapid adoption of small area LCDs within electronic products.

The first purely synthetic liquid crystal *p*-azoxyanisole **3** was synthesised by Gatterman and Ritschke in 1890. Later Georges Friedel identified three different types of liquid crystal phases, *i.e.*, cholesteric, nematic and smectic phases in 1922 and his publication "Les Etats Mesomorphes de la Matière", introduced this terminology into the literature. He also observed the effects on liquid crystalline phases of magnetic and electric fields.[8, 9]
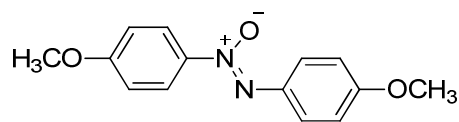
3

Figure **4:** *Structure of (Z)-1, 2-bis(4-methoxyphenyl)diazene oxide.*

The British scientist G. W. Gray published a book about liquid crystals in 1962.[10] The American chemist G. Brown established the Liquid Crystal Institute at Kent State University in 1965 and I.G. Chrystyakov started a special working group for liquid crystals in Moscow. A series of liquid crystal displays were invented in the late 1960's and early 1970's. These early reports of flat-panel displays stimulated a new and sustained research effort into liquid crystal in general and the syntheses of new liquid crystals for use in LCDs.[10]

In 1973, George W. Gray synthesised the terphenyl and cyanobiphenyl classes of liquid crystals, which were the first commercially successful liquid crystals due to their chemical, photochemical and electrochemical stability over a wide temperature range.
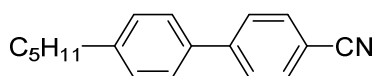
4
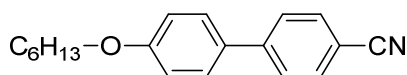
5
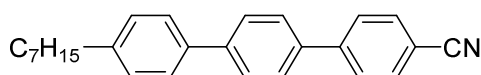
6

Figure **5:** *Structures of first stable commercial liquid crystals.*

This molecular structure was in contrast to existing liquid crystals used in LCDs which contained labile linking groups, such as the light sensitive azo- and azoxy-groups, and the imino-group in stilbenes, such as MBBA **2**. Furthermore, the use of the cyanobiphenyls rendered the use of frit sealing unnecessary and therefore the production of LCDs was much simplified and substantially cheaper.[12]

In the intervening years thousands of nematic and smectic liquid crystals have been developed for different applications, such as the TN-LCD reported in 1970[14] and the surface stabilised ferroelectric liquid crystal display (SSFLC) using chiral smectic liquid crystals

reported in 1980.[15] E Merck of Darmstadt, Germany, is the biggest chemical manufacturer of nematic liquid crystals today. Merck sold more than 20 tons liquid crystals in 1999 and the amount of nematic liquid crystalline mixtures sold increased to 80 tons in 2004 and will be much higher now due to the wide uptake of LCD monitors for PC's, laptop computers and LCD-TVs.[16]

1.3 Definitions of liquid crystal:

Calamitic liquid crystal materials possess some common features. Among these are a rod-like molecular structure, strong dipoles, rigidity of the long axis and easily polarisablesubstituents. Flexible chains are normally attached one or both ends of the rigid core to provide fluidity.

The specific characteristic feature of the liquid crystalline state is the tendency of the molecules or mesogens to point along a common axis, called the *director*. This is dissimilar to molecules in the isotropic liquid phase, which have no intrinsic order. In the solid crystal state, molecules are highly ordered and also have little translational freedom. The typical characteristic orientational order of the liquid crystal state is between the solid crystalline and isotropic liquid phases and this is the origin of the term liquid crystal ormesogenic state. A schematic representation for molecules in the crystalline solid, liquid crystalline, isotropic liquid phases are shown in the Figure 6.

Temperature

Crystalline solid   **Liquid crystal**   **Isotropic liquid**
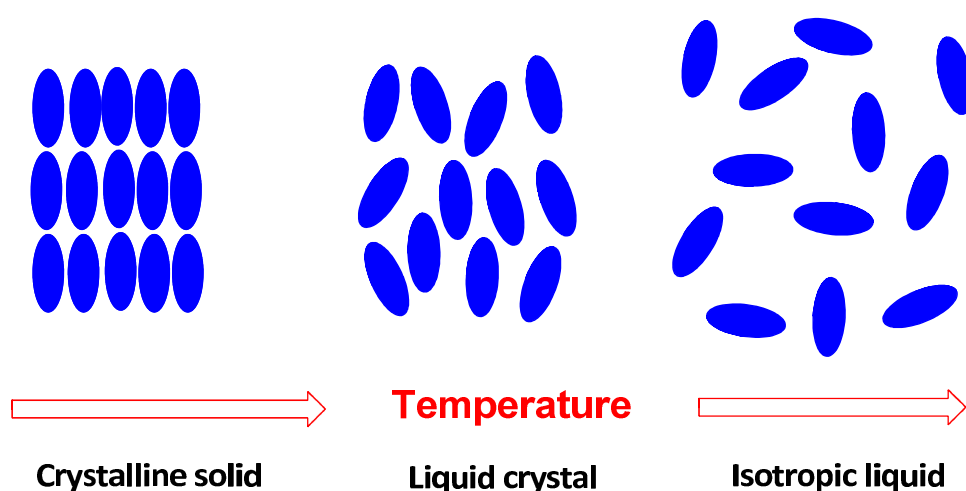
Figure **6:** *A Schematic representation of the formation of a liquid crystal from a crystalline solid on heating, and the formation of the disordered isotropic liquid state on further heating to a higher temperature.*

There are materials which are termed soft crystals, which have long range periodic order in two or three dimensions and these are not liquid crystals. They must be defined as solid crystal because crystalline solid materials clearly show long range periodic order in three dimensions. Substances that flow, are not as ordered as a solid and have some degree of alignment are properly called liquid crystals.[18]

To measure just how much order is present in a material, the order parameter (S) is employed and the definition is shown in Figure 7:

n

θ

$$S = 1/2\ \{3\cos^2\theta - 1\}$$
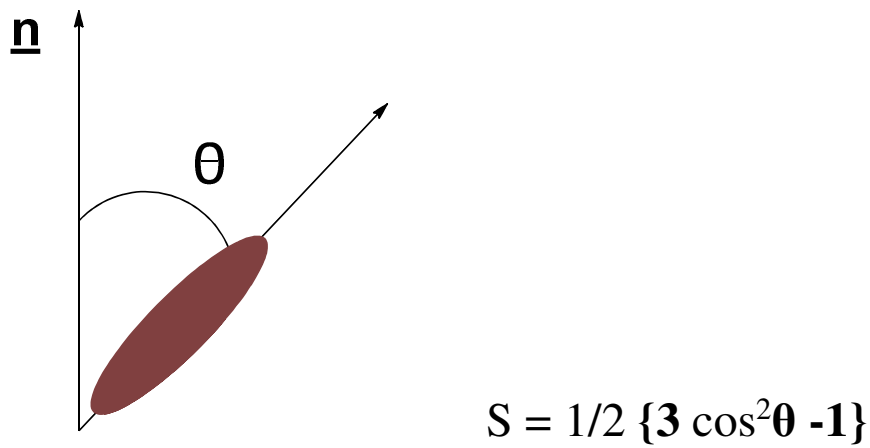
Figure **7:** *Description of the order parameter S.*

'θ' is the angle between the long axes of each individual molecule and that of the director. The brackets are there to imply that an average is taken over a large number of molecules.

A value of S = 0 for the order parameter implies no order *i.e.,* an isotropic liquid, whereas a value of S = 1 would imply that the phase is perfectly ordered *i.e.,* a perfect crystal. Typical values are in the region of 0.3 - 0.7 showing that the molecules are considerably disordered as liquid crystals. The exact value varies as a function of temperature, due to molecular motion. This is illustrated below for a nematic liquid crystal in Figure 8.[19, 20]
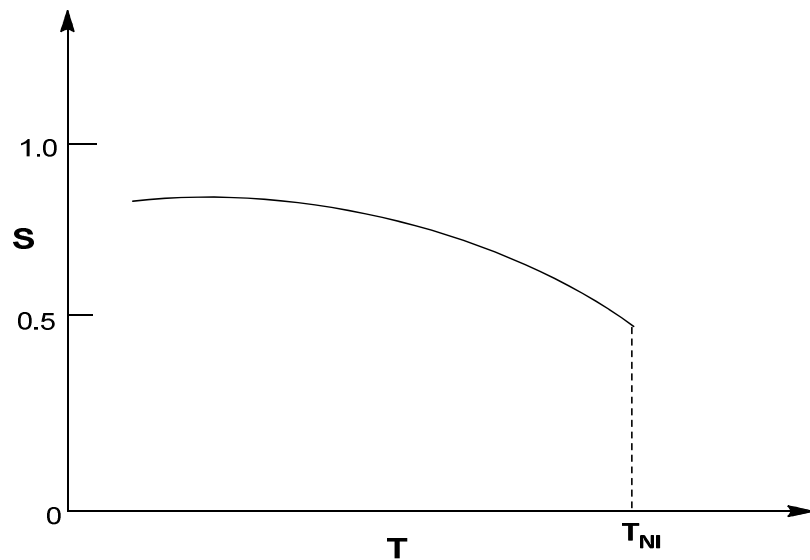
Figure **8:** *Order parameter(*S*) versus temperature (*T*) for a nematic liquid crystal.*

The tendency of the liquid crystal mesogens to point along the director leads to a condition known as anisotropy. This term means that the properties of a material depend on the direction in which they are measured. This nature of liquid crystals is responsible for the specific optical properties exploited in a variety of applications.

Three parameters explain the liquid crystalline structure:

i) Positional Order

ii) Orientational Order

iii) Bond Orientational Order

Each of these three parameters explains the extent to which of the liquid crystal is ordered. Positional order represnts to the extent to which an average molecule or group of molecules shows translational symmetry, just as a crystal unit cell. Orientational order refers a measure of the tendency of the molecules to align along with the director and bond orientational order refers a line joining the centres of nearest-neighbour molecules without requiring a regular spacing along that line. Thus, liquid crystal have a relatively long-range order with respect to the line of centres but only short range positional order along that line.

1.4 Classification of liquid crystals:

Most of the liquid crystal compounds exhibits polymorphism which is simply more than one liquid crystalline state. The term mesophase is used to describe the liquid crystal material "subphases". Mesophases are formed by changing the amount of order in the liquid crystal

materials, either by allowing the molecules to have a degree of translational motion or by imposing order in only one or two dimensions.[19]

There are two main categories of liquid crystals *i.e.*, thermotropic and lyotropic liquid crystals. Thermotropic liquid crystals are formed by the action of heat and lyotropic liquid crystals are formed by the addition of a solvent, such as water for example. Liquid crystals exhibit a strong anisotropy in many of their physical properties; *e.g.*, dependent on the direction of measurement parallel or perpendicular to the long molecular axis.[2, 3, 4, 19]

The variety of liquid crystal phases are characterised by the type of ordering. One can characteriseorientational order, positional order and moreover, order can be either long-range or short-range. Most thermotropic liquid crystals have an isotropic phase at high temperature.Heating will eventually turn them into a conventional liquid phase characterised by random, isotropic molecular ordering and flow behaviour like fluid. At lower temperature, a liquid crystal might possess one or more phases with short-range orientational order andimportant anisotropic orientational structure while still having the capability to flow.[22, 23]

In liquid crystalline phases, ordering is extensive on the molecular scale with domain sizes, in the order of micrometers (µm), but generally does not extend to the macroscopic scale as often occurs in crystalline solids. However some techniques, such as an applied electric fieldor the use of boundaries, can be used to create a single ordered domain in a macroscopic liquid crystal sample. The ordering in a liquid crystal might extend along only one dimension, but with the material being essentially disordered in the other two directions. [2, 3, 4]
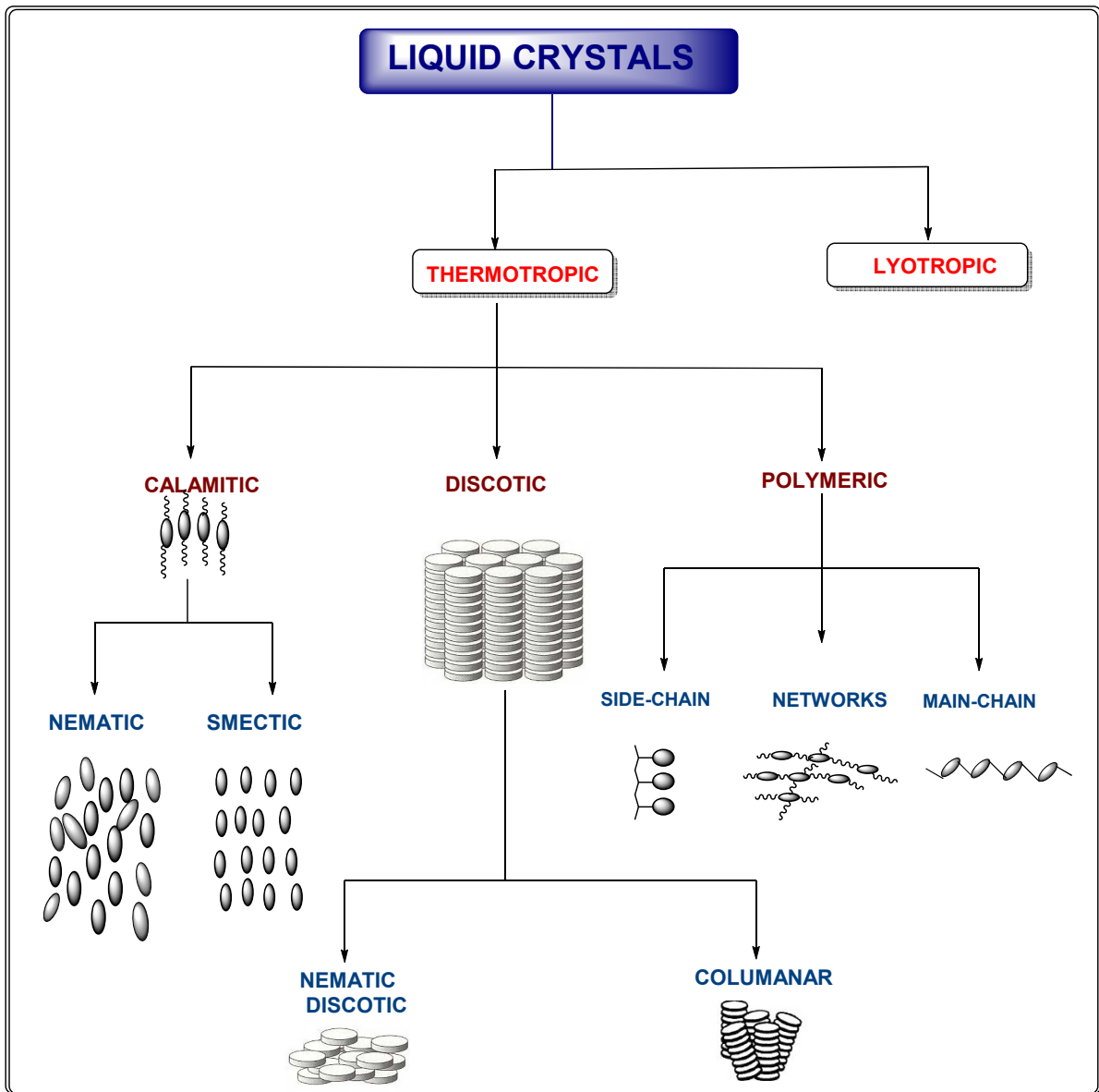
Figure **9:** *A schematic representation of the main types of thermotropic liquid crystalline mesophase*.

1.4.1 Thermotropic liquid crystals:

Thermotropic phases are those that occur in a particular temperature range. If the temperature is raised to a certain level, thermal motion will destroy the delicate cooperative ordering of the liquid crystal phase, driving the material into an isotropic liquid phase. At lower temperatures, most liquid crystal materials form a crystal.[22, 23]

Most of the thermotropic liquid crystal materials show variety of phases with the temperature change. For example, a specific liquid crystal molecule (mesogen) may show various smectic, nematic, columnar, cubic and isotropic liquid phases when the temperature is increase.[24]

1.4.2 Lyotropic liquid crystals:

A lyotropic crystal ntains of two or more components and show liquid-crystalline properties in specific concentration ranges. In the lyotropic LC phases, solvent molecules fill the space around the compounds and gave fluidity to the system. In contrast to thermotropic LC's, lyotropics show the degree of freedom of concentration that enables them to create different phases.

A compound which has two immiscible, hydrophobic and hydrophilic parts within the same molecule is called amphiphilic. Most amphiphilic compounds exhibit lyotropic liquid crystalline phase sequences depending on the volume balances between the hydrophobic part and hydrophilic part. These structures are formed through micro-phase segregation of two incompatible components on a nanometer scale.

1.4.3 Metallotropic liquid crystals

Liquid crystal phases can be found in low-melting inorganic phases like $ZnCl_2$ that have a structure of linked tetrahedral, which easily form glasses. The addition of long chain soap-like molecules leads to a series of new phases that show different types of liquid crystalline behaviour both as a function of temperature and of the organic-inorganic composition ratio. This type of liquid crystalline material has been named metallotropic.[33, 35]

1.4.4 Calamitic liquid crystals:

Calamitic liquid crystals (Greek calamai: long and thin) are usually made up of long rod-like molecules usually containing aromatic or alicyclic five membered or six membered rings with two flexible and/or polar end groups. The known phases of calamitic liquid crystals are nematic, smectic, cubic and columnar mesophases. When, a calamitic liquid crystal is heated in the crystalline state (Cr), the rod like molecules begin to vibrate. At the point when the vibration energy overcomes the attractive forces between the molecules the solid starts to melt. Smectic mesophases can form on heating, when the attractive forces between the ends

of the long, thin rod-like molecule are overcome, while the inter-molecular interactions between the sides of the molecules are maintained. This gives rise to a layered structure, where the molecular long axes are oriented more or less parallel to each other. This thermally-induced transition is known as a crystal to smectic transition (Cr-Sm).

Thee Nematic mesophase (N) is formed on heating when both the attractive forces between the ends of the molecules and the interaction between the sides of the molecules are overcome at the same time. This thermal transition gives rise to a non-layer structure, where the molecular long axes are more or less oriented in the same direction. This thermal transition is known as a crystalline to nematic transition (Cr-N).

If a smectic liquid crystal is heated further it may form a nematic phase, *i.e.*, by overcoming the attractive forces between the molecular axes. This is called the smectic to nematic transition (Sm-N). If all the remaining forces are overcome simultaneously, whether in the smectic or in the nematic phase, the molecules move in a random manner to form an isotropic liquid (I), where there is no positional or orientational order. These thermal transitions correspond to the smectic and nematic clearing point (Sm-I or N-I) (Figure 10).
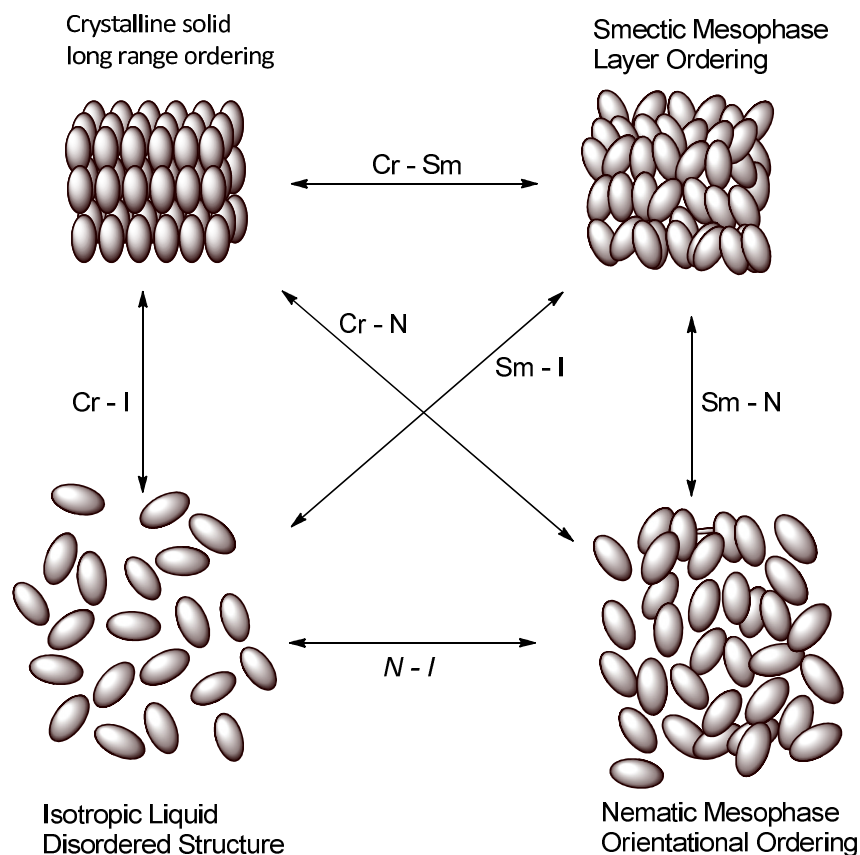
Figure **10:** *Typical transitions in a liquid crystal.*

1.4.5 Discotic phases:

In discotic nematic phases, disk shaped liquid crystal molecules can orient themselves in a layer-like order. If the disk shaped LC's pack into stacks, the phase is called a discotic columnar phase. In this phase, columns themselves may be organised into hexagonal or rectangular arrays. Chiral discotic phases are similar to the chiral nematic phases as shown in the Figure **11**.

Discotic Nematic   Discotic Columnar
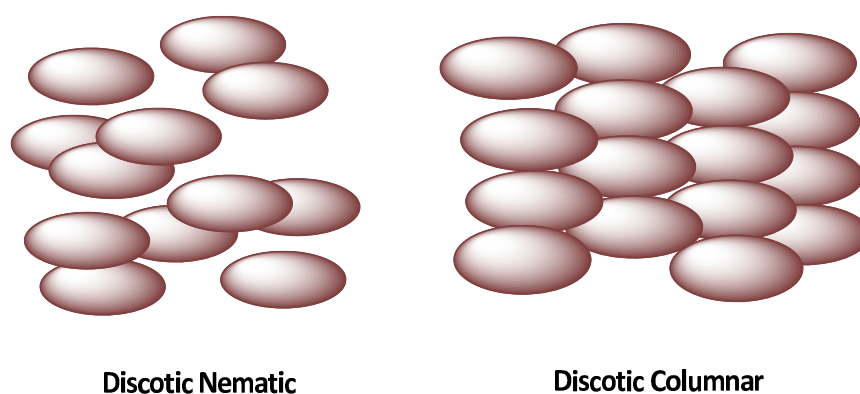
Figure **11:** *Schematic diagram of the nematic and columnar phases of a discotic liquid crystal*.

1.5 Calamitic liquid crystal phases:

1.5.1. Nematic phases:

The nematic phase is the most disordered liquid crystal phase. The word nematic came from the Greek νημα (nema), which means "thread". This term originates from the thread-like topological defects observed in nematics, called disclinations. Nematic phases also show so-called point defects. In this phase, the calamatic molecules have no positional order, but they self-align to have long-range directional order with their long axes almost parallel.[19, 22, 23] Thus, the molecules are free to flow and their centre of mass positions are randomly distributed as in a liquid and still maintain their long-range directional order. Most nematic phases are uniaxial; they have one axis that is longer and preferred, with the other two being equivalent (may be approximated as cylinders or rods). However, a very few examples have been shown to be biaxial nematics, meaning that in addition to orienting their long axis, they also orient along a secondary axis.[26] Nematics have fluidity similar to that of isotropic liquids but they can be easily aligned by an external electric or magnetic field. Aligned nematics have the optical properties of uniaxial crystals and this makes them very useful in LCDs.

The nematic phase is the simplest of the liquid crystalline mesophases. It is essentially a one dimensional ordered elastic fluid, where the molecules have only short range orientational order and no long range positional ordering, leaving the molecules free to rotate, tumble and diffuse throughout the sample. However, as they diffuse throughout the sample the long axes of the rod like molecules tend to align parallel to each other and the average of this alignment is called the director, **n**, and is diagrammatically represented in Figure 12.
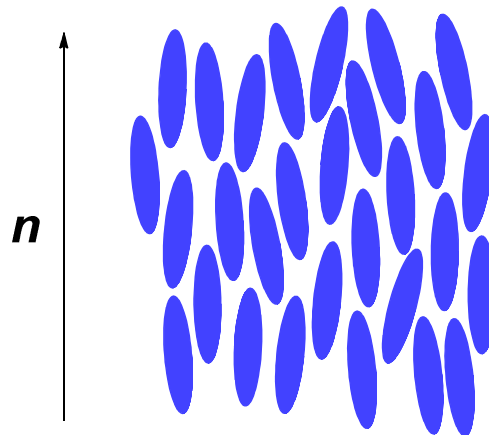
Figure **12:** *Orientation of molecules in a nematic phase*.

1.5.2 Smectic phases:

The smectic phases form well-defined layers that can slide over one another in a manner similar to that of soap. Smectic phases form at lower temperatures than the nematic phases, when the latter is present. Smectic phases are thus, positionally ordered along one direction. In the smectic A phase, the molecules are oriented along the layer normal, while in the smectic C phase they are tilted away from the layer normal and molecules show liquid-like behaviour within the layers. There are many different smectic phases, all characterised by different types, degrees of positional and orientational order.

The smectic phases exhibit a much higher degree of order compared to that of the nematic phase due to the presence of layers within the bulk material. Some of these phases are now regarded as soft crystals as they have been show to have long range positional order and are not any longer defined true liquid crystalline phases.[22, 38]

1.5.2.1 The smectic A phase: [36, 37, 38]

The smectic A phase defines an assembly in which the molecules are free to rotate about their molecular long axis, which is usually perpendicular to the plane of the layer as shown in Figure 13. The molecules do not have positional order within the layers and the layers are free to slide over each other. Molecules may diffuse from one layer to another. The SmA phase is the least ordered of the smectic phases and soft crystals.

The SmA will always precede all other smectic mesophases on cooling from either the isotropic or nematic phases, where a SmA is present in a material; within and between layers there is no translational order, and therefore only short range ordering over a few molecular centres occurs.
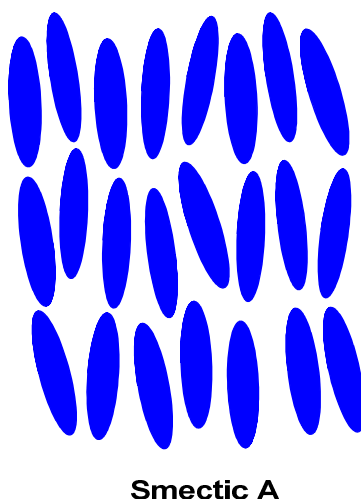
Smectic A

Figure **13:** *A diagrammatic representation of the smectic A phase.*

As the molecules in the SmA phase are arranged in diffuse layers the molecules often have small tilt angles, which are random with respect to the layer normal. In addition to the interdigitation of the terminal chains this makes the layer spacing slightly smaller than the actual length of the molecule.

However, the SmA phase can also exhibit semi-bilayer and bilayer ordering and this can either be caused by interdigitation or partial pairing of molecules. The different types of SmA phases are shown Figure 14 and Figure 15.
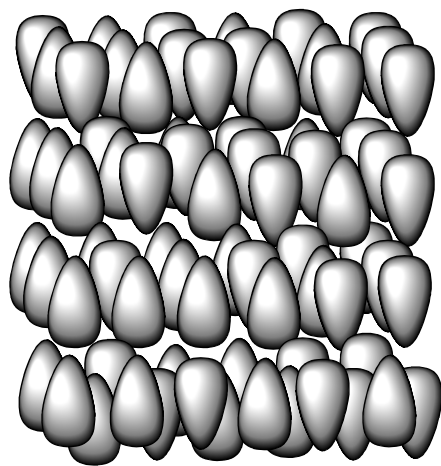
Smectic A$_1$ Phase
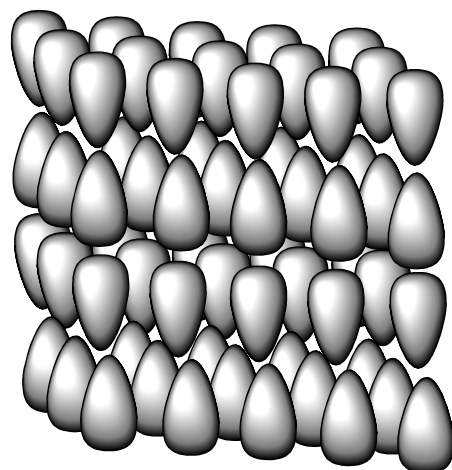
Smectic A$_2$ Phase
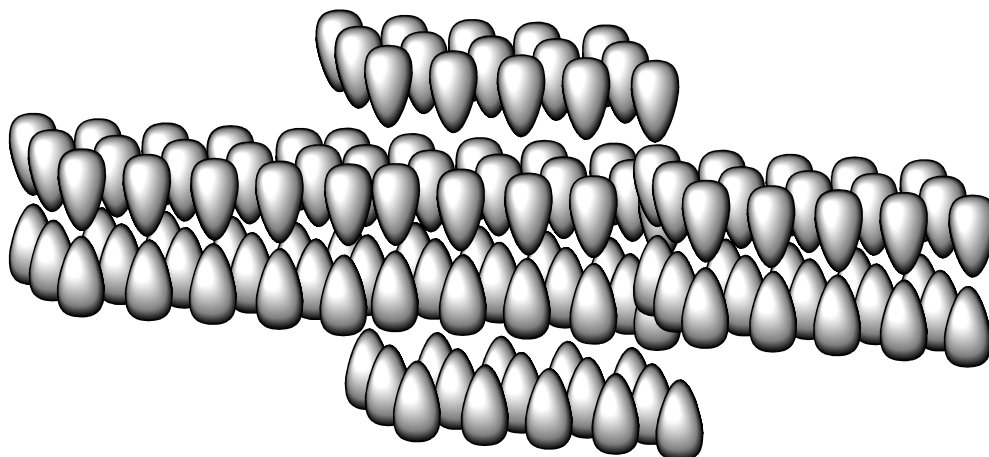
Smectic A Antiphase

Figure **14:** *Structure of Smectic A$_1$, A$_2$ and Ă antiphase.*

The smectic A$_1$ is essentially a monolayer system where the molecules are disordered and do not overlap. The smectic A$_2$ phase has a bilayer and the layer repeating spacing is twice the length of the molecule. The smectic A antiphase is essentially the A$_2$ phase, but has a half layer shift and, at the shift points, this brings about a smectic A$_1$ type structure. These shift points occur every 15 nm or so.

The smectic A_d phase in Figure 14 shows some interdigitation between the molecules. This can be due to polar end groups, such as the cyano group, interacting with the ends of the central core giving interdigitation of the molecules. Frequently, a bilayer of 1.4 times that of the molecular length is observed for this phase.
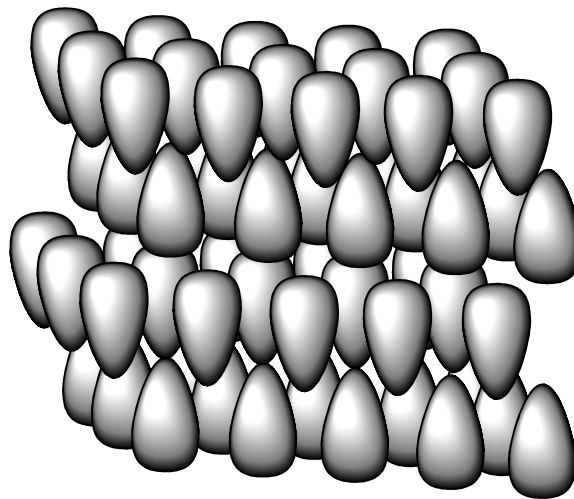
Smectic A$_d$ phase

Figure **15:** *The smectic A$_d$ phase*.

It must be remembered that the diagrams have been simplified as the actual bilayers and pairing of the molecules are in constant flux. [8,9,11]

1.5.2.2 The smectic C phase[36, 37, 38]

SmC is similar to the SmA phase but it has a temperature dependent tilt angle, whereas, the SmA phase may be tilted only locally but will average out to zero over the bulk of the phase. Figure 16 provides a simplistic view of the SmC phase.
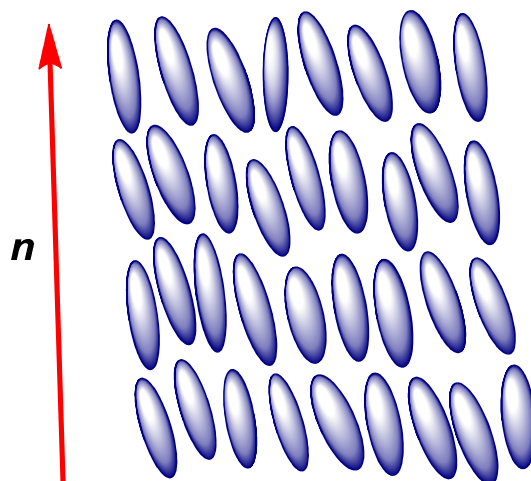
Figure **16:** *A diagrammatic representation of the smectic C phase.*

As can be seen from Figure 15, the long axes of molecules are tilted with respect to the normal of the layers planes. Within the layer the molecules are locally hexagonally closepacked with respect to the director, but this is only over a very short range of about 1.5 nm. Therefore, over a large area the molecules are randomly packed and are tilted roughly in the same direction.

As a consequence of the tilt being preserved over successive layers, the SmC phase has C_{2h} symmetry and is weakly biaxial.

The SmC phase also has a subphase called SmC_{alt} where the tilt angle of the molecule is rotated by $180°$ on passing from one layer to the next, and is shown in Figure 17.
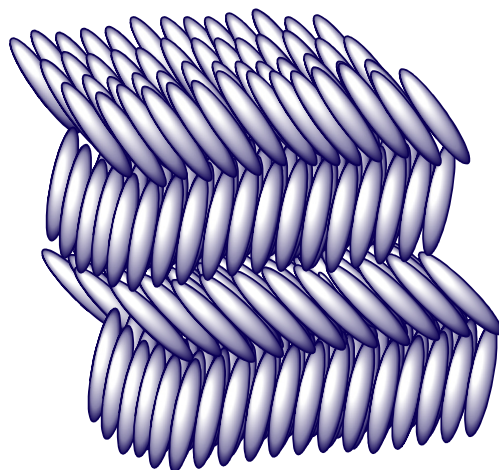
Figure **17:** *A diagrammatic representation of the SmC$_{alt}$ phase.*

Since, the layers of the SmC$_{alt}$ alternate, the overall director is normal to the layer planes. In addition to the alternating phase there are also sub phases for polar materials that are identical to the SmA apart from the fact the SmC versions are tilted, this gives us the SmC$_d$ = SmA$_d$, SmC$_1$ = SmA$_1$ and so on.

Excepting the tilt of the molecular axes of the molecules with respect to the layer plane and layer normal, the smectic C and the SmA mesophase have similar properties.

1.5.3 Chiral phases: [19, 22, 27, 29]

The chiral nematic (N*) phase is termed cholesteric phase from the historic observation in cholesteryl derivatives. Only chiral molecules *i.e.*, those that lack inversion symmetry, can give rise to such a phase. This phase shows a twisting of the molecules perpendicular to the director (n), with the molecular axis parallel to the director. The finite twist angle between adjacent molecules is due to their asymmetric packing. This packing results in longer-range chiral order. [40, 41]

The ordering in the chiral nematic phase is similar to that found in the nematic phase, *i.e.* the long axes of the molecules lie generally pointing towards the director. However, the molecular chirality of the chiral nematic phase causes a gradual change of the director in the bulk and this gives rise to the helicoidal macrostructure shown in Figure-18 for the chiral nematic phase (N* phase).
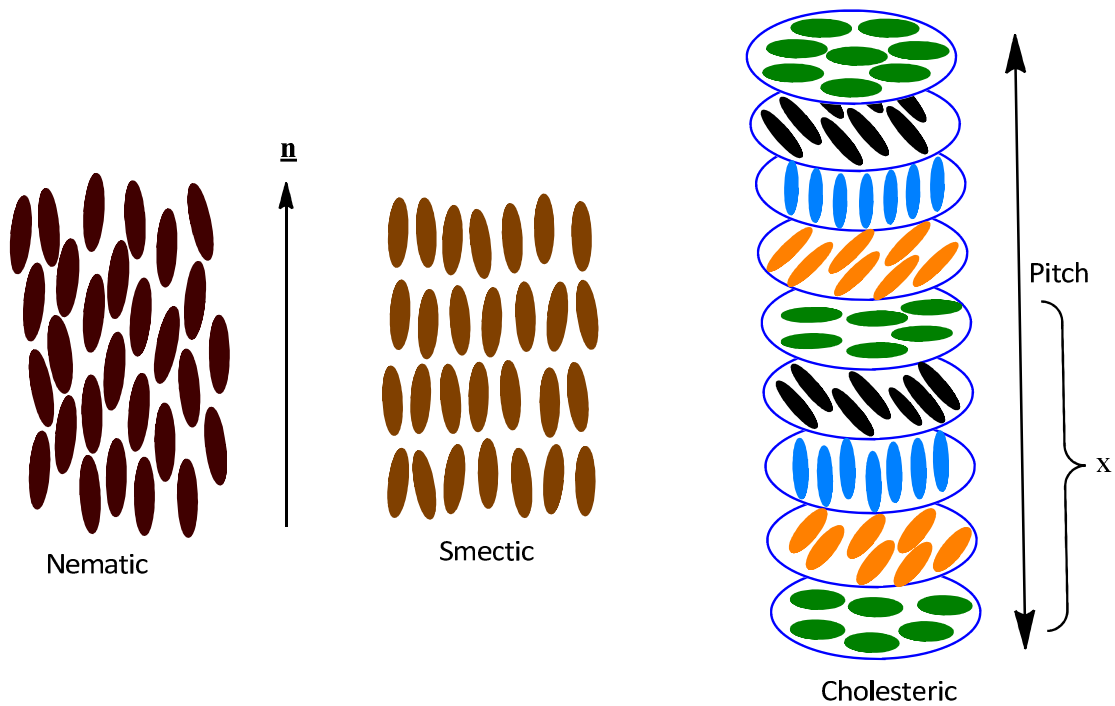
Figure **18:** *Structure of chiral nematic phase compared with achiral phases.*

The full 360º rotation of the chiral nematic director is referred to as the *pitch length p.* However, as n and –n are essentially the same, the structure of the N* phase actually repeats itself every 180º. The pitch length of the material is dependent on temperature. At high temperature, the pitch length is shorter due to the molecules having more thermal energy, causing a greater rotation of the director between molecules, whereas at lower temperatures the pitch length is longer because the molecules have less thermal energy. However, this is not always the case; there are materials that have an increasing pitch length with increasing temperature.[19]

The helix of the chiral nematic phase can either be right or left handed and is dependent on the type of enantiomer and the spacing from the core.[20]

The chiral nematic also has another interesting property in that it can selectively reflect light due to its helical nature and occurs when the pitch length and wavelength of the light λ are of the same order, given in the following equation, where *n* is the refractive index and **p** is the pitch.

$$\lambda = n\mathbf{p}$$

Figure **19**: *Equation relating to selective reflection.*

When circularly polarised light hits the aligned N*, so that the plane of polarisation is parallel to the director then the part which has the same twist sense is reflected and that of the opposite sense is transmitted.

If the pitch of the materials is in the region of white light then coloured light is reflected. As the nematic phase cools the helix will start to unwind and the colour play goes from blue (elevated temperatures) to red once cooled, and is shown graphically in Figure 20.
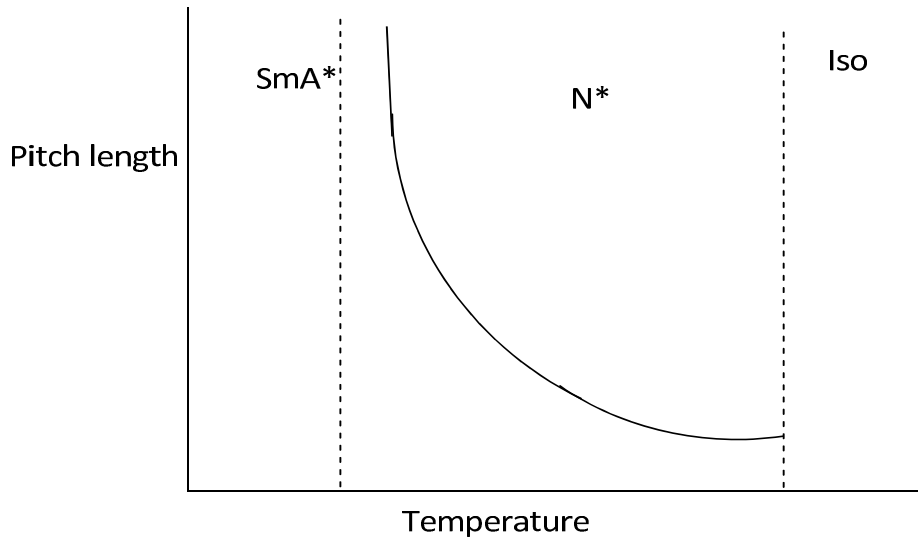
Figure **20:** *Temperature vs. pitch length graph for an N* phase.*

The chiral pitch, *p*, refers to the distance over which the liquid crystal molecules undergo a full 360° twist but the structure of the chiral nematic phase repeats itself every half-pitch, since in this phase directors at 0° and ±180° are equivalent. The pitch, *p*, typically changes when other molecules are added to the liquid crystal host, for example an achiral liquid crystal host material will form a chiral phase if doped with a chiral material or when the temperature is altered, allowing the pitch of a given material to be tuned accordingly. In few liquid crystal systems, the pitch is of the same order as the wavelength of visible light. These systems show specific optical properties like low-threshold laser emission and Bragg reflection[28] and these properties are exploited in a number of optical applications. In the case of Bragg reflection, only the lowest order reflection is allowed if the light is incident along the helical axis, whereas for oblique incidence higher-order reflections become permitted. Cholesteric LC's also shown the unique property that they reflect circularly polarised light when it is incident along the helical axis and elliptically polarised if it comes in indirectly.

1.5.4 Blue phases: [14, 30, 31, 32]

In a small percentage of chiral nematics, blue phases are found between the chiral nematic and isotropic liquid phase. Blue phases have a regular three-dimensional cubic structure of defects with lattice periods of several hundred nanometers and thus blue phases show selective Bragg reflections in the wavelength range of light corresponding to the cubic lattice (Figure 21).

Although blue phases are of interest as tuneable photonic crystals or fast light modulators, the very narrow temperature range within which blue phases exist, usually less than a few Kelvin, is a major limitation. Recently, the stabilisation of blue phases over a temperature range of more than 60 K including room temperature (260-326 K) was demonstrated. Furthermore, electro-optical switching with response times of the order of 10^{-4} s for the stabilised blue phases at 260-326 K has been shown.[32] In May 2008, the first Blue Phase Mode liquid crystal display panel was developed.
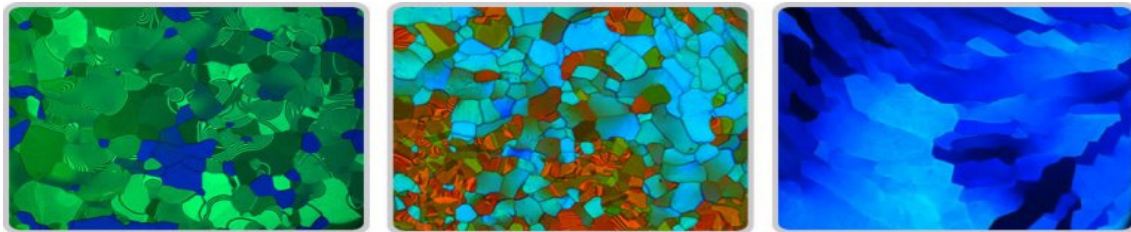
Figure **21**: *Polarising microscopic textures of blue phases, BP I, II & III.*[80]

1.6 The chiral smectic C (SmC*) [37, 42]

The chiral SmC (SmC*) phase just like the chiral nematic has a helical macrostructure and there is a gradual rotation of the local tilt director from layer- to- layer as shown in Figure 22.
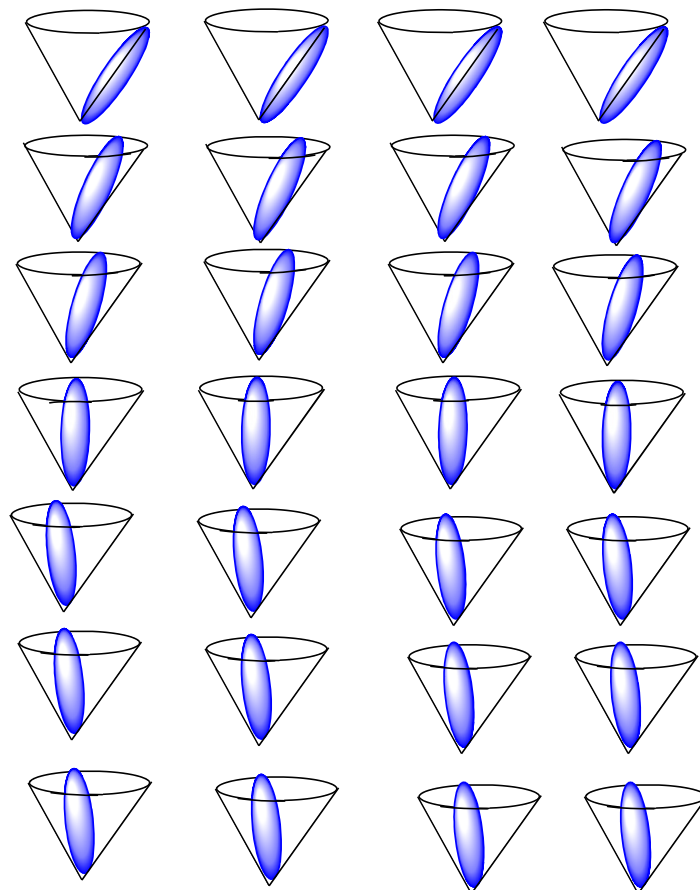
Figure **22:** *A diagrammatic representation of the helical SmC*.*

The tilted molecules of the smectic C* rotate around the cone from layer to layer. The rotation that occurs is always in the same direction and of the same magnitude. This is called the azimuthal angle. This gradual rotation forms the helix, which can either be right or left handed and for simple molecules can be worked out using similar principles to that outlined in the nematic phase but with the inclusion of the inductive effect and direction of polarisation.[43, 44]

The pitch of chiral Smectic C* is usually a few micrometers in length and this indicates that the pitch of the material is made up of thousands of layers, therefore the azimuthal angle is relatively small in the region of one tenth to one hundredth of a degree.

The pitch, just like in the chiral nematic is temperature dependent, however unlike the chiral nematic, the pitch gets tighter as temperature as decreases. The tightening of the pitch is due mainly to the tilt angle becoming larger and layers becoming thinner. In 1974, R.B. Meyer discovered that due to basic symmetry considerations chiral tilted smectic liquid crystal phases ought to be ferroelectric.[45]

1.6.1 Symmetry point of view: [45, 46, 47, 48, 49]

In the achiral SmC phase, the local environment symmetry of each layer consists of:

i) A twofold axis of rotation normal to the tilt direction in the plane of the layer.
ii) A mirror plane normal to the twofold axis and the layer.
iii) A centre of inversion.

This is shown in part (a) of Figure 23 and shows that the SmC phase exhibits C_{2h} symmetry. However, when the molecules have a chiral centre, the local symmetry is reduced to a two fold axis of rotation giving the SmC* phase a C_2 symmetry and is the case for all tilted smectics and disordered crystal phases and is shown in part (b) of Figure 23.
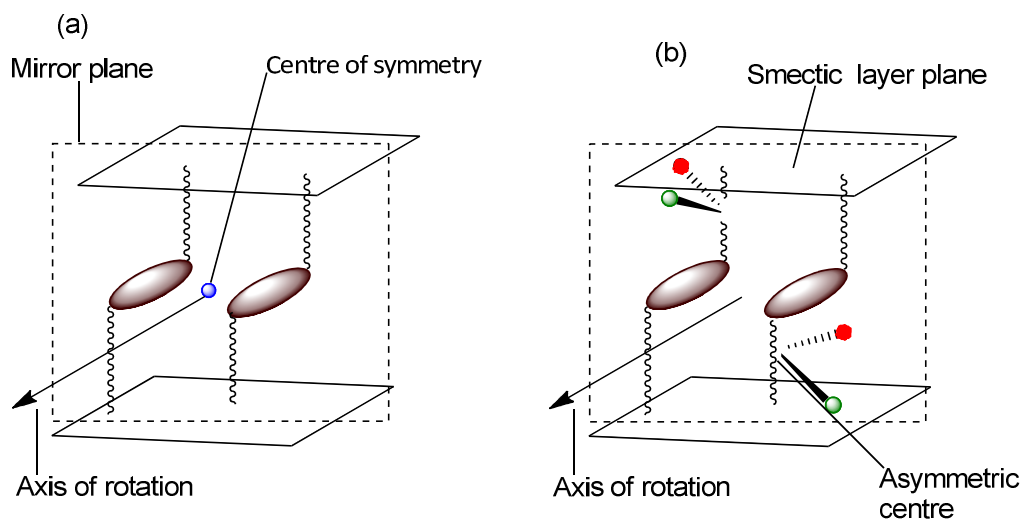
Figure **23**: *Symmetry elements of an achiral smectic (a) and chiral smectic C* phase (b).*

The spontaneous polarisation (Ps) is brought about by the reduction in symmetry and the inequivalence of dipoles due to the chirality and the tilted orientation of the molecules in the phase. Since the molecules in a smectic layer are polar, three spatial components of the macroscopic polarisation exist as shown in Figure 24.
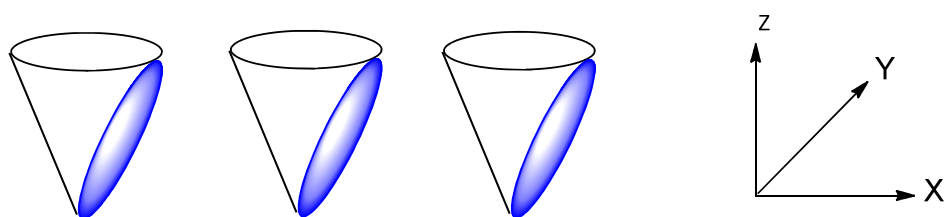
Figure **24**: *Smectic layer and its resultant polarisation vector.*

Applying the C_2 symmetry operation, shown in Figure 24, to the X, Y and Z vectors, X and Z becomes –X and -Z and only Y remains unchanged, therefore the permanent spontaneous polarisation is in the Y direction.

In a 'natural' SmC* phase, the helix leads to gradual precession of the Ps direction from layer to layer and the net Ps cancels. This behaviour is called helielectric. Clark and Lagerwall devised a cell with a rubbed polymer alignment layer and a thin cell gap. The boundary conditions were able to suppress the helix and ferrolectric properties were obtained. The resulting Ps can be reversed by reversing the polarity of an applied field. Changing the direction of the Ps vector is concomitant with the molecular tilt changing direction by rotation around a cone.

1.7 Ferroelectric LCDs

The SmC phase of liquid crystals was first published in 1933, but it was not until 1974 that Robert Meyer predicted its potential ferroelectric behaviour and demonstrated that property in 1975 using DOBAMBC **8** (Figure-25).[45]
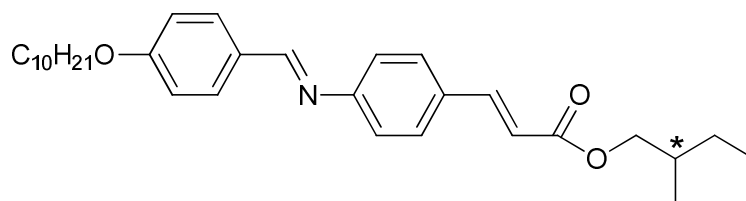
8

Figure **25**: *Structure of DOBAMBC*.

This led to intensive studies on FLC's. In 1980 Clark and Lagerwall demonstrated the concept of the Surface Stabilised Ferroelectric Liquid Crystal device *i.e.*, SSFLC, which was a major step towards the possibility FLC applications. This in turn led to considerable effort in novel FLC materials. Ferroelectric liquid crystal products became feasible and technology began to be commercialised. Initially, the products were direct-view displays and print bars which appeared in 1989.[15]

There is still major interest in ferroelectric liquid crystal technology due to particularly the promise of fast switching and high resolution. These advantages, the possibility for dynamic gray scale and full colour of SSFLC give it great potential for use in demanding applications such as high definition TV's, but there are complications to turn this into reality. These difficulties and the great advances in large area nematic displays explain the lack of major commercial breakthroughs for FLCs in recent years.[19, 45]

Ferroelectric liquid crystal displays have found a successful niche in high definition miniature displays. These displays can be magnified or projected for a full screen image. They can also be used in head mounted displays like those used for virtual reality. These displays are highly portable and also allow for interactivity with the user *e.g.*, image changes with head movement. When displays are supported by the user, the weight of the display is also important. The best way to reduce the weight of that system is to reduce the size of the screen. It is needed so relatively lighter magnification devices can be used to increase the field of view. At the same time, to make the image realistic to the user, the screen resolution must be high. Ferroelectric liquid crystal displays allow for this by their small pixel sizes and

these devices can use reflective illumination to remove bulky and high energy consuming backlighting devices. The bistability provided by surface stabilised ferroelectric liquid crystal devices make them ideal due to low energy consumption. This is a concern for still images since additional power is not required once an image is created and their switching time is fast enough to support high frame rates needed for video. This fast switching time also allows full colour on every pixel by sequential red, green, blue illumination,which means high definition quality on a given display size.[15, 19, 45]

The FLC display materials show faster switching times compared to that of nematic displays and has bistability. However commercial products are very difficult to fabricate, partly due to small gaps (1.5 +/- 0.05 μm). Alignment can be destroyed by mechanical shock due to unstable molecular anchoring at the surface.

Sony has used SiO_2 evaporation for the alignment layers to improve uniformity and contrast ratio. They also made important contribution to gray scale techniques to address the video requirement. The future for ferroelectric LCDs is still uncertain, but if a well aligned display with the higher contrast and wider viewing angle is achieved, they may actually compete with active matrix LCDs. Materials development is one area to be investigated in this regard and the possible rewards make this a worthwhile endeavour. [19, 45, 72]

There are also several antiferroelectric materials under research in USA and Europe but still the contrast ratio is not satisfactory yet, so the manufacturers consider using this technology to be unsafe until these problems are solved.[72]

1.8 Antiferroelectric and ferrielectric phases [19, 49, 50, 51]

Liquid crystals exhibiting tristate switching of the antiferroelectric phase were first discovered in 1988[52-54] and the ferrielectric phase shortly afterwards from a compound called MHPOBC. From then on, a host of antiferro and ferri-type materials have been made. The antiferroelectric phase SmC*$_{anti}$ structure is similar to that of the ferroelectric phase in that each layer has the same tilted structure like the ferroelectric SmC*$_{ferro}$. However, the tilt direction alternates from layer-to-layer giving a herringbone structure. Accordingly the Ps value of the material averages out to zero. The ferrielectric phase SmC*$_{ferri}$ also has an alternating structure but, unlike the SmC*$_{anti,}$ more layers point in one direction, this giving the unwound state of the phase a residual Ps value.[55, 56]

When an electric field is applied to the unwound states of the ferro, ferri- and anti ferro electric phases, the hysteresis response of the Ps value (P) to the applied field (E) is shown in Figure 26 (a) to 28 (a). The structure of the phase that is responsible to this effect is shown in Figure 26 (b) to 28 (b).
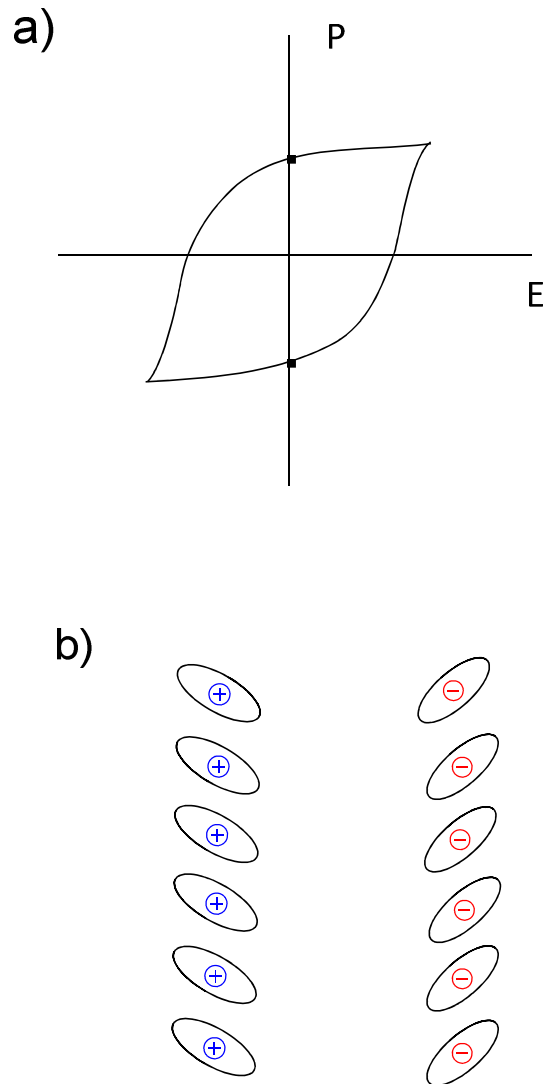
Figure **26:** *The hysteresis response of the ferroelectric phase to an applied electric field and (b) the two tilt directions resulting from applying voltages of opposite polarity.*

(a)

Ps

P

1/3 Ps

E

(b)

r = 1   r = 1/4   r = 2/9   r = 1/5   r = 0
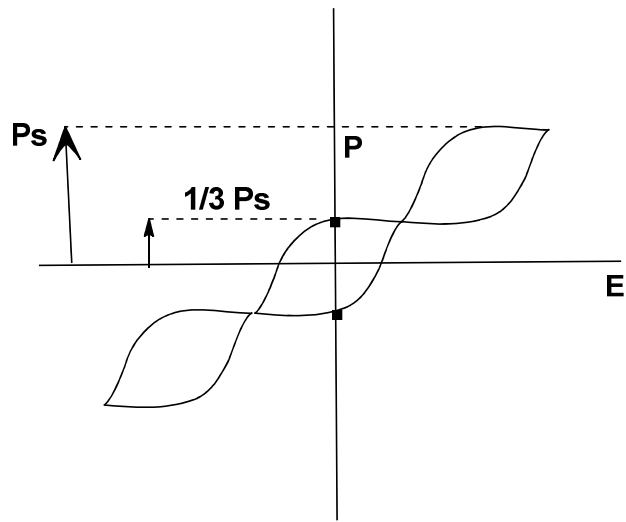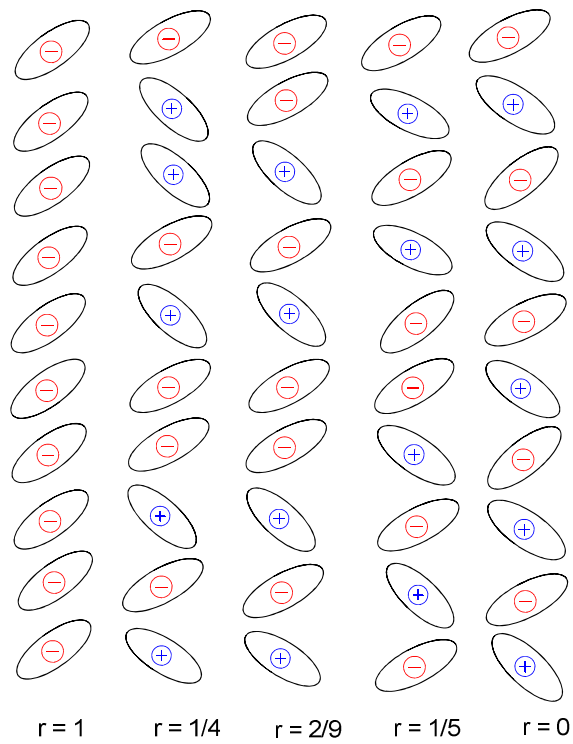
Figure **27:** *The hysteresis response of ferrielectric phase to an applied electric field and (b)*
the inner three columns show different possible arrangements of ferrielectric phase.

(a)

(b)
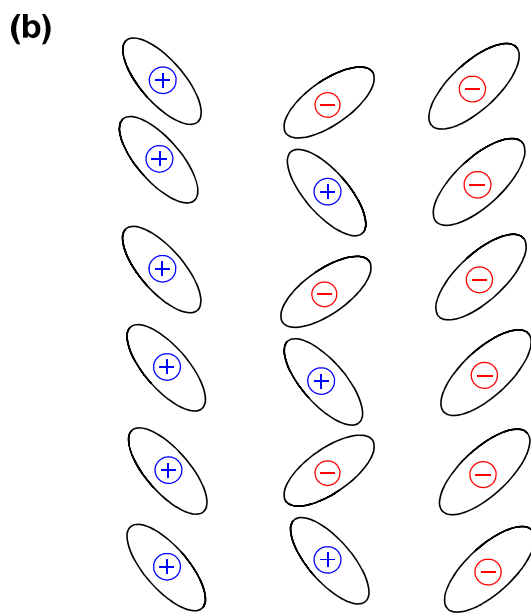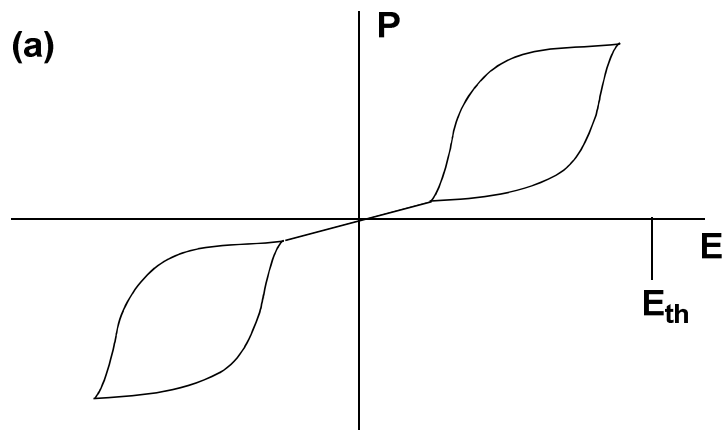
Figure **28: (a)** *The hysteresis response of the antiferroelectric phase to an applied electric field.*

(b) *The middle column shows antiferroelectric structure with no applied electric field; left and right columns shows the result of applying opposite voltages.*

Figure-26 shows the ferroelectric phase. This is again bistable and as indicated on the hysteresis curve, corresponds to the two orientations of the director.

Figure-27 shows the ferrielectric phase which can have various arrangements of the director as show by the inner configurations. This results in a net macroscopic polarisation which is less than the maximum Ps. The ferrielectric phase may exhibit more than three switching states.

Figure-28 shows the antiferroelectric hysteresis and shows that this phase has only one stable state, which is the ground state but the other two states can be achieved by the application of a threshold voltage E_{th}.

The smectic phases can have frustrated phases at the top of their temperature range in a similar fashion to the blue phases. The former are referred to as twist grain boundary phases (TGB). The topic is out of the remit of the research in this thesis and so will not be discussed further. [15, 16]

1.9 Twisted nematic devices:

The twisted nematic first demonstrated by Fergason in 1971 in the US and at the same time, Schadt and Helfrich at Hoffman la Roche were working on the same idea in Europe. In these devices, the liquid crystal is placed between two crossed polarisers and its birefringence controlled by using electricity.[37]

1.9.1 Functioning of polariser in twisted nematic devices:

When the unpolarised light passed through a polarising filter, only one plane of polarisation is transmitted. Then two polarising filters used together transmit light differently depending on their relative orientation. The complete functioning view of polarisers is shown in bFigure-30.
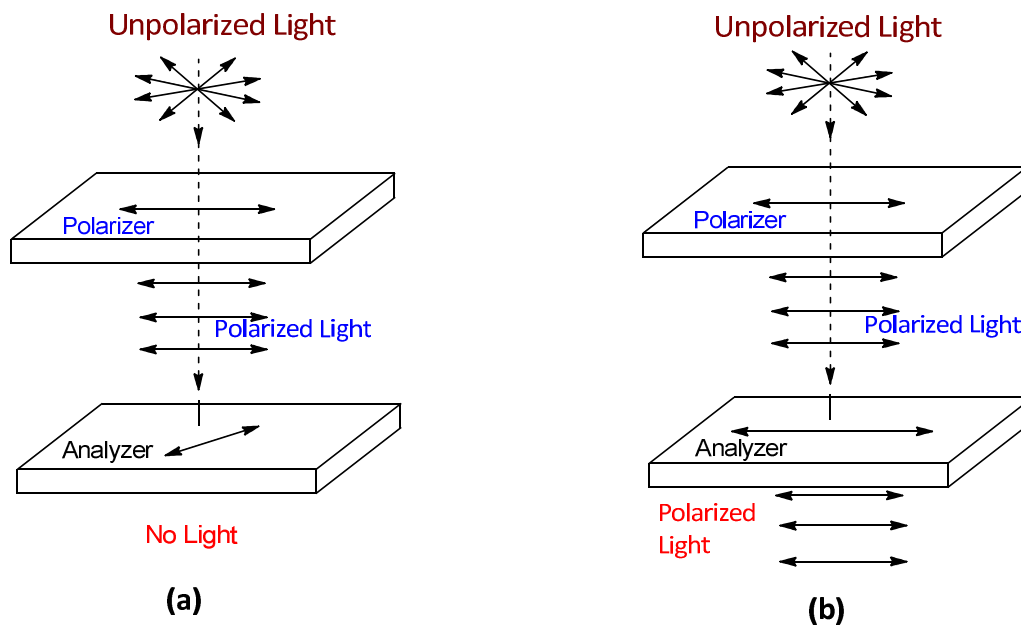
Figure **29**: *The polarising filters in an isotropic medium.*

The system's optical throughout depends on the relative orientation of the polariser and analyzer; when the polarisers are arranged their planes of polarisation perpendicular to each other, the light is blocked (Figure 29a) and the second filter *i.e.,* the analyzer is parallel to the first filter, then the light passed by the first filter is also transmitted by the second filter (Figure 29b).

1.9.2 Twisted nematic liquid crystal cells: [166-171]

A twisted nematic display is made up of, two bounding plates (generally glass slides), each with a transparent conductive coating like indium tin oxide which acts as the electrode, spacers to maintain the cell gap precisely, two crossed polarisers *i.e.,* the polariser and the analyzer and the nematic liquid crystal material. The twisted nematic liquid crystaldevice geometry is shown in Figure 30.
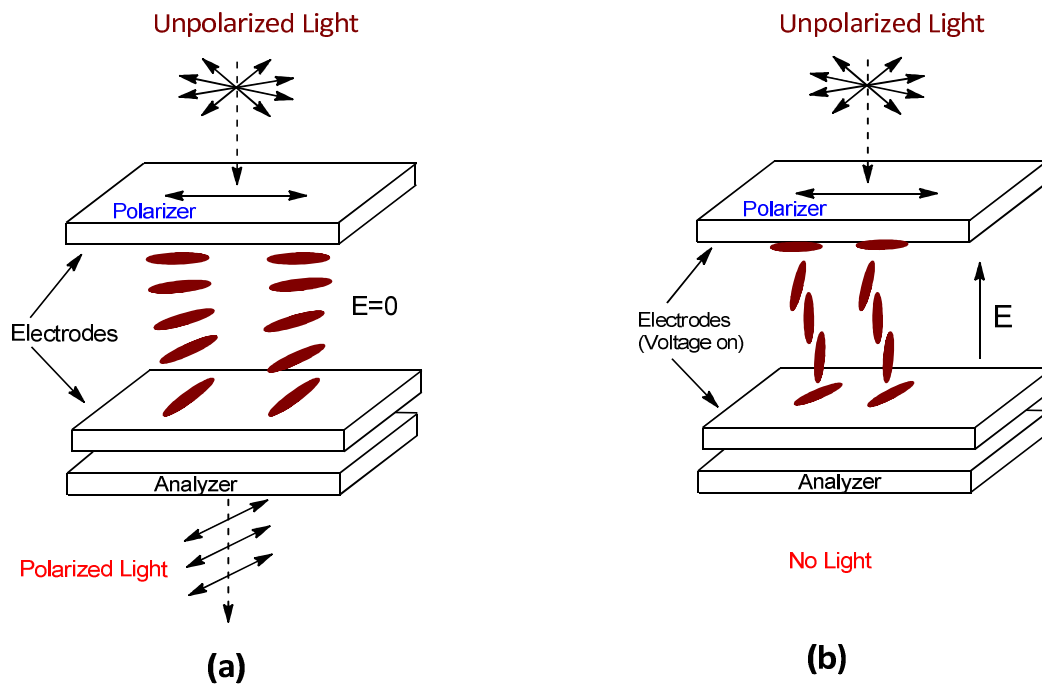
Figure **30**: *The geometry of a twisted nematic device*.

The surfaces of the transparent electrodes are coated with a thin layer of polymer, which surfaces has been brushed in one direction. These trasperant electrodes are filled with the liquid crystal materials. The nematic LC molecules tend to orient with their long axes parallel to this direction. The glass bounding plates are arranged so the molecules adjacent to the top electrode are oriented at a right angle to those at the bottom (Figure 30a). Each polariser is oriented with its easy axis parallel to the rubbing direction of the adjacent electrode.

In the absence of an electric field, the nematic director undergoes a 90°twist within the cell, hence the term twisted nematic. When unpolarised light enters the first polarising filter, it emerges polarised in the same plane as the local orientation of the LC molecules. This twisted arrangement of the LC molecules within the cell then acts as an optical wave guide torotate the plane of polarisation by a quarter turn *i.e.*, 90**°**, so the light which reaches the second polariser can pass through it. In this state the LC cell is transparent.

When the voltage is applied to the electrodes, the LC molecules tend to align with the resulting electric field (Figure 30b) and the optical wave guiding property of the cell is lost so the cell is now dark, as it would be without the LC's present as in Figure-30a. When the electric field is turned off, the molecules relax back to their twisted state and the cell becomes transparent.

The TN device is still employed in cheap displays where values of contrast ratio, refresh rate and viewing angle are not so demanding. However, new modes, namely vertically aligned

nematics and in-plane switching are used in all modern large area active matrix addressed products. Despite the success of these products, there is still a switching speed limitation, where refresh rates of 200 MHz are demanded. Thus the ferroelectric display could still make its mark, if large area stable aligned devices could be achieved.

1.10 Ferroelectric liquid crystal materials: [86, 168]

The nematic and smectic A liquid crystal phases are too symmetric to allow any vector order, ssuch as ferroelectricity. The tilted smectics, however, do allow ferroelectricity if they are composed of chiral molecules. Figure 31 below shows the ferroelectric liquid crystal compound, DOBAMBC **8** and the more recent compound CDRR8 **9** that has been shown to recover ideal bookshelf geometry.

8

9
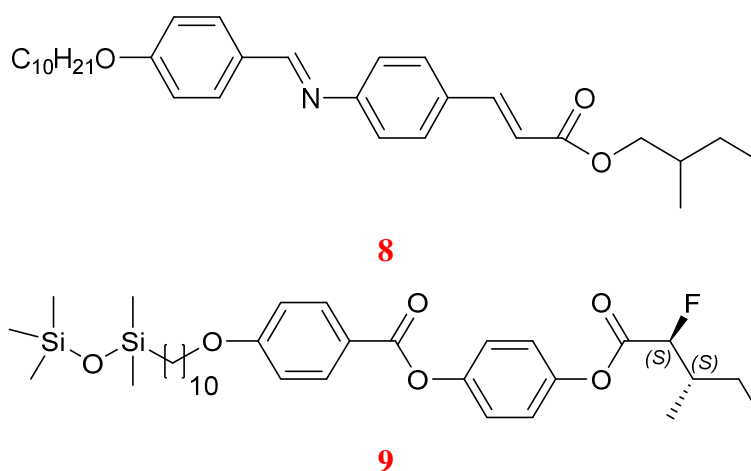
Figure **31:** *Structures of DOBAMBC* **8** *and CDRR8* **9**.

The magnitude of the polarisation depends on temperature, normally decreasing as the tilt angle goes to zero at the SmC* to SmA *phase transition. The geometry of the SmC* phase is shown below in the Figure 32.
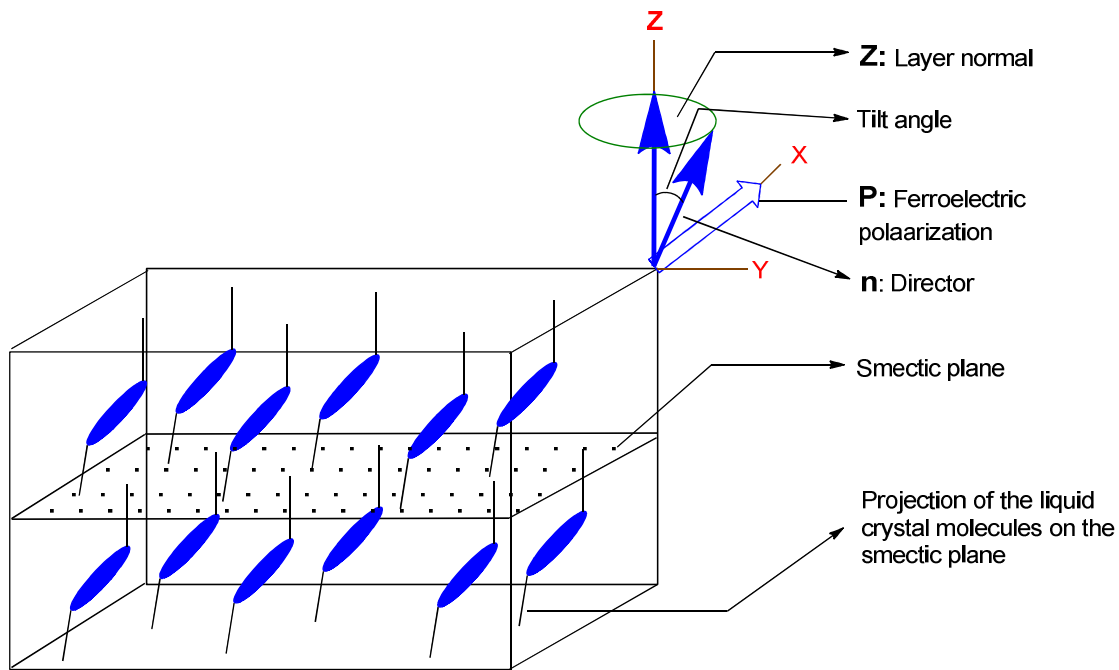
Figure **32:** *Geometry of the smectic C* phase in an FLC device.*

The coupling of the polarisation to applied fields is linear so FLC's can be made to switch quickly, typically within few microseconds and also in a bipolar manner. This makes FLC's ideally suited to electro optic applications. FLC's are now included in several different display technologies, the most popular is the surface-stabilised (SSFLC) geometry.

Clark and Lagerwall's idea is demonstrated in the polarised micrograph of a SmC* phase in Figure 33, where the bottom left portion of the cell shows pitch lines but in a thinner upper portion, helix lines are largely absent. The smectic layers were found to be oriented almost perpendicular to the glass. Further, they discovered that such cells can be switched rapidly between two optically distinct, stable states simply by alternating the sign of an applied electric field.[49]
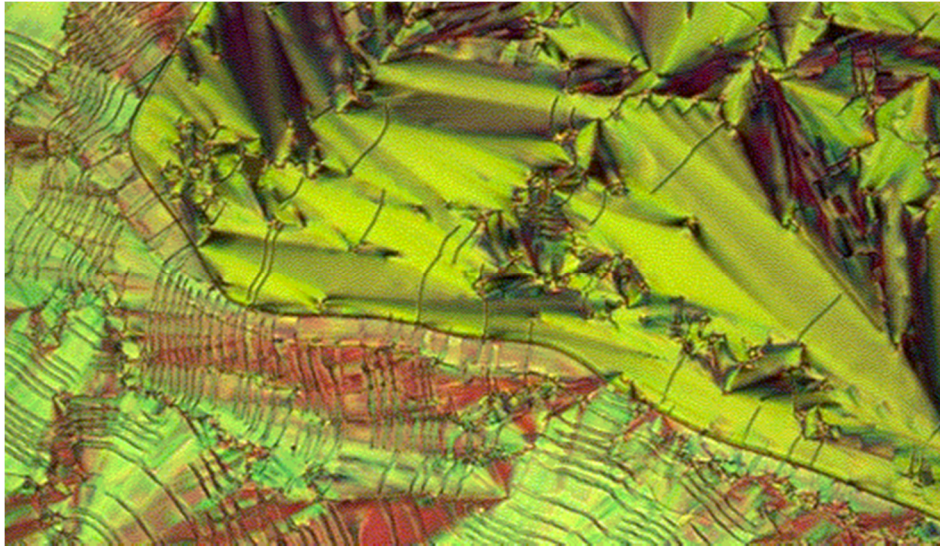
Figure **33:** *The polarised micrograph of FLC.*[49]
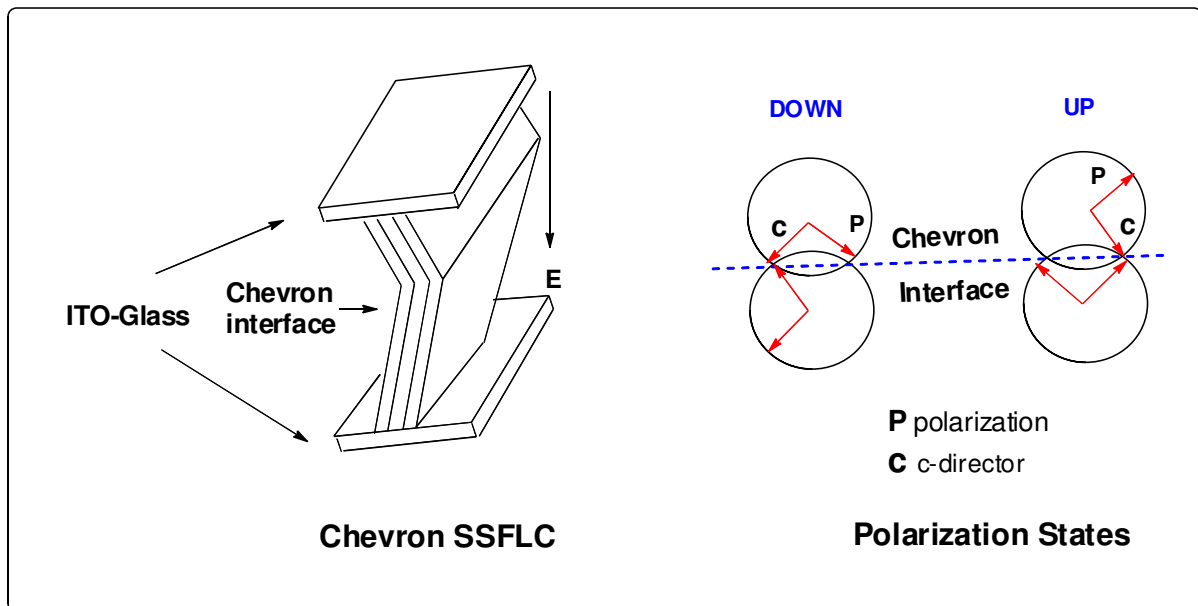
Figure **34:** *Chevron SSFLC and polarisation states.*

It was established by Clark's group, that there are two layer geometries in common *i.e.,* called bookshelf and chevron, shown in Figure-34 above. The electro-optic properties of surface stabilised ferroelectric liquid crystals depend strongly on the layer geometry and also on the nature of the orienting properties of the glass plates.[164, 165]

In order for an SSFLC device to act as an optical shutter giving bright and dark states, the typical geometry is shown in Figure 35. The material ideally has a tilt angle of 22.5° and therefore the director will switch though a cone of 45°. When the field is applied in one

direction, Ps will align with it and the director will align along the direction of one of the polarisers and this will give a dark state. When the opposite electric field is applied, the Ps will rotate 180°. The director will then be 45° away from where it used to be, bisecting the two polarisers. [168-170]

In this geometry, the two components of the light, one polarised parallel and one polarised perpendicular to the director will travel at different speeds through the liquid crystal material. If the thickness can be controlled so that the component perpendicular to the director will be 180º out of phase from where it started, then the resulting light's polarisation will be 90º rotated and will be able to penetrate through the crossed polariser. See Figure 35 below.
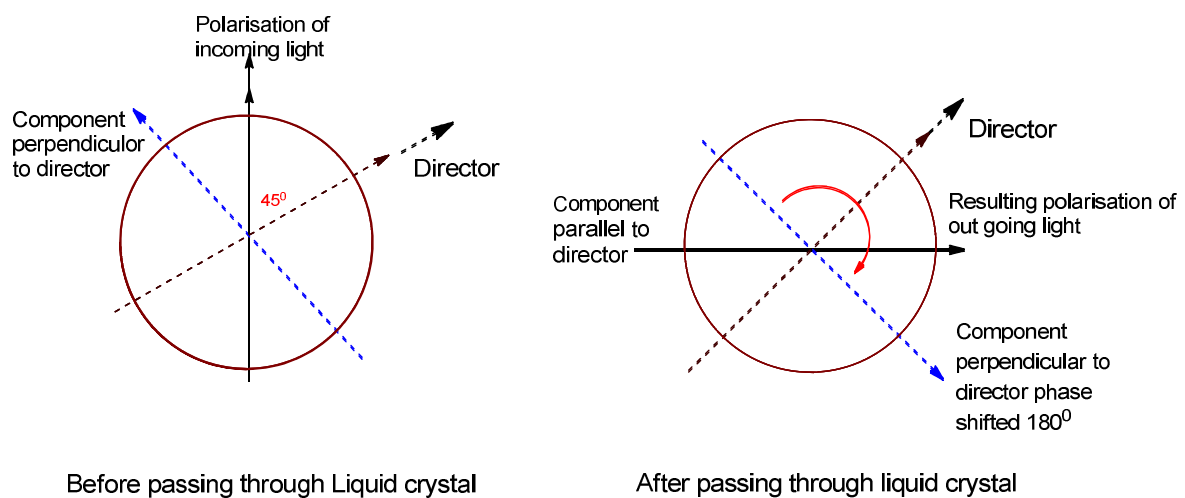
Figure **35:** *Modification of polarisation by ferroelectric displays.*

Before passing through the liquid crystal, the components of light polarised parallel and perpendicular to the director can be separated. After passing through the liquid crystal film, the perpendicular component is shifted in phase by 180º. The resulting linear polarisation is rotated 90º from its original direction. SSFLCD's have high switching speeds in part because an electric field is necessary for both turning a pixel on and for off. However, problems in development of this kind of display persist. The most difficult issue to resolve has been the orientation of the director throughout all the layers of the film.[166]

1.11 The effect of the temperature on Spontaneous Polarisation:

The temperature dependence of the spontaneous polarisation of ferroelectric liquid crystals is similar to that of other FLC materials. One of the main characteristic properties of FLC materials is initial rapid rise of spontaneous polarisation as temperature drops below the critical value (T_{crit}).
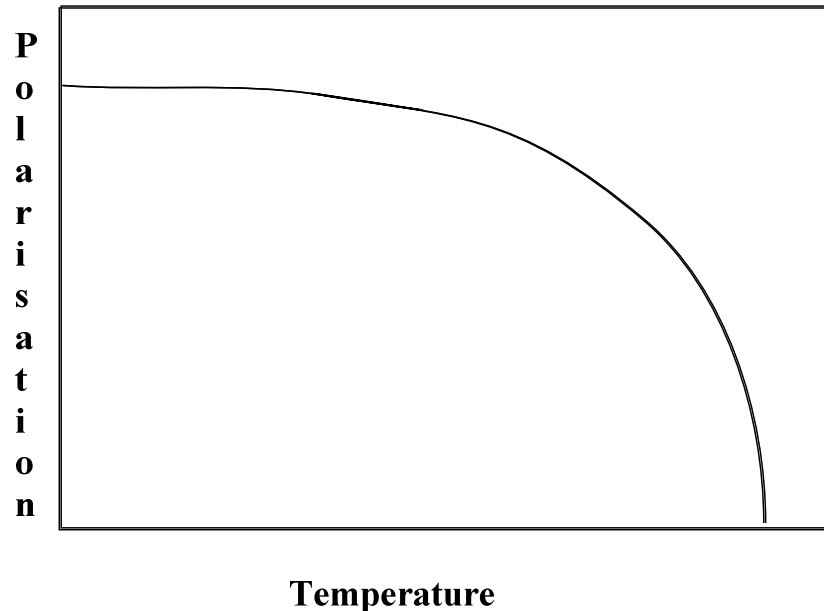
Temperature

Figure **36:** *Schematic representation of spontaneous polarisation Vs temperature.*

In crystalline ferroelectric materials, this initial rapid rise in spontaneous polarisation is due to the interactions of the elementary dipoles in the material with each other, producing an internal field which lines up the dipoles causing saturation of the spontaneous polarisation. In FLCs, although the molecules are actually undergoing a rapid reorientation about their long axis, from symmetry considerations, a time averaging process results in a molecular dipole moment along a 2-fold symmetry axis. This is the molecular polarisation, lying in the smectic layer plane and perpendicular to the long axis of the molecule, as first noted by R. B. Meyer. The interaction of this ensemble of molecular polarisations then leads to the temperature dependence of the spontaneous polarisation which could be observed in an SSFLC where the helielectric effect is avoided.[37]

The molecular tilt angle, q, away from the layer normal to the SmC* layer plane follows a similar temperature dependence to the spontaneous polarisation, rising rapidly at first, then asymptotically approaching a final low temperature value, before crystallisation.[74]

1.12 Advantages and Disadvantages of SSFLCs:

The SSFLC displays, despite the advantages of micro-second switching, high contrast, good viewing angle, bistable switching and ease of multiplexing, did not become the dominant display technology.

The switching time of surface stabilised ferroelectric liquid crystal display is much more less than that of other LC technologies. In SSFLC displays, shutters are capable of 70 μs transition time because of the coupling of the Ps vector to the applied electric field. The clear advantage to this is the increased speed in switching from the white state to the black state and vice versa for video.

Another advantage of fast switching is the ability to use sequential colouring *i.e.*, a colour is created by rapid succession of the additive primary colours blue, green, and red. The eye fuses the sequence into a single colour. If switching time was not fast enough, it would be necessary to sub-divide every pixel into green, red and blue in order to create a colour. This would necessitate making the display larger in order to get a less grainy colour image.

A problem with this matrix structure is a transverse electric field at the pixel edge that can cause misalignment. However, SSFLC's thin cell gap reduces this effect to such an extent that it is not observed under realistic conditions.

The surface stabilised liquid crystal displays have a high aperture ratio (the ratio between the optically active areas and the total area per pixel in a matrix). This is because it is a direct-driven panel, so transistor, gate sources and gate bus do not cover a lot of area as in the addressed matrix. The fact that these cases do not apply to SSFLCs make a pixel size of 5μ by 5μ feasible with the best resolution by standard graphic techniques corresponding to a size of 20μ by 20μ. The highly realistic and pixel size would yield a resolution sufficient for high definition TVs when used in a 35mm slide.

Because in the relaxed state *i.e.*, the white state, the effective cone angle is not near to the optimum value of 45° and contrast is also limited. With commonly observed tilt angles of 15 to 20°, the contrast would be around 30:1 and the black state does not undergo this limitation so the contrast could be 100:1 in this state. However, the black state is affected by partial switching in the refresh mode. This effect reduces the dynamic contrast even more, to a value of 7:1. The contrast can be improved by increasing the effective cone angle.

One good property about the contrast of surface stabilised liquid crystal display devices is that it is almost independent of viewing angle, this is because the optical axis is switched around an axis parallel to the light path. Ideally the optic axis would stay parallel to the cell plane, in other words, the optical axis never turns out into the direction of the observer where directional variations can cause large changes in the extinction. Thus, unlike common liquid crystal displays, SSFLC's can be observed from small angles to the plane of the display without a major loss of contrast. The tilt and chevron structure weaken the SSFLCs contrast at sharp angles because they cause inhomogeneities in the director alignment.

The main reason for this is alignment is the defects were not acceptable for a large area display, but the technology has found a niche application in LCOS micro displays.Commercial FLC mixtures still produce chevron layers, but the ideal situation is a stable bookshelf alignment.Conventional ferroelectric host materials possess an I – N* - SmA* - SmC* phase sequence. Layer shrinkage leads to chevron formation; chevrons are a cause of defects and do not give optimal contrast ratio.[71]
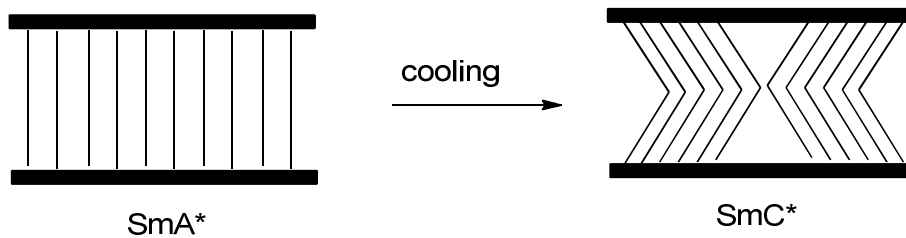
Figure **37:** *Chevron layer formation and defects in SSFLC's.*

1.13 Layer curvature:

The natural tendency towards curvature may also be a significant driving force in the formation of defects. Conventional liquid crystal materials have a narrower cross sectional terminal chain compared to the mesogenic core and this will lead to curvature if one considers a single smectic layer (Figure 38). The effect is partly negated in the phase due to interdigitation of the terminal chains between the layers. Nevertheless, there is still a drving force towards curvature as observed in the natural focal conic fan texture of thermal polarising microscopy. Curvature leads to poor alignment in devices and interdigitation probably reduces the potential tilt angle of a material.
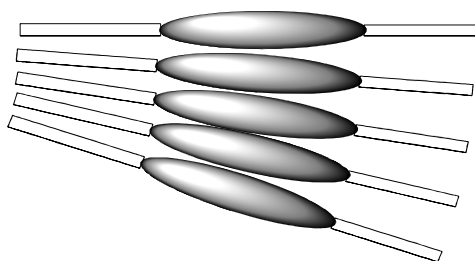
Figure **38:** *Formation of layer curvature*.

2.0 Conventional materials used for host mixtures (fluorinated terphenyls and phenylpyrimidines):

Liquid crystal materials for displays are a mixture of different components. There are many reasons for this but the major reason is to achieve the minimum crystallisation temperature (eutectic) and to get a wide liquid crystalline temperature range. Fluorination has been very beneficial to liquid crystal science due to the significant influence of fluorine on mesomorphic behaviour and related physical properties.[57-60]

The mesogenic behaviour of liquid crystalline molecules is an important aspect to understand before discussing the fluorinated liquid crystal molecules. Molecules with a liquid crystalline mesophase have a degree of intermolecular association between that of a three dimensional crystal and an isotropic liquid. To modify these intermolecular associations, a perturbing substituent or group can be included in the molecular structure that changes the separation of the molecules and modifies the strength of the intermolecular forces.[61]

The fluorine atom is used frequently in the design of liquid crystal molecules to obtain lower viscosity, strong dipole moments, but without decreasing chemical stability in comparison to a C-H bond. Fluorine's small size (1.47 Å) comparable to the size of hydrogen (1.20 Å) means that decreases in length to breadth ratio are marginal. The fluorine atom is a suitable oxygen mimic due to its insignificant steric impact, but at the same it introduces substantial polarity.[58]

2.1 Current FLC mixtures and research aims:

As explained in the previous section, the mono-atomic nature, high electronegativity, low polarisability, small size and strength of the C-F bond has been essential in enabling stable LCs to be synthesised with the desired electrooptic and visco-elastic properties needed for display applications. Compounds very similar to those in Figure 41 are present in large area television displays and in smaller liquid crystal display screens and thus, a multibillion pound industry relies on the benefits of fluorinated LC's. The nematic phase is exploited in most displays. In general, increasing the length of the terminal chains can also be employed to increase smectic vs nematic phase stability. The FLC mixtures were prepared from an achiral host mixture and a chiral dopant. Low viscosity mixtures were developed during the collaboration between QinetiQ, formerly The Defence Evaluation Research Agency (DERA) and the Liquid Crystal Research Group at Hull University. [65, 73, 119]

One such mixture (Figure 39) consists of dialkyldifluoroterphenyls, with fifty percent of the mixture made of two end-ring substituted compounds and the other half from a middle ring difluorinated-material. This mixture has wide SmC phase temperature range, a low melting point and an I – N – SmA – SmC phase sequence, which provides good alignment. It is very stable, has low viscosity and the tilt angle is high enough to give good optical contrast.[34, 39, 161]
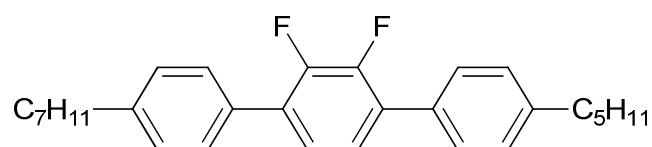
Cryst 36.5 (SmC 24.0) N 111.5 I (^{o}C)

50%
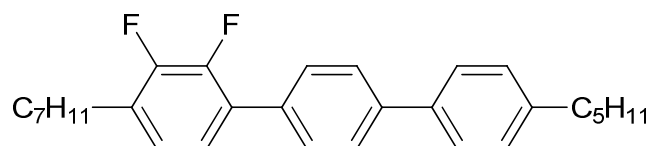
Cryst 56.0 SmC 105.5 SmA 131.0 N 136.0 I (^{o}C)

25%
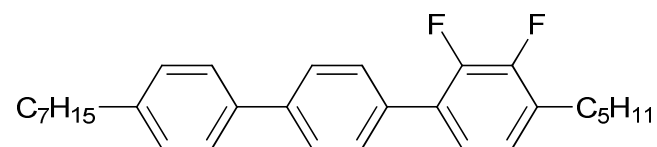
Cryst 65.5 SmI 74.5 SmC 118.5 SmA 135.0 N 137.0 I (^{o}C)

25%

Figure **39:** *The transition temperatures for host mixture components of KCHM211.*

It is interesting to note that 50% of the mixture is a compound with a monotropic SmC phase at 25° C and is essentially a nematogen but the transition temperature of the final mixture referred to as KCHM211 has a much higher SmC – SmA phase transition.

KCHM211 Cryst ~ 11 SmC 87.2 SmA 99.5 N 122.5 ℃ I

KCHM211 + 7 % w/w BE8OF2N SmC* 67.2 SmA* 97.7 N* 113.5 ℃ I

Figure **40:** *Transition temperatures of host mixture KCHM211 and with 7% w/w dopant BE80F2N.*

Mixture of these three components has led to a reduction in melting point, but still it is not really low enough to make a commercial device, however the mixture can be held below the melting point for long periods without crystallising. The chiral dopant BE8OF2N selected by

DERA as part of the Ferroelectric Liquid Crystal research programme with Hull was originally synthesised by Merck. A 7% w/w mixture with KCHM211 produces a mixture with a Ps of 16 nC cm^{-2} and a pitch length of 14 µm at the N*-SmA* phase transition and provides good alignment. The transition temperatures in Figure 40 shows that the most dramatic effect of the dopant, is the reduction of the SmC* - SmA* phase transition by 20 °C. The SmA* - N* transition is barely altered and the clearing temperature is reduced by nearly 9.0 °C; however the latter is beneficial since it reduces the temperature at which electrooptic cells need to be filled.
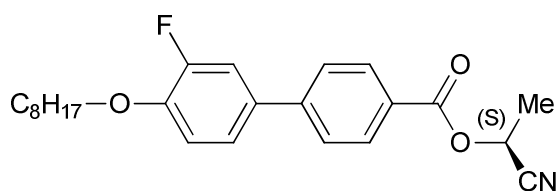
10

Figure **41:** *The non mesogenic dopant BE8OF2N.*

2.2 Fluoro substitution at a lateral position:

Substituting fluorine at a lateral position within the core, exerts a small steric effect because, comparative to a hydrogen atom, the fluorine atom that thrust outward from the side of the molecules will sterically force the molecules apart and disorder the smectic molecular packing. In general, often the melting point will be reduced and the liquid crystalline phase stability as well. A lateral fluoro substituent increases the lateral dipole within a molecule and this may promote tilted SmC phase and thus shows promise in the formulation of ferroelectric compounds. By combining the steric and polarity effects of fluorine, some significant changes in the physical properties can result without too much disruption of the molecular packing.[66, 67]

The examples below, show how addition of fluoro substituents have reduced melting points and clearing points of the terphenyls to give practically useful materials. It also demonstrates the large change in phase type caused by moving the fluorine; for example, the middle ring difluoro compound is a nematogen but when the fluorine substituents are moved to the end ring, the smectic phase is enhanced, including a wide temperature range SmC phase. Monofluoroterphenyl end ring compounds have a crystal B phase but this is completely suppressed in an end ring difluoroterphenyl. Moving a monofluoro substituent from the

middle ring to the inner position on the end ring changes orthogonal smectic behaviour to a broad temperature range SmC phase (Fig. 42).[68, 69]

C 192.0 SmA 213.0 I ($^{\circ}$C)

C 51.5 B 62.0 SmA 109.5 N 136.5 I ($^{\circ}$C)

C 72.5 SmC 80.0 N 136.0 I ($^{\circ}$C)

C 60.0 N 120.0 I ($^{\circ}$C)

C 81.0 SmC 115.5 SmÀ 131.5 N142.0 I ($^{\circ}$C)
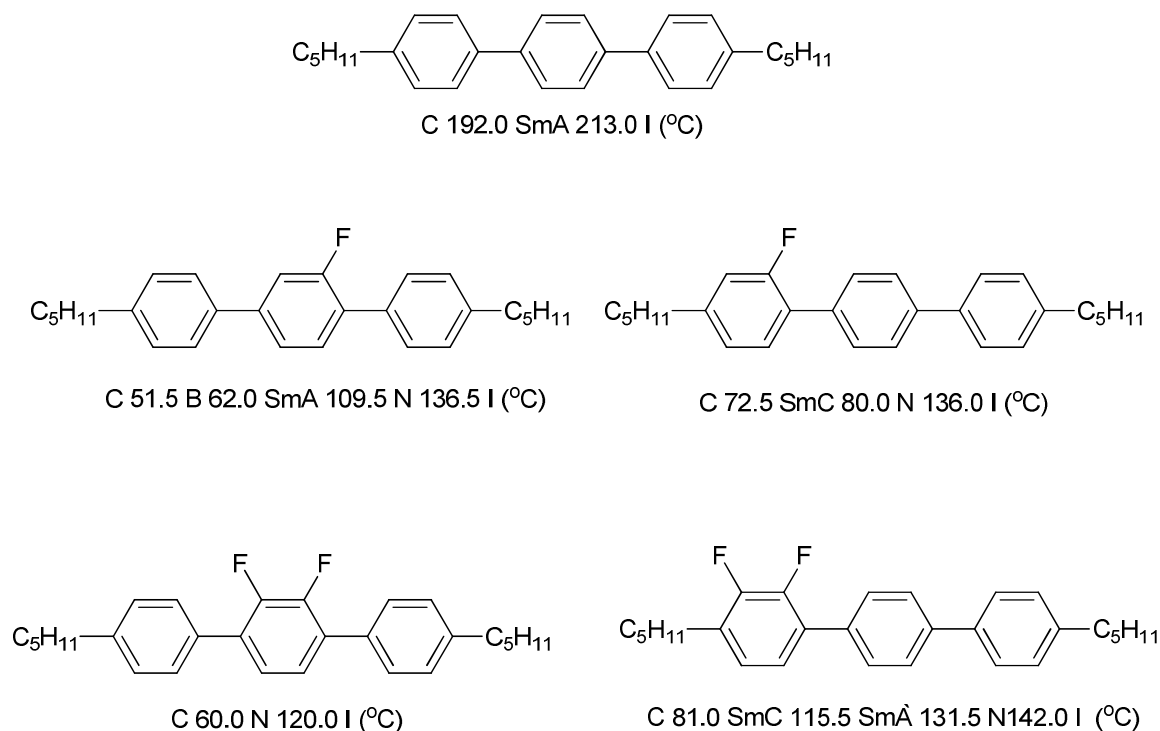
Figure **42:** *Effect of fluoro substituents on transition temperatures.*[65]

2.3 The effect of bulky end groups in ferroelectric liquid crystal materials:

Typical ferroelectric liquid crystal molecules consist of a rigid core and end-tail groups with a chiral centre located on one or both groups and most of the FLC molecules end-tail groups are hydrocarbon chains. However, there have been few studies on the effect of replacing the alkyl chains partially with cyclic groups, fluoro carbons or siloxy units. In contrast to the stiff fluoro carbons and replacing of alkyl chains by flexible dimethylsiloxane groups as end tails is expected to lower the phase transition temperatures with higher in thermal stability of the ferroelectric liquid crystal materials. These dimethylsiloxane groups are bulkier in the size of end group and more flexible and exhibit more irregular conformations, compared to their alkyl chains counter parts. This gave the effect of reducing the shape anisotropy to the molecules and its degree of crystallinity. The reduction of crystallinity to below ambient temperatures is of great interest from an application point of view. This approach of

decreasing the crystallinity of mesogens has been performed already in side-chain liquid crystal polymers.[57]

The organosiloxane LMM liquid crystal materials have attracted reasonable interest because their electro-optical properties are similar to those of classical low molar mass liquid crystals, indicating faster switching times in the nematic[100], SmA, SmA* [101], SmC* [103-105] and SmC$_A$*[106, 107] phases. Commonly such materials show a high mobility of their side groups, tilt angles, temperature independent layer spacing and good mechanical properties associated with the microscopic self assembly of siloxane moieties.

Low molecular mass organosiloxane monomesogen and bimesogens show a number of extraordinary microscopic and macroscopic properties. Microscopically it has been shown that the siloxane moiety may be controlled to induce de Vries-like behaviour and SmA* phases in materials that otherwise only exhibited SmC* phases[114]. Macroscopically, such materials have been incorporated into devices based on, for example, light scattering,[108] birefringence,[107-109] dichroism,[110] fluorescence,[111] photochromism[112] and optical nonlinearity[113].

Depending on their siloxane content, these moieties may be used to control the anticlinic (antiferroelectric) or synclinic (ferroelectric) behaviour of the phase using the same bimesogenic groups. The anticlinic state may be balanced by more indirect effects including entropic ones[120]. The especially interesting feature of these materials with ferroelectric[105] or antiferroelectric phases, is the large tilt angle (45º) dependant on the packing of the mesogen btween the bulky siloxane moieties. The molecular tilt of most siloxane bimesogens is temperature independent over a broad temperature range.[159] These materials can easily be uniformly aligned in a bookshelf geometry, with the smectic layers being normal to the confining surfaces. They do not give rise to chevron defects and switching times of the order of 10 μs to 100s of μs are observed. These materials were very interesting in photonics applications because of their good mechanical stability. Beamsteering devices and optical phase modulators in Liquid Crystal On Silicon (LCOS) devices[115] have employed siloxane bimesogens. Siloxane spacers linking two mesogenic molecules in such bimesogens may give rise to antiferroelectric or ferroelectric phases depending on the number of silicon atoms in their siloxane units.[105, 107, 159]

The optical, electro-optical behaviour of these siloxane bimesogens posssessed a wide temperature range of antiferroelectric phase, with high Ps and high molecular tilt in the field-induced ferroelectric phase.[125]

X = Br, Cl, F

44
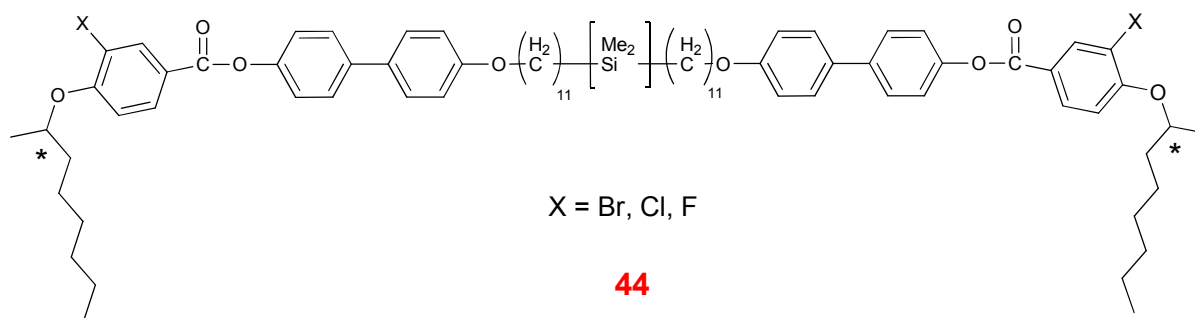
The homologues, Cl11-3-11Cl, Br11-3-11Br, and F11-3-11F are the materials whose properties were explained; F, Cl and Br refer to the halogen substituent in the molecule; 11 refers to the number of methylene spacers in the alkyl chain and 3 refers to the number of silicon atoms in the siloxane moiety.

Table 1. Physical properties of the organosiloxane compounds at a fixed temperature of 220 ℃.[125]

Compound	Clearing temp/℃	Mesophase	Melting temp./℃	Ps/nCcm^{-2}	Tilt angle/º
F11-3-11F	121	SmC$_A$*	51.2	101	40.4
Cl11-3-11Cl	110	SmC$_A$*	55.2	119	41.7
Br11-3-11Br	106	SmC$_A$*	50	135	43.5

Electro-optical properties of the above three bimesogenic siloxane compounds, in which two mesogenic groups were connected by a siloxane unit containing benzoate ester mesogens and 3 silicon atoms were laterally substituted with Br, Cl or F. These materials show an AF phase over a broad temperature range and a high molecular tilt in the AF phase nearer to the 45 ℃.

9
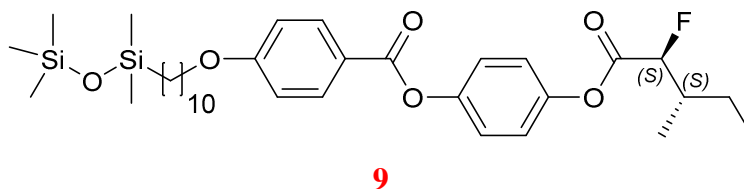
Figure **43**: *The molecular structure of compound CDRR8.*

The family of organosiloxane as a bulky end group materials were explains a series of useful and interesting properties for FLC applications. These materials were crystallise at lower temperatures and both the SmA[*] and the SmC[*] phases observed in a lower temperature regions, which is useful for FLC device applications. This type of organosiloxane materials has a large electroclinic effect without the distortion of an alignment such as a stripe texture[87] and also shows pyroelectric coefficient much higher than that of inorganic materials.[88]

Some organosiloxane materials exhibit a very small layer contraction in the Smectic C[*]phase over the transition from the Smectic A* to Smectic C[*]phases.[89] Specific interest of this fact is to determine the structures of the phases, in which the tilt of the director from the layer normal does not lead to layer shrinkage. This property gives the possibility of preparing perfect ferroelectric liquid crystal displays without any problems in the alignment caused by a change in layer spacing like stripe textures and chevrons.[160]

The pyroelectric coefficient, dielectric permittivity and the smectic layer thickness of a novel ferroelectric organosiloxane LC material **55** was measured as a function of the bias electric field. The material yielded a very high Ps (~240 nC/cm^2) in the smectic C[*] phase. This materials also exhibited unexpected behaviour of pyroelectric coefficient and the smectic layer thickness in a temperature range just below the phase transition from the smectic A[*] to the SmC* phase. This behaviour is explained in terms of new statistical theory based on order parameters of the smectic C[*] phase. The ferroelectric liquid crystal compound, 12KN5DSi **55** is shown below in the Figure 44.[160]

55

C 10 SmC 40.5 SmA 59 I °C
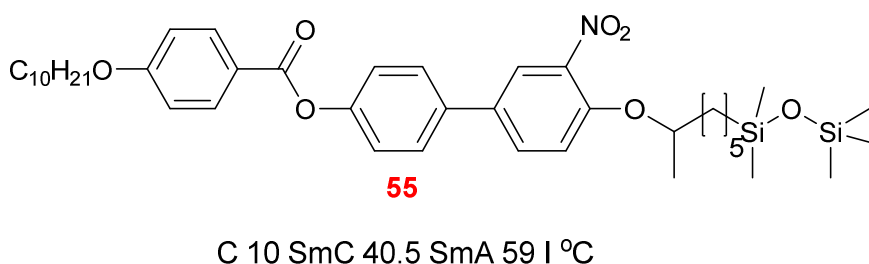
Figure **44:** *Structure and phase transitions of compound 12KN5DSi* **55**.

A high electroclinic effect and a very small layer contraction suggest there are similarites to the de Vries materials[90, 91] and recently, the latter have been intensively investigated.[92-94] In the de Vries phase, the molecules are tilted as in the SmC[*], but the azimuthal directions of the tilt in different smectic layers are oriented randomly or without long-range correlation.[90] This led to uniaxial symmetry of the phase of SmA[*] and the symmetry of every smectic layer is

biaxial. This hypothesis is supported by the fact that each smectic layer has a spontaneous polarisation when the molecules are chiral. This type of phase was also suggested to exist by Fukuda [95] and by Inui *et al.*[96] In connection with the V-shaped switching, it was named as random smectic C* (SmC$_R$*).[97, 160]

In the second type of de Vries model,[91] the molecules were tilted, but the azimuthal directions of their tilts were spread randomly in every smectic layer. In this case, the symmetry of this phase is uniaxial because every smectic layer is uniaxial like that in the ordinary SmA* phase. In this type of model, the smectic layers do not have a Ps, but when the molecules were chiral, it has large susceptibility to the electric field that becomes apparent through a specific electroclinic effect.[160]

Recently, a more realistic theory was proposed which successfully explains the main properties of conventional and so-called de Vries-type smectic LC's and also explains the origin of the anomalously weak layer contraction at the smectic A*– smectic C* transition. In contrast to the previous models, the recent statistical theory is based on a complete set of order parameters of the SmC* phase.[97, 98]

Several ferroelectric organosiloxane materials which exhibit room temperature SmC* phase and low melting points (4 ºC) are shown in Figure 45.[87]
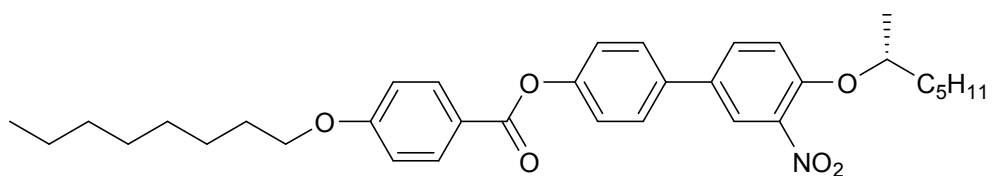
KN86   K 58.9 "C SmA* 68.7 °C Iso
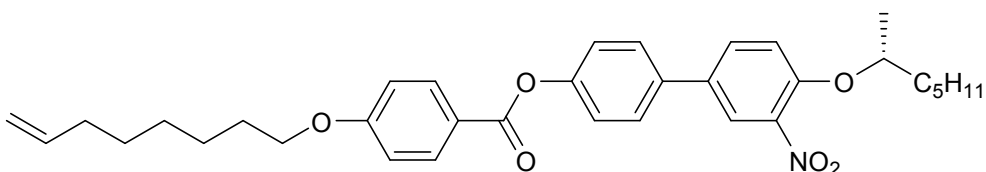
DKN85   K 27.5 "C SmA 61.1 "C Iso
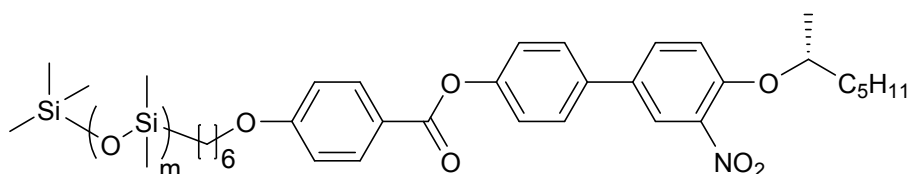
DSiKN65   K < 5 "C SmC* 48.2 SmA* 51 I °C

m=0   SiKN65

m=1   DSiKN65

m=2   TSiKN65

Figure **45**: *Structures of organosiloxane materials: KN86, DKN85, DSiKN65.*

Table 2. Transition temperatures for the ferroelectric organosiloxane liquid-crystalline series:[87]

Compound	phase sequence (°C)
SiKN65	SmC* 48.2 SmA*51 I
DSiKN65	SmC* 40.5 SmA*55 I
TSiKN65	SmC* 23 SmA* 55.5 I

For all the above samples the melting point is below 5 °C.

The electrooptic properties of ferroelectric materials are very sensitive to number of siloxy units attached to the hydrocarbon chain at the non-chiral end of the compound. These siloxy groups decreases the crystallization temperatures of the materials and maintains low switching times even at ambient temperatures.[87]

The inclusion of an ether-linked cyclobutane or oxetane ring at the terminal position of a chain is possible to promote the formation of anticlinic behaviour in compounds containing the weakly polar and less sterically hindered chiral 2-methylbutyl moiety and there is a marked odd/even effect which either promotes synclinic or anticlinic behaviour. Table 3 show the transition temperatures for the conventional materials and Tables 4 and 5 contain analogues with bulky end groups.[126]

Table 3. Basic structure and transition temperatures of series **1** of conventional compounds **56**.[126]

56
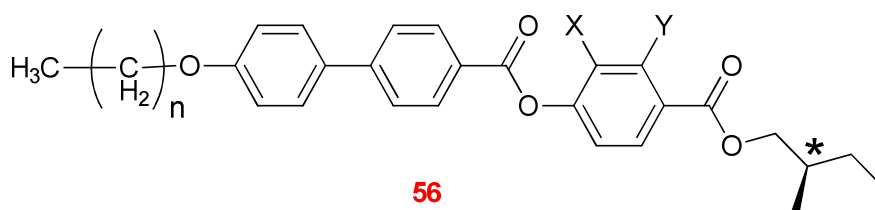
Compound	n	x	y	Transition temperaturesa/°C
1.1	**14**	**H**	**H**	**K 82.2 SmC* 127.4 SmA* 168.2 Iso**
1.2	14	H	F	K 60.7 SmC* 123.7 SmA* 165.8 Iso
1.3	14	F	H	K 72.7 SmC* 99.9 SmA* 139.3 Iso
1.4	**15**	**H**	**H**	**K 73.7 SmC* 127.6 SmA* 167.3 Iso**
1.5	15	H	F	K 53.1 SmC* 122.5 SmA* 164.8 Iso
1.6	15	F	H	K 71.0 SmC* 98.1 SmA* 138.5 Iso

Table 4. Basic structure and transition temperatures of series 2 of conventional materials.[126]
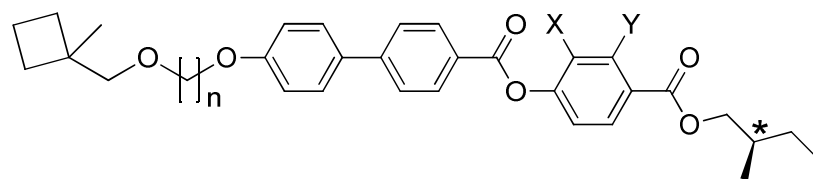
57

Compound	n	x	y	Transition temperaturesa/uC
2.1	**10**	**H**	**H**	**K 32.8 SmC* 125.7 SmA* 146.7 Iso**
2.2	10	H	F	K 41.8 SmC* 123.9 SmA* 147.6 Iso
2.3	10	F	H	K 36.1 SmC* 101.5 SmA* 115.7 Iso
2.4	**11**	**H**	**H**	**K 59.4 SmC$_A$* 88.9 SmC* 124.0 A 146.8 Iso**
2.5	11	H	F	K 38.2 SmC$_A$* 89.8 C* 119.3 A 145.7 Iso
2.6	11	F	H	K 68.1 SmC* 101.2 SmA*117.1 Iso

Table 5. Basic structure and transition temperatures of series **3** of compounds.[126]
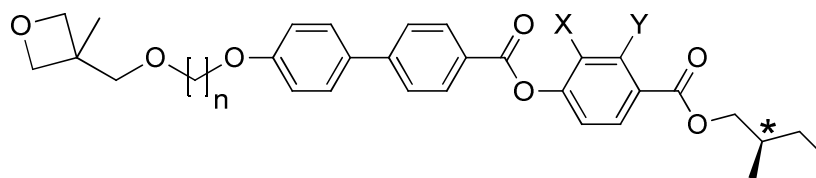
58

Compound	n	X	y	Transition temperaturesa/°C
3.1	**10**	**H**	**H**	**K 25.6 SmC* 101.3 SmA* 135.3 Iso**
3.2	10	H	F	K 220.1SmC* 98.9 SmA* 143.7 Iso
3.3	10	F	H	K 31.3 SmC* 54.7 SmA* 108.0 BP 111.2 Iso
3.4	**11**	**H**	**H**	**K 52.0 SmC$_A$* 70.0 SmC* 104.5 SmA* 130.5 Iso**
3.5	11	H	F	K 32.4 SmC$_A$* 65.0 SmC*112.3 SmA* 124.9 Iso
3.6	11	F	H	K 73.4 SmC* 74.8 SmA* 102.6 Iso

There is clearly a strong effect on melting point and transition temperatures, when replacing thinner alkyl chains with bulky end groups in the molecule. The transition temperatures are significantly lower when introduced bulky end groups in to the molecule.

The combination of the 2-methylbutyl group and long alkoxy chains at the smectic layer interfaces strongly promote synclinic behaviour, which is expected from the current structure–property relationships based on the fact that for anticlinic behaviour a terminal branched chain, typically a 1-methylheptyl unit is required. Examination of cyclobutane (series 2) and oxetane (series 3) reveals much more varied behaviour. For the compounds with a decamethylene spacer (2.1–2.3 and 3.1–3.3) the mesophase behaviour is similar to that of the alkoxy compounds in series.[126]

The bulky cyclic group does not support the formation of a higher order smectic phase. This provides further evidence that this type of group may interfere with the organisation of the molecules at the interface via reduction of the interlayer interactions through steric crowding. It has been shown that the inclusion of a small bulky group at the terminal of an alkyl chain in a typical ferroelectric liquidcrystal can alter the interactions at the smectic layer interfaces sufficiently to promote anticlinic phase behaviour. Indeed, one ofthe major problems for commercialisation of antiferroelectric (AF) LCDs is the need for pitch compensation. Although these materials show extremely high switching thresholds, a 2-methylbutyl group provides a longer pitch than a 1-methylheptyl group.[126]

Organosiloxane 2-phenyl pyrimidine mesogens with chiral (R,R)-2,3-difluorooctyloxy side-chains compounds form chiral smectic A*, smectic C* phases and exbhit alignment properties and specific electro-optical properties as SSFLC's, including one of the fastest optical rise times (11 µs at T – TAC= -10 K and 6 V µm^{-1}) for an organosiloxane mesogen.[127]
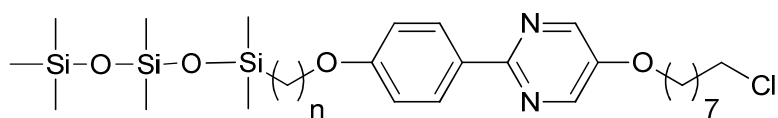
59

59a, n=11 : Cr 48 SmC 89 SmA 98 I

59b, n=6 : Cr 45 SmC 76 SmA 85 I
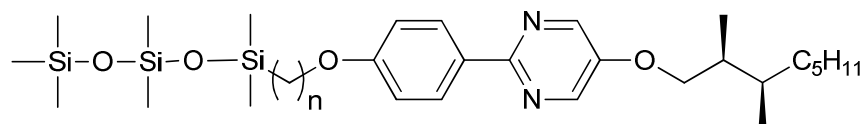
60

60a, n=11; **60b**, n=6

Figure **46:** *The structures and transition temperatures of organosiloxane phenylpyrimidine compounds **59, 60**.*[127]

The lamellar smectic phases were formed by calamitic mesogens containing of two paraffinic side-chains connected to a rigid aromatic core. The difference in conformational rigidity and Van der Waals forces between aromatic and alkyl segments, a type of amphiphilicity, is extremely sensitive to changes in the length of the paraffinic side-chains and the electronic properties of the aromatic core.[129] The formation of smectic phases can be strongly supported by the design of more prominent amphiphilicity combining calamitic mesogens, for example, lipophilic and hydrophilic segments, hydrocarbon and fluorocarbon segments, or hydrocarbon and siloxane segments. The addition of an oligomeric siloxane end-group to a calamitic mesogen has been shown to promote formation of lamellar smectic phases. This is due to the tendency of paraffinic groups and siloxane end groups to nanosegregate into distinct sublayers[130-141]forming a so-called 'virtual siloxane backbone' that allows dopant compatibilization.[142] Examples of chiral organosiloxane liquid crystal mesogens C10C*B[134] Cl11-Si3, Br11-Si3,[135] DSiKN65 and TSiKN65,[87] are shown in Figure 46.

Another interesting property of the siloxane terminated chiral mesogens is an unusually small layer contraction (<1%) upon transition from the orthogonal SmA* phase to the tilted SmC* phase.[140-145] This is mainly applicable to the formulation of LC mixtures for SSFLC device applications, because standard calamitic mesogens were characterised by layer contractions

in the range of 7 to 10%. This results in a twisting of the smectic layers into chevron geometry and the formation of *zigzag* defects reduces the optical quality of surface stabilised ferroelectric liquid crystal displays.[146] The design of materials with a SmA to SmC layer contraction of 1% (so called 'de Vries-like') has not been fully rationalised,[147] although recent studies demonstrates that calamitic liquid crystal materials with low orientational order and high lamellar order are likely to show this behaviour.[148,149] The most 'de Vries-like' materials feature nanosegregating structural elements such as partially fluorinated side chains or siloxane endgroups that strongly support lamellar order.[146] Recent studies showed that addition of a trisiloxane endgroup on one side chain of an achiral 2-phenylpyrimidine mesogen typically lower the layer contraction upon transition from the SmA to the SmC phase and further reduction in layer contraction is produced by addition of chloro endgroups on the other side of the chain. For example compounds **59a** and **59b**;[150] in the case of **59b**, the SmA to SmC phase transition results in a layer contraction of only 1.6%, which is comparable to that achieved with other 'de Vries-like' materials.[146, 127]

The 2-phenylpyrimidine trisiloxane mesogens **60a** and **60b**, which feature the Displaytech (*R*, *R*)-2,3-difluorooctyloxy chiral side chain compounds, compared their electrooptical properties as neat ferroelectric SmC* materials to those of the US Naval Research Lab (NRL) materials TSiKN65 and DSiKN65 below in Table 5 and Figure 47.[87]

Table 6. Spontaneous polarization Ps, optical tilt angle θ opt, optical rise time τ_{10-90} and rotational viscosity η measured in the SmC* phase at T - TAC = -10 K for compounds **60a**, **60b**, TSiKN65, DSiKN65 and C10C*B.[87, 127]

Compound	$PS/nC\ cm^{-2}$	θ_{opt}/deg	$\tau_{10-90}/\mu s^a$	$\eta/mPa\ s^a$
60a	-88 ± 2^b	34 ± 1^b	11 ± 1^b	371 ± 34^b
60b	-40 ± 3^b	34 ± 1^b	37 ± 6^b	372 ± 26^b
DSiKN65	219^c	30^c	184^c	2832^c
TSiKN65	185^c	34^c	606^c	5390^c
$C_{10}C*B$	70^d	26^d	$8^{d,e}$	$200^{d,e}$

^{a} Measured with a square wave AC field of 6 V μm^{-1} at 100 Hz in ITO glass cells with a rubbed nylon alignment layer and a 5.5 μm spacing. ^{b} Average of fifteen measurements from five different films; error is ±2 standard deviations. ^{c} Taken from a single film. ^{d} From ref. 30. ^{e} Measured with a square wave AC field of 20 V μm^{-1} at 100 Hz.
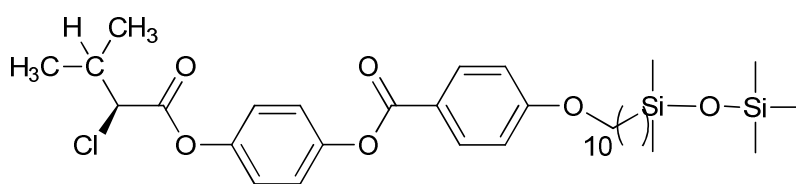
C$_{10}$C*B: Cr 0 SmC* 56 I
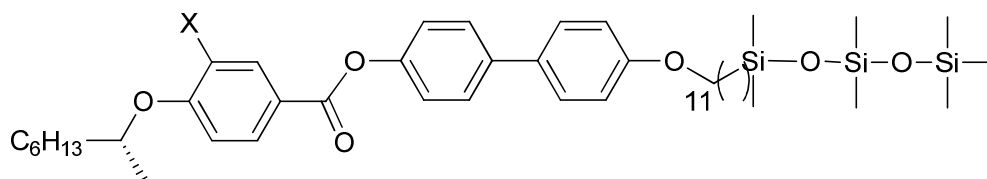
Br11-Si$_3$, X=Br: Cr 46 SmC* 88 I

Cl11-Si$_3$, X=Cl: Cr 41 SmC* 92 I
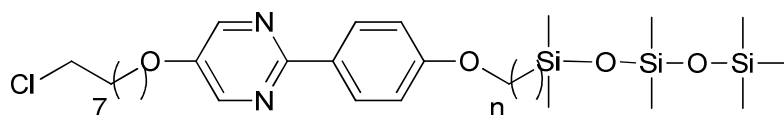
59a, n=11 : Cr 48 SmC 89 SmA 98 I

59b, n=6 : Cr 45 SmC 76 SmA 85 I
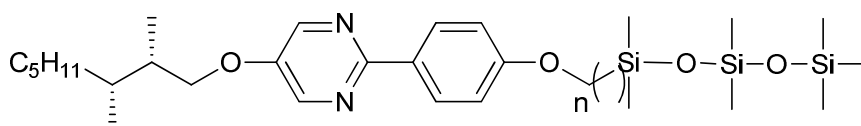
60a, n=11; **60b**, n=6

Figure **47**: *The structures and transition temperatures of chiral organosiloxane mesogens C10C*B, Cl11-Si₃, Br11-Si₃, DSiKN65 and TSiKN65.*[127]

61 n = 14 or 15
X = H or F; Y = H or F

62 m = CH$_2$ n = 10 or 11
m = O X = H or F; Y = H or F

KN86 C 58.9 "C SmA 68.7 Is0 °C

DKN85 C 27.5 "C SmA 61.1 Iso °C

DSiKN65 C < 5 "C SmC* 48.2 SmA 51 I °C
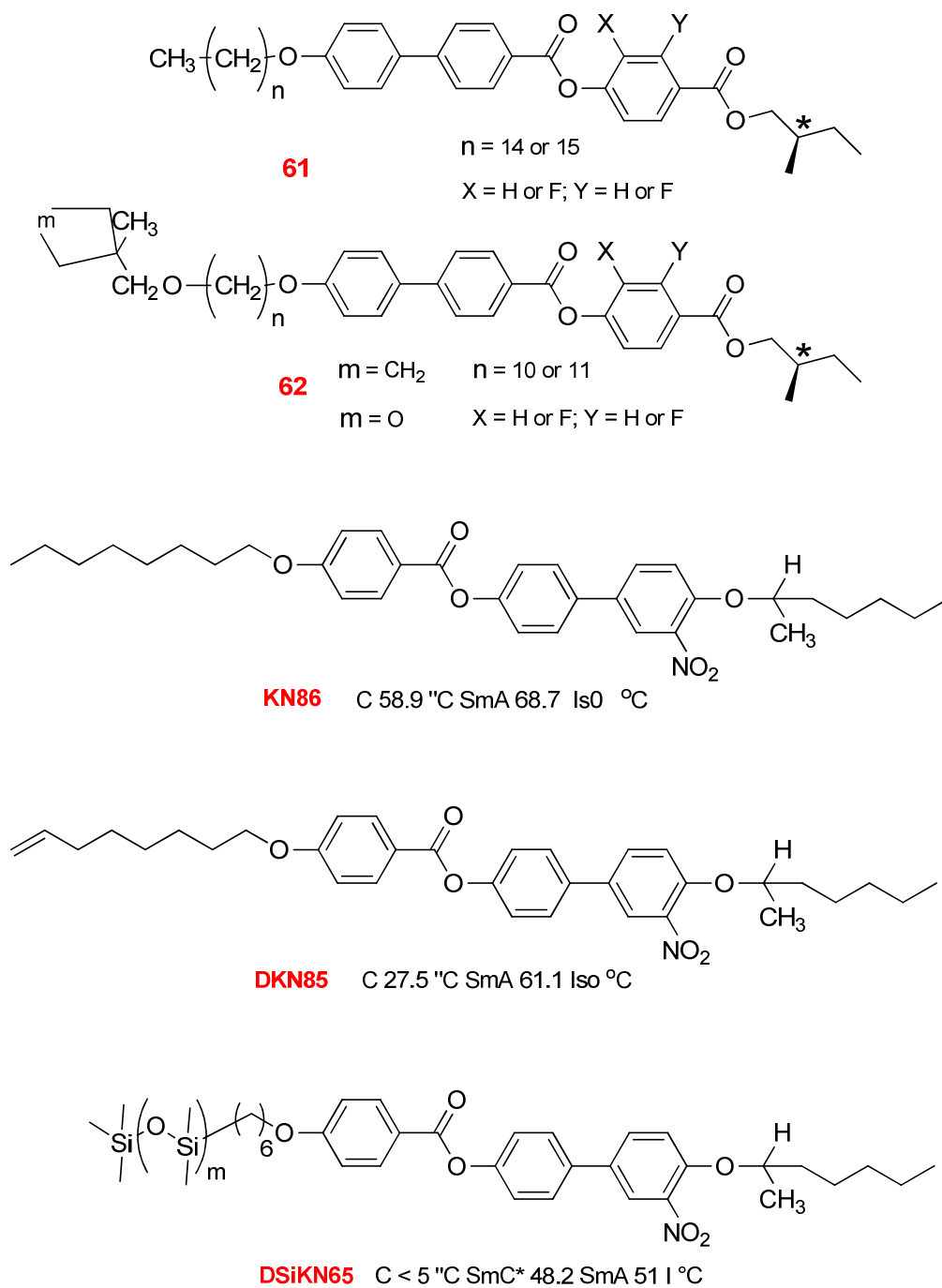
Figure **48**: *The structures and tnasition temperatures of chiral organosiloxane mesogens*
KN86, DKN85, DSiKN65.[87]

The two above mentioned organosiloxane phenylpyrimidines mesogens that form chiral SmA* and SmC* liquid crystal phases and optical rise time measurements at T-TAC= -10 K show that **60a** and **60b** are the fastest switching liquid crystals with a trisiloxane endgroup.

2.4 de Vries-like Materials:

The "de Vries-like" LC materials are *characterised* by a maximum layer contraction of < 1% upon transition from SmA-SmC phase. A new design of de Vries-like materials is based on a frustration between one structural element that promotes the formation of a SmC phase e.g., a trisiloxane-terminated side chain and one that promotes the formation of a SmA phase either a chloro-terminated side chain or a 5-phenylpyrimidine core. The mesogens 5-(4-(1,1-(1,1,1,3,3,5,5-heptamethyltrisiloxanyl)-undecyloxy)phenyl)-2-(1-alkyloxy)pyrimidine go through SmA to SmC phase transitions with maximum layer contractions ranging from 0.5% to 1.4%. A comparison of reduction factors R and f suggests that this behaviour is due in part to a pronounced negative thermal expansion in the SmC phase that counter balances the layer contraction caused by increasing tilt.[153].
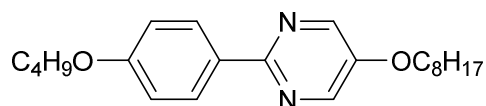
PhP1

Although there are few examples of liquid crystals with de Vries-like properties, there is still no strategy for the rational design of this type of material.[152] In an effort to develop de Vries-like liquid crystal host materials that are structurally related to components of ferroelectric liquid crystal mixtures and increasing the "de Vries character", analogues of **PhP1** were synthesised, integrating one structural element that supports the formation of a SmC phase (e.g., trisiloxane end group) and one that supports the formation of a SmA phase (e.g., chloro-terminated side-chain).[154]

2.5 The new design of ferroelectric mixtures with bulky terminal groups for bookshelf geometry:

A series of compounds were synthesised with a trimethylsilyl or a tertiarybutyl group unit as a bulky terminal group, separated from the core by a short chain e.g., dimethylene, and the other terminal chain being either heptyl or octyloxy. These compounds were synthesised using low temperature lithiations and palladium-catalysed cross-coupling reactions.

The bulky terminal chains containing liquid crystal materials exhibit strong smectic phase stability, mainly smectic C along with a limited temperature range of nematic phase. In most cases, the upper limit of SmC phase is higher than comparable analogues with conventional unbranched terminal chains. This high smectic C phase stability results from a phase separation effect due to the incompatibility of the conventional unbranched terminal chain and the spherical bulky group, hence implying that the smectic 'layers' are well defined and such definition of the layers bodes well for bookshelf geometry in FLC mixtures.[158]

The ortho difluoroterphenyl compounds are one of the best host materials for FLC mixtures. Both alkyl- alkyl and alkyl-alkoxy analogues support a wide temperature range SmC phase, low melting points and the dialkyl analogues confer low viscosity. These materials also show an optical anisotropy suitable for small cell spacings with high resistivity.[155-157]

Difluoroterphenyl materials, were prepared in which the core unit has been retained, but one of the terminal chains was substituted with a short, bulky unit. A tertiary butyl group and the slightly larger trimethylsilyl group were located very close to the terphenyl core. These two bulky units were used as terminal chains in order to affect the maximum influence on the molecular properties. It is expected that the bulky terminal chain will be incompatible with the conventional unbranched terminal chain, causing phase separation, thus making the smectic layers more distinct, less inter-dependent and be conducive towards a bookshelf alignment. [155-157]

All the possible ortho-difluoroterphenyl cores (1,2 and 3) were prepared, in combination with the two conventional terminal chains, heptyl (b), octyloxy (a) and the two bulky terminal units of trimethylsilyl (Si) and tertiarybutyl (C). Such combinations provided a total of twelve novel liquid crystals as shown in Figure 49 and enabled a comprehensive investigation of melting points, transition temperatures and mesophase morphology in comparison with known analogues with conventional terminal chains. [155-157]
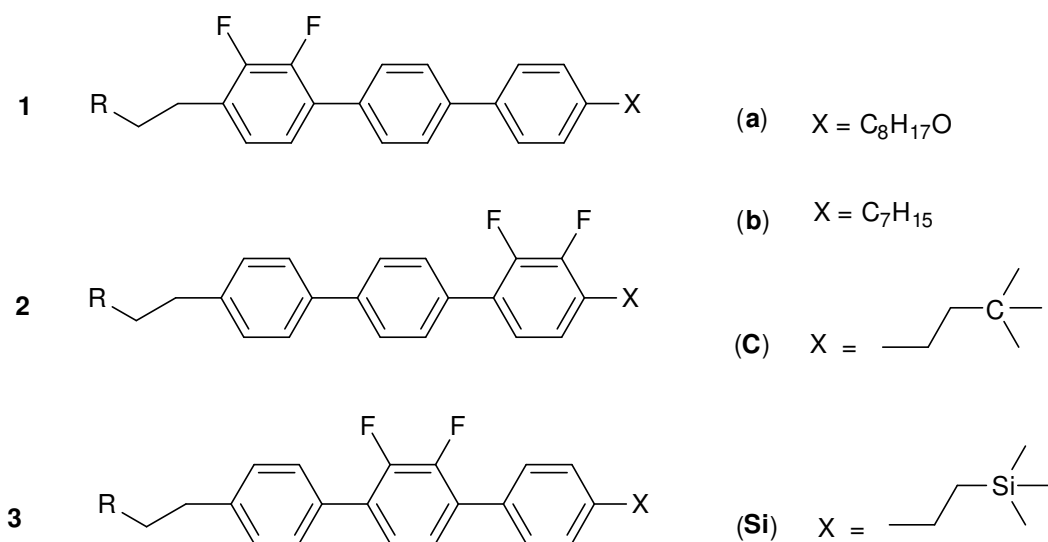
Figure **49**: *The general molecular structures of the targeted novel materials.*

Table 7. The transition temperatures of those compounds with the fluoro substituents in the end ring containing the bulky terminal unit and known compounds for comparison.[158]

63
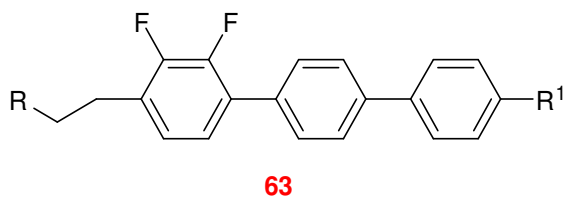
Compound			Transition temperatures/ºC								
No	R	R^1	C		SmC		SmA		N		I
1aC	**Me₃C**	a	●	95.0	●	156.0	●	----	●	-----	●
1bC	**Me₃C**	b	●	86.0	●	125.0	●	129.6	●	-----	●
1aSi	**Me₃Si**	a	●	81.0	●	141.5	●	----	●	-----	●
1bSi	**Me₃Si**	b	●	57.5	●	106.1	●	119.5	●	-----	●
1ak	**C₃H₇**	a	●	89.0	●	155.5	●	165.0	●	166.0	●
1bk	**C₃H₇**	b	●	65.5	●	118.5	●	135.0	●	137.0	●

a = C$_8$H$_{17}$O, b = C$_7$H$_{15}$.

All alkyl chains are shown in the above table are unbranched (Except where indicated).

Table 8. The transition temperatures of those compounds with the fluoro substituents in the end ring containing the linear terminal unit and known compounds for comparison.[158]

64
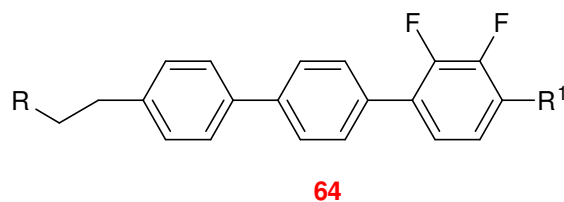
Compound			Transition temperatures/°C										
No	R	R^1	C		SmC		SmA		N		I		
2aC	Me₃C	a	●	81.0	●	131.0	●	----	●	-----	●		
2bC	Me₃C	b	●	71.0	●	101.0	●	----	●	-----	●		
2aSi	Me₃Si	a	●	78.8	●	118.6	●	----	●	-----	●		
2bSi	Me₃Si	b	●	66.7	●	78.9	●	----	●	-----	●		
2ak	C₃H₇	a	●	93.5	●	144.0	●	148.0	●	159.0	●		
2bk	C₃H₇	b	●	56.0	●	105.5	●	131.0	●	136.0	●		

a = C$_8$H$_{17}$O, b = C$_7$H$_{15}$.

All alkyl chains are shown in the above table are unbranched (Except where indicated).

Table 9. The transition temperatures of those compounds with the fluoro substituents in the centre ring, and known compounds for comparison.[158]

65
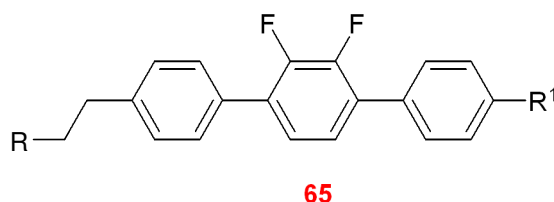
Compound			Transition temperatures/°C									
No	R	R^1	C		SmC		SmA		N		I	
3aC	Me₃C	a	●	89.0	●	106.9	●	----	●	14.4	●	
3bC	Me₃C	b	●	60.0	●	76.0	●	----	●	77.7	●	
3aSi	Me₃Si	a	●	56.1	●	101.9	●	----	●	-----	●	
3bSi	Me₃Si	b	●	58.9	●	61.7	●	----	●	-----	●	
3ak	C₃H₇	a	●	48.5	●	95.0	●	----	●	141.5	●	
3bk	C₃H₇	b	●	36.5	●	24.0	●	----	●	111.5	●	

Here is a = C$_8$H$_{17}$O, b = C$_7$H$_{15}$.

All alkyl chains are shown in the above table are unbranched (Except where indicated).

According to the above data, it was concluded that the introduction of bulky, short terminal groups into difluoroterphenyl core compounds generated a considerable change to mesomorphic properties when compared with the parent materials possessing conventional unbranched terminal chains. The introduction of the short, bulky terminal units greatly improved the stability of the SmC phase and since it is the class of compound which shows by far the lowest viscosity, so this class of novel materials may be good candidates to formulate FLC mixtures.[158]

3.0 Results and discussion:

3.1 Project Outline: 1 Siloxane bookshelf materials

The literature review demonstrated the success of a variety of bulky end groups in supporting high tilt SmC phases over a wide temperature range and sometimes with a low m.p. Some of the examples synthesised exhibit de Vries behaviour which can lead to low layer shrinkage in the SmC* phase and thus, the ideal bookshelf alignment. Few examples such as CDRR8, self rectifying alignment materials as well as bookshelf geometry materials were shown in Figure 46. Some structure activity relationships from this approach area fairly clear but the molecular design required to produce self-rectifying behaviour is not apparent at this stage.

The proposal is to match approximately, the dimension of an aromatic mesogenic core with a bulky silane in the terminal chain: Support for this approach arises from previous work on siloxane compounds such as the fluoroesters (CDDR8 and CDRR3, Figure50). This molecule consists of a bulky end group from the siloxane and a branched chiral chain at the opposite end. One explanation is that the large cross-sectional area of the end groups prevents curvature in the layers and supports bookshelf geometry. A direct I – SmC* transition and a lack of interdigitation gives high tilt, smaller variation of tilt angle with temperature and the little or no apparent detectable SmA* phase, reduces layer shrinkage. It is unusual that a compound with a direct I-SmC* transition has such good alignment because typically, an I-N*-SmA*-SmC* sequence is required to set up a stable layered geometry across the cell.
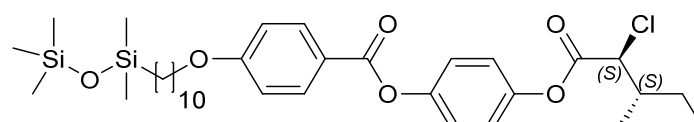
Crys 14.8 SmC* 48.7 °C Iso

CDRR3
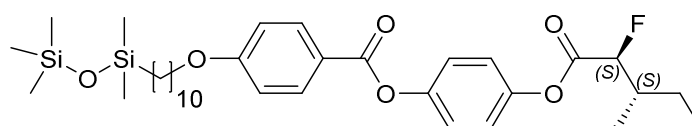
Smc* 59.4 °C Iso (mp could not be determined by DSC)

CDRR8

Figure **50:** *Self-rectifying materials for LCOS Devices.*

These siloxanes with a halogenated alkyl ester as end-groups, an aromatic ester as mesogenic core were not easy to synthesise and in particular, not amenable to scale-up. In addition, the central ester group was unstable. The aim was to follow what we thought were key structural features but to make a stable compound with a wide SmC* phase and that could be readily synthesised and purified without course to repeated column chromatography or preparative HPLC.

The difluoroterphenyl core was chosen as it has these characteristics and is proven by its use in large area displays over several years. Siloxane was replaced with silane *i.e.* oxygen replaced by methylene to give a chemically more stable bulky group. It is arguable whether siloxanes are unstable or whether impurities lead to their loss of performance in devices over time, but in any case, the silane provides a stable substitute, although with a different polarity. The targets are achiral, with the aim of ultimately formulating stable, high tilt, bookshelf aligned, wide temperature range SmC* phase achiral host mixtures. Addition of novel and known chiral dopants would generate ferroelectric behaviour. It is likely that not of the all desirable properties would be achieved, but inroads into some should be a realistic target.

The first targets were disilanes, closely analogous to the pentamethyldisiloxanes (**20**) used in previous materials but linked to a difluoroterphenyl core. These materials were synthesised as outlined in Scheme 1.

20

i)   a = Mg

ii) b = 0 ºC, THF

iii) c = K$_2$CO$_3$, butanone

iv) d = Karstedt's catalyst, toluene

v) e = BuLi, THF, -78 ºC, B(OMe)$_3$, HClaq.

vi) f = UHP, 65-70 ºC

vii) g = AlCl$_3$, DCM
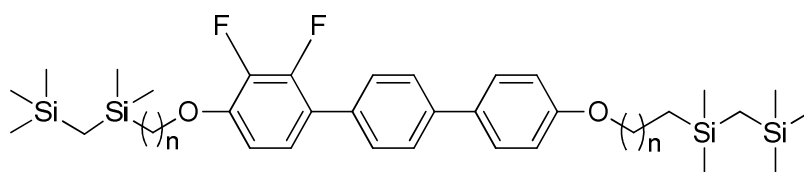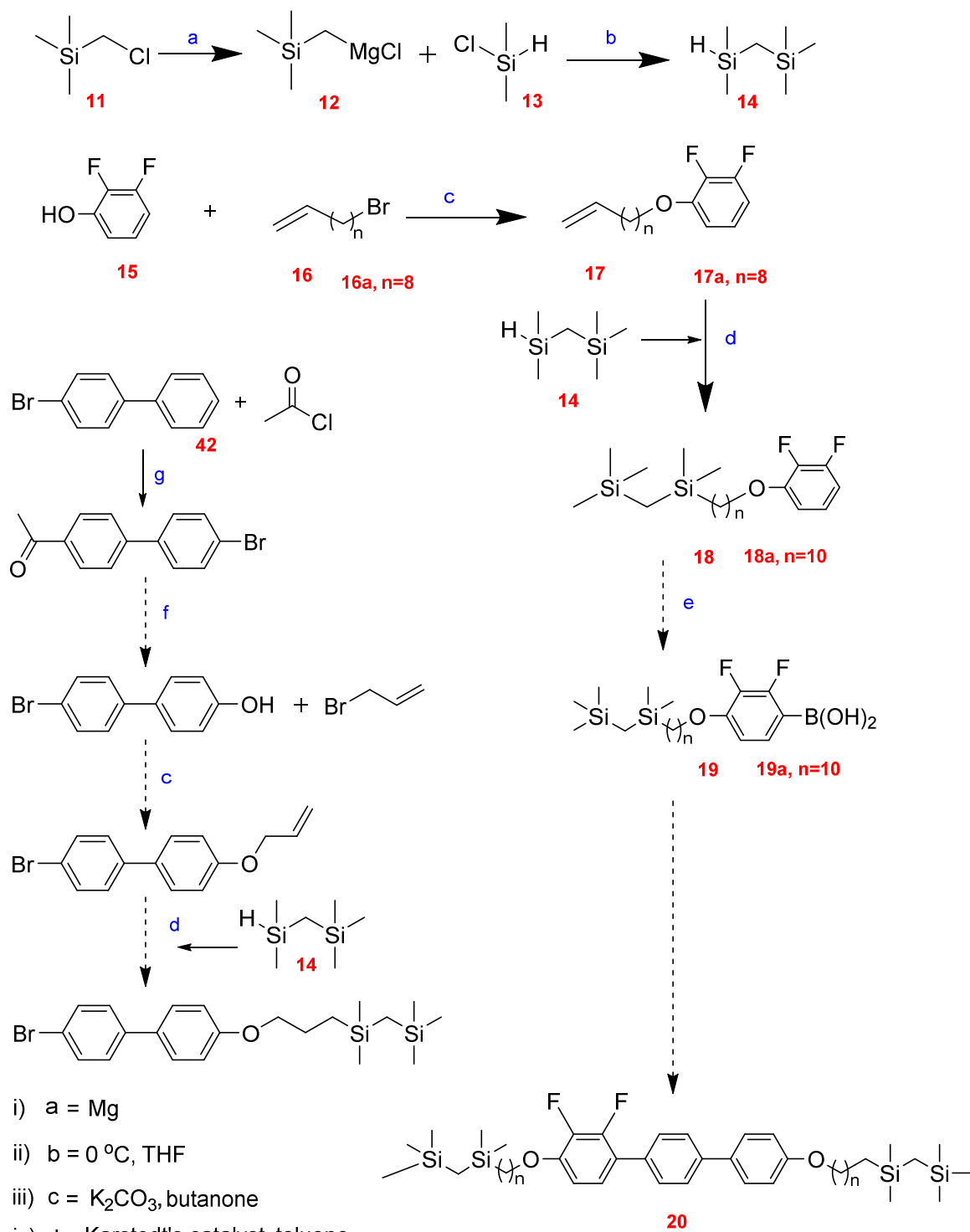
Scheme 1

3.2 Attempted synthesis of 4'-bromo-(1,1'-biphenyl)-4-ol:

4'-Bromo-(1,1'-biphenyl)-4-ol was a key intermediate in Scheme 1 and other schemes but surprisingly for such a simple structure it is very expensive and not suitable for preparing multi-gram quantities of final products. It seemed worthwhile to find a practical synthetic route that was economic and amenable to scale-up. The route began with 4'-bromo-1,1'-biphenyl.

The route involved conventional chemistry, beginning with a Friedel Crafts acylation (Step g) followed by a Baeyer-Villiger oxidation. The literature suggests urea hydrogen peroxide as a cheaper and potentially safer alternative to *m*-chloroperbenzoic acid, which would be better for scale up. We tried to synthesise urea hydrogen peroxide (UHP) by heating urea and hydrogen peroxide at reflux, but didn't get pure urea. Commercially available UHP and the ketone were heated with no solvent as a mix at 60-120 ℃. No product was formed and only starting material was recovered. There was little literature information to go on for the experimental details; perhaps the higher melting point of bromobiphenyl compared to those used in the literature was a major factor. At this point, other issues in the synthesis of these targets led us to halt development of this route.

The pentamethyl disilane **14** was prepared by a published route in which chloromethyltrimethyl silane **11** was converted to a Grignard **12** and reacted in situ with chlorodimethylsilane **13** and purified by distillation. The silane **14** was attached to the alkenyloxy intermediate **17a** *via* Karstedt's catalysed hydrosilylation. A problem arose in the last step when making the difluorophenylboronic acid **19** by low temperature lithiation of compound **18** followed by reaction of the lithium salt with trimethyl borate. The majority of the product was a liquid and showed no aromatic peaks in the ^{1}H NMR spectrum.

The bottom fraction of product was white solid and appeared to contain something resembling a boronic acid according to the ^{1}H NMR spectrum, but the subsequent coupling reaction was not a success. This latter problem would be hard to circumvent without a route which involved hydrosilylation in the final step. It was decided to prepare simpler target bulky end groups with silanes that were more straightforward to prepare. Since this early work, Lemieux has synthesised phenylpyrimidines with terminal disilanes.

Several explanations are possible, one being that the n-BuLi had deteriorated or addition of trimethylborate was too soon after the addition of n-BuLi. The latter is unlikely. Another explanation is that n-BuLi deprotonated the compound **18a** between the two silyl groups

instead of *ortho* to the aromatic difluoro substituents. This would explain the hard to analyse ^{1}H NMR spectra obtained. Silicon stabilises a negative charge on a deprotonated methylene group α to silicon but this is not normally compete with deprotonation of a proton *ortho* to an aromatic fluoro-subsituent. However, in the case of a 1,3 disilyl system, the doubly activated methylene group may be more reactive than the aromatic proton *ortho* to a fluoro-substituent.

3.3 Proposal for new silane materials:

The simpler proposal was to match the size and cross sectional area of a fluorinated mesogenic core with that of a butyldimethylsilyl terminal group. Bulky end groups prevent curvature in the layers. Lack of interdigitation gives high tilt, smaller variation of tilt angle with temperature and little or no SmA phase reduces layer shrinkage.
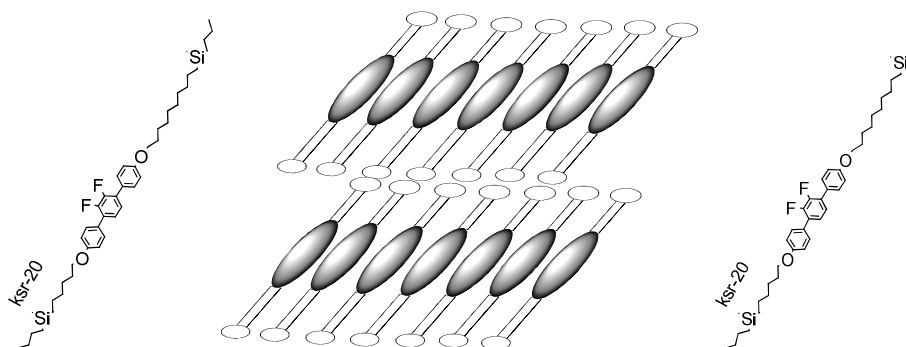
Figure **51:** *Layer formation of bulky end group materials.*

A typical target molecule **30** has a butyldimethylsilyl end-group which is to easy to synthesise and perhaps more suitable for scale-up than siloxanes or the disilanes. The bulky silane group should support tilted smectic phase and suppress nematic and orthogonal smectic phases; in a similar manner to that shown for siloxanes. Synthesis of the simple silanes was straightforward (Scheme 2) following Karstedt's catalytic hydrosilylation of an alkene with commercially available butyldimethylsilane **24**.

21a, n= 2
21b, n= 3
21c, n= 4
21d, n= 8

n=2,3,4,8

23a, n= 2
23b, n= 3
23c, n= 4
23d n= 8

25a, n= 2
25b, n= 3
25c, n= 4
25d, n= 8

28a, n= 2
28b, n= 3
28c, n= 4
28d, n= 8

25a, n= 2
25b, n= 3
25c, n= 4
25d, n= 8

29a, n= 2
29b, n= 3
29c, n= 4
29d, n= 8

30a, m= 8 n= 4
30b, m= 8 n= 2
30c, m= 4 n= 2
30d, m= 8 n= 8
30e, m= 8 n= 3

a = K_2CO_3, butanone, reflux,
b = toluene, Karstedt"s catalyst
c = BuLi, THF, -70 °C, $B(OMe)_3$, HCl
d = 1,2-dimethoxyethane, $Pd(PPh_3)_4$,
    2M Na_2CO_3.

Scheme-2

Scheme-3

a = K_2CO_3, butanone, reflux

b = toluene, Karstedt's catalyst

c = 1,2-dimethoxyethane, $Pd(PPh_3)_4$,
    2M Na_2CO_3.

31

21

21c, n= 4
21e, n= 5
21f, n= 6

32

32a n= 4
32b n= 5
32c n= 6

24

33

33a n= 4
33b n= 5
33c n= 6

29

29a, m= 8
29b, m= 4

34

34a, m= 8   n= 4
34b, m= 8   n= 5
34c, m= 8   n= 6
34d, m= 4   n= 4
34e, m= 4   n= 5
34f, m= 4   n= 6

36

25

25a, n = 2
25d, n = 8

a

37

37a, n = 2
37b, n = 8

i) a = 1,2-dimethoxyethane, Pd(PPh$_3$)$_4$,
2M Na$_2$CO$_3$.

Scheme-4

38
DA 39

33b, n = 5

39

39, n = 5

i) a = 1,2-dimethoxyethane, Pd(PPh$_3$)$_4$,
   2M Na$_2$CO$_3$.

Scheme-5

40

40a, m = 8
40b, m = 6

33b, n = 5

41

41a, m = 8, n = 5
41b, m = 6, n = 5

i) a = 1,2-dimethoxyethane, $Pd(PPh_3)_4$,
2M Na_2CO_3.

Scheme-6

Scheme 2 was planned in order to prepare difluoroterphenyls with a difluorophenyl ring in the middle and butyldimethylsilane groups on both ends. 4-Bromophenol was reacted with a ω-bromoalkenes and the product was hydosilylated with butyldimethylsilane to produce the 4-bromoaryl intermediates **25**. These liquid intermediates were coupled to 2,3-difluoropehnylboronic **27** acid under standard Suzuki Miyaura conditions using aqueous sodium carbonate, 1,2-dimethoxyethane and tetrakistriphenylphospine palladium as the catalyst. There are a wide variety of alternative conditions for this reaction and some may give higher yields, but this method is reliable and the catalyst can be prepared in multigram quantity and kept refridgerated for many months without substantial deterioration. Adding the silane **24** to the double bond prior to coupling is more efficient in yield terms, but more importantly, the double bond migrates to the internal position under Suzuki conditions. The terminal alkene presumably forms a π-bond to Pd, rearranges to a σ-complex and then to the π-complex with the double bond now in the more stable internal position. This was observed fromm the alkenic signals of the ^{1}H NMR spectrum. A similar rearrangement occurred while purifying compound **23d** in the first step of Scheme 2. Purification by high vacuum distillation was carried out. ^{1}H NMR showed the major alkene isomer was the

thermodynamically more stable internal double bond between C_8 and C_9. The integration values for the terminal double bond to the external double bond at 5.42 ppm in a ratio of 1:3.46. The ratio prior to distillation was 1:0.0084; presumably the high temperature with or without the aid of acid catalysis caused the double bond to shift.

Following this result, this and similar products were simply purified by filtration through silica gel and drying using an oil pump to reduce the chance of thermal rearrangement of the double bond.

Scheme 3 was devised to prepare analagous trifluoroterphenyl. The only difference was to employ 4-bromo-3-fluorophenol **31** to introduce an inner fluoro-substituent on an end ring. The conventional trifluoroterphenyl materials have lower mellting points in comparison to the difluoro-analogues. This often makes purification difficult as crystallistion requires cooling and the product comes out of solution in a liquid crystal-rather than a crystal phase. The proved to be the case for several of the materials and repeated column chromatography was requried in order to reach a suitable level of purity and this led to considerable loss of mass. Purity was determined by reverse hplc for these final products; ^{1}H or ^{19}F NMR spectroscopy often did not give clear evidence of impurities as aromatic and aliphatic signals overlapped.

Schemes 4, 5 and 6 show the synthetic routes to monofluoroterphenyls. The conventional materials (Figure 42) show a similar reduction in melting point in comparison to terphenyl but have ordered smectic phases in some case and a lower dielectric anisotropy than the difluorterphenyl compounds. In displays, they are have been superceded by the di- and triflruoterpehnyls but the effect on phase behaviour of bulky groups on the terminal chain has received little or no attention as far as we can tell and these compounds deserve to be investigated. The biphenyl boronic acid was available in the laboratory (coutesy of D. Allan) and thus one Suzuki-Miyaura coupling was required to construct the three ring core. Purificationm by chromatography was also quite straight forward and certainly, much easier than for the trifluoroterphenyls. In the following sections mechanisms for the key reactions involved are discussed.

3.4 Mechanism for Karstedt's catalyst reaction:

The intermediate compounds **25**, **33** weres synthesised using butydimethylsilane, a terminal alkene **23**, **32** and Karstedt's catalyst. This reaction has been key to the synthesis of all hydrosilylation reactions.

$$R_3SiH + R'CH=CH_2 \xrightarrow{\text{Pt}} R_3SiCH_2CH_2R'$$

Figure **52:** *Platinum-catalyzed hydrosilylation reaction.*
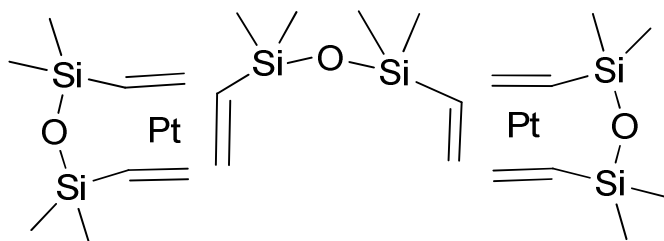
Figure **52:** *Structure of Karstedt's catalyst.*[76]
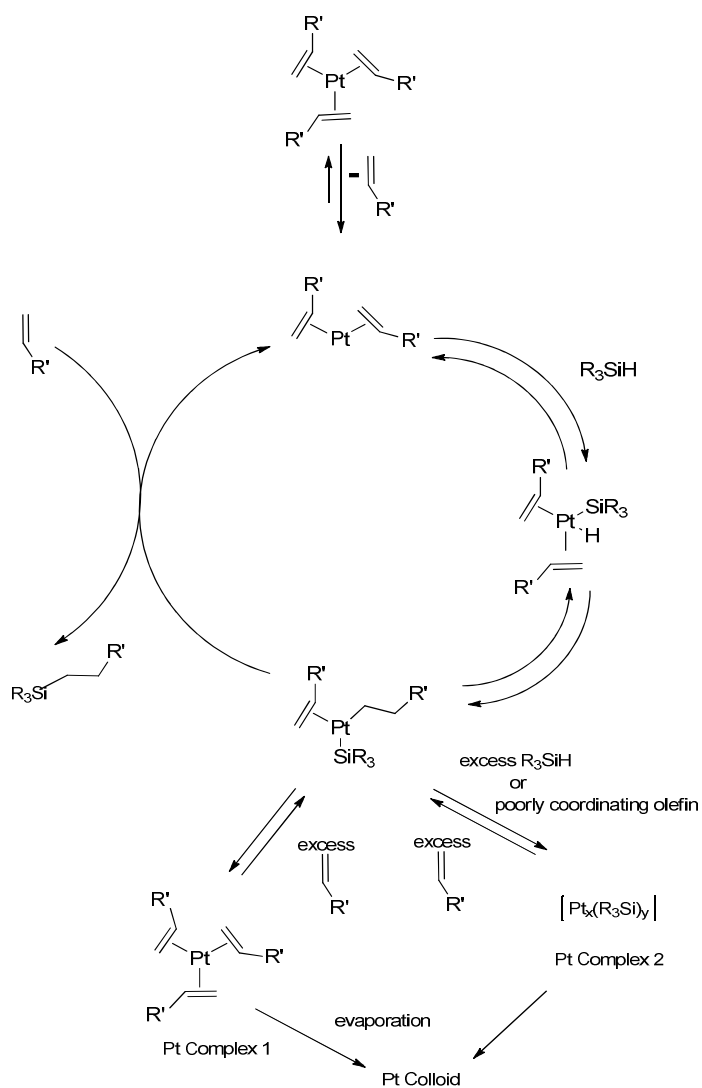
Figure **53:** *Reaction mechanism for hydrosilylation catalyzed by Karstedt's catalyst.*[78]

89

3.4.1 Mechanism discussion:

An overall reaction mechanism[78] is show in Figure 54. During the induction period, the Pt (0) precatalyst undergoes dissociation of the bridging olefin to form a mono nuclear, two-coordinate complex. The oxidative addition of R_3SiH leads to formation of a Pt (II) complex, which is followed by migratory insertion of the olefin into the Pt-H bonds. The reversibility of these steps is supported by the reaction with deuteriosilane in which high levels of deuterium were incorporated into the hydrosilylation products of M^{vinyl} M^{vinyl}. After hydrosilylation of the M^{vinyl} M^{vinyl} ligand, which conclude the induction period, the catalytic cycle proceeds with the added olefin. Certainly we cannot rule out that olefin exchange may also be occurring during the induction period.

Steps in the catalytic cycle are same as those appearing during the induction period. Evidence in support of the catalytic cycle includes kinetic data which support a positive order in hydrosilane and an inverse dependence on olefin concentration. In situ EXAFS analysis indicates that the catalyst is mononuclear and contains Pt-Si and Pt-C bonds regardless of the stoichiometry of the reagents. The absence of vinylsilane products is consistent with migratory insertion of the olefin into the Pt-H bond. The kinetic isotope effect suggests that Si-H bond breaking occurs prior or during the rate-determining step. The determining step is most likely reductive elimination since no Pt-H bonds are observe by NMR or IR spectroscopy.

The platinum end products are dependent on the stoichiometry of the reagents. With high olefin concentration, a Pt(olefin)$_3$ complex is formed. Under conditions of high hydrosilane concentration, a multinuclear Pt cluster is formed with silyl ligands. The products can interconvert by addition of the appropriate reagent probably through the intermediacy of species 4. Conditions that favour formation of Pt complex 2 (absence of oxygen with poor reagents for hydrosilylation, excess hydrosilane, and poorly coordinating olefins) can result in low conversion and olefin bond isomerisation.[78]

The most important aspect for the success of the reaction and its use in these syntheses is the stereospecific addition of the silane on the α-carbon of the alkene. Any significant β-additon would give a byproduct that would be almost impossible to separate by conventional silica chromatography and it would probably co-crystallise with the desired α-addition product.

3.5 Mechanism for Suzuki coupling reaction:

The intermediate compound **28** and final products **30**, **34**, **37** and **39** were synthesised by Suzuki-Miyaura coupling. Compound **28** was prepared with the bromophenoxyalkyldimethylsilane **25** and the difluorophenylboronic acid **27**. This reaction is key to the synthesis of all the fluorinated terphenyls developed over many years and is used by industry. The general Suzuki coupling reaction mechanism, using sodium hydroxide as base, is illustrated in Figure 54.
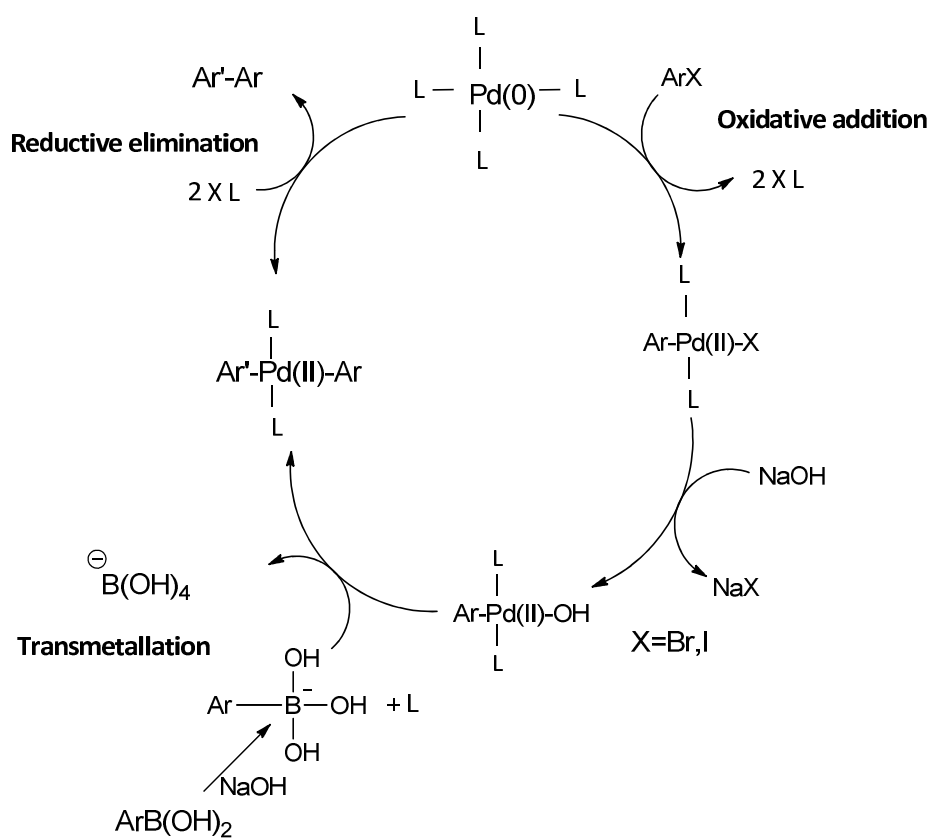
Figure **54**: *Catalytic cycle for Suzuki coupling reaction.*

30
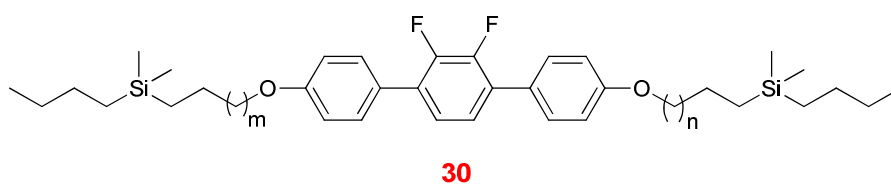
The intermediate step in the synthesis of compound **28** and final step in the synthesis of compounds **30**, **34**, **37** and **39** were *via* the Suzuki coupling reaction. Palladium-catalysed coupling between an aryl bromide and an aryl boronic acid formed a C-C bond and generated the desired biphenyl and terphenyl structure of **28**, **30**, **34**, **37** and **39**. A catalytic cycle of this Suzuki coupling reaction is shown in Figure 55. The cycle is initiated by the oxidative addition of the aryl bromide to the stabilized Pd (0) species. A base RO' is introduced in the coordination sphere of Pd. The transmutation step transferred the Ar' group from the metal boron to the metal palladium to generate an intermediate containing Ar, Ar', B(OH)$_2$, and RO in the coordination sphere of palladium. Two reductive eliminations from this intermediate produced the coupling Ar-Ar' products **28**, **30**, **34**, **37** and **39**.[75, 76]

The butyldimethylsilane moety was characterised by a number of techniques. ^{1}H NMR was carried out in the absence of tetramethylsilane and gave a 6 H singlet at $\delta_H = 0$ for the methyl groups and a 4 H mulitplet at, for example $\delta_H = 0.50$ to 0.63 for the two methylenes adacent to the silicon in compound **37a**. ^{29}Si NMR (I = 1/2) would be an ideal method for identifying the butyldimethylsilane group and for detecting impurities, but for important practical drawbacks The receptivity relative to ^{1}H NMR is 3.68×10^{-4} and the T$_1$ relxation time is long so 10-20 seconds may be required between scans. Many of these disadvantages can be overcome using ^{29}Si DEPT NMR since there is a *J* Si-H coupling to the adjacent methyl and methylene groups. The DEPT sequence give several advantages: enhancement of the signal due to polarisation transfer, removal of the broad signals created by the quartz tube in the probe and most significantly, reduction of the repetition rate which depends on the T$_1$ relaxation times of ^{1}H rather than ^{29}Si, and these times can be shorter by two orders of magnitude. Despite this, the ^{29}Si NMR data could not be obtained for every compound due to the heavy demand on the machines and for much of the research time, the department only had one functioning spectrometer. The difluoroterphenyl silane **28c** gave a singlet for $\delta_{Si} = 2.77$, which is expected, since the reference compound for ^{29}Si is tetramethylsilane ($\delta_{Si} = 0$).

The final products were purified by column chromatography (15% DCM in hexane) followed by recrystallisation (with ethanol-toluene). The purity was confirmed with HPLC and elemental analysis. The mass spectrum showed a single molecular ion peak and no nearby smaller peaks found. Despite this, the phase transitions were broader than would be expected for a very pure compound. One of the final products **30c** was 95.53% pure. For

this compound we used 3 times column chromatography and 4 recrystallisations, but didn't get more than 95.53% purity, Purification by preparative HPLC couldn't be avoided. The final products **28**, **30**, **34**, **37** and **39** were investigated for their liquid crystalline phase behaviour by polarising microscopy and DSC.

3.6 Characterisation

Polarising microscopy of compounds **30a**, **30b**, **30c**, **30d** and **30e** showed only a SmC to Iso transition, but in the compound **30a**, DSC showed a double peak (at 81.5 ºC) at the clearing point when cooling at 0.2 ºC/min. There may be a short range N to SmC phase present, but the transitions are too broad to see clearly anything by microscopy. Broad transitions usually indicate impure compounds, but the HPLC showed 99.6%, eluting after 10.84 min and a total elution time of 40 min. This indicates a high level of purity, and was confirmed by CHN analysis and NMR spectroscopy.

30a
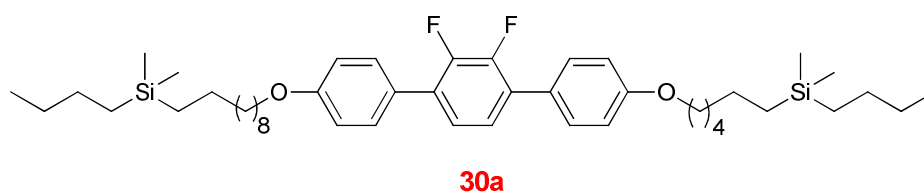
The typical Schlieren texture of one of the final products (**30a**) is shown in Figure 55a.

a) *Polarising microscopy image of the Schlieren texture of the SmC phase for compound **30a** at 81.0 °C, just below the clearing temperature. High birefringence indicated a probable high tilt angle.*
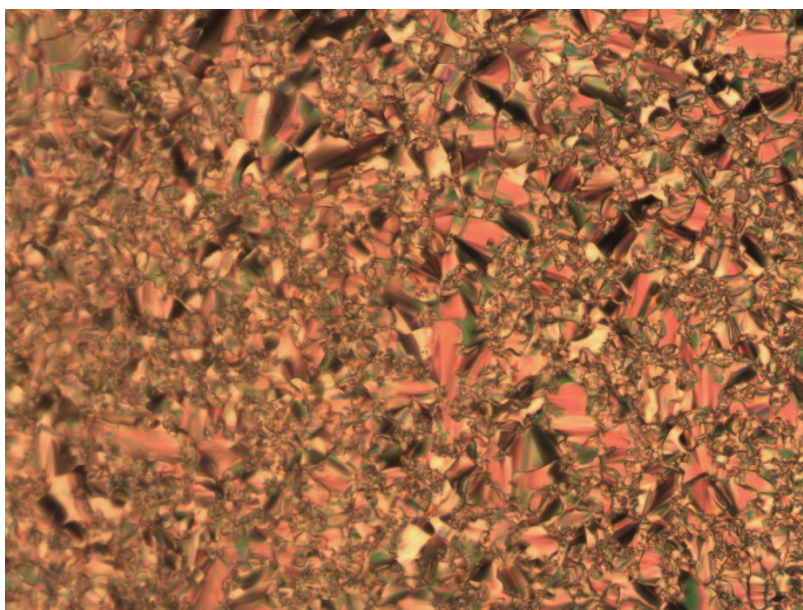
b) *Polarising microscopy image of the Schlieren texture of the SmC phase for compound 34a at 48.0°C.*

Figure **55:** *Polarising microscopy images of the Schlieren texture of the SmC phases of a) 30a, b) 34a.*

3.6.1. Transition temperatures of middle ring difluorobutyldimethylsilanes:

The phase transition temperatures of the all the targeted ferroelectric liquid crystal host materials **20a**, **20b**, **20c**, **20d** and **20e, AA21, AA22** determined by POM are summarised in Table **10**, although the melting temperatures were obtained from DSC thermograms. Compounds **AA21**, **AA22**.[162]

Material	Phase sequence /°C
30c	Heating: C 37.6 SmC 54.7 I (ºC), Sample purity: 95.50% Cooling: I 58.5 SmC 35.0 C (ºC)
AA22	Heating: C 24.6 SmC 73.1 I (ºC)
30b	Heating: C 34.0 SmC 76.2 I (ºC) Cooling: I 78.1 SmC 14.02 C I (ºC)
30e	Heating: C 19.2 SmC 92.5 I (ºC) Cooling: I 89.0 SmC 9.77 C I (ºC)
30a	Heating: C 53.7 SmC 82.0 I (ºC) Cooling: I 81.4 SmC 26.0 C (ºC)
AA21	Heating: C 22.1 SmC 92.2 I (ºC)
30d	Heating: C 70.4 SmC 107.3 I (ºC) Cooling: I 106.6 SmC 53.2 C I (ºC)
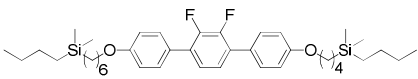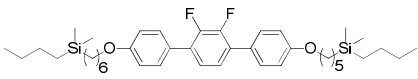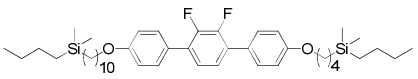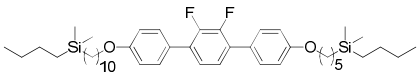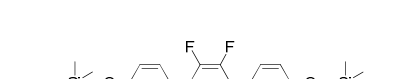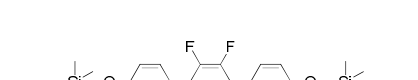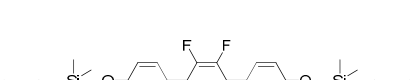
Table 10. The comparison of the transition temperatures of compounds **30c**, **AA22**, **30b**, **30e**, **30a**, **AA21** and **30d**.

30
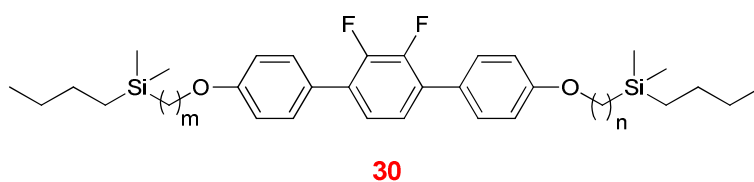
Figure **56**: *Parent structure for the middle ring difluoroterphenylbutyldimethylsilane hostmaterial.*
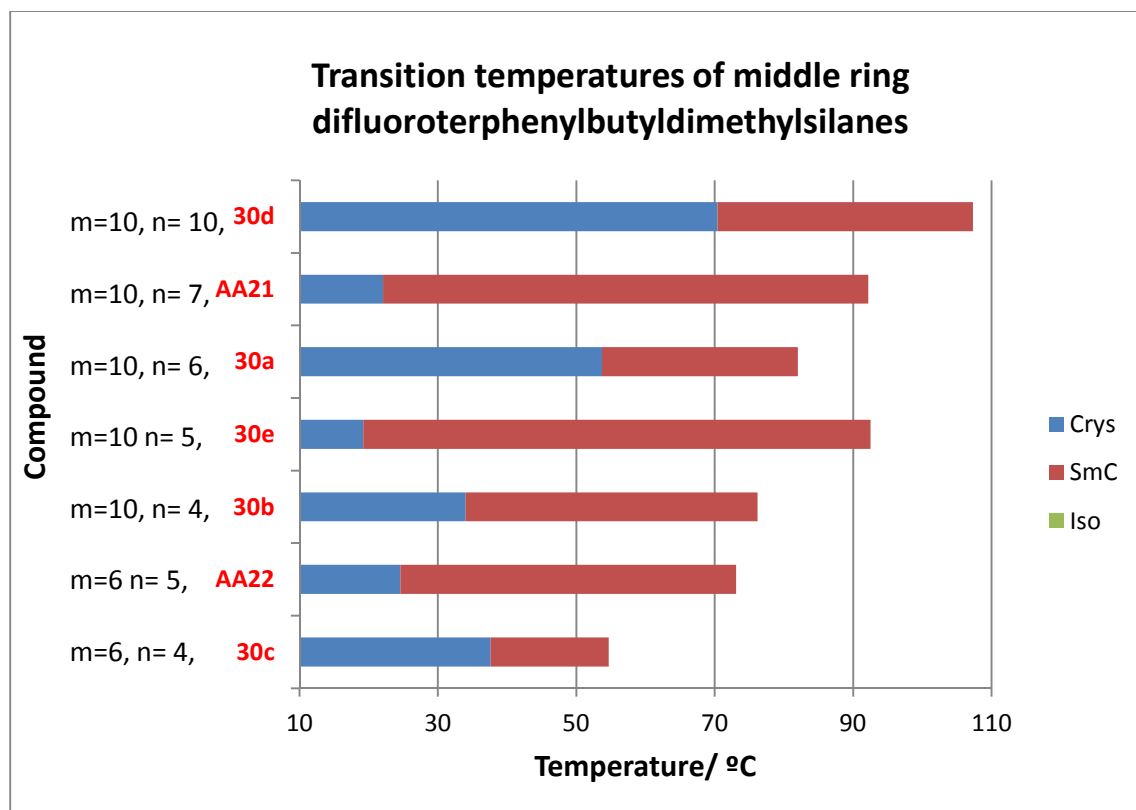
Figure **57**: *Comparison of transition temperatures for the middle ring difluorobutyldimethylsilane host materials.*

The above graph (Figure 58) shows all the difluoroterphenylbutyldimethylsilanes with different side chain length have a Cryst-SmC-Isotropic phase sequence; no nematic phase is present.

Clearing points are proportional to the size of the chain lengths of the compounds. Compound **30d** has long and equal chain lengths and has a high clearing point and therefore a relatively narrow SmC phase temperature, chiefly due to the high melting point. Symmetrical compounds tend to pack better in the crystal and therefore the m.p. is high. When comparing compounds when one chain alters from even to odd and the other chain is the same length,

the melting points decrease and the clearing temperature increases (the so-called odd-even effect); as a result, the SmC phase range increases. This is not an unusual result because when all the atoms in the chain are taken into account, a compound with n being odd has an overall even number of atoms so the conventional odd, even effect is being followed. The compound with a short chain length (**30c** - 95.50% pure) has a low melting point and low SmC-I transition and a longer chain length molecule (**30d**) has a high melting point and wide SmC phase temperature range. The above graph Figure 58 shows, while one side chain length is constant *i.e.,* C_{10} chain and another side chain length is gradually increased, there is an increase in melting point and the SmC-Iso temperature. There is not a huge difference in melting point between **30e** (m = 10, n = 5) and **AA21** (m = 10, n = 7) and the SmC- Iso values are similar, so the effect of alkyl chain length became less as it gets longer. Compound **30e** has the lowest melting point which is around 19 ℃ and a SmC phase temperature range 73.3 ℃. There is a big different in melting point and SmC phase stability between **30c** (m = 6, n = 4) and **30 d** (m = 10, n = 10), that shows the effect of the alkyl chain length. The middle difluoro-compounds are slight broader in the centre of the core and have a transverse dipole in the middle. There are also two transannular twists between a fluorine and proton in adjacent rings leading to a larger dihedral angle. This combination of structural properties favours the nematic phase in simple dialkyl fluoroterphenyls, especially for shorter chain lengths. In these examples, it appears that the effect of the bulky end groups is to strongly support the SmC phase. This effect has been called micro-phase segregation when applied to terminal siloxanes and perfluoroalkyl chains but perhaps it is not always accurate to use this term. These silane bulky end chains may simply support layered phases as the most stable space filling structure, whereas the overlap of rigid cores and interdigitation occurring in a nematic phase would be a higher energy phase structure.

To conclude, the alkyl chain length can increase the clearing point and there is a marked odd-even effect on the m.p. This butylsilane bulky end group strongly supports the SmC phase and completely suppresses the N and SmA phase.

3.6.2 Transition temperatures of Trifluoroterphenylbutyldimethyl silanes (34):

The phase transition temperatures of the all the targeted ferroelectric liquid crystal host materials **34d, 34e, 34f, 34a, 34b** and **34c** determined by POM are summarised in Table 11, although the melting temperatures were obtained from DSC thermograms.
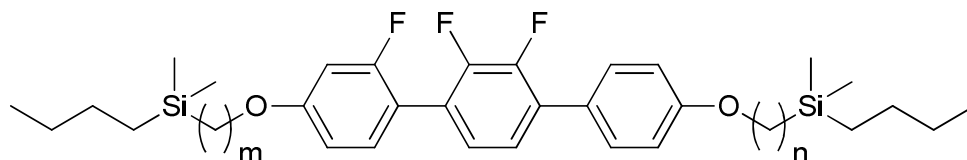
Figure **58:** *The parent structure of trifluoro terphenylbutyldimethylsilane.*

Table 11. Transition temperatures for Trifluoroterphenylbutyldimethyl silanes on cooling: (**34a**, **34b**, **34c**, **34d**, **34e** and **34f**).

Compound	Chain length	C SmC	I
34a	m=6, n=10	7.7	48.3
34b	m=7, n=10	-20	58.4
34c	m=8, n=10	27.0	55.0
34d	m=6, n=6	-4.6	33.0
34e	m=7, n=6	-20	43.5
34f	m=8, n=6	2.3	41.1
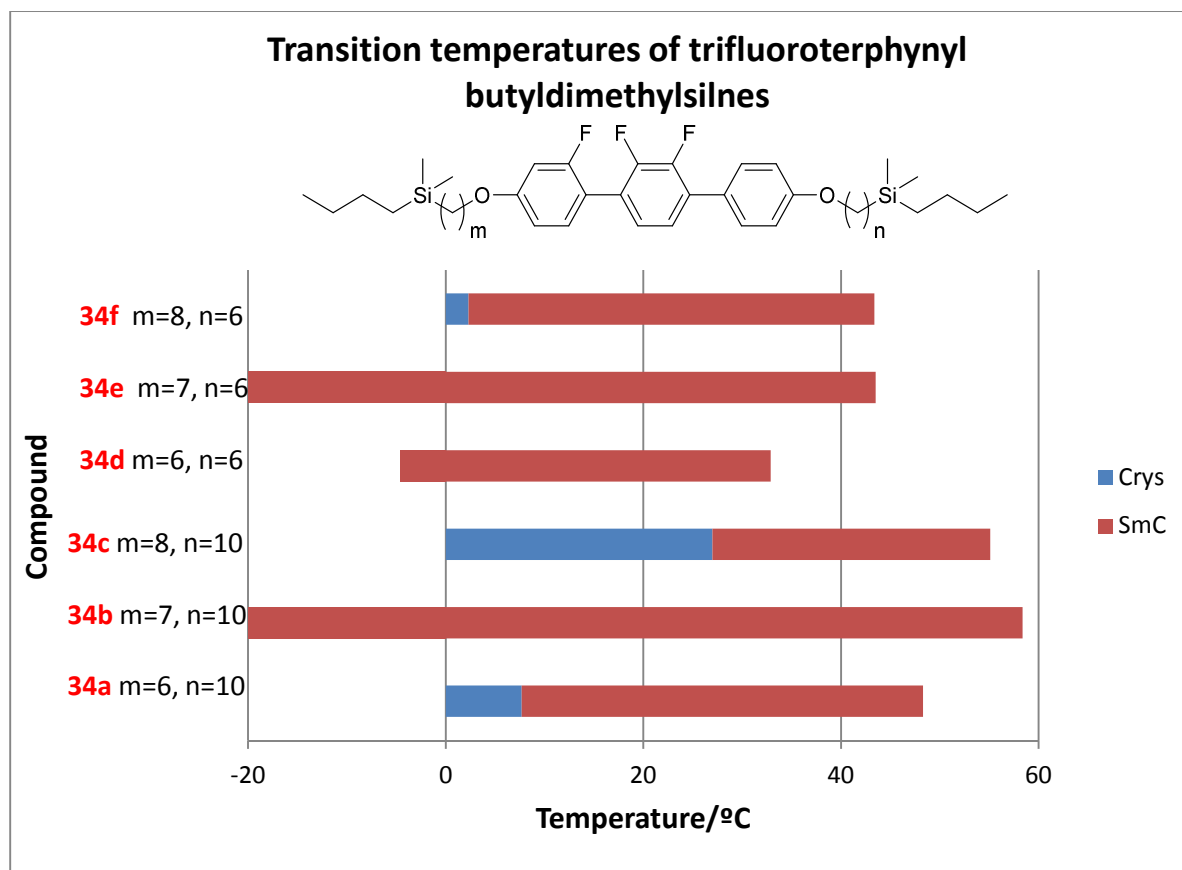
Figure 59: *Comparison of transition temperatures for the trifluoroterphenyl butyldimethylsilane host materials.*

The above graph, Figure 60, shows all the trifluoroterphenylbutyldimethylsilanes with different side chain length show a Cryst-SmC-Isotropic phase sequence; no nematic or SmA phase is present.

In comparison to the difluoroterphenyl analogues (Figure 57, Table 10) melting points and clearing points are reduced. For example, terphenyl **AA21** has transitions of Crys 22.1 SmC 92.2 °C I and the the trifluoroterphenyl **34b** has transitions of Crys -20 SmC 58.4 °C I; both have 7 and 10 methylene groups between linking oxygen and the silicon. Clearing points are proportional to the size of the chain lengths of the compounds. Compound **34b** has long chain lengths and has a high temperature clearing point and therefore a wide temperature range SmC phase present. The almost symmetrical compound **34c** tend to pack better in the crystal and therefore the m.p. is high. When comparing compounds when one chain alters from even to odd and the other chain is the same length, the melting points decrease and the clearing temperature increases; as a result the SmC phase range increases. This is not an unusual result because when all the atoms in the chain are taken into account, a compound

with in being odd has an overall even number of atoms so the conventional odd, even effect is being followed. The compound with even, short chain length (**34d** - 96.93% pure) has a low melting point and low SmC-I transition and a longer chain length molecule (**34b**) has a low crystallisation point and wide SmC phase temperature range. The above graph shows, while one side chain length is constant *i.e.,* C_{10} chain and another side chain length is gradually increased, there is an increase in melting point and the SmC-Iso temperature. There is not a huge difference in crystallisation point between **34e** (m = 7, n = 6) and **34b** (m = 7, n =10) and both compounds did not crystallised until -20ºC, so the effect of alkyl chain length became less as it gets longer. Compound **34b** has the highest clearing point which is around 58.4ºC and a SmC phase temperature range 78.4 ºC. There is a big difference in melting point and SmC phase stability between **34c** (m = 8, n = 10) and **34b** (m = 7, n = 10), that shows the odd-even effect of the alkyl chain length. The trifluoro-compounds are slight broader in the centre of the core and have a transverse dipole in the middle. There are also two transannular twists between a fluorine and proton in adjacent rings leading to a larger dihedral angle. This combination of structural properties favours the nematic phase in simple dialkyl fluoroterphenyls, especially for shorter chain lengths. In these examples, it appears that the effect of the fluorine and bulky end groups is to strongly support the SmC phase. These silane bulky end chains may simply support layered phases as the most stable space filling structure, whereas the overlap of rigid cores and interdigitation occurring in a nematic phase would be a higher energy phase structure.

To conclude, the alkyl chain length can increase the clearing point and there is a marked odd-even effect on the m.p. This butylsilane bulky end group strongly supports the SmC phase and completely suppresses the N and SmA phase.

When compared to middle ring difluoroterphenylbutyldimethylsilanes, the clearing point of trifluoroterphenylbutyldimethylsilane compounds are reduced significantly and would be unsuitable as FLC host materials unless this figure was increased by other components. However, the melting points are also reduced and several examples required being kept at -20 °C in order to crystallise. This shows the effect of a single fluorine in liquid crystal phase behaviour.

3.6.3 Transition temperatures of middle ring monofluoroterphenylbutyldimethyl silanes:

At this stage, results indicated that the butylsilane group was giving some high tilt SmC material. Electrooptic studies, to be detailed later, were problematic as the lack of the N or SmA phase made alignment very difficult. In addition the reduction in clearing point when silanes at both ends were employed meant that the ultimate SmC* temperature of a formulated FLC mxiture would not be sufficiently wide for a practical material. Thus, a simpler approach of attaching a butylsilane at only one end would be synthetically easier and may improve material properties.

Monofluoroterphenyls were the first of this family to be investigated in the 1980s before being superceded by difluoroterphenyls. However it seemed that a combination of monofluorinated core and a bulky end group would be worth investigating.

The phase transition temperatures for conventional known monofluorinated compounds **50, 51, 52** are provided for comparisonalong side butylsilane analogues **37a, 37b** in Table11. Transition temperatures are determined by POM, although the melting temperatures were obtained from DSC thermograms.[37]
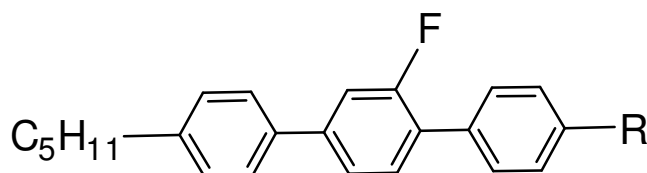
Figure **60**: *The parent structure of middlering monofluoro terphenylbutyldimethylsilane.*

Compound		Transition temperatures/ºC						
	R	C	B	SmI	SmC	SmA	N	I
50	CN	● 82.0	● ----	● ----	● ----	● ----	● 143.0	●
51	C$_5$H$_{11}$	● 51.0	● 62.0	● ----	● ----	● 109	● 136.5	●
52	OC$_8$H$_{17}$	● 40.0	● ----	● 53.5	● 116.5	● 130.0	● 155.0	●
37a	O$(CH_2)_4$Si	● 11.3	● ----	● ----	● 48.0	● 96.5	● ----	●
37b	O$(CH_2)_{10}$Si	● 12.0	● ----	● ----	● 60.0	● 119.4	● ----	●

Table **12:** Transition temperatures for monofluoroterphenyl butyldimethylsilanes on cooling (**50**, **51**, **52**, **37a** and **37b**).

Transition temperatures of middle ring monofluoroterphenyl-butyldimethylsilanes:
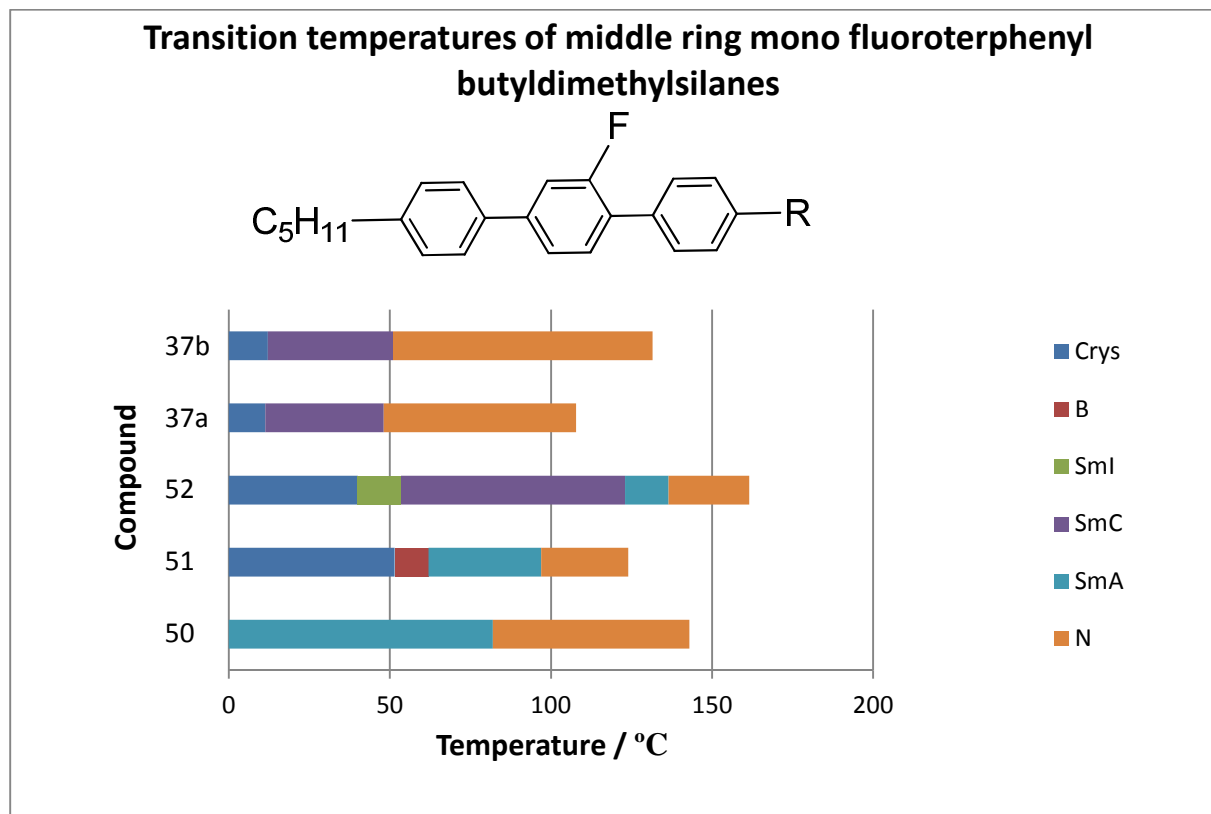
Figure **61**: *Comparison of transition temperatures for the middle ring monofluoroterphenyl butyldimethylsilane host materials.*

Compound **52**, with a conventional octyloxy chains shows ordered smectic phases, including SmI, B, and J phase but does possess a significant SmC temperature in addition to SmA and N phases. The addition of terminal butyldimethylsilane groups suppresses the N phase and have low crystallisation temperatures but the SmC-SmA transition is only around 50 °C, a significant drop from the straight octyloxy chain.

Clearing points are proportional to the size of the chain lengths of the compounds.The symmetrical compound **51** has a short C₅-alkyl chain on both ends and shows a Crys-B-SmA-N-I phase sequence. When one silyl chain increases and the other chain length remains constant *e.g.* pentyl, the crystallisation temperatures decrease very slightly. A general observation is that the bulky end groups suppress nematic phases. It may not be accurate to

state that they support smectic behaviour as the transition from smectic to isotropic is considerable lower than for the octyloxy-molecule **51**. This is not an unusual result because when all the atoms in the chain are taken into account, the butyldimethylsilane gives bulkiness to the one end in the layers so molecules flows easily between the layers, this behaviour of the molecule support smectic behaviour. The compound **37a** with even, short C$_4$- chain with butyl dimethylsilanehas a clearing temperature 96.5ºC and low SmC-I transition and a longer chain length molecule with silane tail **37b** has a low crystallisation point and wide SmC and SmA phase temperature range. There is not a huge difference in crystallisation point between the shorter chain **37a** (butyloxydimethylsilane) and the longer chain **37b** (decyloxydimethyl-silane) which have almost the same crystallisation point in both compounds of around 12.0 ºC, so the effect of alkyl chain length became less in this molecules when bulky silane group present in the end tail. Compound **52** has the highest clearing point which is around 155.0 ºC and an upper SmC phase temperature range of 63 ºC. There is a big difference in melting point and SmC phase stability between **52** (alkoxy end group) and **37b** (alkoxy silane end group), that indicates the bulky silane effect on the phase behaviour. The monofluoro-compounds are slight smaller in the centre of the core, with less transannular twist and a smaller transverse dipole compared to difluoroterphenyls. The weaker dipole may be less supportive of the SmC phase. This combination of structural properties favours the nematic phase in simple middle ring monofluoroterphenyls without bulky groups, especially for shorter chain lengths. In these examples, it appears that the effect of the fluorine and bulky end groups is to strongly support the SmC phase. These silane bulky end chains may simply support layered phases as the most stable space filling structure, whereas the overlap of rigid cores and interdigitation occurring in a nematic phase would be a higher energy phase structure.

To conclude, these bulky end tails decrease the m.p., clearing points and provide low crystallisation temperature. This butyldimethylsilane bulky end group supports the SmC and SmA phases and completely suppresses the N phase in middle ring monofluoro-terphenylsilanes. When compared to trifluoro, middle ring difluoroterphenylbutyldimethyl-silanes, the clearing point of monofluoroterphenylbutyldimethylsilane compounds is much higher.

3.6.4 Transition temperatures of end ring monofluoro terphenylbutyldimethylsilanes:

The middle ring pentylmonofluoroterphenyl silanes had demonstrated that, this simple approach can suppress ordered B phases and support smectic phases, but the upper limit of the SmC phase was a moderate 50 °C. End ring 'inner'monofluoroterphenyls are known to have SmC behaviour so these derivatives were also targetted. The phase transition temperatures from cooling of the all the targeted ferroelectric liquid crystal host materials **39, 41a, 41b** and **53** determined by POM are summarised in Table13, although the crystallisation temperatures were obtained from DSC thermograms.
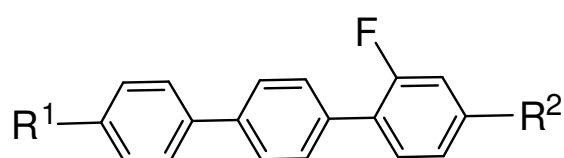
Figure **62**: The parent structure of endring monofluoro terphenylbutyldimethylsilane.

Compound		Transition temperatures/°C								
		C		**J**		**SmC**		**N**		**I**
53	$R^1=C_5H_{11}$, $R^2=OC_8H_{17}$	●	25	●	43.5	●	119	●	158	●
41a	$R^1=C_{10}H_{23}$, $R^2=$	●	75	●	-----	●	-----	●	135.0	●
41b	$R^1=OC_8H_{17}$, $R^2=$	●	87.5	●	-----	●	-----	●	140.6	●
39	$R^1=C_5H_{11}$, $R^2=$	●	56.5	●	-----	●	-----	●	113.5	●

Table **13:** Transition temperatures for endring monofluoroterphenylbutyldimethyl silanes on cooling: (**53**, **41a**, **41b** and **39**).[37]

Transition temperatures for the end ring monofluoro fluoroterphenyl butyldimethyl-silane host materials:
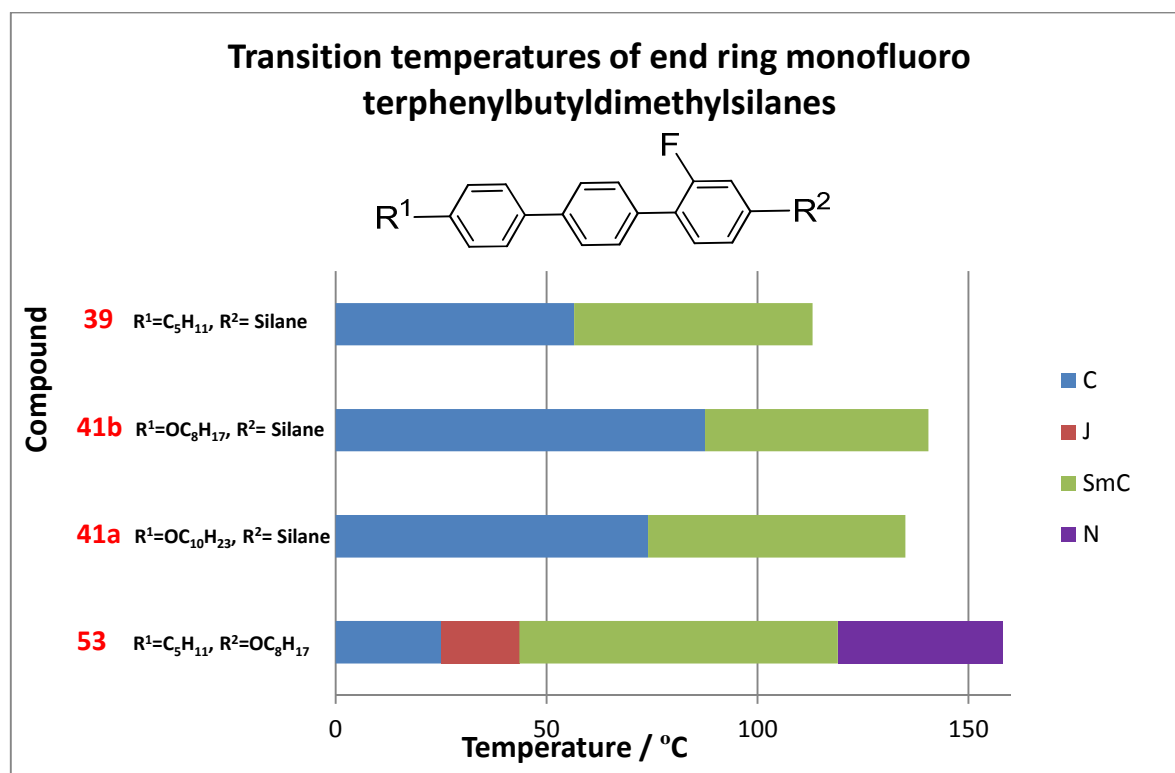
Figure **63:** *The comparison of transition temperatures for the end ring mono fluoroterphenyl butyldimethylsilane host materials*.

The above graph Figure 63 shows, the endring monofluoroterphenylbutyldimethylsilanes with short alkyl chain on the one end and long alkoxy side chain on the other end compound **53** show a different phases over the isotropic-crystal phase transitions including SmC, N and Smectic subphase J on cooling.

Clearing points are proportional to the size of the chain lengths of the compounds. Compound **53** has a long alkoxy chain and has a high clearing point around 158ºC and an N phase. Increasing the butyldimethylsilyl chains on one end and maintaining an n-pentyl chain at the other end, causes the melting points increases. The clearing point temperature decreases with alkyl, alkoxy chains and decreases with butyldimethylsilane tails; as a result the SmC phase range increases. This phenomenon indicates bulky end tail groups support smectic behaviour. The butyldimethylsilane gives bulkiness to the one end in the layers so molecules flows easily between the layers, this behaviour of the molecule, support smectic behaviour. The compound **39** with odd-even, short C_5-alkyl chain and long alkoxysilane on the other endshow a low melting point around 113.5ºC and low SmC-I transition and a longer

chain length molecule with silane end tail **41a, 41b** has a high crystallisation point and wide SmC phase temperature range. The above graph shows, while one side silane chain length is constant *i.e.,* change in another side chain length, size is gradually increased; there is a decrease in melting point and increase in the smectic nature. Compound **53** has the highest clearing point, which is around 158.0 ºC and a SmC phase temperature range 75.5 ºC. The monofluoro-compounds are slight smaller in the centre of the core compared to difluoro, trifluorobutylsilanes so these compounds has high clearing points and low Smectic behaviour than di, trifluorosilane compounds and high clearing points, more smectic behaviour than the middle ring monofluoroterphenyl silanes. This combination of structural properties favours the smectic phase in simple middle ring monofluoroterphenyls without bulky groups, especially for shorter chain lengths. In these examples, it appears that the effect of the fluorine on the end ring and bulky end groups is to strongly support the SmC phase. These silane bulky end chains may simply support layered phases as the most stable space filling structure, whereas the overlap of rigid cores and interdigitation occurring in a nematic phase would be a higher energy phase structure.

To conclude, the alkyl chain length can increase the clearing point and bulky end tails decrease the m.p., clearing points and there is a marked bulky group effect on the m.p. This butylsilane bulky end group, fluorine on the end ring strongly supports the SmC behaviour and completely disappears nematic phase.

When compared to trifluoro, middle ring difluoroterphenylbutyldimethylsilanes, the clearing point of endring monofluoroterphenylbutyldimethylsilane compounds is very high and compared with middle ring monofluoro terphenylbutyldimethylsilanes, lower in m.p., wider in smectic range and it shows the effect of fluorine, bulky end groups in phase behaviour of these materials. A combination of lower melting trifluoroterphenyls with high clearing point mono- and difluoroterphenyls is reasonably promising as a means to a practical low melting point FLC mixture. However, mixtures that were formulated and discussed in the following sections were often governed by the mass of compound available and its purity rather than a compound with the optimum phase transitions.

3.7 Electro-optic studies of the mixtures:

3.7.1. Tilt angles for mixture of 30a and BE8OF2N-(*S*):

The FLC electrooptic properties of the individual component **30a** was examined by mixing with the standard chiral dopant **BE8OF2N** and filling an Instec 5 μm anti-parallel rubbed electrooptic cell in the isotropic phase. Cooling into the SmC* phase was usually carried out with a high frequency square wave applied in order to achieve the best level of alignment although this often required repetition and altering the conditions to optimise alignment. The transition from N* to SmA* phase is considered a key point in setting up the smectic layers across the cell and the cooling rate should be in the 0.2 °C/min region at this point. Electrooptic measurements were made using the integrated Instec automatic liquid crystal tester (ALCT) apparatus, hotstage and software.

The addition of the non-mesogenic dopant can have a marked effect on the transition temperatures. The textures for the 9.9% mixture were hard to analyse as there was very little birefringence to observe. Final transition temperatures and phase identification have still to be confirmed. However, this mixture did showed ferroelectric like switching and the first graph (Figure 64) shows the measured tilt angle over a wide temperature range obtained from rotating the microscope stage until similar levels of darkness were obtained in the two ferrolectric states of the switching cone under crossed polarisers. A low frequency triangular wave field (amplitude 30 V, frequency 1 Hz) was applied. Poor alignment and the difficulty in judging the moment of maximum extinction led to a larger scatter of data than is ideal. More experience of this measurement normally leads to a reduction in the degree of scatter.
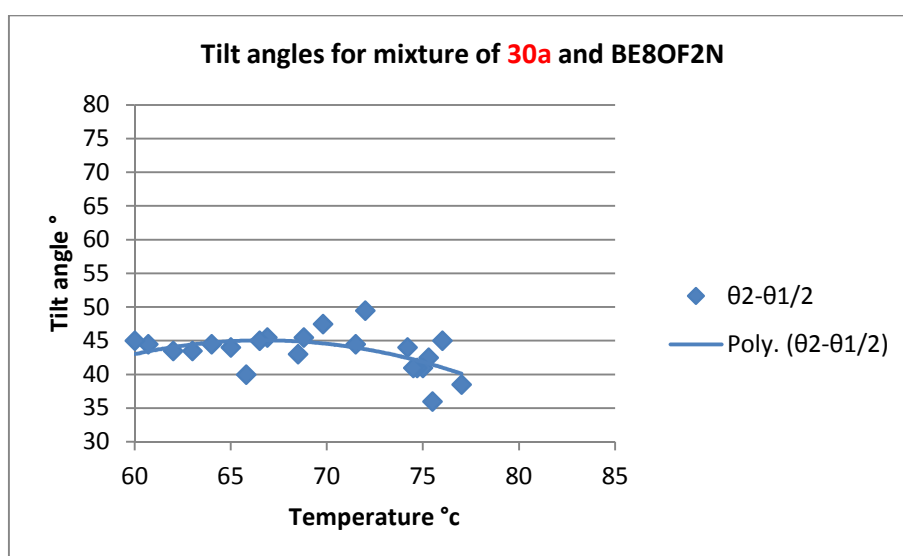
Figure **64:** *Tilt angles for 9.9% mixture of 30a and BE8OF2N.*

Ideal ferroelectric mixtures would have a high SmC tilt (Ideal tilt angle 22.5ºC). Results from siloxanes showed a higher tilt than for simple terminal alkyl chain mesogens. This silane produces a much higher tilt angle than observed for the doped alkyldifluoroterphenyls and the tilt angle remained constant over the temperature range but with a large scatter of data points. The high tilt may be because the bulky silanes and siloxanes prevent interdigitation and allow the molecules tilt more freely. Small angle X-Ray diffraction is required to confirm these tilt angles and perhaps the measurements should be repeated in future studies. The high tilt is useful for particular FLCD modes so these sorts of compounds may be promising in developing very high tilt materials, if good alignment can be achieved. The constant tilt angle is good for alignment and for the optical performance of a display. Tilt angles are not changing over temperatures so the retardation factor will not change and this will give constant contrast over the operating temperature range of a display. Additionally the Ps should not change markedly but the Ps data below does show a significant increase on cooling. Perhaps this is due to the decrease rotation of the molecules on cooling which may increase the average transverse dipole that contributes to Ps.

3.7.2 Ps Values for 9.9% mixture of 30a and BE8OF2N:
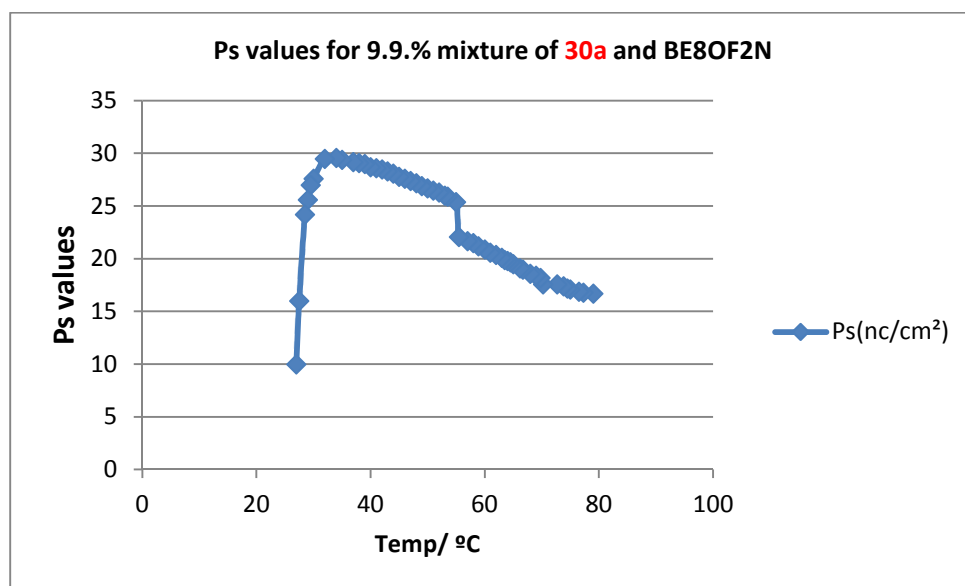
Figure **65:** Ps *values of 9.9% mixture of **30a** and **BE8OF2N**.*

Ps does usually increase as the tilt angle increases, with cooling. In addition molecular motion will decrease on cooling, so one may predict that Ps values would also increase. In the above graph, between 55.5 ºC and 55.0 ºC, there is a step change in Ps values. This may be because of a phase change, for example to an antiferroelectric phase, SmI* or an error that occurred in the experimental set up during the measurement. Both possibilities need checking to confirm the validity of this result. Other mixtures with lower percentages of dopant were prepared, but electrooptics measurements have not been completed yet, however DSC curves were obtained and a peak in the region of the step change was seen. POM showed a textural change at 72 °C but the nature of the transition was not confirmed. Obviously, this is an area that requires careful examination to determine what is happening.

3.8 Phase Diagrams of mixtures:

3.8.1 Phase diagram for mixture of 30a and KC1019:

A key motivation for synthesising the butyldimethylsilanes was to investigate their behaviour when the silanes are combined with conventional fluoroterphenyl liquid crystals orindeed, other silanes. This was in addition to evaluating the individual components and for their potential in more comprehensive mixture formulation. This is because such mixtures are most likely to lead to materials with the desired phase transitions and alignment properties required in an FLC device. The optimum balance of bulky end groups and normal alkyl chains may support SmC phases and maintain a low m.p. Alignment in electrooptic cells is very hard to predict and the number of factors involved, including alignment materials and the conditions employed to achieve alignment require much effort to attain improvements and a greater level of understanding.

The conventional FLC material chosen for the first mixture study was KC1019 which has a relatively low m.p., wide SmC phase temperature range and was available in reasonable quantity to enable several mixtures to be prepared. Compound 30a was selected first, partly for practical reasons, in that there was sufficient quantity and it was of high enough purity for the mixture data to be valid and to allow a number of mixtures to be prepared, still leaving sufficient for later iterations and for electrooptic studies. The first example to be investigated was compound 30a, KC1019 is a high SmC-SmA transition, so it was decided to also mix the same compound with a middle ring difluoroterphenyl KC1020 which is chiefly a nematogen. This would test more severely, how well the bulky end groups support the SmC phase when diluted with normal end chain liquid crystals.

KC1019

Crys 56.0 SmC 105.5 SmA 131.0 N 136.0 °C I

30a
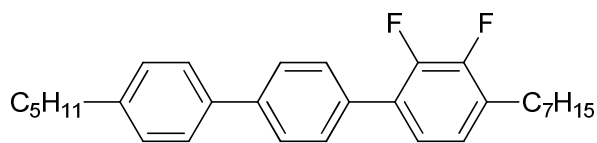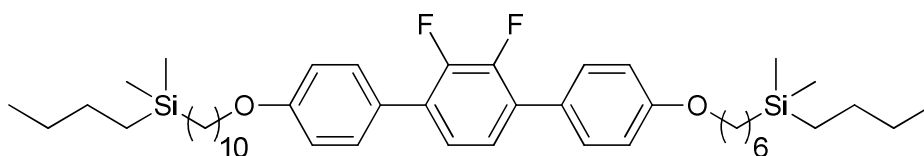
Crys 53.7 SmC 82.0 °C I
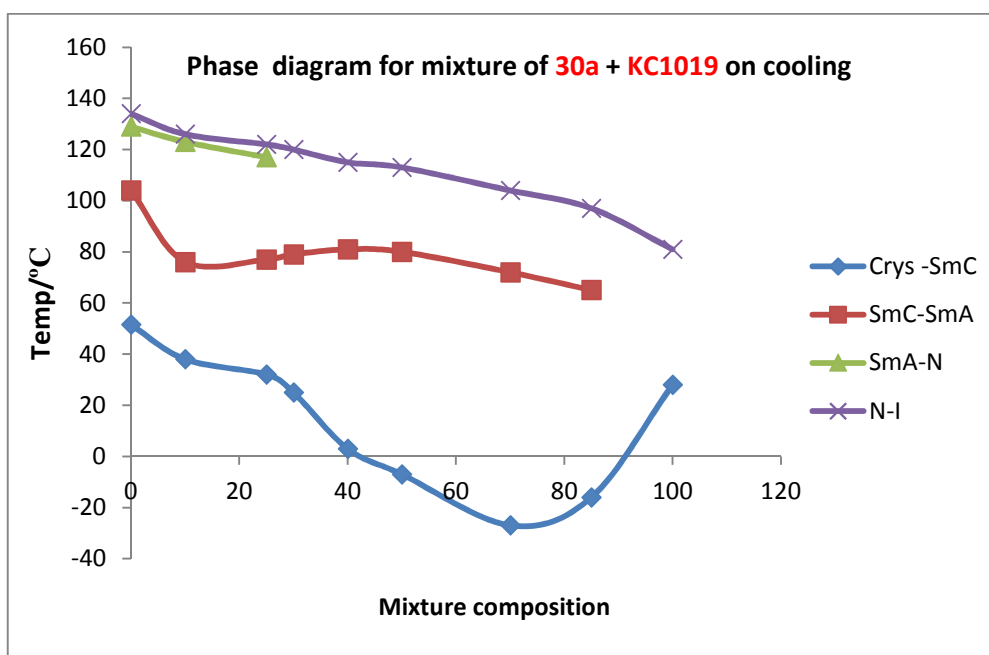
Figure **66**: *Phase diagram of **30a** and **KC1019** mixtures.*

In this mixture investigation, the proportion of silane added 10% to 90% w/w. This was partly on the practical grounds of material availability and on the fact that the SmC phase became dominant by 70% and would almost certainly remain as the only mesophase from

then on. There is a continuous reduction in crystallisation point. Crystallisation is not a thermodynamic value can change with a variety of conditions, but the DSC measurements tend to show a fairly consistant value. The eutectic may be at exactly 70% w/w but the gradient shows no sign that there will be a sudden drop at greater percentages. The phase diagram shows the data obtained *via* POM on cooling for up to a maximum of 90% w/w of the silane **30a**. The cooling data is presented because textures could not easily be identified from the heating data. The above graph shows that while increasing the percentage of silane material **30a** in the mixture, the nematic phase is very soon lost. A nematic phase is considered important to establish alignment in a conventional FLC device, although self rectifying, high tilt materials (CDRR8) are known that possess a direct SmC* - Iso transition. In general the SmC phase becomes dominant as the percentage of silane increase; initially the SmC-SmA phase transition drops for some reason and then increases before being suppressed at 70% between 40% and 90% **30a, 34a, 37a, 41b, 39**. The lowering of the crystallisation temperature and the raising of the SmC-SmA transition temperature leads to a wider temperature range SmC phase overall which is promising for further mixture development. Generally, melting points are moderately high for difluoroterphenyl compounds, but for these binary mixtures, melting points were recorded from the DSC heating curves below 60 ℃. It would not be too ambitious to predict that a reduction in m.p. could not be achieved with further mixture development.

The data for the mixture with the middle ring difluoroterphenyl K1020 are presented below.

3.8.2 Phase diagram for mixtures of compounds 30a and KC1020:

KC1020

Crys 36.5 (SmC 24.0) N 111.5 °C I

30a
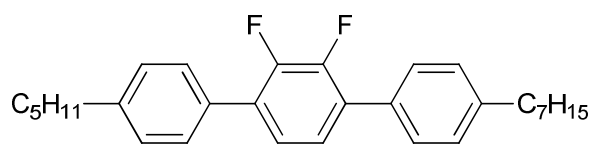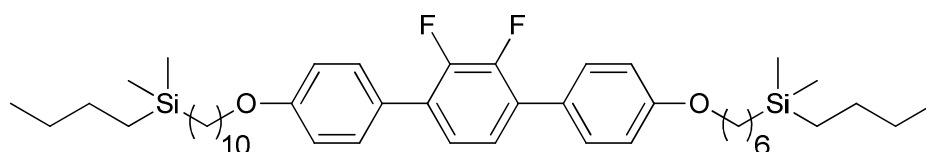
Crys 53.7 SmC 82.0 °C I
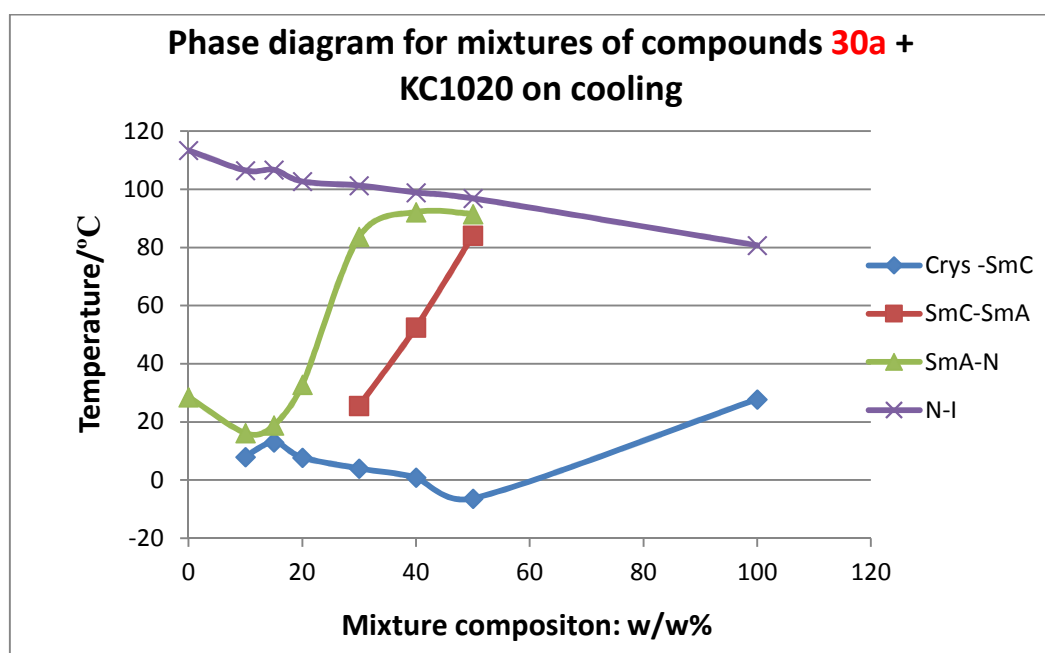
Figure **67:** *Phase diagram of 30a and KC1020 mixtures.*

The phase diagram shows the data obtained *via* POM on cooling for up to a maximum of 50% w/w of the silane **30a** and the 50% mixture data points are then simply connected to the transitions for the pure silane compound. The cooling data is presented because textures

could not easily be identified from the heating data. The main observation is almost the same as for the end ring difluoroterphenyl, and by 50% of silane there is only a short range SmA and N phase. At the same time, the depression in freezing point is around the minimum. This is a promising behaviour if duplicated in an FLC mixture. The short range N and SmA phases would aid alignment and a relatively high tilt would be predicted. Generally, melting points are moderately high for difluoroterphenyl compounds, but for these binary mixtures, melting points, although not shown here, were recorded from the DSC heating curves below 30 °C. The data showing the melting points for this and all 50% mixture are provided in the appendix. It would not be too ambitious to predict that a reduction in m.p. could not be achieved with further mixture development.

Following the support of the SmC phase in the middle ring binary mixtures, it was deemed unnecessary to formulate further mixtures using the end ring compound **KC1019**. All later mixtures used only **KC1020**.

3.8.3. Phase diagram for mixture of the trifluoroterphenyl disilane 34a + KC1020:
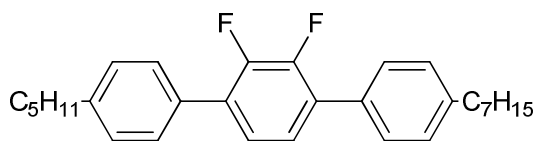
KC1020

Crys 36.5 (SmC 24.0) N 111.5 °C I
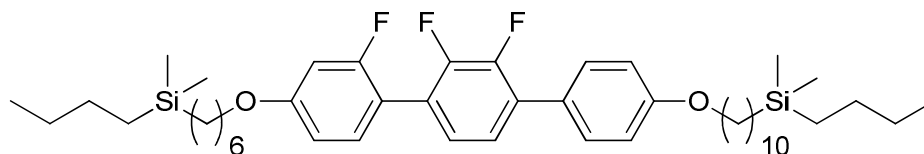
34a

Crys 7.67 SmC 48.3 °C
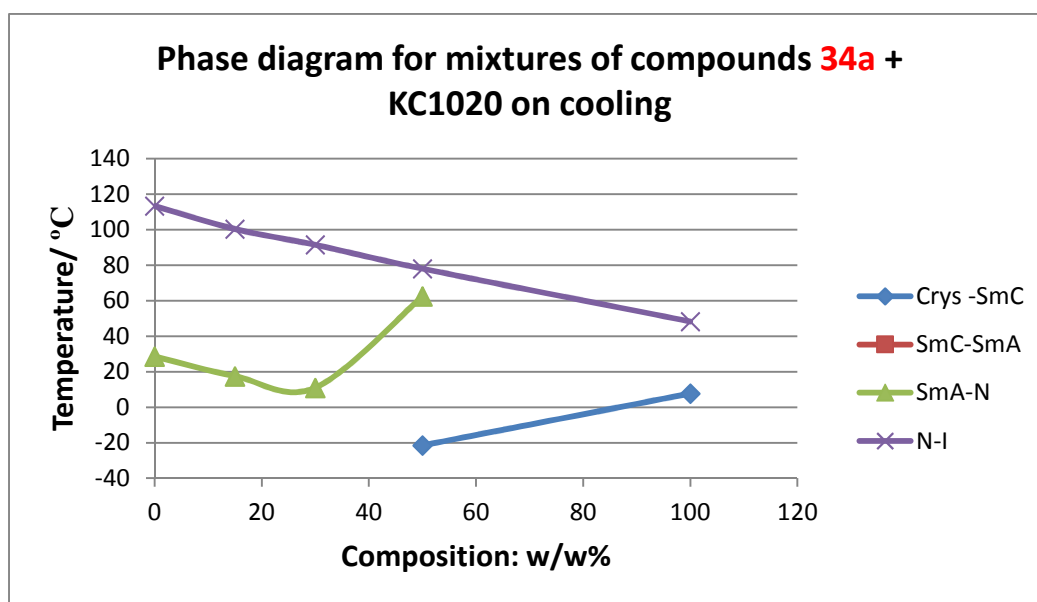
Figure **68:** *Phase diagram of 34a and KC1020 mixtures.*

The phase diagram shows the data obtained *via* POM on cooling for up to a maximum of 50% w/w of the silane **34a**. The trifluoroterphenyl disilane is low melting and with a reasonably high SmC temperature range for these compounds. In this case, the SmC phase is not observed until the 50% mixture and there is a sudden loss of N phase. Further mixtures would need to be formulated to find how the switch from N to SmC occurs. The 50% mixture has a impressively low crystallisation temperature, observed on cooling in the DSC.

3.8.4. Phase diagram for mixture of compounds 37a + KC1020:

KC1020

Crys 36.5 (SmC 24.0) N 111.5 I °C

37a

Crys 11.3 SmC 48.1 SmA 96.5 I °C
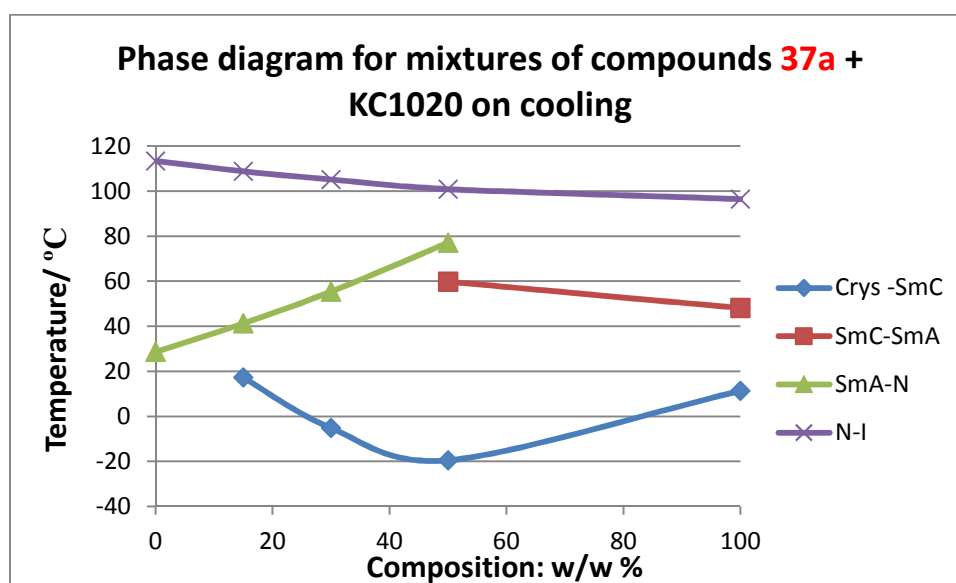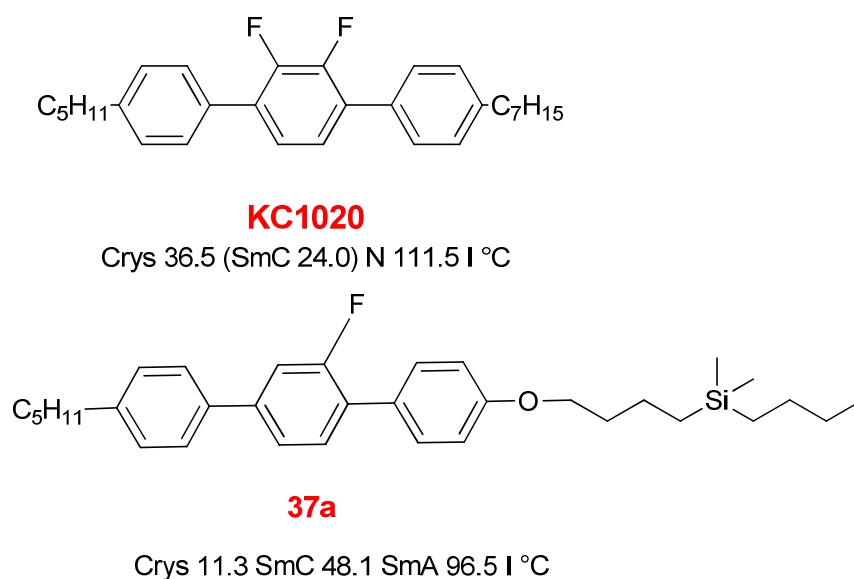
Figure **69:** *Phase diagram of 37a and KC1020 mixtures*

The middle ring monofluoroterphenyl shows a similarly low crystallisation temperature to the trifluoroterphenyl. In this case, at 50% of **37a**, there is a SmC phase up to 60 °C while still maintain a SmA and N phase. This is promising for use in mixtures although the upper limit of the SmC phase is not as high as demanded for commercial devices.

3.8.5. Phase diagram for the mixture of compounds 41b and KC1020:

KC1020

Crys 36.5 (SmC 24.0) N 111.5 I °C

41b

Crys 87.5 SmC 140.6 I °C

Phase diagram for mixtures of compound **41b** + KC1020 on cooling
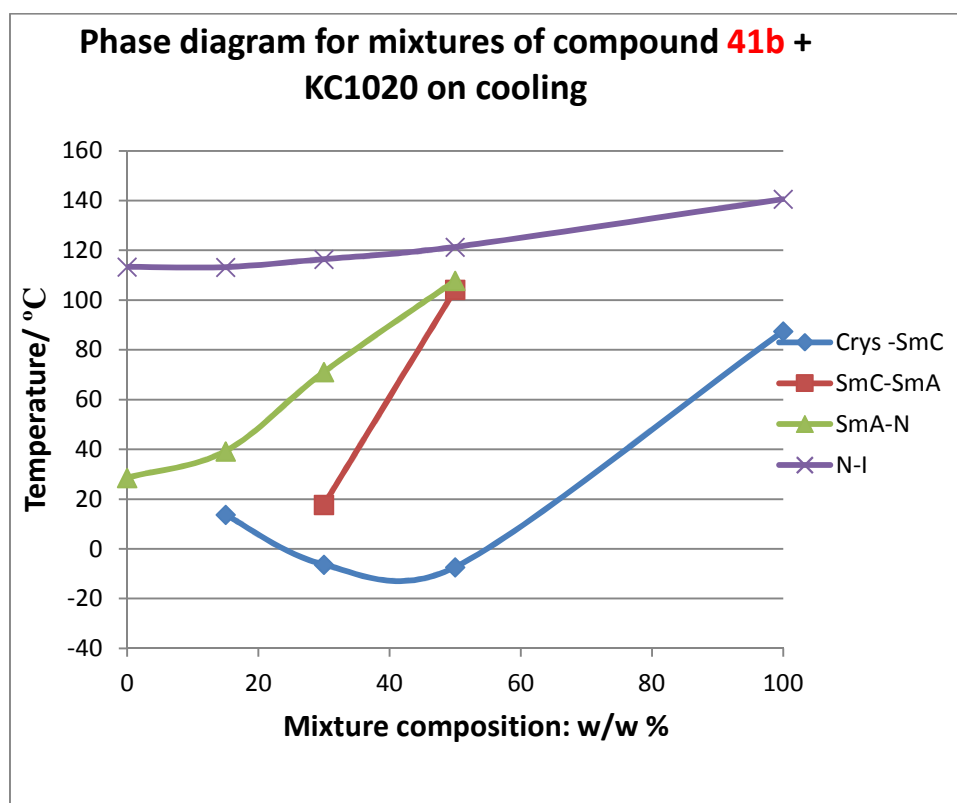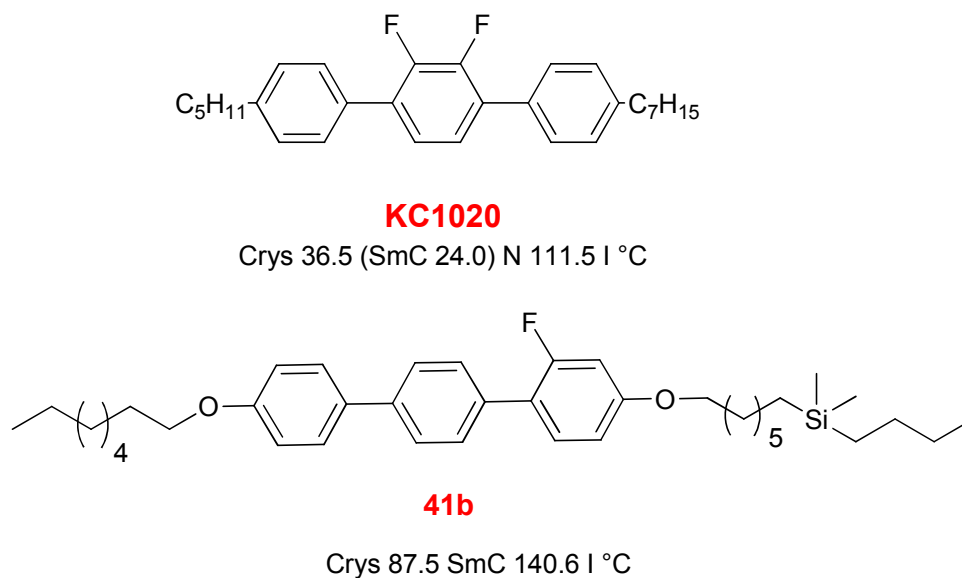
Figure **70:** *Phase diagram of compound **41b** and **KC1020** mixtures.*

The phase diagram shows the data obtained *via* POM on cooling for up to a maximum of 50% w/w of the silane **41b**. Compound **41b** is the endring monofluoroterphenyl analogue of compound **37a** whose behaviour was described previously. Once again there is an impressive depression in freezing point and it appears from the curve that the eutectic does occur near to the 50% value. The more SmC end ring compound shows in that the SmC phase appears earlier in the phase diagram than for **37a** but there is still a small band of SmA and N phase present at 50% w/w. The basic phase behaviour looks ideal for use in FLC mixtures, although there are many more properties that need to be fulfilled.

3.8.6. Phase diagram for mixtures of compounds 39 and KC1020:

KC1020

Crys 36.5 (SmC 24.0) N 111.5 I °C

39

Crys 56.5 SmC 113.5 I °C
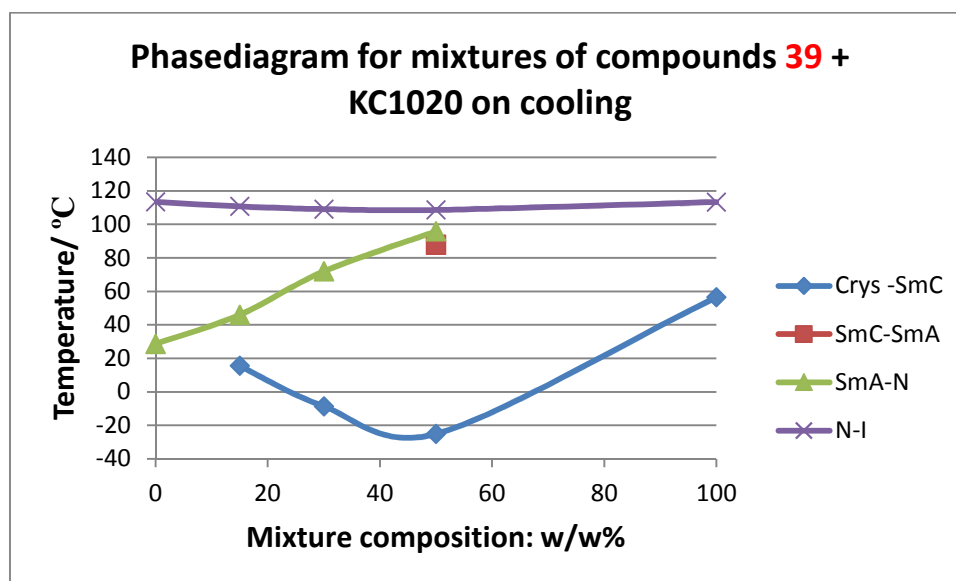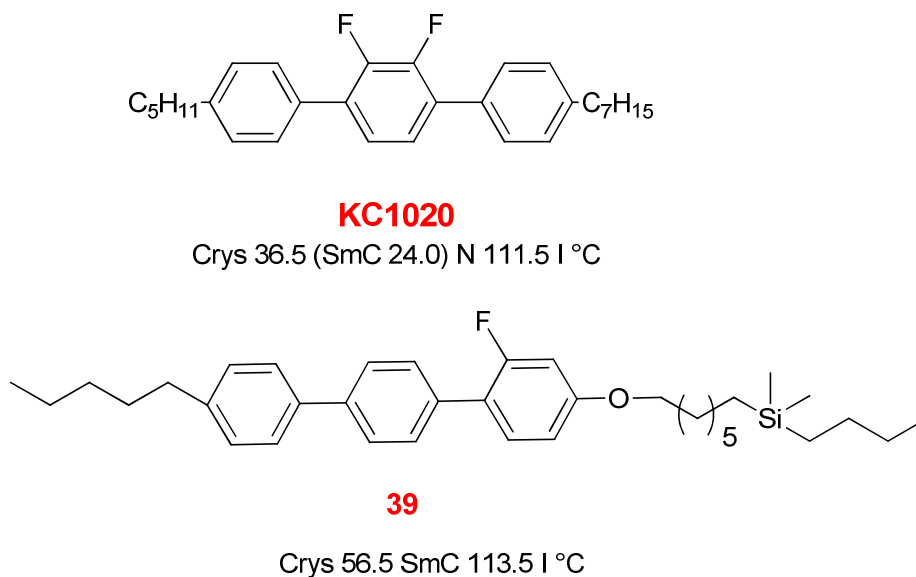
Figure**71:** *Phase diagram of 39 and KC1020 mixtures.*

This compounds differes only in having a longer chain length for the spacer keeping the same at butyldimethylsilane. The phase diagram is therefore quite similar to Figure 72, but the longer chain length supports SmC phase to the extent that SmA behaviour is 'squeezed' out earlier. All the above exampless show a marked drop in crystallisation temperature and so further mixture starting from these eutectics should be capable of obtaining the values of -40 °C or so required by industry.

119

Based on above data, 50% mixtures of compounds **30a**, **34a**, **37a**, **41b**, **39** were selected. These have I-SmA-SmC-C phase sequence and a minimum crystallisation temperature. Each 50% w/w mixture was doped with 7% BE80F2N standard dopant to obtain an FLC material. At that stage, the transition temperatures of the resulting mixtures could not be predicted with certainty and the loss of an N* or SmA* phase may lead to poor alignment. The mixtures were investigated for their phase transitions and then filled in antiparallel rubbed 5 µm thick Instec cells to measure tilt angles and Ps values.

3.9 Transition temperatures for 7% of BE8OF2N in 50% of compound (i) 30a + KC1019, (ii) 30a + KC1020 (iii) 39 + KC1020:

Compound	Transition temperatures/°C								
	C		SmC*		SmA*		N*		I
1. 7% BE8OF2N in **30a** + KC1019	●	-16	●	74.5	●	109.0	●	---	●
2. 7% BE8OF2N in **30a** + KC1020	●	-7.9	●	35.5	●	93.0	●	---	●
3. 7% BE8OF2N in **39** + KC1020	●	-38.8	●	63.5	●	97.0	●	101.5	●

Table **14.** Transition temperatures for the 7% of BE8OF2N in 50% of compounds, (i) **30a** + **KC1019**, (ii) **30a** + KC1020 (iii) **39** + KC1020.

Table 14 show the **t**ransition temperatures on cooling for the three 7% mixtures. Only that from compound **39** has an N* phase, which is generally the most reliable phase sequence to enable good FLC alignment. The value of 7% w/w is a standard amount that gives a moderate Ps of about 20 nCcm^{-2} in the baseline FLC mixture consisting of conventional difluoroterphenyls. That value of Ps enables FLC switching, does not reduce the SmC*-SmA* transition too far below that of the host mixture and has a sufficiently long pitch to enable good alignment. The achiral binary mixtures were chosen, assuming that some N* would be maintained when the chiral dopant was added. It may be possible that mixtures with marginally less silane component could be found that possess an N* phase. This will probably be at the expense of higher crystallisation temperatures lower SmC*-SmA* temperatures.

3.9.1. Electrooptic studies of the mixture of 7% BE8OF2N in 50 % of compounds 30a +KC1019:

3.9.1.1 Tilt angles for the mixture of 7% BE8OF2N in 50 % of compounds 30a + KC1019:
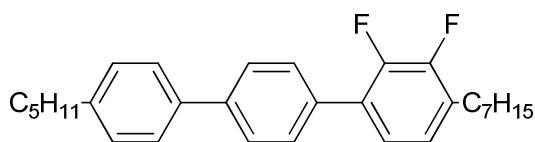
KC1019
Crys 56.0 SmC 105.5 SmA 131.0 N 136.0 °C I
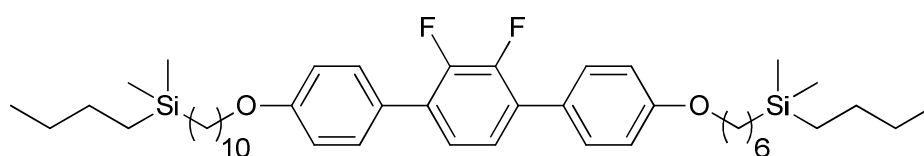
30a
Crys 53.7 SmC 82.0 °C I
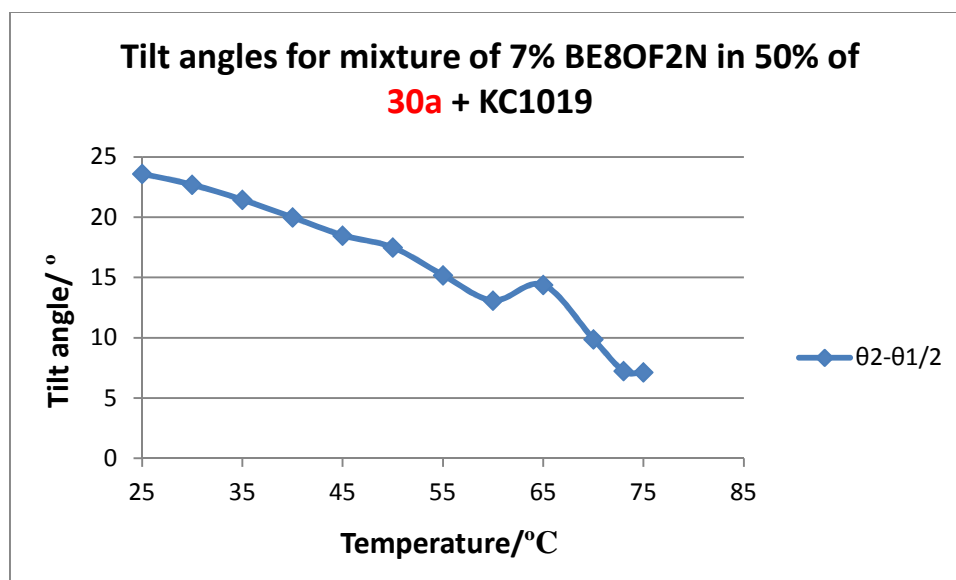
Figure **72:** *Tilt angles of the mixture of 7% BE8OF2N in 50% of compounds 30a + KC1019*.

The FLC electrooptic properties of the 50% mixture of compound **30a +KC1019** was examined by mixing with the standard chiral dopant **BE8OF2N** and filling an Instec 5 μm anti-parallel rubbed electrooptic cell in the isotropic phase. Cooling into the SmC* phase was usually carried out with a high frequency square wave applied in order to achieve the best

level of alignment although this often required repetition and alterating of the conditions to optimise alignment. The transition from N* to SmA* phase is considered a key point in setting up the smectic layers across the cell and the cooling rate should be in the 0.2 °C/min region at this point. Unfortunately, this material has a direct I-SmA* transiton. Electrooptic measurements were made using the integrated Instec automatic liquid crystal tester (ALCT) apparatus, hot stage and software.

The addition of the non-mesogenic dopant can have a marked effect on the transition temperatures. The textures for the 7% mixture were hard to analyse as there was very little birefringence to observe. This was presumably as the material was very prone to homeotropic alignment in the SmA* phase and in the tilted SmC* phase, helicity sometimes cancels the usual Schlieren texture. However this mixture did show ferroelectric like switching and the first graph shows the measured tilt angle over a wide temperature range obtained from rotating the microscope stage until similar levels of darkness were obtained under crossed polarisers. A tilt angle of 22.5° equates to a switching cone angle of 45° which gives maxiumum constrast between the light and dark state. Increasing tilt angle with decreasing temperature is directly linked to increasing Ps, but the ideal FLC material would show no change in tilt angle over its operating temperature range. This is not easy to achieve and the material used in current devices are a compromise between many competing properties. The desire for a constant tilt SmC* angle is one of the reasons for the interest in de Vries compounds.

A low frequency triangular wave field (amplitude 30 V, frequency 1 Hz) was applied. The magnitude and increase in tilt angle with cooling is very much in keeping with similar conventional mixtures using this dopant and a conventional difluoroterphenyl host mixture. The fact that a low crystallisation temperature was obtained from a simple binary mixure was promising for the development of much lower crystallisation termperatures.

3.9.1.2 Ps values for the mixture of 7% BE8OF2N in 50 % of compound 30a + KC1019

Ps values for mixture of 7% BE8OF2N in 50% of compounds 30a + KC1019
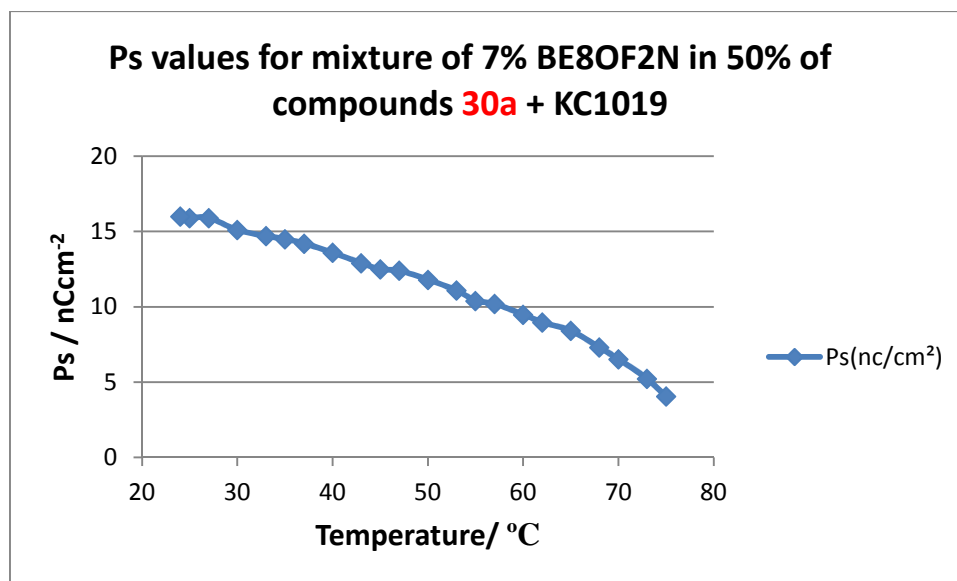
Figure **73:** *Ps values of the mixture of 7% BE8OF2N in 50% of compounds 30a +KC1019*.

Ps values were measured over the SmC* phase using the triangular wave method. Ps values do usually increase as the tilt angle increases, with cooling. In addition molecular motion will decrease on cooling, so one may predict that Ps values would also increase. In the above graph (Figure 73), Ps values are increased around 4 to 16 nC/cm^{-2} on cooling which marginally below that found in the standard mixture KCHM2117.

3.9.2 The mixture of 7% BE8OF2N in 50% of compounds 30a +KC1020.

3.9.2.1Tilt angles of the mixture of 7% BE8OF2N in 50% of compounds30a +KC1020:

KC1020

Crys 36.5 (SmC 24.0) N 111.5 °C I

30a
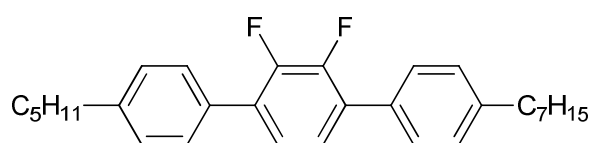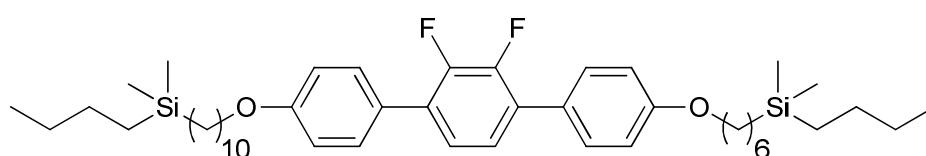
Crys 53.7 SmC 82.0 °C I
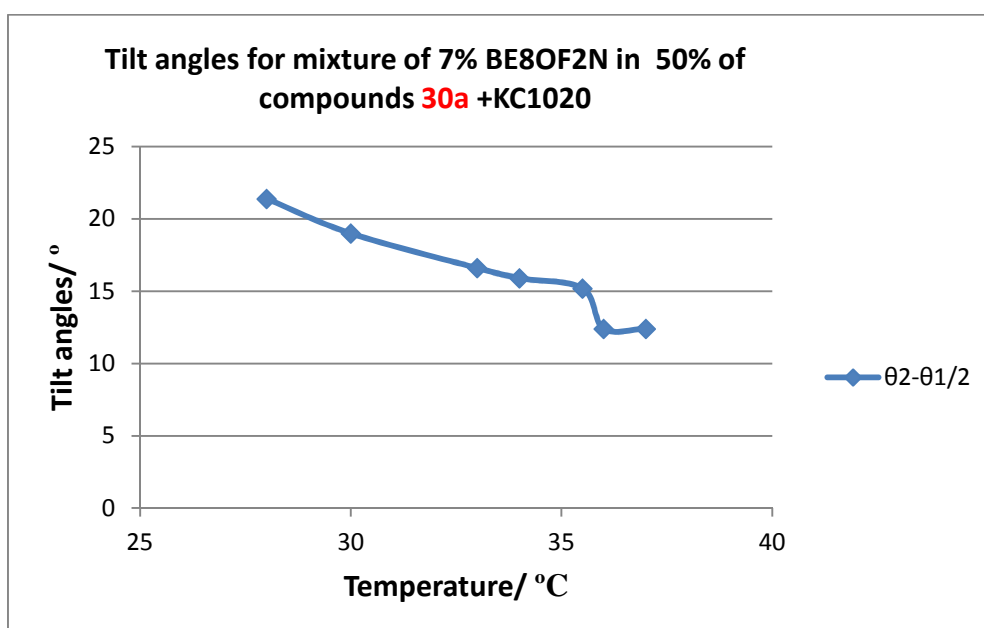
Figure**74:** *Tilt angles of the mixture of 7% BE8OF2N in 50% of 30a + KC1020*.

The FLC electrooptic properties of the mixture of 7% BE8OF2N in **30a + KC1020**, the end ring difluoroterphenyl, w as examined the tilt angle was again, almost the ideal 22.5°, but there was an anomolous kink in the data shortly after the SmC* phase began. This may be a real phenomenon or an artifact of the difficulty in judging the position of the two positions of the SmC* director by eye.

3.9.2.2 Ps values for mixture of 7% BE8OF2N in 50% of compounds *30a* +KC1020

Ps values for mixture of 7% BE8OF2N in 50% of compounds 30a + KC1020
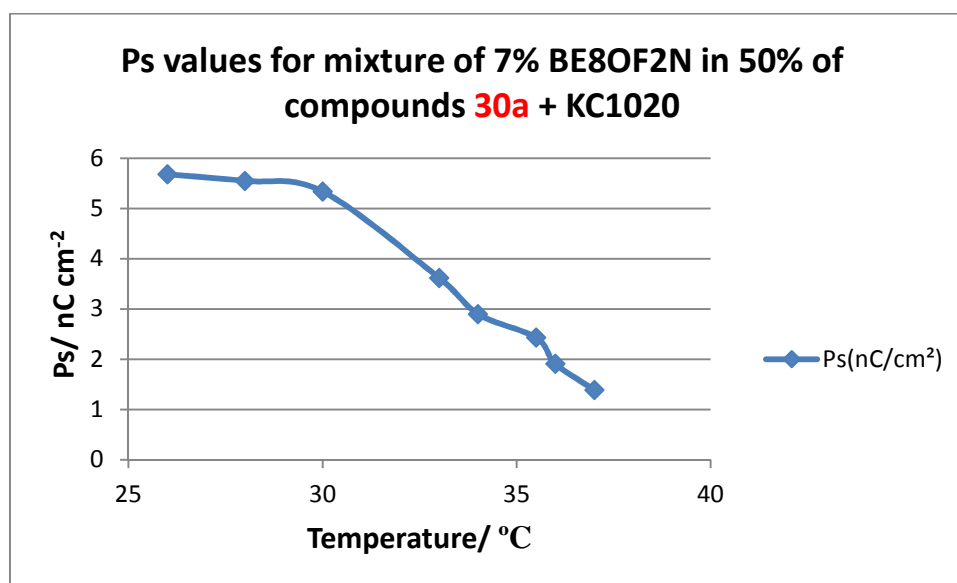
Figure **75:** *Ps values of the mixture of 7% BE8OF2N in 50% compounds of 30a +KC1020*.

Ps values measured over the SmC* phase on cooling, the normal rise in Ps was observed but the maximum value at room temperaturewas only just under 6 nC cm^{-2}. This is contrast to the expected value of around 20 nC cm-. One reason may simply be poor alignment such as there areas where the material is not switching fully or has some domains with the opposite tilt that cancels out part of the Ps. Alternatively, the interaction of the dopant and host mixtures does not enhance the polarisation.

3.9.3 The mixture of 7% BE8OF2N in 50% of compounds 39 +KC1020:

3.9.3.1Tilt angles for 7% BE8OF2N in a 50% mixture of compound 39 +KC1020:

KC1020

Crys 36.5 (SmC 24.0) N 111.5 I °C

39

Crys 56.5 SmC 113.5 I °C
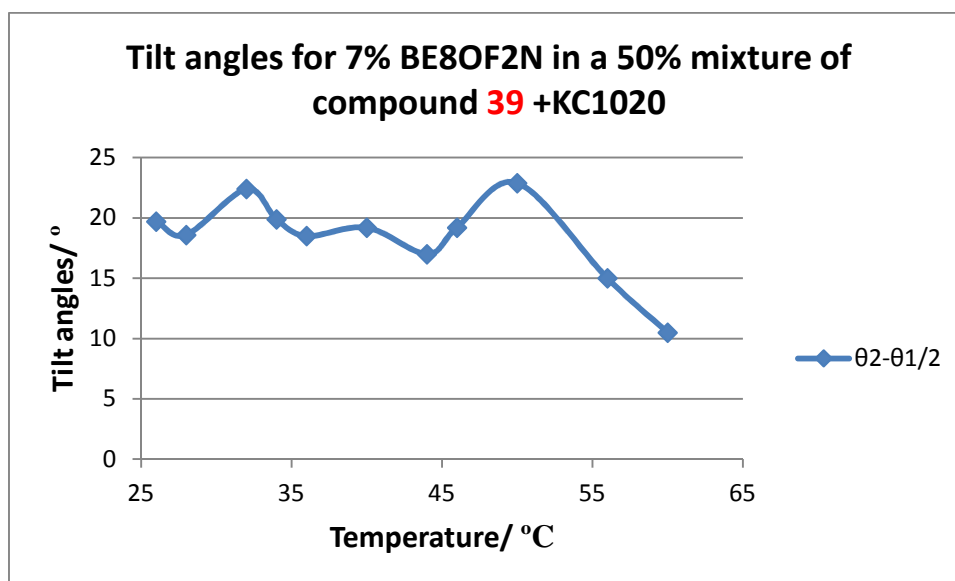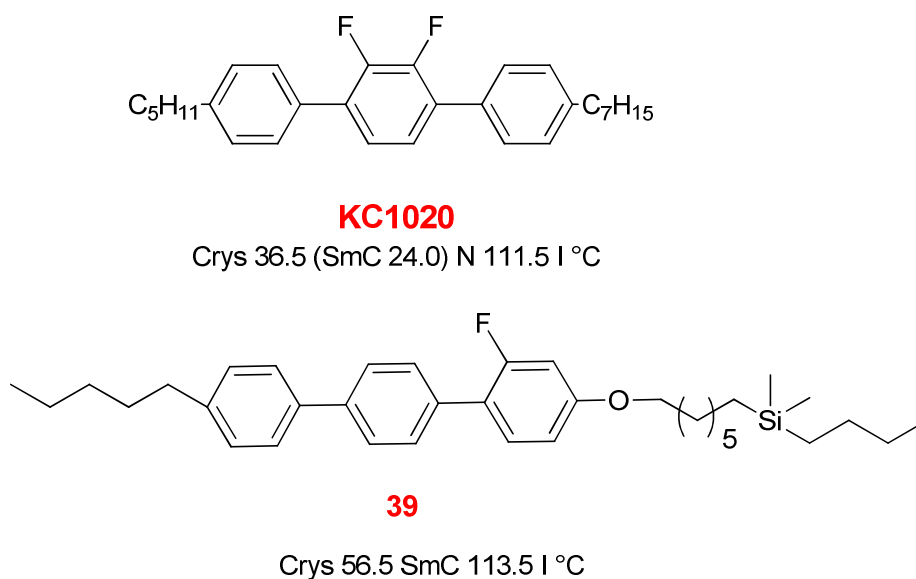
Figure**76:** Tilt angles of the mixture of 7% BE8OF2N in 50% w/w of **39** + **KC1020**.

In this mixture, judging the two switching directions opticallty was particularly difficult and the unsatisfactory scatter of points in Figure 76 was the result of several observations. However, the general trend points to a tilt angle of the required magnitude. In this and other

examples, the optical data should be backed up with small X-ray scattering results. Unsuccessful bids for beam time at the synchrotron source and either breakdowns or lack of available time slots on the departmental kit meant that these measurements were not made within the time of the PhD. However, such measurements will be obtained before publication is considered.

3.9.3.2 Ps values of the mixture of 7% BE8OF2N in 50% of compounds *39* +KC1020
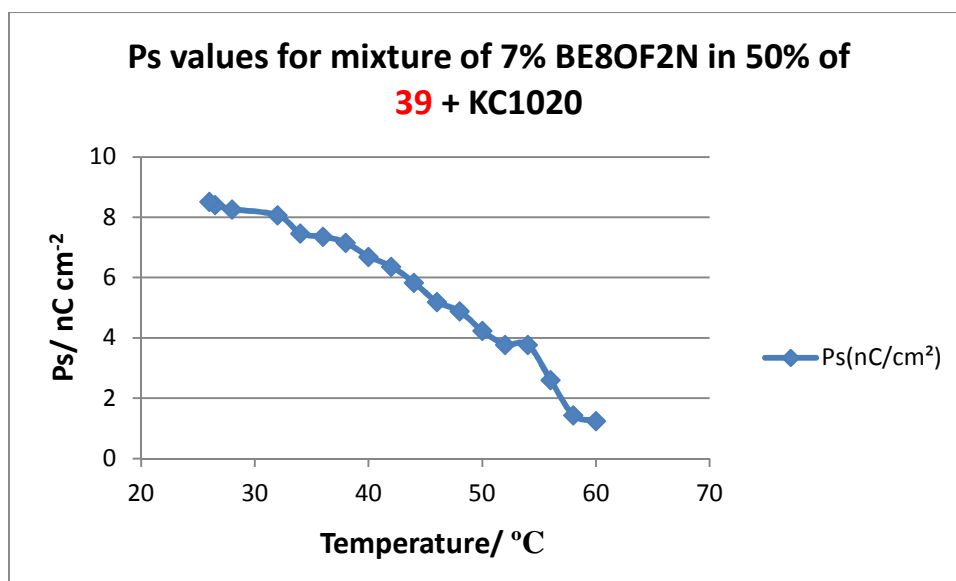
Figure **77:** *Ps values of the mixture of 7% BE8OF2N in 50% w/w of 39 + KC1020.*

Ps values increased on cooling but reached a similar maximum to (8.4 nC/cm^{-2})to that observed for compound 30a. The two types of molecule are quite different and one would expect the difluoroterphenyl to interact with the dopant as a conventional material would. It would seem that another explanation is required relating to poor alignment or incomplete switching. Repetition of the measurements in different cells and careful comparison with known material may help reduce the number of possible explanations.

4.0 Conclusions:

The main aim of the research to prepare stable liquid crystalline compounds and mixtures based on the fluorinated terphenyl mesogenic core. These were designed to be enabling formulation of low melting ferroelectric host materials with a wide SmC temperature range, small variation in tilt angle and uniform, stable alignment in FLC devices. The structural unit under investigation was a terminal silane acting as a bulky, stable moiety which would easy to prepare and suitable for scale up of synthesis.

A route to pentamethyldisilane liquid crystals analogous to pentamethyldisiloxane proved difficult which may be due to lithiation between the two silicon atoms, and also there was a problem with the Baeyer Villiger step in the synthesis of 4-hydroxybromophenyl from 4-bromobiphenyl. The former target was dropped in order to simplify the synthetic route and purification and provide more robust final products

Simpler target bulky butyldimethylsilane end group compounds were selected that were more straightforward to prepare. The initial proposal was to match the cross sectional area of a fluorinated mesogenic core with a butyldimethylsilane terminal group to reduce interdigitation, leading to high, unchanging tilt and uniform alignment based on lack of curvature.

Syntheses proved as straightforward as planned, however the materials required repeated column chromatography in some cases, but it is not known whether the impurities were aleady present in the starting silanes and bromoalkenes or whether they were created in the hydrosilylation, lithiationa and Suzuki coupling reactions. Difluoroterphenyl units linked by oxygen at both end to a spacer and a terminal butyldimethylsilane produced materials were the first to be prepared and showed wide SmC phase temperature ranges. It was considered that as the aim was to formulate these with conventional fluorinated terphenyls and to have a I-N-SmA-SmC phase sequence, it was not necessary to have silanes at both ends. Although bookshelf aligned FLC materials are known with a direct I-SmC* transition, this seems a very hard situation to reproduce. Consequently it was decided to prepare a series of monofluoro, di and trifluoroterphenyls with a pentyl chain at one end and a dibutyldimethyl silane at the other. A few alkoxy analogues to the pentyl substituted terphenyls were prepared for comparison. These are also mainly SmC-Iso compounds and even the middle ring monofluoroterphenyls suppressed the nematic phase. The trifluoroterphenyls were the most difficult to prepare and most significantly, to purify and only modest SmC phase temperature

ranges. Their use in FLC host mixtures would require significant advantages, before being considered.

Selected examples, based mainly on having examples of the main structural types were formulated in binary mixtures with standard middle ring and for one example, an end ring difluoroterphenyl. In nearly every case, the addition of the mono butyldimethylsilane supressed the nematic phase of the dialkyldfluoroterphenyl wide SmC phase temperature ranges. The most impressive property was the drop in crystallisation temperature, sometimes as low as -20 °C and these appear to be a typical eutectic behaviour. Further mixture development from such eutectics could lead to crystallisation temperatures demanded by industry.

The eutectic like mixtures of 50% silane and conventional difluoroterphenyl werew mixed with 7% of the standard chiral dopant BE80F2N and electrooptic measurements to examine the ferroelectric LC parameters. Tilt angles were in the typical region of 20° required by an SSFLC devicc, but Ps measurements varied from values between 15 and 20 nC cm^{-2} whereas others only reach 8-9 nC cm^{-2} The work leaves some questions open and more measurments are required to confirm tilt angles any change in layer shrinkage comparted with typical non-bulky end group mesogens. However, the scope for mixture development to produce materials with a very low crystallisation temperature seems feasible from a relatively simple array of stable silane based liquid crystals.

5.0 Experimental

5.1 General instrumentation and Techniques

Compounds were analysed and purified by using the following methods, equipment and materials.

5.1.1 Nuclear Magnetic Resonance (NMR) Spectroscopy

The structures of all compounds were confirmed by using ^{1}H NMR spectroscopy with a JEOL ECP400 or Jeol JNM LA-400 spectrometer. The residual protic solvent was used as the internal standard [CDCl$_3$, δ_H = 7.26]. The following abbreviations are used to describe the splitting patterns; singlet (s), doublet (d), triplet (t), quartet (q), quintet (quin), multiplet (m) double doublet (dd), doublet of doublet of doublet (ddd), double triplet (dt). The structures of all final compounds were confirmed by using ^{13}C NMR spectroscopy was recorded 100.5 MHz. Deuteriated chloroform was used as the internal standard, and the centre peak of the triplet was set to δ 77.00. ^{19}F NMR was recorded at 376 MHz, reference CFCl$_3$ δ_F = 0 ppm; ^{29}Si NMR recorded at 79 MHz, reference TMS δ_{Si} = 0.

5.1.2 Mass Spectrometry

A mass spectrometer used for analyse the majority of compounds *via* electron impact was a 70 eV Finnigan MAT 1020 GC-MS spectrometer. Mass spectrometry is an analytical technique that measures the mass-to charge ratio of charged particles. It is most generally used to find the composition of a physical sample by generating a mass spectrum representing the masses of sample fragments.

5.1.3 Elemental Analysis

Elemental analysis was carried out on all final compounds to give an indication of purity. The analysis was performed on a Fisons EA 1108 CHN analyser.

5.1.4 Optical Microscopy

All mesophases were characterised and all transition temperatures were determined using an Olympus BH2 polarising microscope in conjunction with a Mettler FP82 hot stage and Mettler FP90 central processor, Photos-JVC TK-C1481 colour video camera using Mettler Studio Capture software. The heating and cooling rates used were 2 ºC/min and 1 ºC/min.

For optical polarising microscopy the thin sample of mesogenic material is sandwiched between a glass microscope slide and glass cover slip. The microscope slide is placed on a stage which can be accurately temperature controlled between polarisers which are crossed at

90° to each other. When analysing mesophase by optical polarising microscopy, the texture that is revealed depends upon how the sample is aligned in addition to being dependent upon the phase structure of the sample. There are two basic forms of alignment for liquid crystalline compounds, homeotropic and homogeneous (planar). Homeotropic alignment is where molecules that constitute the phase structure are oriented such that their long axes (optic axes) are normal to the supporting substrate. When molecules are so oriented polarised light is unaffected by the material and so light cannot pass through the analyser. Hence complete blackness will be seen through the microscope. In tilted smectic phase SmC*, as molecules are tilted with respect to the layer normal, hence tilted stage is required to get homeotropic situation. In homogeneous alignment the constituent molecules of the liquid crystal phase are oriented parallel to the supporting substrates. Such alignment is required for the analysis of ferroelectric liquid crystals for pitch length, spontaneous polarisation and tilt angle. With homogeneous alignment, a thin film of the liquid crystal phase exhibits birefringence and coloured texture results when viewed between crossed polarisers. Optical polarising microscopy enables the identification of the type of liquid crystal and other mesophases from the optical texture that is generated. However the technique is also essential when evaluating the physical properties of liquid crystal in certain phases and over particular temperature ranges. As ferroelectric liquid crystals are evaluated in small electro-optic cells for spontaneous polarisation, tilt angle and switching times. The optical polarising microscopy is essential for such evaluations.

5.1.5 Differential Scanning Calorimetry

Differential Scanning Calorimetry (DSC) is a useful tool to complement the use of optical microscopy to study of liquid crystal phase transitions. DSC is used in determining the heat supplied or extracted during a process such as a phase transition. All transition temperatures were confirmed on a Mettler DSC822e with STARe software, calibrated with indium (156.6 °C 28.45J/g) and zinc (419.47 °C), checked daily with indium ± 0.3. The reference is aluminium. All DSC transition temperatures and melting points are quoted as the onset temperature.

5.1.6 High Performance Liquid Chromatography (HPLC)

The purity of all final compounds were determined by using HPLC, Gilson system comprising- 151 UV/VIS detector, 233XL auto sampler/fraction collector, 321 binary solvent pump, Valvemate column changer, Unipoint ver 3.3 software. Analytical column-

Phenomenex Luna 5µm C18(2) or Si(2) 250 x 25mm and using 60% acetonitrile, 40 % chloroform.

5.1.7 Chromatography

The progress of reactions was frequently monitored by thin layer chromatography (TLC) and capillary gas chromatography (GC). Aluminium backed TLC plates coated with silica gel (60 F_{254} Merck) were utilised. GC was carried out using a Varian CP3800 gas chromatogaph equipped with a 10 m CP-SIL 5CB column. Purification of intermediates and final products was mainly accomplished by column chromatography, using silica gel 60 (230 - 400 mesh) and recrystalised from a suitable solvent. All glassware used was thoroughly cleaned by rinsing with acetone followed by distilled water and then drying in an oven at 100 °C.

5.1.8 Reactions

All reactions were carried out under a nitrogen atmosphere, when aqueous solutions were used as solvent or reagent.

Tetrakis (triphenylphosphine) palladium (0) was prepared according to the literature procedure.[81]

5.1.9 Reagents and reaction solvents

Reagents were supplied by Kingston Chemicals, or purchased from Acros Organics, Avacado, Aldrich, Fisher and Sigma; all were used without further purification.

6.0 Experimental procedures

6.1 Synthesis of Difluoroterphenyl silanes:

((Trimethylsilyl)-methyl)dimethylsilane[172] 14:

The Grignard reagent of trimethylchloromethylsilane (TMCMS) **12** was prepared by reaction of TMCMS (24.6 g, 0.20 mol) **11** and magnesium chips (5.76 g, 0.24 mol) in THF (100 ml). The Grignard reagent was added dropwise into dimethylchlorosilane (DMCS) (18.92 g, 0.20 mol) **13** dissolved in THF (100 ml) at 0 °C. The mixture was stirred at room temperature overnight and quenched with Conc. HCl (30 ml) acidified water and extracted with diethyl ether (3 x 100 ml). The combined organic extracts were washed with water (3 x 150 ml) and dried (Na_2SO_4). The oil was distilled under high vacuum to give (trimethylsilylmethyl)dimethylsilane **14** (12.07 g, 41%) as a clear, colourless oil.

^{1}H NMR δ ($CDCl_3$), -0.24 (2H, d, CH_2), 0.03 (9 H, s, $(CH_3)_3Si$) and 0.09 (6 H, d, J 3.8, $(CH_3)_2SiH$).

1-(Dec-9-enyloxy)-2,3-difluorobenzene 17a:

10-Bromodec-1-ene (30 g, 0.137 mol) **16a**, 2, 3-difluorophenol (18.51g, 0.142 mol) **5** and potassium carbonate (56.48 g, 0.411 mol) were stirred in butanone (500 ml) under reflux in a dry N_2 atmosphere overnight. After confirming the completion of the reaction by TLC, the potassium carbonate was filtered off and butanone was removed *in vacuo.* The reaction mixture was dissolved in diethylether (250 ml), washed with 10% $NaOH_{aq.}$ (200 ml) and water (2 x 100 ml) and dried ($MgSO_4$). The solvent was removed under *vacuo* and the product was distilled under high vacuum to give 1-(dec-9-enyloxy)-2,3-difluorobenzene **17a** (34.50 g, 94%) as a clear, colourless oil. ^{1}H NMR δ ($CDCl_3$), 1.26-1.41 (8 H, m, $CH_2CH_2CH_2$), 1.47 (2 H, quint, J 3.8, $CH_2CH_2CH_2$), 1.82 (2 H, quint, J 3.8, OCH_2CH_2), 2.05 (2 H, q, J 3.8, CH_2CH), 4.03 (2 H, t, J 3.8, OCH_2), 4.94 (1 H, br d, J 17.0, 10.3, CH=CH_2), 5.00 (1 H, br d, J 17.0, 10.3, CH=CH_2), 5.82 (1 H, ddt, J 17.0, 10.2 ,6.8, CH=CH_2), 6.82 (2 H, m, ArH) and 7.11 (1 H, ddt, J 7.2, 6.0, 2.4, 5-H).

(10-(2, 3-Difluorophenoxy)decyl)dimethyl((trimethylsilyl)methyl)silane 18a:

((Trimethylsilyl)methyl)dimethylsilane **14** (14.44 g, 0.0986 mol) and 1-(dec-9-enyloxy)-2,3-difluorobenzene **17a** (13.21 g, 0.0493 mol) was stirred in toluene (60 ml) under dry N_2 for 10 min. Karstedt's catalyst (100 µL) was added and the mixture was stirred under N_2 at room temperature overnight. After confirming the completion of reaction by TLC, toluene was removed in *vacuo.* The oil was purified by column chromatography (silica gel; hexane) and dried (P_2O_5) to give a colourless liquid as a (10-(2, 3-Difluorophenoxy)decyl)dimethyl ((trimethylsilyl)methyl)silane **18a** (16.05 g, 79%).

^{1}H NMR δ (CDCl$_3$), -0.30 (2 H, s, Me$_3$SiCH_2Si), -0.01 (6 H, s, (CH_3)$_2$Si), 0.02 (9 H, s, (CH$_3$)$_3$Si), 0.47 (2 H, t, Si-CH_2-CH$_2$), 1.26 (12 H, quint, *J* 7.2, CH$_2$CH_2CH$_2$), 1.44 (2 H, quint, *J* 7.2, CH$_2$CH_2CH$_2$), 1.79 (2 H, quint, *J* 7.2, 6.8, CH$_2$CH_2CH$_2$), 4.01 (2 H, t, CH$_2$CH_2O), *J* 6.2), 6.68-6.75 (2 H, m, ArH) and 6.95(1 H, ddt, *J* 8.4, 5.9, 2.5, 5-H).

Attempted preparation of (4-((10-(dimethyl((trimethylsilyl)methyl)silyl)decyl)oxy)-2,3-difluorophenyl)boronic acid 19a:

A solution of n-butyl lithium (16.05 ml, 0.039 mol, 2.5 M in hexanes) was added dropwise to stirred solution of (10-(2,3-difluorophenoxy)decyl)dimethyl((trimethylsilyl)methyl)silane (16.05 g, 0.040 mol) **18a** in THF (100 ml) maintaining the temperature below -65 ºC. After addition was complete the mixture was kept below -65 ºC for 1.5 h and trimethylborate (12.06 g, 0.116 mol) in THF (75 ml) was added drop wise maintaining the temperature below -65 ºC. The reaction mixture was allowed to warm to room temperature, stirred at room temperature overnight and quenched with 10% HCl (20 ml) acidified water, extracted with diethyl ether (2 x 100 ml), washed with water (2 x 100 ml) and dried (MgSO$_4$). The solvent was evaporated in *vacuo* to give oil containing a milky coloured precipitate (16.10 g, 91%). No satisfactory ^{1}H NMR was obtained.

1-(4'-Bromo-(1,1'-biphenyl)-4-yl)ethanone 42 :

Aluminium chloride (40.0 g) and dichloromethane (750 ml) were stirred and cooled to 5 ^{0}C. Acetyl chloride (40.2 g) was quickly added to this mixture and cooled to -3 ^{0}C to give a transparent yellow solution. Solid 4-bromophenyl (60 g) was added in small portions over 1.5 h and the mixture was stirred overnight. After confirming the completion of reaction by TLC, the mixture was poured into ¼ of two litre bucket of ice and 37% HCl (200 ml) was added to the ice to destroy the aluminium chloride. The mixture was extracted with DCM (4 x 300 ml). The organic solution was washed with water (3 x 400 ml), 10% NaOH (400 ml), distilled water (3 x 400 ml) and dried (MgSO$_4$). The solvent was removed in *vacuo* to give 1-(4'-bromo-(1,1'-biphenyl)-4-yl)ethanone **42** (from EtOH) as a gold colour fluffy material (64.30 g, 91%). ^{1}H NMR δ (CDCl$_3$), 2.64 (3 H, s, CH$_3$), 7.49 (2 H, d, *J* 8.2, ArH), 7.60 (2 H, d, *J* 8.0, ArH), 7.65 (2 H, d, *J* 8.0, ArH) and 8.03 (2 H, d, *J* 8.0, 2- and 6-H).

Attempted synthesis of

potassium(4-((10-(dimethyl((trimethylsilyl)methyl)silyl)decyl)oxy)-2,3-difluorophenyl) trifluoroborate (Scheme-1):

4-10-(Dimethyl((trimethylsilyl)methyl)silyl)decyloxy)-2,3-difluorophenylboronicacid (2.0 g, 4.0 mmol), potassium hydrogen fluoride (0.9 g, 6.4 mmol) were added to a mixture of methanol (4 ml) and H$_2$O (7 ml) and stirred vigorously for 2 hours. The solid was taken up an acetone heated and filterd hot. No solid was observed and no product was formed because no aromatic protons were observed in the ^{1}H NMR of one liquid fraction. No further work was needed as a consequence.

We stopped the synthesis of pentamethyldisilanes and we moved to synthesis of middle ring difluoroterphenylbutyldimethylsillanes.

6.2 Synthesis of middle ring difluoroterphenylbutyldimethylsilanes:

1-Bromo-4-(dec-9-en-1-yloxy)benzene 23d:

10-Bromodecene (30 g, 0.136 mol) **21d**, 4-bromophenol (25.95 g, 0.15 mol) **22**, potassium carbonate (57 g, 0.15 mol) were stirred in butanone (400 ml) under dry N_2. The reaction mixture was heated under reflux overnight. After confirming the completion of reaction by TLC, the potassium carbonate was filtered off. The butanone was removed in *vacuo*. The reaction mixture was dissolved in diethylether (400 ml), washed with 10% NaOH Aq.solution (200 ml), water (2 x 100 ml) and dried ($MgSO_4$). The solvent was removed in *vacuo* and the product was distilled by high vacuum distillation to give unwanted product. (^{1}H NMR shows the double bond between 8, 9 carbon atoms; may be because high temperature with high vacuum distillation causes a double bond shift from C_9, C_{10} to C_8, C_9). Product weight (36.0 g).

^{1}H NMR δ (CDCl$_3$), 1.27-1.50 (10 H, m, CH$_2$CH_2CH$_2$), 1.77 (2 H, quint, *J* 6.5, CH$_2$CH_2CH$_2$), 2.05 (2 H, q, *J* 6.7, CH$_2$CH_2CH=), 3.90 (2 H, t, *J* 6.4, OCH_2CH$_2$), 5.76- 5.88 (1 H, m, CH$_2$CH=CH$_2$), 6.75 (2 H, d, ArH) and 7.38 (2 H, d, ArH).

m/z (EI) 310 (M$^+$ - C$_{16}$H$_{23}$BrO requires 310), 314.1 (1.6%), 312.1 (1.7), 313.1 (16.8) and 310.1 (100).

1-Bromo-4-(hex-5-en-1-yloxy)benzene 23c:

6-Bromohexene (8.00 g, 0.049 mol) **21c**, 4-bromophenol (0.054 g, 0.15 mol) **22**, potassium carbonate (20.3 g, 0.147 mol) were stirred in butanone (200 ml). The reaction mixture was heated under reflux overnight under dry N_2. After confirming the completion of reaction by TLC, the potassium carbonate was filtered off and butanone was removed *in vacuo*. The crude was dissolved in diethyl ether (200 ml), washed with 10% NaOH $_{aq.}$ (100 ml) water (3 x 50 ml) and dried ($MgSO_4$). The solvent was removed in *vacuo* and the product was distilled by high vacuum distillation to give 1-bromo-4-(hex-5en-1yloxy)benzene (11.50 g, 92%) **23c** as a colourless oil.

^{1}H NMR δ (CDCl$_3$), 1.54 (2 H, m, CH$_2$CH_2CH$_2$), 1.77 (2 H, quint, J 13.3, 6.4, CH$_2$CH_2CH$_2$), 2.10 (2 H, q, J 14.7, 7.3, CH$_2$CH_2CH=), 3.90 (2 H, t, J 6.4, OCH_2CH$_2$), 4.92- 5.06 (2 H, m, CH$_2$CH=CH_2), 5.75- 5.85 (1H, m, CH$_2$CH=CH$_2$), 6.75 (2 H, dt, J 10.2, 5.6, 3.4, ArH) and 7.38 (2 H, dt, J 10.2, 5.6, 3.6, ArH).

^{13}C NMR δ (CDCl$_3$), 26.0 (CH$_2$), 29.0 (CH$_2$), 33.8 (CH$_2$), 68.2 (O-CH$_2$), 112.5 (C$_{ArC}$-Br), 114.2 (=CH$_2$), 116.2 (C-2 and C-6), 132.0 (C-3 and C-5), 139.0 (-CH$_2$=), 158.2 (C$_1$).

m/z (EI) 254 (M$^+$ - C$_{12}$H$_{15}$BrO requires 254), 257.0 (12.8%), 255.0 (13), 256.0 (97) and 254.0 (100).

1-Bromo-4-(dec-9-en-1-yloxy)benzene 23d:

10-Bromodecene (30 g, 0.136 mol) **21d**, 4-bromophenol (25.95 g, 0.15 mol) **22**, potassium carbonate (57 g, 0.15 mol) were stirred in butanone (400 ml). The reaction mixture was heated under reflux overnight. After confirming the completion of reaction by TLC, the potassium carbonate was filtered off and butanone was removed *in vacuo*. Dissolved reaction mixture in diethylether (200 ml) and washed with 10% NaOH $_{aq.}$ solution (200 ml), water (2 x 100 ml) and dried (MgSO$_4$). The butanone was removed in *vacuo*, the crude product was dissolved in hexane and product was purified by filtration through silica gel. The solvent was removed in *vacuo*, dried (P$_2$O$_5$) to give 1-bromo-4-(dec-9-en-1-yloxy)benzene (41.00 g, 97%) **23d** as a colourless oil.

^{1}H NMR δ (CDCl$_3$), 1.25-1.65(10 H, m, CH$_2$CH_2CH$_2$), 1.77 (2 H, quint, J 6.7, OCH$_2$CH_2CH$_2$), 2.05 (2 H, q, J 6.9, CH$_2$CH_2CH=), 3.90 (2 H, t, J 6.6, OCH_2CH$_2$), 4.90- 5.04 (2 H, m, CH$_2$CH=CH_2), 5.75- 5.88 (1 H, m, CH$_2$CH=CH$_2$), 6.77 (2 H, dt, J 10.0, 5.4, 3.2, ArH) and 7.36 (2H, dt, J 10.0, 5.4, 3.2, ArH).

^{13}C NMR δ (CDCl$_3$), 26.0 (CH$_2$), 29.0 (CH$_2$), 29.3(CH$_2$), 29.4 (CH$_2$), 33.8 (CH$_2$), 68.2 (O-CH$_2$), 112.5 (C$_{ArC}$-Br), 114.2 (=CH$_2$), 116.2 (C-2 and C-6), 132.0 (C-3 and C-5), 139.0 (-CH$_2$=), 158.2 (C$_1$).

m/z (EI) 310 (M$^+$ - C$_{12}$H$_{15}$BrO requires 310), 314.1 (1.6%), 312.1 (1.7), 313.0 (16.8), 311.1 (17.6), 312.1 (97.3) and 310.1 (100).

(6-(4-Bromophenoxy)hexyl)(butyl)dimethylsilane 25c:

1-Bromo-4-(hex-5en-1yloxy)benzene (11.00 g, 43.0 mmol) **23c**, butyldimethylsilane (10 g, 86.2 mmol) **24** were stirred in toluene (40 ml) with Karstedt's catalyst (80 µL) under dry N_2 at room temperature overnight. After confirming the completion of reaction by TLC, toluene was removed in *vacuo*. The product was purified by column chromatography (silica gel; hexane) and dried (P_2O_5), to give (6-(4-bromophenoxy)hexyl)(butyl)dimethylsilane (12.70 g, 79 %) **25c** as a colourless liquid.

^{1}H NMR δ (CDCl$_3$), 0.00 (6 H, s, CH$_2$Si(C*H$_3$*)$_2$CH$_2$), 0.53 (4 H, m, C*H$_2$*Si(CH$_3$)$_2$C*H$_2$*),), 0.93 (3 H, t, *J* 6.9, CH$_2$C*H$_3$*), 1.24- 1.56 (10 H, m, CH$_2$C*H$_2$*CH$_2$), 1.80 (2 H, quin, *J* 6.7, OCH$_2$C*H$_2$*), 3.95 (2 H, t, *J* 6.5, OC*H$_2$*CH$_2$), 6.81 (2 H, dt, *J* 10.2, 5.6, 3.4, ArH) and 7.40 (2 H, dt, *J* 10.2, 5.6, 3.4, ArH);

^{13}C NMR δ (CDCl$_3$), -3.3 ((CH$_3$)$_2$ Si), 13.8 (CH$_3$), 14.9 (CH$_2$), 15.2 (CH$_2$), 23.8 (CH$_2$), 25.6 (CH$_2$), 26.1 (CH$_2$), 26.6 (CH$_2$), 29.0 (CH$_2$), 33.3 (CH$_2$), 68.2 (O-CH$_2$), 112.5 (C$_{ArC}$), 116.3 (C-2 and C6), 132.1 (C-3 and C-5), 158.2 (C$_1$); δ^{29}Si, 2.76 (s).

m/z (EI) 372 (M$^+$ - C$_{18}$H$_{31}$BrOSi requires 372), 374.1 (2.0%), 372.1 (3), 374.0 (4), 371.1 (20), 370.1 (99.4) and 372.1 (100).

(10-(4-Bromophenoxy)decyl)(butyl)dimethylsilane 25d:

1-Bromo-4-(dec-9-en-1-yloxy)benzene (41.0 g, 0.132 mol) **23d**, butyldimethylsilane (30 g, 0.264 mol) **24**, were stirred in toluene (160 ml) with Karstedt's catalyst (320 µL) under dry N_2 at room temperature for overnight. After confirming the completion of reaction by TLC, the toluene was removed in *vacuo*. The product was purified by column chromatography (silica gel; hexane) and dried (P_2O_5), to give (10-(4-bromophenoxy)decyl)(butyl) dimethylsilane (48.75 g, 86%), **25d** as a colourless liquid.

^{1}H NMR δ (CDCl$_3$), 0.00 (6 H, s, -CH$_2$-Si(C*H$_3$*)$_2$-CH$_2$-), 0.46-0.59 (4 H, m, C*H$_2$*Si(CH$_3$)$_2$C*H$_2$*), 0.94 (3 H, t, *J* 6.9, CH$_2$C*H$_3$*), 1.18- 1.54 (18 H, m, CH$_2$C*H$_2$*CH$_2$), 1.82 (2 H, quin, *J* 6.5, OCH$_2$C*H$_2$*), 3.95 (2 H, t, *J* 6.4, OC*H$_2$*CH$_2$), 6.81 (2 H, d, ArH) and 7.40 (2 H, d, ArH);

^{13}C NMR δ (CDCl$_3$), -3.3 (2xCH$_3$), 13.8 (CH$_3$), 14.9 (CH$_2$), 15.2 (CH$_2$), 23.8 (CH$_2$), 25.9 (CH$_2$), 26.1 (CH$_2$), 26.6 (CH$_2$), 29.0 (CH$_2$), 33.3 (CH$_2$), 68.2 (CH$_2$), 112.5 (C$_4$), 116.3 (C-2 and C6), 132.1 (C3 and C5), 158.2 (C-O); δ^{29}Si, 2.73 (s).

m/z (EI) 428 (M$^+$ - C$_{22}$H$_{39}$BrOSi requires 428), 430.2 (3.2%), 427.2 (24), 426.2 (99), and 428.0 (100).

Butyl(6-((2',3'-difluoro-[1,1'-biphenyl]-4-yl)oxy)hexyl)dimethylsilane 28c:

Tetrakis(triphenylphosphine)palladium (0.47 g, 0.4 mmol) and (2,3-difluorophenyl)boronic acid (8.30 g, 52.5 mmol) **27** were added sequentially to a stirred mixture of (6-(4-bromophenoxy)hexyl)(butyl)dimethylsilane (12.0 g, 32.32 mmol) **25c** and 1,2-dimethoxy ethane (150 ml) under dry N$_2$. The reaction mixture was heated under reflux overnight. After confirming the completion of reaction by TLC, the cooled mixture was poured into water and the product was extracted into ether (3 x 100 ml), washed with brine, dried (MgSO$_4$). The solvent was removed in *vacuo*. The product was purified by column chromatography (Silica gel, 1% ethyl acetate in hexane), butyl(6-((2',3'-difluoro-[1,1'-biphenyl]-4-yl)oxy)hexyl)dimethylsilane (9.20 g, 70%), **28c** as a colourless oil.

^{1}H NMR δ (CDCl$_3$), 0.00 (6 H, s, CH$_2$Si(C*H*$_3$)$_2$CH$_2$), 0.49-0.59 (4 H, m, C*H*$_2$Si(CH$_3$)$_2$C*H*$_2$), 0.93 (3 H, t, J 6.9, CH$_2$C*H*$_3$), 1.26- 1.57 (10 H, m, CH$_2$C*H*$_2$CH$_2$), 1.85 (2 H, quin, J 13.5, 6.6, OCH$_2$C*H*$_2$), 4.05 (2 H, t, J 6.6, OC*H*$_2$CH$_2$), 7.03 (2 H, d, ArH), 7.11-7.17 (2 H, m, ArH), 7.18-7.24 (1 H, m, ArH) and 7.52 (2 H, d, ArH);

^{13}C NMR δ (CDCl$_3$), -3.3 ((CH$_3$)$_2$ Si), 13.8 (CH$_3$), 14.9 (CH$_2$), 15.2 (CH$_2$), 23.8 (CH$_2$), 25.7 (CH$_2$), 26.1 (CH$_2$), 26.6 (CH$_2$), 29.1 (CH$_2$), 33.4 (CH$_2$), 68.0 (O-CH$_2$), 114.5 (C-2 and C-6), 115.3 (2 x CH), 123.9 (C-5), 125.0 (C-6), 130.0 (C$_3$), 130.1 (C$_5$), 130.5 (C-1), 145.5 (F-C-2), 151.5 (F-C-3), 158.2 (C-O); δ^{29}Si, 2.77 (s).

m/z (EI) 404 (M$^+$ - C$_{24}$H$_{34}$F$_2$OSi requires 404), 406.2 (3.3%), 406.2 (5), 405.2 (26), and 404.0 (100).

1-Bromo-4-(but-3-en-1-yloxy)benzene 23a:

4-Bromobutene (25 g, 0.185 mol) **21a**, 4-Bromophenol (36 g, 0.203 mol), **22**, potassium carbonate (76.6 g, 0.55 mol) were stirred in acetone (400 ml), The reaction mixture was heated under reflux overnight under a dry N$_2$. After confirming the completion of reaction by TLC, the potassium carbonate was filtered off, and acetone was removed in *vacuo* and the reaction mixture was dissolved in diethylether (200 ml), washed with 10% NaOH $_{aq.}$ solution (200 ml) and water (2 x 100 ml), dried (MgSO$_4$). Crude was dissolved in hexane, the product was purified by filtration through silica gel. The solvent was removed in *vacuo*, dried (P$_2$O$_5$),

gave 1-bromo-4-(but-3-en-1-yloxy)benzene (12.0 g, 47%), **23a** as a colourless oil. ^{1}H NMR δ (CDCl$_3$), 2.40-2.50 (2 H, m, CH$_2$C*H*$_2$CH=), 3.89 (2 H, t, *J* 6.6, OCH$_2$C*H*$_2$), 4.90- 5.12 (2 H, m, CH$_2$CH=C*H*$_2$), 5.75- 5.86 (1 H, m, CH$_2$C*H*=CH$_2$), 6.70 (2 H, d, ArH) and 7.28 (2 H, d, ArH).

^{13}C NMR δ (CDCl$_3$), 34.2 (CH$_2$), 68.2 (O-CH$_2$), 112.5 (C$_{ArC}$-Br), 114.2 (=CH$_2$), 116.2 (C-2 and C-6), 132.0 (C-3 and C-5), 139.0 (-CH$_2$=), 158.2 (C$_1$).

m/z (EI) 226 (M$^+$ - C$_{10}$H$_{11}$BrO requires 226), 229.0 (10.7 %), 227.0 (11), 228.0 (97) and 226 (100).

(4'-((6-(Butyldimethylsilyl)hexyl)oxy)-2,3-difluoro-[1,1'-biphenyl]-4-yl)boronicacid 29c:

A solution of n-butyllithium (2.5 ml, 6.0 mmol, 2.5 M in hexanes) was added to a cooled (-78 ^{0}C) solution of butyl(6-((2',3'-difluoro-[1,1'-biphenyl]-4-yl)oxy)hexyl)dimethylsilane (2.5 g, 21.0 mmol), **28c**, THF (150 ml), the temperature maintained for 1.5 hr. Added trimethylborate (2 g, 18.6 mmol) portion wise, whilst keeping the temperature below -60 ^{0}C, stirred for overnight. After confirming the completion of reaction by TLC, added 4M HCl (8 ml) and stirred for an hour, the product was extracted into ether (3 x 50 ml), washed with brine (2 x 50 ml) and dried (MgSO$_4$). The solvent was removed in *vacuo*, to give (4'-((6-(butyldimethylsilyl)hexyl)oxy)-2,3-difluoro-[1,1'-biphenyl]-4-yl)boronicacid (3.0 g, 33%), **29c** as a white colour solid.

^{1}H NMR δ (CDCl$_3$), 0.00 (6 H, s, CH$_2$Si(C*H*$_3$)$_2$CH$_2$), 0.47-0.65 (4 H, m, C*H*$_2$Si(CH$_3$)$_2$C*H*$_2$) 0.93 (3 H, m, CH$_2$C*H*$_3$), 1.22- 1.52 (10 H, m, CH$_2$C*H*$_2$CH$_2$), 1.85 (2 H, m, OCH$_2$C*H*$_2$), 2.05 (2 H, s, B-O*H*), 4.05 (2 H, t, *J* 6.60, OC*H*$_2$CH$_2$), 7.10 (2 H, d, ArH), 7.11-7.17 (2 H, m, ArH), 7.38-7.46 (2 H, m, ArH) and 7.56 (2 H, d, ArH).

^{13}C NMR δ (CDCl$_3$), -3.3, 13.8, 14.9, 15.2, 23.8, 25.7, 26.1, 26.6, 29.1, 33.4, 68.0, 114.5 (C-2 and C-6), 115.3, 123.9, 125.0, 130.0, 130.1, 130.5, 145.5, 151.5, 158.2.

m/z (EI) 448 (M$^+$ - C$_{24}$H$_{35}$BF$_2$O$_3$Si requires 448), 450.2 (4.3%), 449.2 (6), 447.2 (25), and 448 (100); δ^{29}Si, 2.77 (s).

Butyl(6-((4''-((10-(butyldimethylsilyl)decyl)oxy)-2',3'-difluoro-[1,1':4',1''-terphenyl]-4-yl)oxy)hexyl)dimethylsilane 30a:

Tetrakis(triphenylphosphine)palladium (0.01 g) and (4'-((6-(butyldimethylsilyl)hexyl)oxy)-2,3-difluoro-[1,1'-biphenyl]-4-yl)boronic acid (2.95 g, 6.6 mmol), **29c** were added sequentially to stirred mixture of (10-(4-bromophenoxy)decyl)(butyl)dimethylsilane (1.98 g, 4.65 mmol), **25d** and DME (30 ml) under N_2 atmosphere. The stirred mixture was heated under reflux overnight. After confirming the completion of reaction by TLC, the cooled mixture was poured into water and the product was extracted into ether (3 x 75 ml), washed with brine, dried (MgSO$_4$) and the solvent was removed in *vacuo*. The crude product was purified by column chromatography (silica gel; 10% DCM in hexane) give a butyl(6-((4''-((10-(butyldimethylsilyl)decyl)oxy)-2',3'-difluoro-[1,1':4',1''-terphenyl]-4-yl)oxy)hexyl)dimethylsilane (1.75 g, 50.14%), **30a** as a white crystals. Purity 99.63 (HPLC); (Found: C, 72.65; H, 9.88; $C_{46}H_{72}F_2O_2Si_2$ requires C, 73.54; H, 9.66).

^{1}H NMR δ (CDCl$_3$), 0.01 (12 H, d, CH$_2$Si(CH_3)$_2$CH$_2$), 0.50-0.59 (8 H, m, CH_2Si(CH$_3$)$_2$CH_2), 0.94 (6 H, t, *J* 5.6, CH$_2$CH_3), 1.28- 1.58 (28 H, m, CH$_2$CH_2CH$_2$), 1.86 (4 H, quin, *J* 6.4, OCH$_2$CH_2), 4.07 (4 H, t, *J* 6.6, OCH_2CH$_2$), 7.05 (4 H, d, ArH), 7.26 (2 H, m, ArH) and 7.57 (4 H, d, ArH);

^{13}C NMR δ (CDCl$_3$); Me$_4$Si); -3.3, 13.8, 20.8, 24.0, 25.6, 25.9, 26.2, 29.6, 34.7, 68.7, 114.9, 125.6, 128.1, 129.7, 148.1, 159.2.

m/z (EI) 750 (M$^+$- $C_{46}H_{72}F_2O_2Si_2$ requires 750), 298 (11%), 115 (20), 59 (66) and 32 (100); ^{29}Si, 2.75 (s), 2.90 (s); δ^{19}F, 143.54, F (s).

(4-(4-Bromophenoxy)butyl)(butyl)dimethylsilane 25a:

1-Bromo-4-(but-3-en-1-yloxy)benzene (11.5 g, 50.66 mmol), **23a**, butyldimethylsilane (11.75 g, 10.13 mmol), **24**, were stirred in toluene (80 ml) with Karstedt's catalyst (130 µL) under dry N_2 at room temperature overnight. After confirming the completion of reaction by TLC, the toluene was removed in *vacuo.* The product was purified with column chromatography (silica gel; 2% ethyl acetate in hexane), dried (P$_2$O$_5$), to give (4-(4-bromophenoxy)butyl)(butyl)dimethylsilane (16 g, 92%), **25a** as a colourless liquid.

^{1}H NMR δ (CDCl$_3$), 0.00 (6 H, s, CH$_2$Si(CH$_3$)$_2$CH$_2$), 0.44-0.62 (4 H, m, CH$_2$Si(CH$_3$)$_2$CH$_2$), 0.91 (3 H, t, J 6.9, CH$_2$CH$_3$), 1.20- 1.59 (6 H, m, CH$_2$CH$_2$CH$_2$), 1.81 (2 H, quin, J 6.8, OCH$_2$CH$_2$), 3.95 (2 H, t, J 6.4, OCH$_2$CH$_2$), 6.80 (2 H, d, ArH) and 7.39 (2 H, d, ArH).

^{13}C NMR δ (CDCl$_3$), -3.3 (2xCH$_3$), 13.8 (CH$_3$), 23.8 (CH$_2$), 25.9 (CH$_2$), 26.1 (CH$_2$), 26.6 (CH$_2$), 33.3 (CH$_2$), 68.2 (CH$_2$), 112.5 (C$_4$), 116.3 (C-2 and C6), 132.1 C3 and C5), 158.2 (C-O); δ^{29}Si, 2.73 (s).

m/z (EI) 344 (M$^+$ - C$_{16}$H$_{27}$BrOSi requires 344), 346.1 (1.5 %), 343.1 (22), 342.1 (98) and 344 (100).

Butyl(10-((2',3'-difluoro-[1,1'-biphenyl]-4-yl)oxy)decyl)dimethylsilane 28d:

Tetrakis(triphenylphosphine)palladium (0.658 g) and (2,3-difluorophenyl)boronic acid (9.60 g, 60.8 mmol), **17** were added sequentially to a stirred mixture of (10-(4-bromophenoxy)decyl)(butyl)dimethylsilane (20.0 g, 46.8 mmol) **25d** and DME (250 ml), and heated under reflux overnight under a N$_2$ atmosphere. After confirming the completion of reaction by TLC, the cooled mixture was poured into water and the product was extracted into ether (3 x 100 ml), washed with brine, dried (MgSO$_4$) and the solvent was removed in *vacuo*. The product was purified by column chromatography (silica gel; 2 % EA in hexane), recrystallised from ethanol, toluene, gave butyl (10-((2', 3'-difluoro-[1,1'-biphenyl]-4-yl)oxy)decyl)dimethylsilane (16 g, 74 %), **28d** as a colourless solid.

^{1}H NMR δ (CDCl$_3$), 0.00 (6 H, s, -CH$_2$-Si(CH$_3$)$_2$-CH$_2$-), 0.51-0.55 (4 H, m, CH$_2$Si(CH$_3$)$_2$CH$_2$), 0.93 (3 H, t, J 7.0, CH$_2$CH$_3$), 1.26- 1.58 (18 H, m, CH$_2$CH$_2$CH$_2$), 1.86 (2 H, quin, J 6.6, OCH$_2$CH$_2$), 4.05 (2 H, t, J 6.6 , OCH$_2$CH$_2$), 7.03 (2 H, d, ArH), 7.11-7.25 (2 H, m, ArH), 7.31 (1 H, s, ArH) and 7.53 (2 H, dd, J 8.8, 1.48, ArH).

^{13}C NMR δ (CDCl$_3$), -3.3 ((CH$_3$)$_2$ Si), 13.8 (CH$_3$), 14.9 (CH$_2$), 15.2 (CH$_2$), 23.8 (CH$_2$), 25.7 (CH$_2$), 26.1 (CH$_2$), 26.6 (CH$_2$), 29.1 (CH$_2$), 33.4 (CH$_2$), 68.0 (O-CH$_2$), 114.5 (C-2 and C-6), 115.3 (2 x CH), 123.9 (C-5), 125.0 (C-6), 130.0 (C$_3$), 130.1 (C$_5$), 130.5 (C-1), 145.5 (F-C-2), 151.5 (F-C-3), 158.2 (C-O);

m/z (EI) 460 (M$^+$ - C$_{28}$H$_{42}$F$_2$OSi requires 460), 463 (1.5 %), 462 (6), 461 (34) and 460 (100); δ^{29}Si, 2.76 (s).

1-Bromo-4-(pent-4-en-1-yloxy)benzene 23b:

5-Bromopentene (18 g, 0.121 mol), **21b**, 4-bromophenol (23 g, 0.133 mol), **22**, potassium carbonate (50.0 g, 0.362 mol) were stirred in acetone (250 ml) under dry N_2. The reaction mixture was heated under reflux overnight. After confirming the completion of reaction by TLC, potassium carbonate was filtered off, acetone was removed in *vacuo* and the reaction mixture was dissolved in diethylether (250 ml), washed with 10% NaOH $_{aq.}$ solution (150 ml), water (2 x 100 ml) and dried ($MgSO_4$). The crude material was dissolved in 2% EA in hexane; the product was purified by filtration through silica gel. The solvent was removed in *vacuo*, dried (P_2O_5), to give 1-bromo-4-(pent-4-en-1-yloxy)benzene (27.30 g, 94%), **23b** as a colourless oil.

^{1}H NMR δ ($CDCl_3$), 1.88-1.97 (2 H, quin, *J* 14.1,6.4, $CH_2CH_2CH_2$), 2.24-2.32 (2 H, m, $CH_2CH_2CH=$), 3.98 (2 H, t, *J* 6.4, OCH_2CH_2), 5.03- 5.15 (2 H, m, $CH_2CH=CH_2$), 5.83-5.96 (1 H, m, $CH_2CH=CH_2$), 6.83 (2 H, d, ArH), and 7.41 (2 H, d, ArH).

^{13}C NMR δ ($CDCl_3$), 29.0 (CH_2), 33.8 (CH_2), 68.2 ($O-CH_2$), 112.5 ($C_{ArC}-Br$), 114.2 ($=CH_2$), 116.2 (C-2 and C-6), 132.0 (C-3 and C-5), 139.0 ($-CH_2=$), 158.2 (C_1).

m/z (EI) 240 ($M^+ - C_{11}H_{13}BrO$ requires 240), 243 (12 %), 241 (12), 242 (97) and 240 (100).

Butyl(6-((4''-(4-(butyldimethylsilyl)butoxy)-2',3'-difluoro-[1,1':4',1''-terphenyl]-4-yl)oxy)hexyl)dimethylsilane 30c:

Tetrakis(triphenylphosphine)palladium(0.01g) and (4'-((6-(butyldimethylsilyl)hexyl)oxy)-2,3-difluoro-[1,1'-biphenyl]-4-yl)boronic acid (1.63 g, 3.7 mol) **29c** were added sequentially to a stirred mixture of (4-(4-bromophenoxy)butyl)(butyl)dimethylsilane (1.00g, 2.9 mmol), **25a** and DME (30 ml) under N_2 atmosphere. The reaction mixture heated under reflux overnight. After confirming the completion of reaction by TLC, the cooled mixture was poured into water and the product was extracted into ether (3 x 75 ml), washed with brine, dried ($MgSO_4$) and the solvent was removed in *vacuo*. The crude product was purified by column chromatography (silica gel; 10% DCM in hexane) to give butyl(6-((4''-(4-(butyldimethylsilyl)butoxy)-2',3'-difluoro-[1,1':4',1''-terphenyl]-4-yl)oxy)hexyl)dimethylsilane (1.83 g, 95%) **30c** as a colourless solid. Purity: 95.5% (HPLC); Found: C, 72.28; H, 9.28; $C_{40}H_{60}F_2O_2Si_2$ requires C, 72.02; H, 9.07.

^{1}H NMR δ (CDCl$_3$), 0.01 (12 H, d, CH$_2$Si(CH_3)$_2$CH$_2$, 0.50-0.64 (8 H, m, CH_2Si(CH$_3$)$_2$CH_2), 0.93 (6 H, t, J 6.76, CH$_2$CH_3), 1.26- 1.60 (16 H, m, CH$_2$CH_2CH$_2$), 1.81-1.93 (4 H, m, OCH$_2$CH_2), 4.06 (4 H, sext, J 10.44,6.44, 3.88, OCH_2CH$_2$), 7.04 (4 H, d, ArH), 7.25 (2 H, m, ArH), 7.56 (4 H, d, ArH);

^{13}C NMR δ (CDCl$_3$); Me$_4$Si); -3.3, 13.8, 20.8, 24.0, 25.6, 25.9, 26.2, 29.6, 34.7, 68.7, 114.9, 125.6, 128.1, 129.7, 148.1, 159.2.

m/z (EI) 666 (M$^+$ - C$_{40}$H$_{60}$F$_2$O$_2$Si$_2$ requires 666), 355 (8%), 206(8), 115 (25), 73 (48), 59(100) and 32 (35); ^{29}Si, 2.76 (s), 2.92 (s); δ^{19}F, 143.54, F (s).

(4'-((10-(butyldimethylsilyl)decyl)oxy)-2,3-difluoro-[1,1'-biphenyl]-4-yl)boronic acid 29d:

A solution of n-butyllithium (15 ml, 0.033 mol, 2.5 M in hexanes) was added drop wise to stirred, cooled (-78 ^{0}C) solution of butyl(10-((2',3'-difluoro-[1,1'-biphenyl]-4-yl)oxy)decyl)dimethylsilane(15 g, 0.0326 mol), **28d** in THF (300 ml) and maintain it for 1.5 h. Tri methyl borate (11.56 ml~10.17 g, 0.0978 mol) was added drop wise, whilst keeping the temperature below -60 ^{0}C. Reaction mixture was stirred overnight. After confirming the completion of reaction by TLC, added 4 molar HCl (40 ml) and stirred for half an hour, extracted into ether (3 x 200 ml), washed with brine (2 x 200ml), dried (MgSO$_4$) and the solvent was removed in *vacuo* to give (4'-((10-(butyldimethylsilyl)decyl)oxy)-2,3-difluoro-[1,1'-biphenyl]-4-yl)boronicacid (16.4 g, 99.80%) **29d** as a colourless solid.

^{1}H NMR δ (CDCl$_3$), 0.00 (6 H, s, CH$_2$Si(CH_3)$_2$CH$_2$), 0.52 (4 H, broad t, J 9.0, CH_2Si(CH$_3$)$_2$CH_2), 0.91 (3 H, t, J 6.6, CH$_2$CH_3), 1.25- 1.53 (18 H, m, CH$_2$CH_2CH$_2$),1.75-1.85 (2 H, m, OCH$_2$CH_2), 2.05 (2 H, s, B-OH), 4.07 (2 H, m, OCH_2CH$_2$), 7.11 (2 H, d, ArH), 7.31-7.47 (2 H, m, ArH) and 7.57 (2 H, d, ArH).

^{13}C NMR δ (CDCl$_3$), -3.3, 13.8, 14.9, 15.2, 23.8, 25.7, 26.1, 26.6, 29.1, 33.4, 68.0, 114.5 (C-2 and C-6), 115.3, 123.9, 125.0, 130.0, 130.1, 130.5, 145.5, 151.5, 158.2;

m/z (EI) 504 (M$^+$ - C$_{28}$H$_{43}$BF$_2$O$_3$Si requires 504), 507 (1 %), 506 (3), 504 (9), 505 (32) and 504 (100).

(5-(4-Bromophenoxy)pentyl)(butyl)dimethylsilane 25b:

1-Bromo-4-(pent-4-en-1-yloxy)benzene (6.25g, 25.9 mmol), (**13b**), butyldimethylsilane (6.00 g, 51.7 mmol), **24** were stirred in toluene (50 ml) with Karstedt's catalyst(70 µL) under dry N_2 at room temperature for overnight. After confirming the completion of reaction by TLC, toluene was removed in *vacuo*. The product was purified with column chromatography (silica gel; 2% EA in hexane), dried (P_2O_5) to give (5-(4-bromophenoxy)pentyl) (butyl)dimethylsilane (9.00 g, 97.40%), **25b** as a colourless liquid.

^{1}H NMR δ (CDCl$_3$), 0.00 (6 H, s, CH$_2$Si(C*H*$_3$)$_2$CH$_2$), 0.51-0.57 (4 H, m, C*H*$_2$Si(CH$_3$)$_2$C*H*$_2$), 0.92 (3 H, t, *J* 6.9, CH$_2$C*H*$_3$), 1.26- 1.56 (8 H, m, CH$_2$C*H*$_2$CH$_2$), 1.82 (2 H, quin, *J* 13.7, 6.8, OCH$_2$C*H*$_2$), 3.95 (2 H, t, *J* 6.6, OC*H*$_2$CH$_2$), 6.82 (2 H, d, ArH) and 7.41 (2 H, d, ArH).

^{13}C NMR δ (CDCl$_3$), -3.3 (2xCH$_3$), 13.8 (CH$_3$), 23.8 (CH$_2$), 25.9 (CH$_2$), 26.1 (CH$_2$), 26.6 (CH$_2$), 29.0 (CH$_2$), 68.2 (CH$_2$), 112.5 (C$_4$), 116.3 (C-2 and C6), 132.1 (C3 and C5), 158.2 (C-O); δ^{29}Si, 2.74 (s).

m/z (EI) 358 (M$^+$ - C$_{17}$H$_{29}$BrOSi requires 358), 360 (3 %), 359 (20), 357 (24) and 358 (100).

Butyl(10-((4''-(4-(butyldimethylsilyl)butoxy)-2',3'-difluoro-[1,1':4',1''-terphenyl]-4-yl)oxy)decyl)dimethylsilane 30b:

Tetrakis(triphenylphosphine)palladium (0.01 g) and (4'-((10-(butyldimethylsilyl)decyl)oxy)-2,3-difluoro-[1,1'-biphenyl]-4-yl)boronic acid (2 g, 4.0 mmol), **29d** were added sequentially to stirred mixture of (4-(4-bromophenoxy)butyl)(butyl)dimethylsilane (0.96 g, 2.8 mol), **25a** and DME (15 ml) under N_2 atmosphere. The stirred mixture was heated under reflux overnight. After confirming the completion of reaction by TLC, the cooled mixture was poured into water and the product was extracted into ether (3 x 75 ml), washed with brine, dried (MgSO$_4$). The solvent was removed in *vacuo*. The crude product was purified by column chromatography (silica gel; 10% DCM in hexane) to give butyl(10-((4''-(4-(butyldimethylsilyl)butoxy)-2',3'-difluoro[1,1',4',1''-terphenyl]-4-yl)oxy)decyl)dimethylsilane (1.50 g, 74%) **30b** as a colourless solid. Purity: 98.79% (HPLC); Found: C, 72.85; H, 9.71; C$_{44}$H$_{68}$F$_2$O$_2$Si$_2$ requires C, 73.08; H, 9.48;

^{1}H NMR δ (CDCl$_3$), 0.01 (12 H, d, CH$_2$Si(C*H*$_3$)$_2$CH$_2$), 0.49-0.66 (8 H, m, C*H*$_2$Si(CH$_3$)$_2$C*H*$_2$), 0.94 (6 H, td, *J* 9.0, 6.9, 2.04, CH$_2$C*H*$_3$), 1.27- 1.59 (24 H, m, CH$_2$C*H*$_2$CH$_2$), 1.88 (4 H, sext,

J 21.4, 15.0, 6.6, OCH$_2$C*H*$_2$), 4.08 (4 H, q, *J* 10.8, 6.4, OC*H*$_2$CH$_2$), 7.05 (4 H, d, ArH), 7.24-7.28 (2 H, m, ArH), 7.57, (4 H, d, ArH);

^{13}C NMR δ (CDCl$_3$); Me$_4$Si); -3.3, 13.8, 20.8, 24.0, 25.6, 25.9, 26.2, 29.3, 29.6, 34.7, 68.4, 68.7, 114.9, 125.6, 128.1, 129.3, 129.7, 148.1, 159.2.

m/z (EI) 722 (M$^+$ - C$_{44}$H$_{68}$F$_2$O$_2$Si$_2$ requires 722), 525 (5%), 355 (12), 115 (31), 59 (100) and 41 (17); ^{29}Si, 2.76 (s), 2.92 (s); δ^{19}F, 143.55, F (s).

(((2',3'-difluoro-[1,1':4',1''-terphenyl]-4,4''-diyl)bis(oxy))bis(decane-10,1-diyl))bis(butyldimethylsilane) 30d:

Tetrakis(triphenylphosphine)palladium(0.01 g) and (4'-((10-(butyldimethylsilyl)decyl)oxy)-2,3-difluoro-[1,1'-biphenyl]-4-yl)boronic acid (2.016 g, 4.0 mmol) **29d** were added sequentially to stirred mixture of (10-(4-bromophenoxy)decyl)(butyl)dimethylsilane (1.20 g, 2.8 mol), **25d** and DME (15 ml) under N$_2$ atmosphere. The stirred mixture was heated under reflux for overnight. After confirming the completion of reaction by TLC, the cooled mixture was poured into water and the product was extracted into ether (3 x 75 ml), washed with brine, dried (MgSO$_4$). The solvent was removed in *vacuo*, the crude product was purified by column chromatography (silica gel; 10% DCM in hexane) to give (((2',3'-difluoro-[1,1':4',1''-terphenyl]-4,4''-diyl)bis(oxy))bis(decane-10,1-diyl))bis(butyldimethylsilane) (1.50 g, 74%), **30d** as a white colour solid. Purity: 99.49 % (HPLC); Found: C, 74.38; H, 9.99; C$_{50}$H$_{80}$F$_2$O$_2$Si$_2$ requires C, 74.23; H, 10.11.

^{1}H NMR δ (CDCl$_3$), 0.00 (12 H, s, CH$_2$Si(C*H*$_3$)$_2$CH$_2$), 0.53 (8 H, m, C*H*$_2$Si(CH$_3$)$_2$C*H*$_2$), 0.94 (6 H, t, *J* 6.9, CH$_2$C*H*$_3$), 1.26- 1.56 (36 H, m, CH$_2$C*H*$_2$CH$_2$), 1.87 (4 H, quin, *J* 13.7, 6.7, OCH$_2$C*H*$_2$), 4.07 (4 H, t, *J* 6.4, OC*H*$_2$CH$_2$), 7.05 (4 H, d, ArH), 7.26 (2 H, m, ArH), 7.57, (4 H, d, ArH);

^{13}C NMR δ (CDCl$_3$); Me$_4$Si); -3.3, 13.8, 20.8, 24.0, 25.6, 25.9, 26.2, 29.3, 29.6, 34.7, 68.7, 114.9, 125.6, 128.1, 129.3, 129.7, 148.1, 159.2.

m/z (EI) 806.66 (M$^+$ - C$_{50}$H$_{80}$F$_2$O$_2$Si$_2$ requires 806), 808.66 (34%), 807.64 (67), 650.20 (3), 591.21 (6), 430.09 (16) and 385.12 (20); ^{29}Si, 2.75 (s), 2.90 (s); δ^{19}F, 143.53, F (s).

Butyl(5-((4''-((10-(butyldimethylsilyl)decyl)oxy)-2',3'-difluoro-[1,1':4',1''-terphenyl]-4-yl)oxy)pentyl)dimethylsilane 30e:

Tetrakis(triphenylphosphine)palladium(0.01 g) and (4'-((10-(butyldimethylsilyl)decyl)oxy)-2,3-difluoro-[1,1'-biphenyl]-4-yl)boronic acid (2 g, 4.0 mmol), **29d** were added sequentially to stirred mixture of (5-(4-bromophenoxy)pentyl)(butyl)dimethylsilane (1.85 g, 5.2 mol), **25b** DME (20 ml), add 2M Na$_2$CO$_3$ sol(20 ml), under N$_2$ atmosphere. The stirred mixture was heated under reflux overnight. After confirming the completion of reaction by TLC, the cooled mixture was poured into water and the product was extracted into ether (3 x 75ml), washed with brine, dried (MgSO$_4$), the solvent was removed in *vacuo*. The crude product was purified by column chromatography (silica gel; 10% DCM in hexane) to give butyl(5-((4''-((10-(butyldimethylsilyl)decyl)oxy)-2',3'-difluoro-[1,1':4',1''-terphenyl]-4-yl)oxy)pentyl)dimethylsilane (1.33 g, 49%), **30e** as a white colour solid. Purity: 98.85 % (HPLC); Found: C, 73.25; H, 9.62; C$_{45}$H$_{70}$F$_2$O$_2$Si$_2$ requires C, 73.32; H, 9.57;

^{1}H NMR δ (CDCl$_3$), 0.01 (12 H, d, CH$_2$Si(C*H*$_3$)$_2$CH$_2$), 0.50-0.63 (8 H, m, C*H*$_2$Si(CH$_3$)$_2$C*H*$_2$), 0.94 (6 H, td, *J* 1.8, 6.9, 8.8, CH$_2$C*H*$_3$), 1.26- 1.58 (26 H, m, CH$_2$C*H*$_2$CH$_2$), 1.87 (4 H, m, OCH$_2$C*H*$_2$), 4.06 (4 H, t, *J* 6.4, OC*H*$_2$CH$_2$), 7.05 (4 H, d, ArH), 7.26 (2 H, m, ArH), 7.57, (4 H, d, ArH).

^{13}C NMR δ (CDCl$_3$); Me$_4$Si); -3.3, 13.8, 20.5, 20.8, 24.0, 25.6, 25.9, 26.2, 29.3, 29.6, 34.7, 68.4, 68.7, 114.9, 125.6, 128.1, 129.3, 129.7, 148.1, 159.2.

m/z (EI) 736 (M$^+$ - C$_{45}$H$_{70}$F$_2$O$_2$Si$_2$ requires 736), 355 (8%), 298 (8), 206 (6), 115 (30), 99 (8), 59 (100) and 41 (14); ^{29}Si, 2.75 (s), 2.90 (s); δ^{19}F, 143.53, F (s).

Butyl(4-((2',3'-difluoro-[1,1'-biphenyl]-4-yl)oxy)butyl)dimethylsilane 28a:

Tetrakis(triphenylphosphine)palladium(0.165 g) and (2,3-difluorophenyl)boronic acid (3.6 g, 23.0 mmol), **27** were added sequentially to stirred mixture of (4-(4-bromophenoxy)butyl)(butyl)dimethylsilane (6 g, 17.5 mmol), **25a** DME (50 ml), and 2M Na$_2$CO$_3$ sol (50 ml), under N$_2$ atmosphere. The stirred mixture was heated under reflux overnight. After confirming the completion of reaction by TLC, the cooled mixture was poured into water and the product was extracted into ether (3 x 100 ml), washed with brine, dried (MgSO$_4$). The solvent was removed in *vacuo*. The crude product was purified by column chromatography (silica gel; hexane) to give butyl(4-((2',3'-difluoro-[1,1'-biphenyl]-4-yl)oxy)butyl)dimethylsilane (5.5 g, 84%), **28a** as a colourless oil.

^{1}H NMR δ (CDCl$_3$), 0.00 (6 H, s, CH$_2$Si(CH_3)$_2$CH$_2$), 0.48-0.63 (4 H, m, CH_2Si(CH$_3$)$_2$CH_2), 0.91 (3 H, t, J 7.0, CH$_2$CH_3), 1.23- 1.57 (6 H, m, CH$_2$CH_2CH$_2$), 1.85 (2 H, quint, J 6.6, OCH$_2$CH_2), 4.03 (2 H, t, J 6.4, OCH_2CH$_2$), 7.03 (2 H, d, ArH), 7.07-7.14 (2 H, m, ArH), 7.15-7.22 (1 H, m, ArH), 7.49 (2 H, d, ArH).

^{13}C NMR δ (CDCl$_3$), -3.3 ((CH$_3$)$_2$ Si), 13.8 (CH$_3$), 23.8 (CH$_2$), 23.9(CH$_2$), 24.1 (CH$_2$), 26.6 (CH$_2$), 26.7 (CH$_2$), 33.4 (CH$_2$), 68.0 (O-CH$_2$), 114.5 (C-2 and C-6), 115.3 (2 x CH), 123.9 (C-5), 125.0 (C-6), 130.0 (C$_3$), 130.1 (C$_5$), 130.5 (C-1), 145.5 (F-C-2), 151.5 (F-C-3), 158.2 (C-O).

m/z (EI) 376 (M$^+$ - C$_{22}$H$_{30}$F$_2$OSi requires 376), 378 (3%), 377 (5), 377.2 (24) and 376 (100); δ^{29}Si, 2.77 (s).

6.3 Synthesis of Trifluoroterphenyl silanes:

1-Bromo-2-fluoro-4-(hex-5-en-1-yloxy)benzene 32a:

6-Bromohexene (11.0 g, 0.068 mol) **21c**, 4-bromo-3-fluorophenol (14.3 g, 0.075 mol) **31**, potassium carbonate (28.0 g, 0.206 mol) were stirred in butanone (240 ml). The reaction mixture was heated under reflux overnight under dry N$_2$. After confirming the completion of reaction by TLC, the potassium carbonate was filtered off and butanone was removed *in vacuo*. The crude was dissolved in diethylether (200 ml), washed with 10% NaOH$_{aq}$. solution (140 ml) water (3 x 100 ml) and dried (MgSO$_4$). The solvent was removed in *vacuo* and the product was purified by filtration through a bed of silica (hexane) to gave 1-bromo-2-fluoro-4-(hex-5en-1-yloxy)benzene (16.50 g, 88%) **32a** as a colourless oil.

^{1}H NMR δ (CDCl$_3$), 1.47-1.59 (2 H, m, CH$_2$CH_2CH$_2$), 1.78 (2 H, quint, J 13.4, 6.4, CH$_2$CH_2CH$_2$), 2.45 (2 H, q, J 14.7, 7.3, CH$_2$CH_2CH), 3.91 (2 H, t, J 6.4, OCH_2CH$_2$), 4.95-5.07 (2 H, m, CH$_2$CHCH_2), 5.75- 5.88 (1 H, m, CH$_2$CHCH$_2$), 6.59 (1 H, ddd, J 10.2, 5.6, 3.4, 5-H), 6.68 (1 H, dd, J 10.6, 2.8, 3-H) and 7.38 (1 H, dd, 8.9, 8.1, 6-H).

^{13}C NMR δ (CDCl$_3$); Me$_4$Si); 26.0, 28.7, 33.9, 68.7, 101.7, 104.7, 114.0, 115.7, 133.8, 139.0, 158.0, 166.0.

m/z (EI) 272 (M$^+$ - C$_{12}$H$_{14}$BrFO requires 272), 274 (1%), 275 (12), 274 (97) and 272 (100).

1-Bromo-2-fluoro-4-(hept-6-en-1-yloxy)benzene 32b:

7-Bromoheptene (9.0 g, 0.052 mol) **21e**, 4-bromo-3-fluorophenol (11.0 g, 0.057 mol) **31**, potassium carbonate (22.0 g, 0.154 mol) were stirred in butanone (200 ml). The reaction mixture was heated under reflux overnight under dry N_2. After confirming the completion of reaction by TLC, the potassium carbonate was filtered off and butanone was removed *in vacuo*. The crude was dissolved in diethylether (200 ml), washed with 10% NaOH $_{Aq.}$solution (100 ml) water (3 x 100 ml) and dried (MgSO$_4$). The solvent was removed in *vacuo* and the product was purified by filtration through a bed of silica (hexane) to 1-bromo-2-fluoro-4-(hept-6-en-1-yloxy)benzene (13.40 g, 90%) **32b** as a colourless oil.

^{1}H NMR δ (CDCl$_3$), 1.40-1.50 (4 H, quint, *J* 11.2, 7.3 CH$_2$C*H*$_2$CH$_2$), 1.72-1.83 (2 H, m, CH$_2$C*H*$_2$CH$_2$), 2.03-2.13 (2 H, m, CH$_2$C*H*$_2$CH), 3.90 (2 H, t, *J* 6.5, OC*H*$_2$CH$_2$), 4.92- 5.05 (2 H, m, CH$_2$CHC*H*$_2$), 5.74- 5.87 (1 H, m, CH$_2$C*H*CH$_2$), 6.55-6.62 (1 H, ddd, *J* 11.6, 8.9, 3.8, Ar*H*), 6.64-6.70 (1 H, dd, *J* 10.4, 2.6, Ar*H*) and 7.34-7.41 (1 H, dd, *J* 8.7, 8.1, Ar*H*);

^{13}C NMR δ (CDCl$_3$); Me$_4$Si); 26.0, 29.6, 29.7, 33.9, 68.7, 101.7, 104.7, 114.0, 115.7, 133.8, 139.0, 158.0, 166.0.

m/z (EI) 286 (M$^+$ - C$_{13}$H$_{16}$BrFO requires 286), 290 (1%), 289 (14), 288 (97) and 286 (100).

1-Bromo-2-fluoro-4-(oct-7-en-1-yloxy)benzene 32c:

8-Bromooctene (10.0 g, 0.0518 mol) **21f**, 4-bromo-3-fluorophenol (11.0 g, 0.057 mol) **31**, potassium carbonate (21.0 g, 0.155 mol) were stirred in butanone (200 ml). The reaction mixture was heated under reflux overnight under dry N_2. After confirming the completion of reaction by TLC, the potassium carbonate was filtered off and butanone was removed *in vacuo*. The crude was dissolved in diethylether (200 ml), washed with 10% NaOH $_{aq.}$solution (100 ml) water (3 x 100 ml) and dried (MgSO$_4$). The solvent was removed in *vacuo* and the product was purified by filtration through a bed of silica (hexane) to gave 1-bromo-2-fluoro-4-(oct-7-en-1-yloxy)benzene (14.20 g, 87%) **32c** as a colourless oil.

^{1}H NMR δ (CDCl$_3$), 1.20-1.60 (8 H, m, CH$_2$C*H*$_2$CH$_2$), 1.77 (2 H, quin, *J* 13.2, 6.5, CH$_2$C*H*$_2$CH$_2$), 2.06 (2 H, q, *J* 14.0, 6.7, CH$_2$C*H*$_2$CH), 3.90 (2 H, t, *J* 6.5, OC*H*$_2$CH$_2$), 4.91-5.04 (2 H, m, CH$_2$CHC*H*$_2$), 5.75- 5.87 (1 H, m, CH$_2$C*H*CH$_2$), 6.59 (1 H, ddd, *J* 11.6, 8.7, 2.8, Ar*H*), 6.68 (1 H, dd, *J* 10.4, 2.8, Ar*H*), 7.38 (1 H, dd, *J* 8.9, 8.1, Ar-*H*).

^{13}C NMR δ (CDCl$_3$); Me$_4$Si); 26.0, 29.6, 29.7, 33.9, 68.7, 101.7, 104.7, 114.0, 115.7, 133.8, 139.0, 158.0, 166.0.

m/z (EI) 300 (M$^+$ - C$_{14}$H$_{18}$BrFO requires 300), 304 (1%), 303 (15), 302 (97) and 300 (100).

(6-(4-Bromo-3-fluorophenoxy)hexyl)(butyl)dimethylsilane 33a:

1-Bromo-2-fluoro-4-(hex-5-en-1-yloxy)benzene (8.0 g, 29.3 mmol) **32a**, and butyldimethylsilane (7.0 g, 58.6 mmol) **24** were stirred in toluene (75 ml) with Karstedt's catalyst (80 µL) under dry N$_2$ at room temperature overnight. After confirming the completion of reaction by TLC, toluene was removed in *vacuo.* The product was purified by column chromatography (silica gel; hexane) and dried (P$_2$O$_5$), to give (6-(4-bromo-3-fluorophenoxy)hexyl)(butyl)dimethylsilane (10.50 g, 92 %) **33a** as a colourless liquid.

^{1}H NMR δ (CDCl$_3$), 0.00 (6 H, s, CH$_2$Si(C*H*$_3$)$_2$CH$_2$), 0.44-0.53 (4 H, m, -C*H*$_2$Si(CH$_3$)$_2$C*H*$_2$), 0.87 (3 H, t, *J* 6.9, -CH$_2$C*H*$_3$), 1.20- 1.49 (10 H, m, CH$_2$C*H*$_2$CH$_2$), 1.76 (2 H, quin, *J* 13.3, 6.53, OCH$_2$C*H*$_2$), 3.90 (2 H, t, *J* 6.7, OC*H*$_2$CH$_2$), 6.60 (1 H, ddd, *J* 10.6, 8.8, 2.9, ArH), 6.68 (1 H, dd, *J* 10.4, 2.6, ArH), 7.38 (1 H, dd, *J* 9.0, 8.2, ArH); δ^{19}F, 149.11, F (s).

^{13}C NMR δ (CDCl$_3$); Me$_4$Si); -3.4, 13.8, 20.5, 20.9, 24.2, 26.0, 26.2, 29.0, 29.6, 33.7, 68.4, 101.7, 104.7, 114.2, 133.6, 158.2, 166.0.

m/z (EI) 390 (M$^+$ - C$_{18}$H$_{30}$BrFOSi requires 390), 392 (2%), 390 (3), 389 (20), 388 (99) and 390 (100).

(7-(4-Bromo-3-fluorophenoxy)heptyl)(butyl)dimethylsilane 33b:

1-Bromo-2-fluoro-4-(hept-6-en-1-yloxy)benzene (8.0 g, 29.3 mmol) **32b**, butyldimethylsilane (7.0 g, 58.6 mmol) **24** were stirred in toluene (75 ml) with Karstedt's catalyst (80 µL) under dry N$_2$ at room temperature overnight. After confirming the completion of reaction by TLC, toluene was removed in *vacuo.* The product was purified by column chromatography (silica gel; hexane) and dried (P$_2$O$_5$), to give (7-(4-bromo-3-fluorophenoxy)heptyl)(butyl)dimethylsilane (10.50 g, 92 %) **33b** as a colourless liquid.

^{1}H NMR δ (CDCl$_3$), 0.00 (6H, s, CH$_2$Si(C*H*$_3$)$_2$CH$_2$), 0.43-0.52 (4 H, m, C*H*$_2$Si(CH$_3$)$_2$C*H*$_2$), 0.87 (3 H, t, *J* 7.1, CH$_2$C*H*$_3$), 1.20- 1.48 (12 H, m, CH$_2$C*H*$_2$CH$_2$), 1.77 (2 H, quin, *J* 13.4, 6.7, OCH$_2$C*H*$_2$), 3.91 (2 H, t, *J* 6.5, OC*H*$_2$CH$_2$), 6.59 (1 H, ddd, *J* 10.6, 8.7, 2.8, ArH), 6.68 (1 H, dd, *J* 10.6, 8.7, 2.8, ArH), 7.38 (1 H ,dd, *J* 8.8, 8.1, ArH); δ^{19}F, 149.10, F (s).

^{13}C NMR δ (CDCl$_3$); Me$_4$Si); -3.4, 13.8, 20.5, 20.9, 24.2, 26.0, 26.2, 29.0, 29.3, 29.6, 33.7, 68.4, 101.7, 104.7, 114.2, 133.6, 158.2, 166.0.

m/z (EI) 404 (M$^+$ - C$_{19}$H$_{32}$BrFOSi requires 404), 406 (3%), 403 (25), 405 (26), 402 (98) and 404 (100).

(8-(4-Bromo-3-fluorophenoxy)octyl)(butyl)dimethylsilane 33c:

1-Bromo-2-fluoro-4-(oct-7-en-1-yloxy)benzene (7.0 g, 23.2 mmol) **32a**, butyldimethylsilane (5.40 g, 46.5 mmol) **24** were stirred in toluene (75 ml) with Karstedt's catalyst (70 µL) under dry N$_2$ at room temperature overnight. After confirming the completion of reaction by TLC, toluene was removed in *vacuo*. The product was purified by column chromatography (silica gel; hexane) and dried (P$_2$O$_5$), to give (8-(4-bromo-3-fluorophenoxy)octyl)(butyl)dimethyl-silane (8.75 g, 90 %) **33c** as a colourless liquid.

^{1}H NMR δ (CDCl$_3$), 0.00 (6 H, s, CH$_2$Si(C*H*$_3$)$_2$CH$_2$), 0.42-0.52 (4 H, m, C*H*$_2$Si(CH$_3$)$_2$C*H*$_2$), 0.87 (3 H, t, *J* 6.9, CH$_2$C*H*$_3$), 1.20- 1.48 (14 H, m, CH$_2$C*H*$_2$CH$_2$), 1.77 (2 H, quin, *J* 13.4, 6.7, OCH$_2$C*H*$_2$), 3.90 (2 H, t, *J* 6.5, OC*H*$_2$CH$_2$), 6.59 (1 H, ddd, *J* 11.8, 8.9, 2.8, ArH), 6.68 (1 H, dd, *J* 10.4, 2.6, ArH), 7.38 (1 H ,dd, *J* 8.6, 8.1, ArH); δ^{19}F, 149.10, F (s).

^{13}C NMR δ (CDCl$_3$); Me$_4$Si); -3.4, 13.8, 20.5, 20.9, 24.2, 26.0, 26.2, 29.0, 29.3, 29.6, 33.7, 68.4, 101.7, 104.7, 114.2, 133.6, 158.2, 166.0.

m/z (EI) 418 (M$^+$ - C$_{20}$H$_{34}$BrFOSi requires 418), 420 (3%), 417 (5), 419 (21), 416 (99) and 418 (100).

Butyl(6-((4''-((10-(butyldimethylsilyl)decyl)oxy)-2,2',3'-trifluoro-[1,1',4',1''-terphenyl]-4-yl)oxy)hexyl)dimethylsilane 34a:

Tetrakis(triphenylphosphine)palladium (0.02 g) and (4'-((10-(butyldimethylsilyl)decyl)oxy)-2,3-difluoro-[1,1'-biphenyl]-4-yl)boronicacid (1.60 g, 4.1 mmol), **29a** were added sequentially to stirred mixture of (6-(4-bromo-3-fluorophenoxy)hexyl)(butyl)dimethylsilane (1.63 g, 3.2 mmol), **33a** and DME (50 ml) under N$_2$ atmosphere. The stirred mixture was heated under reflux overnight. After confirming the completion of reaction by TLC, the cooled mixture was poured into water and the product was extracted into ether (3 x 100 ml), washed with brine, dried (MgSO$_4$), the solvent was removed in *vacuo*. The crude product was

purified by column chromatography (silica gel; 10% DCM in hexane) give a butyl(6-((4''-((10-(butyldimethylsilyl)decyl)oxy)-2,2',3'-trifluoro-[1,1',4',1''-terphenyl]-4-yl)oxy)hexyl)dimethylsilane (0.52 g, 16%) **34a** as a white colour solid. Purity: 98.99 % (HPLC); Found: C, 71.63; H, 9.54; $C_{45}H_{70}F_2O_2Si_2$ requires C, 71.83; H, 9.30.

^{1}H NMR δ (CDCl$_3$), 0.00 (12 H, m, CH$_2$Si(CH_3)$_2$CH$_2$), 0.50-0.63 (8 H, m, CH_2Si(CH$_3$)$_2$CH_2), 0.93 (6 H, td, J 1.8, 6.9, 8.8, CH$_2$CH_3), 1.27- 1.50 (28 H, m, CH$_2$CH_2CH$_2$), 1.85 (4 H, m, OCH$_2$CH_2), 4.06 (4 H, t, J 6.4, OCH_2CH$_2$), 6.8 (2 H, d, ArH), 7.04 (2H, m), 7.33 (3 H, m, ArH), 7.56 (2 H, d, ArH);

^{13}C NMR δ (CDCl$_3$); Me$_4$Si); -3.4, 13.8, 15.2, 23.8, 23.9, 25.9, 26.0, 26.2, 26.6, 29.0, 29.1, 29.2, 29.3, 29.4, 29.5, 29.6, 33.3, 33.7, 68.1, 68.4, 102.2, 102.4, 110.7, 114.2, 114.3, 123.6, 124.1, 125.6, 126.7, 129.8, 129.9, 130.0, 131.6, 149.4, 149.5, 159.2, 160.8, 161.6.

m/z (EI) 768 (M$^+$ - $C_{46}H_{71}F_3O_2Si_2$ requires 768), 771 (1%), 770 (7), 769 (50) and 768 (100); δ^{19}F, -143.4, -139.6, -112.3 F (s), δ^{29}Si, 2.74, 2.77 (s).

Butyl(7-((4''-((10-(butyldimethylsilyl)decyl)oxy)-2,2',3'-trifluoro-[1,1',4',1''-terphenyl]-4-yl)oxy)heptyl)dimethylsilane 34b:

Tetrakis(triphenylphosphine)palladium (0.02 g) and (4'-((10-(butyldimethylsilyl)decyl)oxy)-2,3-difluoro-[1,1'-biphenyl]-4-yl)boronicacid (1.60 g, 3.2 mmol), **29a** were added sequentially to stirred mixture of (7-(4-bromo-3-fluorophenoxy)heptyl)(butyl)dimethylsilane (1.68 g, 4.2 mmol), **33b** and DME (50 ml) under N$_2$ atmosphere. The stirred mixture was heated under reflux overnight. After confirming the completion of reaction by TLC, the cooled mixture was poured into water and the product was extracted into ether (3 x 100 ml), washed with brine, dried (MgSO$_4$), the solvent was removed in *vacuo*. The crude product was purified by column chromatography (silica gel; 10% DCM in hexane) give a butyl(7-((4''-((10-(butyldimethylsilyl)decyl)oxy)-2,2',3'-trifluoro-[1,1',4',1''-terphenyl]-4-yl)oxy)heptyl)dimethylsilane (0.82 g, 25%) **34b** as a white colour solid. Purity: 98.99 % (HPLC); Found: C, 72.25; H, 9.49; $C_{45}H_{70}F_2O_2Si_2$ requires C, 72.07; H, 9.39.

^{1}H NMR δ (CDCl$_3$), 0.00 (12 H, d, CH$_2$Si(CH_3)$_2$CH$_2$), 0.49-0.59 (8 H, m, CH_2Si(CH$_3$)$_2$CH_2), 0.94 (6 H, td, J 1.8, 6.9, 8.8, CH$_2$CH_3), 1.27- 1.45 (22 H, m, CH$_2$CH_2CH$_2$), 1.50 (4 H, m, OCH$_2$CH_2), 4.06 (4 H, q, J 6.4, OCH_2CH$_2$), 6.81 (4 H, d, ArH), 7.04 (2 H, m, ArH), 7.20, (2 H, m, ArH), 7.36, (1 H, dd, J 8.6, 8.1, ArH), 7.58, (2 H, d, ArH) ;

^{13}C NMR δ (CDCl$_3$); Me$_4$Si); -3.4, 13.8, 15.2, 23.8, 23.9, 25.9, 26.0, 26.2, 26.6, 29.0, 29.1, 29.2, 29.3, 29.4, 29.5, 29.6, 33.3, 33.7, 68.1, 68.4, 102.2, 102.4, 110.7, 114.2, 114.3, 123.6, 124.1, 125.6, 126.7, 129.8, 129.9, 130.0, 131.6, 149.4, 149.5, 159.2, 160.8, 161.6.

m/z (EI) 782 (M$^+$ - C$_{47}$H$_{73}$F$_3$O$_2$Si$_2$ requires 782), 784 (7%), 783 (51) and 782 (100); δ^{19}F, -143.4, -139.6, -112.3 F (s), δ^{29}Si, 2.74, 2.77 (s).

Butyl(8-((4''-((10-(butyldimethylsilyl)decyl)oxy)-2,2',3'-trifluoro-[1,1':4',1''-terphenyl]-4-yl)oxy)octyl)dimethylsilane 34c:

Tetrakis(triphenylphosphine)palladium (0.02 g) and (4'-((10-(butyldimethylsilyl)decyl)oxy)-2,3-difluoro-[1,1'-biphenyl]-4-yl)boronicacid (1.73 g, 4.15 mmol), **29a** were added sequentially to stirred mixture of (8-(4-bromo-3-fluorophenoxy)octyl)(butyl)dimethylsilane (1.60 g, 3.20 mmol), **33c** and DME (50 ml) under N$_2$ atmosphere. The stirred mixture was heated under reflux overnight. After confirming the completion of reaction by TLC, the cooled mixture was poured into water and the product was extracted into ether (3 x 100 ml), washed with brine, dried (MgSO$_4$) and the solvent was removed in *vacuo*. The crude product was purified by column chromatography (silica gel; 10% DCM in hexane) to give butyl(8-((4''-((10-(butyldimethylsilyl)decyl)oxy)-2,2',3'-trifluoro-[1,1':4',1''-terphenyl]-4-yl)oxy)octyl)dimethylsilane (0.30 g, 9%) **34c** as a white colour solid. Found: C, 73.33; H, 9.48; C$_{45}$H$_{70}$F$_2$O$_2$Si$_2$ requires C, 72.31; H, 9.48.

^{1}H NMR δ (CDCl$_3$), 0.00 (12 H, d, CH$_2$Si(C*H*$_3$)$_2$CH$_2$), 0.49-0.59 (8 H, m, C*H*$_2$Si(CH$_3$)$_2$C*H*$_2$), 0.93 (6 H, t, *J* 6.9, CH$_2$C*H*$_3$), 1.26- 1.45 (32 H, m, CH$_2$C*H*$_2$CH$_2$), 1.87 (4 H, q, 6.56, 13.68, OCH$_2$C*H*$_2$), 4.04 (4 H, q, *J* 6.5, OC*H*$_2$CH$_2$), 6.83 (2 H, m, ArH), 7.05 (2 H, dd, *J* 2.2, 8.96, ArH), 7.4, (1 H, m, ArH), 7.57 (2 H, dd, *J* 3.5, 8.7, ArH);

^{13}C NMR δ (CDCl$_3$); Me$_4$Si); -3.4, 13.8, 15.2, 23.8, 23.9, 25.9, 26.0, 26.2,26.3, 26.6, 29.0, 29.1, 29.2, 29.3, 29.4, 29.5, 29.6, 33.3, 33.7, 68.1, 68.4, 102.2, 102.4, 110.7, 114.2, 114.3, 123.6, 124.1, 125.6, 126.7, 129.8, 129.9, 130.0, 131.6, 149.4, 149.5, 159.2, 160.8, 161.6.

m/z (EI) 796 (M$^+$ - C$_{48}$H$_{75}$F$_3$O$_2$Si$_2$ requires 796), 800 (1%), 798 (7), 798 (19), 797 (63) and 796 (100); δ^{19}F, -143.4, -139.6, -112.3 F (s), δ^{29}Si, 2.74, 2.77 (s).

(((2,2',3'-Trifluoro-[1,1',4',1''-terphenyl]-4,4''-diyl)bis(oxy))bis(hexane-6,1-diyl))bis(butyldimethylsilane) 34d:

Tetrakis(triphenylphosphine)palladium (0.02 g) and (4'-((6-(butyldimethylsilyl)hexyl)oxy)-2,3-difluoro-[1,1'-biphenyl]-4-yl)boronic acid (1.10 g, 2.5 mmol), **29b** were added sequentially to stirred mixture of (6-(4-bromo-3-fluorophenoxy)hexyl)(butyl)dimethylsilane (1.26 g, 3.2 mmol), **33a** and DME (50 ml) under N_2 atmosphere. The stirred mixture was heated under reflux overnight. After confirming the completion of reaction by TLC, the cooled mixture was poured into water and the product was extracted into ether (3 x 100 ml), washed with brine, dried (MgSO$_4$) and the solvent was removed in *vacuo*. The crude product was purified by column chromatography (silica gel; 10% DCM in hexane) to give (((2,2',3'-trifluoro-[1,1',4',1''-terphenyl]-4,4''-diyl)bis(oxy))bis(hexane-6,1-diyl))bis(butyldimethylsilane) (0.61 g, 26%) **34d** as a white colour solid. Found: C, 70.51; H, 9.16; $C_{45}H_{70}F_2O_2Si_2$ requires C, 70.74; H, 8.90.

^{1}H NMR δ (CDCl$_3$), 0.00 (12 H, d, CH$_2$Si(CH_3)$_2$CH$_2$), 0.49-0.59 (8 H, m, CH_2Si(CH$_3$)$_2$CH_2), 0.93 (6 H, t, *J* 6.92, CH$_2$CH_3), 1.25- 1.49 (16 H, m, CH$_2$CH_2CH$_2$), 1.85 (4 H, m, OCH$_2$CH_2), 4.04 (4 H, q, *J* 6.5, 14.3, OCH_2CH$_2$), 6.75-6.85 (2H, m), 7.04 (2 H, d, ArH), 7.36 (1 H, m, ArH), 7.56, (2 H, dd, *J* 3.48, 8.8, ArH);

^{13}C NMR δ (CDCl$_3$); Me$_4$Si); -3.4, 13.8, 15.0, 23.8, 25.7, 26.1, 26.6, 29.0, 29.2, 29.4, 29.5, 29.6, 29.7, 33.3, 33.4, 33.7, 68.1, 68.5, 102.2, 110.7, 114.2, 114.3, 123.6, 125.6, 126.7, 129.8, 129.9, 130.0, 131.7, 146.9, 147.0, 159.2, 160.6, 161.6.

m/z (EI) 713 (M$^+$ - $C_{42}H_{63}F_3O_2Si_2$ requires 712), 715 (3%), 713 (10), 713 (45), and 712 (100); δ^{19}F, -143.4, -139.6, -112.3 F (s), δ^{29}Si, 2.74, 2.77 (s).

Butyl(6-((4''-((7-(butyldimethylsilyl)heptyl)oxy)-2',2'',3'-trifluoro-[1,1',4',1''-terphenyl]-4-yl)oxy)hexyl)dimethylsilane 34e:

Tetrakis(triphenylphosphine)palladium (0.02 g) and (4'-((6-(butyldimethylsilyl)hexyl)oxy)-2,3-difluoro-[1,1'-biphenyl]-4-yl)boronic acid (1.10 g, 2.5 mmol), **29b** were added sequentially to stirred mixture of (7-(4-bromo-3-fluorophenoxy)heptyl)(butyl)dimethylsilane (1.30 g, 3.2 mmol), **33b** and DME (50 ml) under N_2 atmosphere. The stirred mixture was heated under reflux overnight. After confirming the completion of reaction by TLC, the

cooled mixture was poured into water and the product was extracted into ether (3 x 100 ml), washed with brine, dried (MgSO$_4$) and the solvent was removed in *vacuo*. The crude product was purified by column chromatography (silica gel; 10% DCM in hexane) to give butyl(6-((4''-((7-(butyldimethylsilyl)heptyl)oxy)-2',2'',3'-trifluoro-[1,1',4',1''-terphenyl]-4-yl)oxy)hexyl)dimethylsilane (0.40 g, 17%) **34e** as a colourless solid. Found: C, 70.93; H, 9.27; C$_{45}$H$_{70}$F$_2$O$_2$Si$_2$ requires C, 71.03; H, 9.01.

^{1}H NMR δ (CDCl$_3$), 0.00 (12 H, s, CH$_2$Si(CH_3)$_2$CH$_2$), 0.49-0.59 (8 H, m, CH_2Si(CH$_3$)$_2$CH_2), 0.93 (6 H, t, *J* 6.9, CH$_2$CH_3), 1.25- 1.55 (22 H, m, CH$_2$CH_2CH$_2$), 1.86 (4 H, quin,, *J* 13.48, 6.7, OCH$_2$CH_2), 4.05 (4 H, q, *J* 6.5, OCH_2CH$_2$), 6.77-6.85 (2H, m) 7.04 (2 H, td, *J* 2.84, 4.88, ArH), 7.36 (1 H, m, ArH), 7.54-7.59, (2 H, m, ArH);

^{13}C NMR δ (CDCl$_3$); Me$_4$Si); -3.4, 13.8, 15.0, 23.9, 25.7, 26.0, 26.2, 26.6, 29.0, 29.1, 29.2, 29.3, 33.4, 33.6, 68.1, 68.5, 102.2, 110.7, 114.2, 114.3, 123.6, 124.2, 125.6, 126.7, 129.08, 129.9, 130.0, 130.3, 131.7, 147.0, 147.3, 149.9, 159.2, 160.8.

m/z (EI) 727 (M$^+$ - C$_{45}$H$_{70}$F$_2$O$_2$Si$_2$ requires 726), 729 (1%), 728 (7), 727 (46) and 726 (100); δ^{19}F, -143.4, -139.6, -112.3 F (s), δ^{29}Si, 2.74, 2.77 (s).

Butyl(8-((4''-((6-(butyldimethylsilyl)hexyl)oxy)-2,2',3'-trifluoro-[1,1',4',1''-terphenyl]-4-yl)oxy)octyl)dimethylsilane 34f:

Tetrakis(triphenylphosphine)palladium (0.02 g) and (4'-((6-(butyldimethylsilyl)hexyl)oxy)-2,3-difluoro-[1,1'-biphenyl]-4-yl)boronic acid (1.10 g, 2.50 mmol), **29b** were added sequentially to stirred mixture of (8-(4-bromo-3-fluorophenoxy)octyl)(butyl)dimethylsilane (1.35 g, 3.25 mmol), **33c** and DME (50 ml) under N$_2$ atmosphere. The stirred mixture was heated under reflux overnight. After confirming the completion of reaction by TLC, the cooled mixture was poured into water and the product was extracted into ether (3 x 100 ml), washed with brine, dried (MgSO$_4$) and the solvent was removed in *vacuo*. The crude product was purified by column chromatography (silica gel; 10% DCM in hexane) to give butyl(8-((4''-((6-(butyldimethylsilyl)hexyl)oxy)-2,2',3'-trifluoro-[1,1',4',1''-terphenyl]-4-yl)oxy)octyl)dimethylsilane (0.40 g, 17%) **34f** as a colourless solid. Found: C, 71.19; H, 9.37; C$_{44}$H$_{67}$F$_3$O$_2$Si$_2$ requires C, 71.30; H, 9.11.

^{1}H NMR δ (CDCl$_3$), 0.00 (12 H, d, CH$_2$Si(CH_3)$_2$CH$_2$), 0.49-0.59 (8 H, m, CH_2Si(CH$_3$)$_2$CH_2), 0.93 (6 H, t, *J* 6.9, CH$_2$CH_3), 1.26- 1.58 (24 H, m, CH$_2$CH_2CH$_2$), 1.86 (4 H, quin, *J* 13.7, 6.8

, OCH$_2$CH_2), 4.06 (4 H, q, *J* 6.8, OCH_2CH$_2$), 6.76-6.86 (2H, m), 7.05 (2 H, td, ArH), 7.33-7.40 (1 H, m, ArH), 7.57-7.60, (2 H, d, ArH);

^{13}C NMR δ (CDCl$_3$); Me$_4$Si); -3.4, 13.8, 15.0, 23.9, 25.7, 26.0, 26.2, 26.6, 29.0, 29.2, 29.3, 33.4, 33.6, 68.1, 68.5, 102.2, 110.7, 114.2, 114.3, 123.6, 124.2, 125.6, 126.7, 129.08, 129.9, 130.0, 130.3, 131.7, 147.0, 147.3, 149.9, 159.2, 160.8.

m/z (EI) 741 (M$^+$ - C$_{44}$H$_{67}$F$_3$O$_2$Si$_2$ requires 740), 743 (1%), 741 (10), 742 (11), 741 (48) and 740 (100); δ^{19}F, -143.4, -139.6, -112.3 F (s), δ^{29}Si, 2.74, 2.77 (s).

Butyl(4-((2'-fluoro-4''-pentyl-[1,1':4',1''-terphenyl]-4-yl)oxy)butyl)dimethylsilane 37a:

Tetrakis(triphenylphosphine)palladium (0.02 g) and (3-fluoro-4'-pentyl-[1,1'-biphenyl]-4-yl)boronic acid (2.16 g, 7.57 mmol), **36** were added sequentially to stirred mixture of (8-(4-bromo-3-fluorophenoxy)octyl)(butyl)dimethylsilane (2 g, 5.82 mmol), **25a** and DME (50 ml) under N$_2$ atmosphere. The stirred mixture was heated under reflux overnight. After confirming the completion of reaction by TLC, the cooled mixture was poured into water and the product was extracted into ether (3 x 100 ml), washed with brine, dried (MgSO$_4$) and the solvent removed in *vacuo*. The crude product was purified by column chromatography (silica gel; 10% DCM in hexane) to give butyl(4-((2'-fluoro-4''-pentyl-[1,1':4',1''-terphenyl]-4-yl)oxy)butyl)dimethylsilane (1.2 g, 48%) **37a** as a colourless solid. . Found: C, 78.31; H, 8.99; C$_{33}$H$_{45}$FOSi requires C, 78.31; H, 9.23.

^{1}H NMR δ (CDCl$_3$), 0.00 (6 H, s, CH$_2$Si(CH_3)$_2$CH$_2$), 0.50-0.63 (14 H, m, CH_2Si(CH$_3$)$_2$CH_2), 0.88-0.97 (6 H, m, CH$_2$CH_3), 1.25- 1.54 (10 H, m, CH$_2$CH_2CH$_2$), 1.68 (2 H, quin, *J* 14.7, 7.1 OCH$_2$CH_2), 4.04 (2 H, t, *J* 6.2, OCH_2CH$_2$), 7.01 (2H, dt, *J* 9.8, 5.1, 3.0, ArH), 7.30 (1 H, s, ArH), 7.36-7.52, (4 H, m, ArH), 7.54-7.59, (4 H, m, ArH);

^{13}C NMR δ (CDCl$_3$); Me$_4$Si); -3.4, 13.8, 15.0 ,20.5, 22.5, 26.1, 26.6, 29.7, 31.1, 31.5, 35.6, 67.7, 114.2, 114.4, 114.5, 122.6, 127.0, 127.2, 127.7, 129.0, 130.0, 130.6, 137.0, 141.6, 142.7, 158.8, 161.2.

m/z (EI) 504 (M$^+$ - C$_{33}$H$_{45}$FOSi requires 504), 505 (8%), 184 (8), 333 (6), 368 (30), 425 (80), 482 (90) and 41 (14); δ^{19}F, -118.1, F (s).

Butyl(10-((2'-fluoro-4''-pentyl-[1,1':4',1''-terphenyl]-4-yl)oxy)decyl)dimethylsilane 37b:

Tetrakis(triphenylphosphine)palladium (0.02 g) and (3-fluoro-4'-pentyl-[1,1'-biphenyl]-4-yl)boronic acid (1.74 g, 6.0 mmol), **36** were added sequentially to stirred mixture of (10-(4-bromophenoxy)decyl)(butyl)dimethylsilane (2.0 g, 4.67 mol), **25d** and DME (50 ml) under N_2 atmosphere. The stirred mixture was heated under reflux overnight. After confirming the completion of reaction by TLC, the cooled mixture was poured into water and the product was extracted into ether (3 x 100 ml), washed with brine, dried ($MgSO_4$) and the solvent was removed in *vacuo*. The crude product was purified by column chromatography (silica gel; 10% DCM in hexane) to give butyl(4-((2'-fluoro-4''-pentyl-[1,1':4',1''-terphenyl]-4-yl)oxy)butyl)dimethylsilane (0.3 g, 11%) **37b** as a colourless solid. Found: C, 79.83; H, 10.00; $C_{39}H_{57}FOSi$ requires C, 79.53; H, 9.76.

^{1}H NMR δ (CDCl$_3$), 0.00 (6 H, s, CH$_2$Si(C*H*$_3$)$_2$CH$_2$), 0.49-0.57 (4 H, m, C*H*$_2$Si(CH$_3$)$_2$C*H*$_2$), 0.88-0.97 (6 H, m, CH$_2$C*H*$_3$), 1.25- 1.54 (24 H, m, CH$_2$C*H*$_2$CH$_2$), 2.39 (4 H, quin, *J* 3.7, 1.8 , OCH$_2$C*H*$_2$), 2.73 (2 H, quin, *J* 3.4, 1.6, OC*H*$_2$CH$_2$), 4.08(2H, t, *J* 6.5) 7.10 (3 H, dt, *J* 9.8, 4.9, 2.8, ArH), 7.37 (3 H, dt, *J* 9.8, 4.1, 2.5, ArH), 7.55-7.68, (3 H, m, ArH), 7.72 (2 H, dt, *J* 9.8, 4.1, 2.5, ArH);

^{13}C NMR δ (CDCl$_3$); Me$_4$Si); -3.4, 13.8, 15.0 ,20.5, 22.5, 26.1, 26.6, 29.7, 29.8, 29.9, 31.1, 31.5, 33.0, 35.6, 67.7, 114.2, 114.4, 114.5, 122.6, 127.0, 127.2, 127.7, 129.0, 130.0, 130.6, 137.0, 141.6, 142.7, 158.8, 161.2.

m/z (EI) 588 (M$^+$ - C$_{39}$H$_{57}$FOSi requires 588), 531 (2%), 391 (8), 334 (6), 277 (30), 248 (8), 59(100) and 43 (14); δ^{19}F, -118.1, F (s).

6.4 Synthesis of Mono fluoroterphenyl silanes:

Butyl(7-((4''-(decyloxy)-2-fluoro-[1,1':4',1''-terphenyl]-4-yl)oxy)heptyl)dimethylsilane 41a:

Tetrakis(triphenylphosphine)palladium (0.02 g) and (4'-(decyloxy)-[1,1'-biphenyl]-4-yl)boronic acid (1.7 g, 4.81 mmol), **40a** were added sequentially to stirred mixture of (7-(4-bromo-3-fluorophenoxy)heptyl)(butyl)dimethylsilane (1.5 g, 3.70 mmol), **33b** and DME (50 ml) under N_2 atmosphere. The stirred mixture was heated under reflux overnight. After confirming the completion of reaction by TLC, the cooled mixture was poured into water and the product was extracted into ether (3 x 100 ml), washed with brine, dried (MgSO$_4$) and the solvent removed in *vacuo*. The crude product was purified by column chromatography (silica gel; 10% DCM in hexane) to give butyl(7-((4''-(decyloxy)-2-fluoro-[1,1':4',1''-terphenyl]-4-yl)oxy)heptyl)dimethylsilane (0.2 g, 11%) **41a** as a colourless solid. Found: C, 77.79; H, 10.00; $C_{41}H_{61}FO_2Si$ requires C, 77.79; H, 9.71.

^{1}H NMR δ (CDCl$_3$), -0.05 (6 H, t, *J* 3.0, CH$_2$Si(C*H*$_3$)$_2$CH$_2$), 0.49-0.58 (4 H, m, C*H*$_2$Si(CH$_3$)$_2$C*H*$_2$), 0.90-0.97 (6 H, m, CH$_2$C*H*$_3$), 1.20- 1.51 (26 H, m, CH$_2$C*H*$_2$CH$_2$), 1.80 (4 H, quin, *J* 7.2, 14.6, OCH$_2$C*H*$_2$), 4.04 (4 H, quin, *J* 13.8, 6.5, OC*H*$_2$CH$_2$), 6.68-6.80 (2H, m), 6.98 (2 H, dt, *J* 9.4, 4.9, 2.6 , ArH), 7.05 (4 H, d, ArH), 7.25 (4 H, m, ArH), 7.52-7.60 (3 H, m, ArH);

^{13}C NMR δ (CDCl$_3$); Me$_4$Si); -3.3, 13.8, 14.1 , 22.7, 23.8, 25.9, 26.0, 26.1, 26.6, 29.0, 29.1, 29.2, 29.3, 29.4, 29.5, 29.6, 31.8, 33.6, 68.1, 68.4, 102.4, 110.8, 114.8, 120.7, 126.6, 128.0, 129.0, 130.8, 133.0, 134.1, 139.6, 159.1, 159.7, 161.6.

m/z (EI) 632 (M$^+$ - $C_{41}H_{61}FO_2Si$ requires 632), 635 (8%), 386 (8), 246 (6), 115 (3), 55 (100) and 41 (14); δ^{19}F, 115.4, F (s).

Butyl(7-((2-fluoro-4''-(octyloxy)-[1,1':4',1''-terphenyl]-4-yl)oxy)heptyl)dimethylsilane 41b:

Tetrakis(triphenylphosphine)palladium (0.02 g) and (4'-(decyloxy)-[1,1'-biphenyl]-4-yl)boronic acid (1.6 g, 4.81 mmol), **40b** were added sequentially to stirred mixture of (7-(4-bromo-3-fluorophenoxy)heptyl)(butyl)dimethylsilane (1.5 g, 3.70 mmol), **33b** and DME (50 ml) under N_2 atmosphere. The stirred mixture was heated under reflux overnight. After confirming the completion of reaction by TLC, the cooled mixture was poured into water and

the product was extracted into ether (3 x 100 ml), washed with brine, dried (MgSO$_4$) and the solvent removed in *vacuo*. The crude product was purified by column chromatography (silica gel; 10% DCM in hexane) to give butyl(7-((4"-(decyloxy)-2-fluoro-[1,1':4',1"-terphenyl]-4-yl)oxy)heptyl)dimethylsilane (1.22 g, 54%) **41b** as a colourless solid. Found: C, 77.39; H, 9.80; C$_{39}$H$_{57}$FO$_2$Si requires C, 77.43; H, 9.50.

^{1}H NMR δ (CDCl$_3$), 0.00 (6 H, t, *J* 3.7 CH$_2$Si(C*H$_3$*)$_2$CH$_2$), 0.50-0.57 (4 H, m, C*H$_2$*Si(CH$_3$)$_2$C*H$_2$*), 0.90-0.97 (6 H, m, CH$_2$C*H$_3$*), 0.28- 1.48 (22 H, m, CH$_2$C*H$_2$*CH$_2$), 1.86 (4 H, quin, *J* 14.6, 7.3, OCH$_2$C*H$_2$*), 4.05 (4 H, quin, *J* 14.3, 6.8, OC*H$_2$*CH$_2$), 6.73-6.85 (2 H, m, ArH), 7.03 (2 H, dt, *J* 9.37, 4.8, 2.6, ArH), 7.31 (4 H, m, ArH), 7.58-7.68 (3 H, m, ArH);

^{13}C NMR δ (CDCl$_3$); Me$_4$Si); -3.3, 13.8, 14.1, 22.7, 23.8, 25.9, 26.2, 26.6, 29.0, 29.1, 29.2, 29.4, 31.8, 33.6, 68.1, 68.4, 102.6, 110.8, 114.8, 120.7, 126.6, 128.0, 129.0, 130.8, 133.0, 134.1, 139.6, 159.1, 159.7, 161.6.

m/z (EI) 604 (M$^+$ - C$_{39}$H$_{57}$FO$_2$Si requires 604), 449 (8%), 292 (8), 168 (6), 115 (30), 99 (8), 59 (8) and 43 (4); δ^{19}F, -118.1, F (s).

Butyl(7-((2-fluoro-4"-pentyl-[1,1':4',1"-terphenyl]-4-yl)oxy)heptyl)dimethylsilane 39:

Tetrakis(triphenylphosphine)palladium (0.02 g) and (4'-(decyloxy)-[1,1'-biphenyl]-4-yl)boronic acid (1.6 g, 4.81 mmol), **40b** were added sequentially to stirred mixture of (7-(4-bromo-3-fluorophenoxy)heptyl)(butyl)dimethylsilane (1.5 g, 3.70 mmol), **33b** and DME (50 ml) under N$_2$ atmosphere. The stirred mixture was heated under reflux overnight. After confirming the completion of reaction by TLC, the cooled mixture was poured into water and the product was extracted into ether (3 x 100 ml), washed with brine, dried (MgSO$_4$) and the solvent removed in *vacuo*. The crude product was purified by column chromatography (silica gel; 10% DCM in hexane) to give butyl(7-((4"-(decyloxy)-2-fluoro-[1,1':4',1"-terphenyl]-4-yl)oxy)heptyl)dimethylsilane (1.22 g, 54%) **39** as a colourless solid. Found: C, 79.53; H, 10.08; C$_{36}$H$_{51}$FOSi requires C, 79.07; H, 9.40.

^{1}H NMR δ (CDCl$_3$), 0.00 (6 H, t, *J* 3.3, CH$_2$Si(C*H$_3$*)$_2$CH$_2$), 0.51-0.55 (4 H, m, C*H$_2$*Si(CH$_3$)$_2$C*H$_2$*), 0.90-1.0 (6 H, m, CH$_2$C*H$_3$*), 1.26- 1.45 (16 H, m, CH$_2$C*H$_2$*CH$_2$), 1.71 (2 H, quin, *J* 14.6, 7.3, OCH$_2$C*H$_2$*), 1.86 (2 H, quin, *J* 13.6, 6.7, ArCH$_2$C*H$_2$*), 2.70 (2H, t, *J* 7.6, ArC*H$_2$*CH$_2$), 4.04 (2H, t, *J* 6.6, OC*H$_2$*CH$_2$), 6.74-6.85 (2 H, m, ArH), 7.31 (4 H, m, Ar*H*), 7.57-7.65 (4 H, m, Ar*H*), 7.69 (1H, dt, *J* 8.4, 3.9, Ar*H*);

^{13}C NMR δ (CDCl$_3$); Me$_4$Si); -3.4, 13.8, 15.0 ,20.5, 22.5, 24.0, 26.1, 26.6, 29.6, 31.1, 31.5, 33.0, 35.6, 67.7, 112.2, 114.2, 122.6, 127.2, 127.7, 129.0, 130.0, 137.0, 138.0, 142.7, 158.8, 161.2.

m/z (EI) 546, (M$^+$ - C$_{36}$H$_{51}$FOSi requires 546.4), 391 (8%), 334 (8), 315 (6), 277 (30), 167 (8), 59 (100) and 43 (4); δ^{19}F, -115.5, F (s).

7.0 References:

1.   W. Heintz, *J. Prakt. Chem.*, 1855, **66**, 1.

2.   O. Lehmann, *Z. Physik. Chem.,* 1889, **4**, 462

3.   A. W. C. Fries, *"Electroluminescent Liquid Crystals for Organic Light-Emitting Diodes"*, Practical Report, University of Hull, 2004.

4.   M. P. Aldred, PhD thesis, University of Hull, 2004.

5.   F. Reinitzer, *Monatsch. Chem.*, 1888, **9**. 422.

6.   H. Kelker and B. Scheurle, *Angew. Chem. Int. Ed.,* 1969, **8**, 884.

7.   G. W. Gray, K. J. Harrison and J. A. Nash. *Electronics Lett.,* 1973, **9**, 130.

8.   L. Gattermann and A. Rischke, *Ber. Dtcsh. Chem. Ges.,* 1890, **23**, 1738.

9.   G. Friedel, *Ann. Phys.,* 1922, **18**, 273.

10.   H. Coles, D. Demus, J. W. Goodby, G. W. Gray, H. W. Spiess and V. Vill, Wiley-VCH, Weinheim, *Handbook of Liquid Crystals*, 2A, Chapter IV, **2**, 1998.

11.   G. W. Gray, K. J. Harrison and J. A. Nash, *Electron*. Lett., 1973, **10**, 130.

12.   T. Uchida, *Mol. Cryst. Liq. Cryst.,* 1985, **123**, 15.

13.   A. F. Schenz, V. D. Neff and T. W. Schenz, *Mol. Cryst. Liq. Cryst.,* 1973, **23**.

14.   M. Schadt and W. Helfrich, *Appl. Phys. Lett*., 1971, **18**, 127.

15.   N. A. Clark and S. T. Lagerwall, *Appl. Phys. Lett*., 1980, **36**, 899.

16.   P. Kirsch and Merck KGAA, *20th Int. Liq.Cryst. Conf*. (ILCC-20), Ljubljana, Slovenia, 2004.

17.   O. R. Lozman, PhD Thesis, Univeristy of Leeds, 2000.

18.   M. P. Aldred, PhD Thesis, University of Hull, 2004.

19.   P. J. Collings, and M. Hird, *Introduction to Liquid Crystals*, Taylor and Francis, Bristol, 1997.

20.   A. de Vries, *Liq.Cryst., Proc. Int. Conf. in Pramana. Suppl ,* Bangalore, 1, **93**, 1973.

21.   F. Reinitzer, *Monatsch. Chem*., 1888, **421**.

22.   P. G. de Gennes and J. Prost, *The Physics of Liquid Crystals*. Oxford, Clarendon Press, 1993.

23.   S. Chandrasekhar, *Liquid Crystals* (2nd ed.), Cambridge, Cambridge University Press, 1992.

24.   Y. Shao and T. W. Zerda, *J. Chem. Phys*., B*,* 1998, **102**, 3387.

25.   J. A. Rego, A. A. H. Jamie, L. A. MacKinnon and G. Elysse*, Liq. Cryst*., 2010, **37,** 37.

26. L. A. Madsen, T. J. Dingemans, M. Nakata, and E. T. Samulski, *Phys. Rev. Lett.,* 2004, **92**, 145505.

27. I. Dierking, *Textures of Liquid Crystals*, Wiley-VCH, Weinheim, 2003, 54.

28. V. I. Kopp, B. Fan, H. K. M. Vithana and A.Z. Genack, *Opt. Lett., 1998,* **23**, 1707.

29. T. J. Sluckin, D. A. Dunmur and H. Stegemeyer, *Crystals that flow: classic papers from the history of liquid crystals*, Taylor and Francis, London, 2004.

30. H. Kleinert and K. Maki, *Fortschritte der Physik*, 1981, **29**, 219.

31. T. Seideman. *Rep. Prog. Phys*., 1990, **53**, 659.

32. H. J. Coles and M. N. Pivnenko, *Nature*, 2005, **436**, 997.

33. J. D. Martin, C. L. Keary, T. A. Thornton, M. P. Novotnak, J. W. Knutson and J. C.W. Folmer, *Nat. Mater.*, 2006, **5**, 271.

34. M. Moreno-Maňas, M. Pérez, and R. Pleixats, *J. Org. Chem.*, 1996, **61**, 2346.

35. M. P. Aldred, PhD thesis, "*Charge Transporting and Electroluminescent Liquid Crystals for Organic Light-Emitting Diode*", University of Hull, 2004.

36. J. W. Goodby, *J. Mater. Chem.,* 1991, **1,** 307.

37. M. Hird, *Chem. Soc. Rev.,* 2007, **36**, 2070.

38. G. W. Gray and J. W. Goodby, *Smectic Liquid Crystals*, Leonard-Hill, Glasgow-London, 1984.

39. N. Iranpoor, H.Firouzabadi and D. Khalili, *Org. Biomol. Chem.*, 2010, **8**, 4436.

40. H. Coles, *Handbook of Liquid Crystals*, D. Demus, J. W. Goodby, G. W. Gray, H. W. Spiess and V. Vill, Wiley-VCH, Weinheim, 1998, Vol. 2A, Chapter IV, Section 2, 1.

41. D.G. McDonnnell, *Thermotropic Liquid Crystals*, G. W. Gray, J. Wiley and Sons, Chichester, 1987.

42. J .W. Goodby, *Ferroelectric liquid crystals*, Gordon and Breach science Publishers, 1991.

43. J. W. Goodby, E. Chin, T. M. Leslie, J. M. Geary and J. S. Patel, *J. Am. Chem. Soc.,* 1986, **108**, 4729.

44. J. W Goodby, and E. Chin, *J. Am. Chem. Soc.,* 1986, **108**, 4736.

45. R. B. Meyer, L. Liebert, L. Strzelecki and P. Keller, *J. Phys. (Paris) Lett,* 1975, **36,** L69.

46. R. B. Meyer, *Mol. Cryst. Liq. Cryst.,* 1977, **40**, 33.

47. S. T. Lagerwall and I. Dahi*, Mol. Cryst. Liq. Cryst.,* 1984, **114**, 151.

48. M. Glendenning, PhD Thesis, University of Hull, 1998.

49. S.T. Lagerwall, *Ferroelectric and Antiferroelectric liquid crystals.* Wiley- VCH, 1999.

50. I. Nishiyama, *Adv. Mater.*, 1994, **6**, 966.

51. A. Fukuda, Y. Takanashi, T. Isozaki, K. Ishikawa and H. Takezoe, *J. Mater. Chem.*, 1994, **4**, 997.

52. A. D. L. Chandani, T. Hagiwara, Y. Suziki, Y.Ouchi, H. Takezoe and A. Fukuda, *Jap. J. Appl. Phys.*, 1988, **27**, 729.

53. A. D. L. Chandani, Y. Ouchi, H. Takezoe, A. Fukuda, K. Furukawa and A. Kishi, *Jap. J. Appl. Phys.,* 1989, **28**, 1261.

54. A. D. L. Chandani, E. Gorecka, Y. Ouchi, H. Takezoe and A. Fukuda, *Jap. J. Appl. Phys.,* 1989, **28**, 1264.

55. K. Hiraoka, A.Taguchi, Y. Ouchi, H. Takezoe and A. Fukuda, *Jap. J. Appl. Phys.,* 1990, **29,** 103.

56. E. Gorecka, A. D. L. Chandini, Y. Ouchi, H. Takezoe and A. Fukuda, *Jap. J. Appl. Phys.,* 1990, **29**, 131.

57. S. J. Cowling, A. W. Hall and J. W. Goodby, *Liq. Cryst.*, 2005, **32**, 1483-1498.

58. Y. Shirota, *J. Mater. Chem.*, 2000, **10**, 1.

59. Q. Pei and Y. Yang, *Chem. Mater.*, 1995, **7**, 1568.

60. W. Huang, W. Lyu, H. Meng, J. Pei and S.F.Y. Li, *Chem. Mater.*, 1998, **10**, 3340.

61. M. Hird and K. J. Toyne, *Mol. Cryst. Liq. Cryst. Sci. and Tech*. Sect. A, 1998, **323**, 1.

62. S. Takamastu, M. Suefuji, T. Mitote and M. Mastumura, *Mol. Cryst. Liq. Cryst.*, 1981, **66**, 123.

63. A. V. Ivashchenko, E. I. Kovshev, V. T Lazareva, E. K. Prudnikova, V.V. Titov, T.Z. Verkoval, M. I. Barnik and L. M. Yagupolski, *Mol. Cryst. Liq. Cryst.*, 1981, **67**, 235.

64. V. V. Titov, T.I. Zverkova, E. I. Kovshev, Y. N. Fialkov, S. V. Shelazhenko and L. M. Yagupolski, *Mol. Cryst. Liq. Cryst.*, 1978, **47**, 1.

65. Z. N. Kayani, R. A. Lewis and S. Naseem, *J. Mol. Liq.*, 2013, **180**, 74.

66. H. J. Deutscher, H. M. Vorbrodt and H. Zaschke. *Z. Chem.*, 1981, **21**, 9.

67. L. A. Karamysheva, E. I. Kovshev, A. I. Pavluchenko, K. V. Roitman, V. V. Titov, S. I. Torgova and M. F. Grebenkin, *Mol. Cryst. Liq. Cryst.*, 1981, **67**, 897.

68. R. Cai and E.T. Samulski. *Liq. Cryst.*, 1991, **9**, 617.

69. K. Dimitrova, J. Hauschild, H. Zaschke and H. J. Schubert, *J. Prakt. Chem.,* 1980, **322**, 933.

70. B. L. Feringa and R. Eelkema, *Org. Biomol. Chem.*, 2006, **4**, 3729.

71.   D. M. Walba, K. F. Eidman, and R. C. Haltiwanger, *J. Org. Chem.,* 1989, **54**, 4939.

72.   I. Dierking, F. Giesselmann, J. Schacht and P. Zugenmaier, *Liq. Cryst.*, 1995, **19**, 179.

73.   Z. N. Kayani, R. A. Lewis and S. Naseem, *J. Mol. Liq.*, 2012, **175**, 72.

74.   R. B. Meyer, L. Liebert, L. Strzelecki, and P. Keller, *J. Phys. Lett.* (Paris), 1975, **69,** 36.

75.   T. Sakurai, N.Mikami, M.Ozaki, and K.Yoshino, *J. Chem. Phys.*, 1986, **85**, 585.

76.   M. Moreno-Mañas, M. Perez and R. Pleixats, *J. Org. Chem.*, 1996, **61**, 2346.

77.   S. R. Renn and T.C. Lubensky, *Phys. Rev. A,* 1988, **38**, 2132.

78.   F. Faglioni, M. Blanco, W.A. Goddard and D. Saunders. *J. Phys. Chem.,* 2002, **106**, 1714.

79.   A. J. Chalk and J. F. Harrod, *J. Am. Chem. Soc.* 1965, **87**, 16.

80.   I. Dierking, *Textures of liquid crystals*, Weinheim: Wiley-VCH, 2003, 168.

81.   D. R. Coulson, *Inorg. Synth.*, 1972, **13**, 121.

82.   N. Miyama, T. Yanagi and A. Suzuki, *Synth.Commun.*, 1981, **11**, 73.

83.   R. B. Millar and S. Dugar, *Organometallics*, 1984, **3**, 1261.

84.   J. W. Goodby and T. M. Leslie, *Mol. Crys. Liq. Cryst.,* 1984, **110**, 175.

85.   H. R. Brand, P. E. Cladis and P. L. Finn, *Phys. Rev. A.,*1985, **31**, 361.

86.   N. A. Clark and S. T. Lagerwall, *Appl. Phys. Lett.*, 1980, **36**, 899-901.

87.   J. Naciri, J. Ruth, G. Crawford, R. Shashidhar and B. R. Ratna, *Chem. Mater.*, 1995, **7**, 1397.

88.   J. Naciri, D. K. Shenoy, P. Keller, S. Gray, K. Crandall and R. Shashidhar, *Chem. Mater.*, 2002, **14**, 5134.

89.   M. S. Spector, P. A. Heiney, J. Naciri, B. T. Weslowski, D. B. Holt and R. Shashidhar, *Phys. Rev. E: Stat., Nonlinear, Soft Matter Phys.,* 2000, **61**, 1579.

90.   A. de Vries, *Mol. Cryst. Liq. Cryst*, 1977, **41**, 27.

91.   A. de Vries, A. Ekachai and N. Spielberg, *Mol, Cryst. Liq. Cryst.*, 1979, **49**, 143-152.

92.   F. Giesselmann, J. P. F. Lagerwall, G. Andersson and M. D. Radcliffe, *Phys. Rev. E: Stat., Nonlinear, Soft Matter Phys.,* 2002, **66**, 5.

93.   N. A. Clark, T. Bellini, R. F. Shao, D.Coleman, S. Bardon, D. R. Link, J. E. Maclennan, X. H. Chen, M. D. Wand, D. M. Walba, P. Rudquist and S. T. Lagerwall, *Appl. Phys. Lett.*, 2002, **80**, 4097.

94.   J. P. F. Lagerwall, F. Giesselmann and M. D. Radcliffe, *Phys. Rev. E: Stat., Nonlinear, Soft Matter Phys.* 2002, **66**, 11.

95.   A. Fukuda, *Proceedings, Asia Display 95 Digest* 1995, **61–63**.

96.   S. Inui, N. Iimura, T. Suzuki, H. Iwane, K. Miyachi, Y. Takanishi and A. Fukuda, *J. Mater. Chem.* 1996, **6**, 671.

97.   M. V. Gorkunov, F. Giesselmann, J. P. F. Lagerwall, T. J. Sluckin and M. A. Osipov, *Phys. Rev.E: Stat., Nonlinear, Soft Matter Phys.* 2007, **75**, 4.

98.   M. V. Gorkunov, M. A. Osipov, J. P.F. Lagerwall and F. Giesselmann, *Phys. Rev. E: Stat., Nonlinear, Soft Matter Phys.* 2007, **76**, 16.

99.   R. Korlacki, V. P. Panov, A. Fukuda, J. K. Vij, C. M. Spillmann and J. Naciri, *Phys. Rev. E: Stat., Nonlinear, Soft Matter Phys.* 2010, **82**, 7.

100.   E. A. Corsellis and H. J. Coles. *Mol. Cryst. Liq. Cryst.,* 1995, **261**, 71.

101.   J. Newton, H. J. Coles, P. Hodge and J. Hannington. *J. Mater. Chem.*, 1994, **4**, 869.

102.   M. Redmond, H. J. Coles, E. Wischerhoff and R. Zentel, *Ferroelectrics*, 1993, **148**, 323.

103.   H. J. Coles, H. Owen, J. Newton and P. Hodge*, Liq. Cryst.*, 1993, **15**, 739.

104.   H. J. Coles, H. Owen, J. Newtona and P. Hodge, *Proc. SPIE*, 1995, **22**, 2408.

105.   P. Kloess, J. McComb, H. J. Coles and R. Zentel, *Ferroelectrics*, 1996, **180**, 233.

106.   W. K. Robinson, P. Kloess, C. Carboni and H. J. Coles. *Liq. Cryst.*, 1997, **23**, 309.

107.   W. K. Robinson, C. Carboni, P. Kloess, S. P. Perkins and H. J. Coles, *Liq. Cryst.*, 1998, **25**, 301.

108.   H. J. Coles, I. Butler, K. Raina, J. Newton, J. Hannington and D. Thomas, *Proc. SPIE*, 1995, **14**, 2408.

109.   W. K. Robinson, P. Lehmann and H. J. Coles, *Mol. Cryst. Liq. Cryst.*, 1999, **229**, 328.

110.   H. Owen, H. J. Coles, J. Newton and P. Hodge, *Mol. Cryst. Liq. Cryst.*, 1994, **151**, 257.

111.   P. De Hondt, S. Perkins and H. J. Coles, *Mol. Cryst. Liq. Cryst.*, 2001, **263**, 366.

112.   J. Newton, H. G. Walton, H. J. Coles and P. Hodge*, Mol. Cryst. Liq. Cryst.*, 1995, **107**, 260.

113.   E. Wischerhoff, R. Zental, M. Redmond, O. Mondain- Monval and H. J. Coles, *Macromol. Chem. Phys.*, 1994, **195**, 1593.

114.   M. N. Pivnenko, O. Hadler, M. J. Coles, M. Grassman, P. R. Davies, J. P. Hannington and H. J. Coles, *Proc. SPIE*,**16**, 5289.

115.   H.J. Coles, K. Takatoh, P. Kloess and M.J. Coles, *U.K. Patent GB2 317 186B*, 1996.

116.   D.E. Shoosmith, A. Remnant, S.P. Perkins and H.J. Coles, *Ferroelectrics*, 2000, **75**, 243.

117. P. Lehmann, W.K. Robinson and H. J. Coles, *Mol. Cryst. Liq. Cryst.*, 1999, **221**, 328.

118. N. Olsson, I. Dahl, B. Helgee and L. Komitov, *J. Mater. Chem.*, 2007, **17**, 2517.

119. Z. N. Kayani, R. A. Lewis and S. Naseem, *J. Mol. Liq.*, 2012, **170**, 11-19.

120. D. Guillon, M. A. Osipov, S. Mery, M. Siffert, J. F. Nicoud, C. Bourgogne and P. Sebastiao, *J. Mater. Chem.*, 2001, **11**, 2700.

121. M. Ibn-Elhaj, A. Skoulios, D. Guillon, J. Newton, P. Hodge and H. J. Coles, *J. Phys. II Fr*, 1996, **6**, 271.

122. E. A. Corsellis, D. Guillon, P. Kloess and H. J. Coles, *Liq. Cryst.*, 1997, **23**, 235.

123. T. Murias, A. C. Ribeiro, D. Guillon, D. Shoosmith and H. J. Coles, *Liq. Cryst.*, 2002, **29**, 627.

124. J. Naciri, G. P. Crawford, B. R. Ratna and R. Shashidhar, *Ferroelectrics*, 1993, **148,** 297**.**

125. H. J. Coles, M. N. Pivnenko, Lehmann and L. Komitov, *Liq. Cryst.*, 2005, **2**, 32.

126. S. J. Cowling and J. W. Goodby, *Chem. Commun.*, 2006, 4107-4109.

127. J. C. Roberts, N. Kapernaum, F. Giesselmann, M. D. Wand and R. P. Lemieux, *J. Mater. Chem.*, 2008, **18**, 5301.

128. (a) C. Tschierske, *J. Mater. Chem.*, 1998, **8**, 1485; (b) J. W. Goodby, G. H. Mehl, I. M. Saez, R. P. Tuffin, G. Mackenzie, R. Auze´ly- Velty, T. Benvegnu and D. Plusquellec, *Chem. Commun.*, 1998, 2057; (c) C. Tschierske, *J. Mater. Chem.*, 2001, **11**, 2647. (d) C. Tschierske, *Annu. Rep. Prog. Chem., Sect. C*, 2001, **97**, 191.

129. (a) T. Hegmann, M. R. Meadows, M. D. Wand and R. P. Lemieux, *J. Mater. Chem.*, 2004, **14**, 185; (b) C. S. Hartley, N. Kapernaum, J. C. Roberts, F. Giesselmann and R. P. Lemieux, *J. Mater. Chem.*, 2006, **16**, 2329.

130. M. D. Wand, R. Vohra, D. M. Walba, N. A. Clark and R. Shao, *Mol. Cryst. Liq. Cryst.*, 1991, **202**, 183.

131. K. Sunohara, K. Takatoh and M. Sakamoto, *Liq. Cryst.*, 1993, **13**, 283.

132. J. Newton, H. Coles, P. Hodge and J. Hannington, *J. Mater. Chem.*, 1994, **4**, 869.

133. H. Poths, E. Wischerhoff, R. Zentel, A. Schoenfeld, G. Henn and F. Kremer, *Liq. Cryst.*, 1995, **18**, 811.

134. M. Ibn-Elhaj, A. Skoulios, D. Guillon, J. Newton, P. Hodge and H. J. Coles, *J. Phys. II*, 1996, **6**, 271.

135. W. K. Robinson, C. Carboni, P. Kloess, S. P. Perkins and H. J. Coles, *Liq. Cryst.*, 1998, **25**, 301.

136.   P. Sebastiao, S. Mery, M. Sieffert, J. F. Nicoud, Y. Galerne and D. Guillon, *Ferroelectrics*, 1998, **212**, 133.

137.   H. J. Coles, S. Meyer, P. Lehmann, R. Deschenaux and I. Jauslin, *J. Mater. Chem.*, 1999, **9**, 1085.

138.   J. Z. Vlahakis, K. E. Maly and R. P. Lemieux, *J. Mater. Chem.*, 2001, **11**, 2459.

139.   J. Naciri, D. K. Shenoy, P. Keller, S. Gray, K. Crandall and R. Shashidhar, *Chem. Mater.*, 2002, **14**, 5134.

140.   J. Naciri, C. Carboni and A. K. George, *Liq. Cryst.*, 2003, **30**, 219.

141.   O. E. Panarina, Y. P. Panarin, F. Antonelli, J. K. Vij, M. Reihmann and G. Galli, *J. Mater. Chem.*, 2006, **16**, 842.

142.   (a) J. C. Dubois, P. Le Barny, M. Mauzac and C. Noel, *Handbook of Liquid Crystals*, E. D. Demus, J. W. Goodby, G. W. Gray, H. W. Piess and V. Vill, Wiley-VCH, Weinheim, 1998, vol. 3, 207; (b) M. Rossle, R. Zentel, J. P. F. Lagerwall and F. Giesselmann, Liq. Cryst., 2004, 31, 883; (c) M. Rössle, D. Schollmeyer, R. Zentel, J. P. F. Lagerwall, F. Giesselmann and R. Stannarius, *Liq. Cryst.*, 2005, **32**, 533.

143.   M. S. Spector, P. A. Heiney, J. Naciri, B. T. Weslowski, D. B. Holt and R. Shashidhar, *Phys. Rev. E*, 2000, **61**, 1579.

144.   O. E. Panarina, Y. P. Panarin, J. K. Vij, M. S. Spector and R. Shashidhar, *Phys. Rev. E*, 2003, **67**, 051709.

145.   N. Hayashi, T. Kato, A. Fukuda, J. K. Vij, Y. P. Panarin, J. Naciri, R. Shashidhar, S. Kawada and S. Kondoh, *Phys. Rev. E*, 2005, **71**, 041705.

146.   J. P. F. Lagerwall and F. Giesselmann, *Chem. Phys. Chem*, 2006, **7**, 20.

147.   A. de Vries, *J. Chem. Phys.*, 1979, **71**, 25.

148.   (a) M. V. Gorkunov, M. A. Osipov, J. P. F. Lagerwall and F. Giesselmann, *Phys. Rev. E*, 2007, **76**, 051706; (b) M. V. Gorkunov, F. Giesselmann, J. P. F. Lagerwall, T. J. Sluckin and M. A. Osipov, *Phys. Rev. E*, 2007, **75**, 060701.

149.   K. Saunders, D. Hernandez, S. Pearson and J. Toner, *Phys. Rev. Lett.*, 2007, **98**, 197801; K. Saunders, *Phys. Rev. E*, 2008, **77**, 061708.

150.   L. Li, C. D. Jones, J. Magolan and R. P. Lemieux, *J. Mater. Chem.*, 2007, **17**, 2313.

151.   J. C. Roberts, N. Kapernaum, Qing xiang Song, D. Nonnenmacher, K. Ayub, F. Giesselmann and R. P. Lemieux. *J. Am. Chem. Soc*, 2010, **365**, 132.

152.   (a) M. V. Gorkunov, M. A. Osipov, J.P.F. Lagerwall and F. Giesselmann, *Phys. Rev. E* 2007, **76**, 051706; (b) M. V. Gorkunov, F. Giesselmann, J. P. F. Lagerwall, T. J. Sluckin and M. A. Osipov, *Phys. Rev. E*, 2007, **75**, 060701.

153. (a) K. Saunders, D. Hernandez, S. Pearson and J. Toner, *Phys. Rev. Lett.* 2007, **98**, 197801; (b) K. Saunders, *Phys. Rev. E*, 2008, **77**, 061708; (c) K. Saunders, *Phys. Rev. E,* 2009, **80**, 011703.

154. L. Li, C. D. Jones, J. Magolan and R. P. Lemieux, *J. Mater. Chem.,* 2007, **17**, 2313.

155. A. J. Slaney, V. Minter and J. C. Jones, *Ferroelectrics*, 1996, **178**, 65.

156. M. Hird, J. W. Goodby, P. Hindmarsh, R. A. Lewis and K. J. Toyne, *Ferroelectrics*, 2002, **276**, 219.

157. G. W. Gray, M. Hird, D. Lacey, and K. J. Toyne, *J. Chem. Soc.*, *Perkin Trans.* 2, 1989, 2041.

158. I. A. Radini and M. Hird, *Liq. Cryst.*, 2009, **12**, 1417.

159. M. N. Pivnenko, P. Lehmann, L. Komitov and H. J. Coles, *Liq. Cryst.*, 2005, **32**, 173.

160. N. M. Shtykov, V. P. Panov, J. K. Vij and J. Naciri, *Liq. Cryst.,* 2011, **38**, 521.

161. N. Miyaura, K. Yamada, H. Suginome and A. Suzuki, *J. Am. Chem. Soc.*, 1985, **107**, 972.

162. J. S. Patel, *Appl. Phys. Lett.*, 1992, **60**, 280.

163. M. A. Handshy and N. A. Clark, *Ferroelectrics*, 1984, **59**, 69.

164. J. S. Patel and J. W. Goodby, *Mol. Cryst. Liq. Cryst.*, 1987, **117**, 144.

165. M. Johno, A. D. L. Chandani, Y. Ouchi, H. Takezoe and A. Fukuda, *Jpn. J. Appl. Phys.*, 1989, **28**, 119.

166. J. S. Patel, *Appl. Phys. Lett.*, 1985, **47**, 1277.

167. W. J. A. M. Hartmann*, Int. Display Res. Conf.*, 1988, 191.

168. T. P. Rieker, N. A. Clark, G. S. Smith, D. S. Parmar, E. B. Sirota and C. R. Safinya, *Ferroelectrics*, 1987, **59**, 2658.

169. N. A. Clark, T. P. Rieker and J. E. Maclennan, *Ferroelectrics*, 1988, **79**, 85.

170. Y. Ouchi, J. Lee, H. Takazoe, A. Fakuda and K. Kondo, *Jpn. J. Appl. Phys.*,1988, **27**, 725.

171. J. S. Patel, S. D. Lee and J. W. Goodby, *Phys. Rev. A*, 1989, **40**, 2854.

172. M. D. Leatherman, W. Peng, G. A. Policello, S. K. Rajaraman, R. Wagner and Z. Xia, *US Pat.*, 0269467, 2007 ;

Appendix:

DSC thermographs of final compounds:

DSC thermograph of the compound **30a** (KSR-20):

^endo

Integral	204.33 mJ
normalized	64.25 Jg^-1
Onset	53.74 ℃
Peak	55.47 ℃

Integral	25.88 mJ
normalized	8.14 Jg^-1
Onset	81.66 ℃
Peak	82.56 ℃

]3[ksr-20
ksr-20, 3.1800 mg

10
mW

]4[ksr-20
ksr-20, 3.1800 mg

Integral	-161.92 mJ
normalized	-50.92 Jg^-1
Onset	29.79 ℃
Peak	27.13 ℃

Integral	-24.46 mJ
normalized	-7.69 Jg^-1
Onset	81.35 ℃
Peak	80.66 ℃
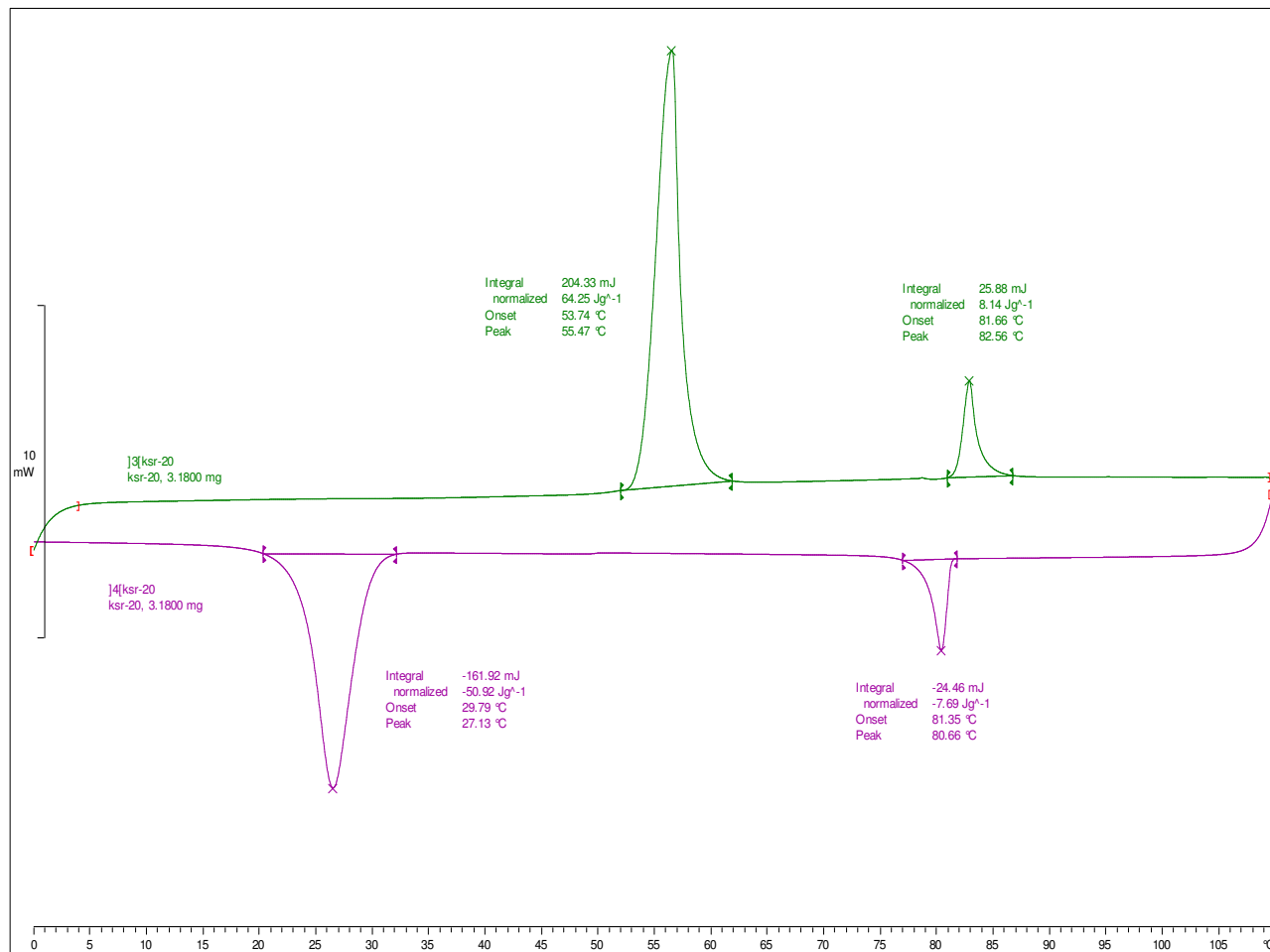
Hull Liquid Crystal Group: METTLER   ***STAR^e SW 8.10***

DSC thermograph of the compound **30c** (KSR-25):

^endo

Integral   129.75 mJ
  normalized   34.60 Jg^-1
Onset   34.47 ℃
Peak   37.50 ℃

Integral   18.47 mJ
  normalized   4.93 Jg^-1
Onset   52.18 ℃
Peak   54.68 ℃

5
mW

]3[ksr-25
ksr-25, 3.7500 mg

]4[ksr-25
ksr-25, 3.7500 mg

Integral   -19.21 mJ
  normalized   -5.12 Jg^-1
Onset   52.04 ℃
Peak   49.49 ℃

0   5   10   15   20   25   30   35   40   45   50   55   60   65   70   75   80   85   ℃
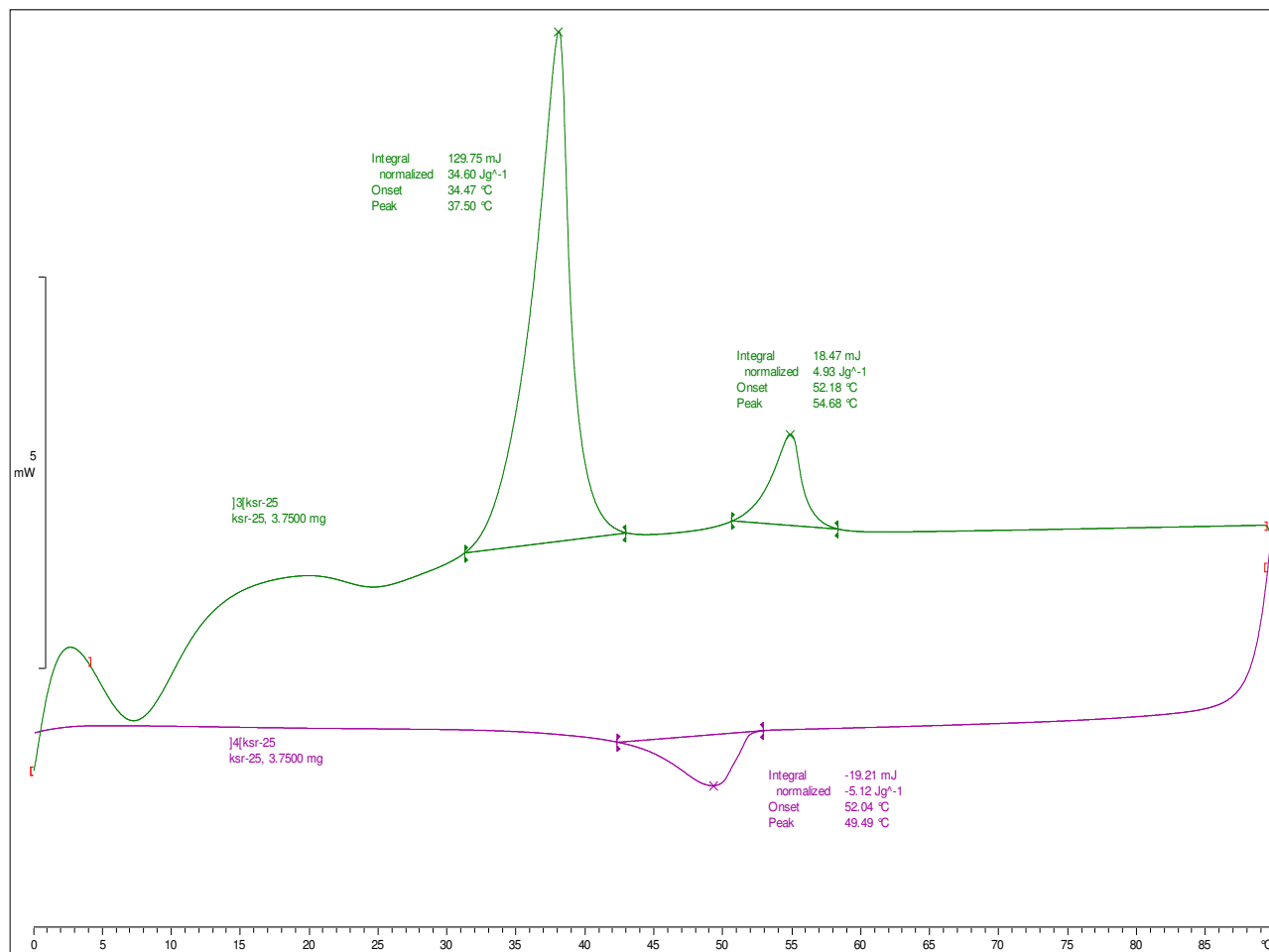
Hull Liquid Crystal Group: METTLER   **STAR^e SW 8.10**

DSC thermograph of the compound **30b** (KSR-28):

^endo   **KSR-28**   **14.10.2011 15:32:45**

Integral   151.38 mJ
normalized   40.80 Jg^-1
Onset   35.54 ℃
Peak   37.34 ℃

Integral   27.19 mJ
normalized   7.33 Jg^-1
Onset   67.31 ℃
Peak   68.76 ℃

]3[ksr-28
ksr-28, 3.7100 mg

Integral   -54.90 mJ
normalized   -14.80 Jg^-1
Onset   7.69 ℃
Peak   12.57 ℃

10
mW

]4[ksr-28
ksr-28, 3.7100 mg

Integral   -26.58 mJ
normalized   -7.16 Jg^-1
Onset   67.11 ℃
Peak   66.17 ℃
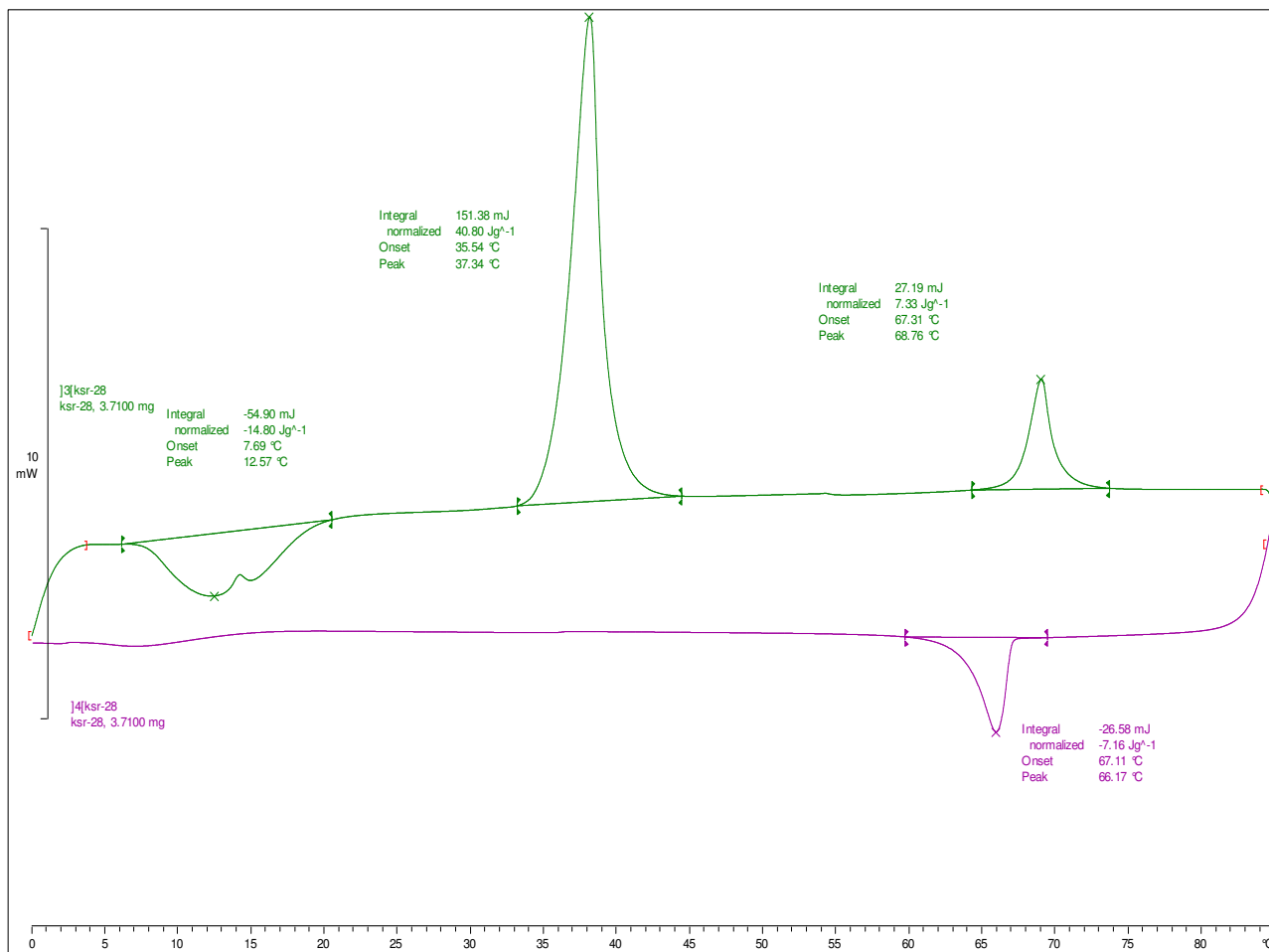
Hull Liquid Crystal Group: METTLER   **STAR^e SW 8.10**

DSC thermograph of the compound **30d**(KSR-29):
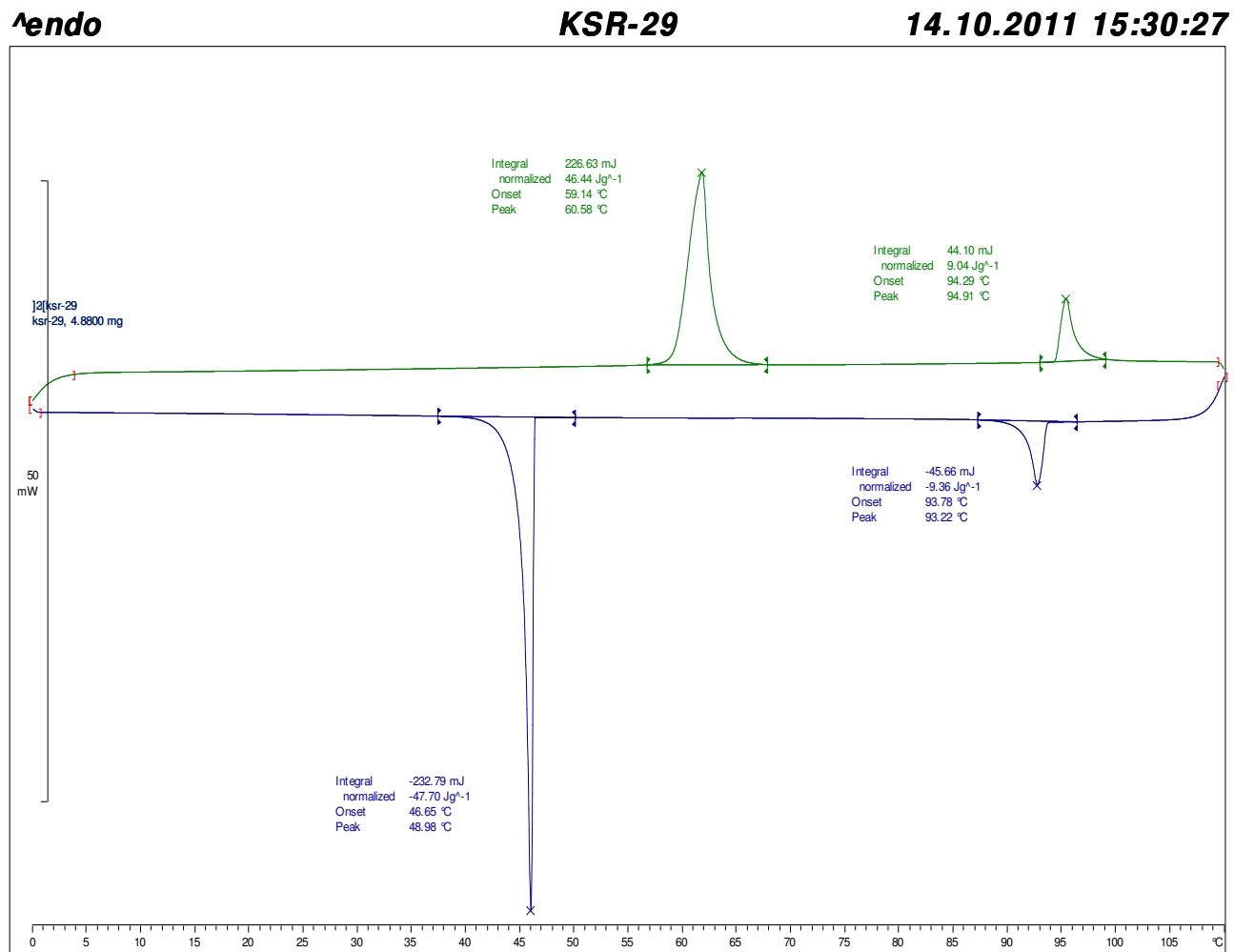
DSC thermograph of the compound **30e** (KSR-30):

^endo   **KSR-30**   **14.10.2011 15:20:34**

Integral   99.95 mJ
normalized   17.23 Jg^-1
Onset   19.26 ℃
Peak   20.64 ℃

Integral   55.32 mJ
normalized   9.54 Jg^-1
Onset   84.99 ℃
Peak   85.98 ℃

]3[ksr-30
ksr-30, 5.8000 mg

]4[ksr-30
ksr-30, 5.8000 mg

Integral   -51.53 mJ
normalized   -8.88 Jg^-1
Onset   84.17 ℃
Peak   83.34 ℃

Integral   -96.43 mJ
normalized   -16.63 Jg^-1
Onset   9.04 ℃
Peak   7.79 ℃

10
mW
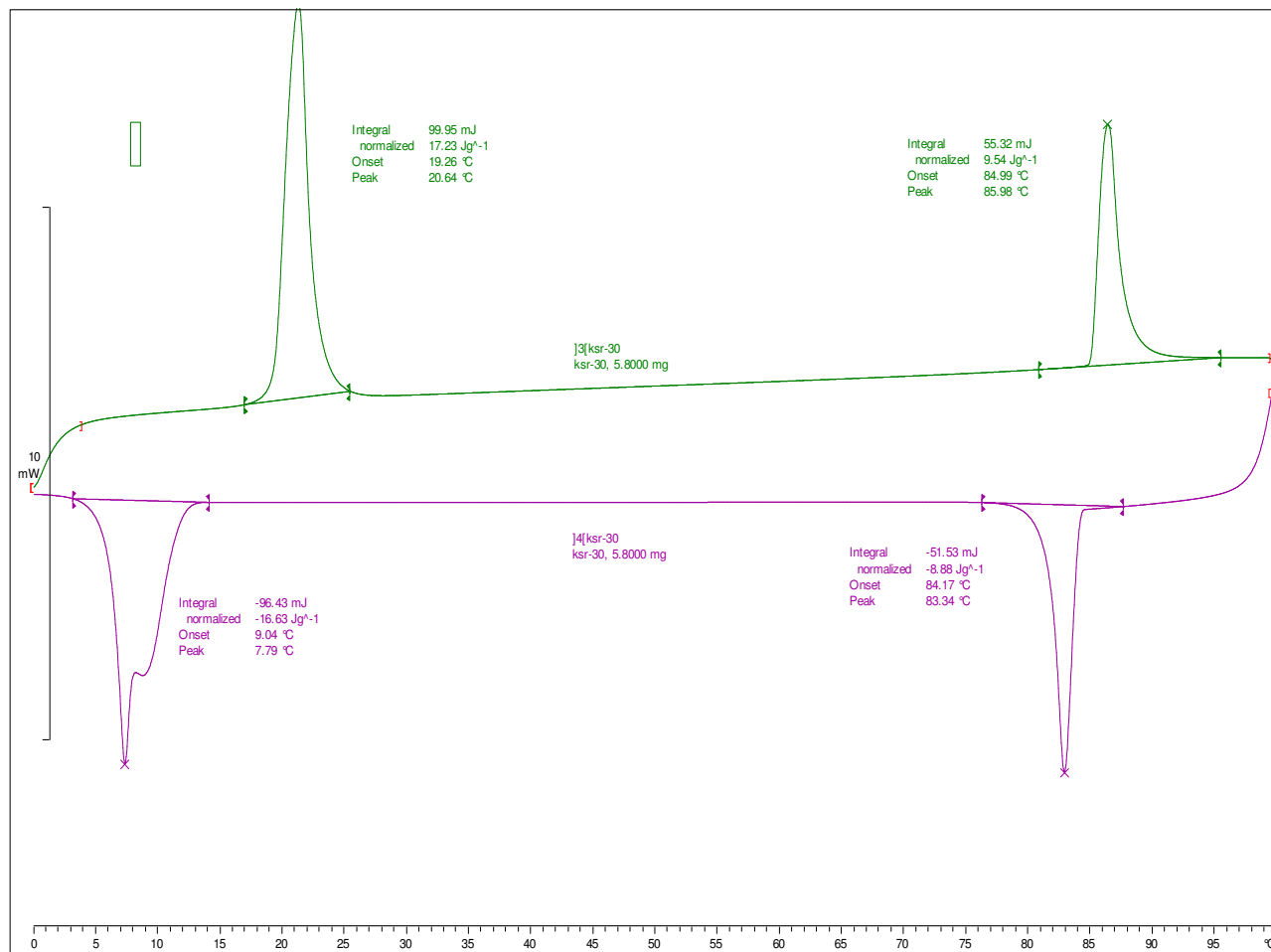
Hull Liquid Crystal Group: METTLER   **STAR^e SW 8.10**

DSC thermograph of the compound **34a** (KSR-38):

^endo

Integral 173.32 mJ
normalized 51.89 Jg^-1
Onset 38.40 ℃
Peak 39.97 ℃

Integral 28.80 mJ
normalized 8.62 Jg^-1
Onset 49.04 ℃
Peak 50.24 ℃

5
mW

]3[KSR-38
KSR-38, 3.3400 mg

]4[KSR-38
KSR-38, 3.3400 mg

Integral -113.22 mJ
normalized -33.90 Jg^-1
Onset 13.89 ℃
Peak 7.67 ℃

Integral -28.25 mJ
normalized -8.46 Jg^-1
Onset 48.91 ℃
Peak 48.35 ℃

-20 -15 -10 -5 0 5 10 15 20 25 30 35 40 45 50 55 60 65 70 ℃

Hull Liquid Crystal Group: METTLER   **STAR^e SW 8.10**

174
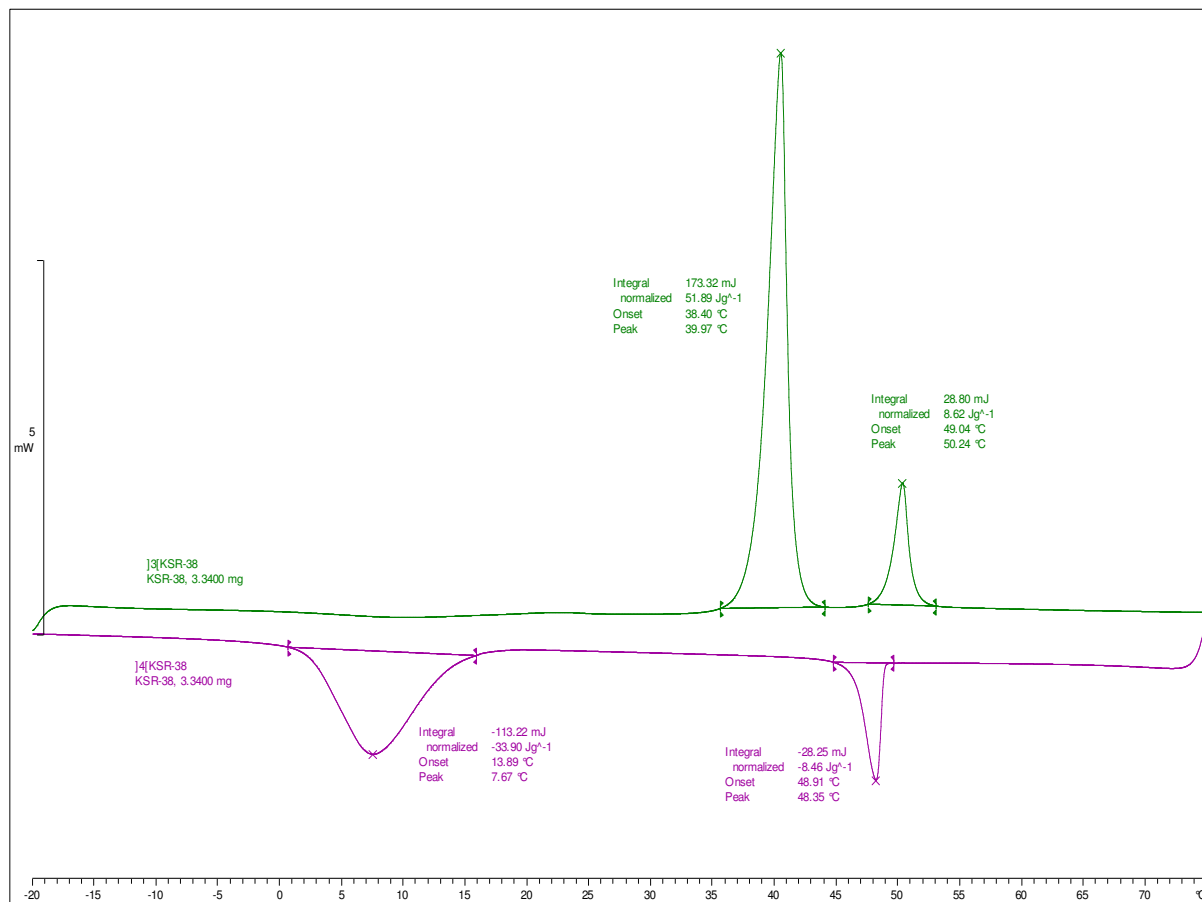
DSC thermograph of the compound **34b** (KSR-39):

^endo

]3[KSR-39
KSR-39, 3.2700 mg

Integral   31.96 mJ
  normalized   9.77 Jg^-1
Onset   59.07 ℃
Peak   60.42 ℃

2
mW

]4[KSR-39
KSR-39, 3.2700 mg

Integral   -28.95 mJ
  normalized   -8.85 Jg^-1
Onset   59.19 ℃
Peak   58.37 ℃

-20 -15 -10 -5 0 5 10 15 20 25 30 35 40 45 50 55 60 65 70 ℃
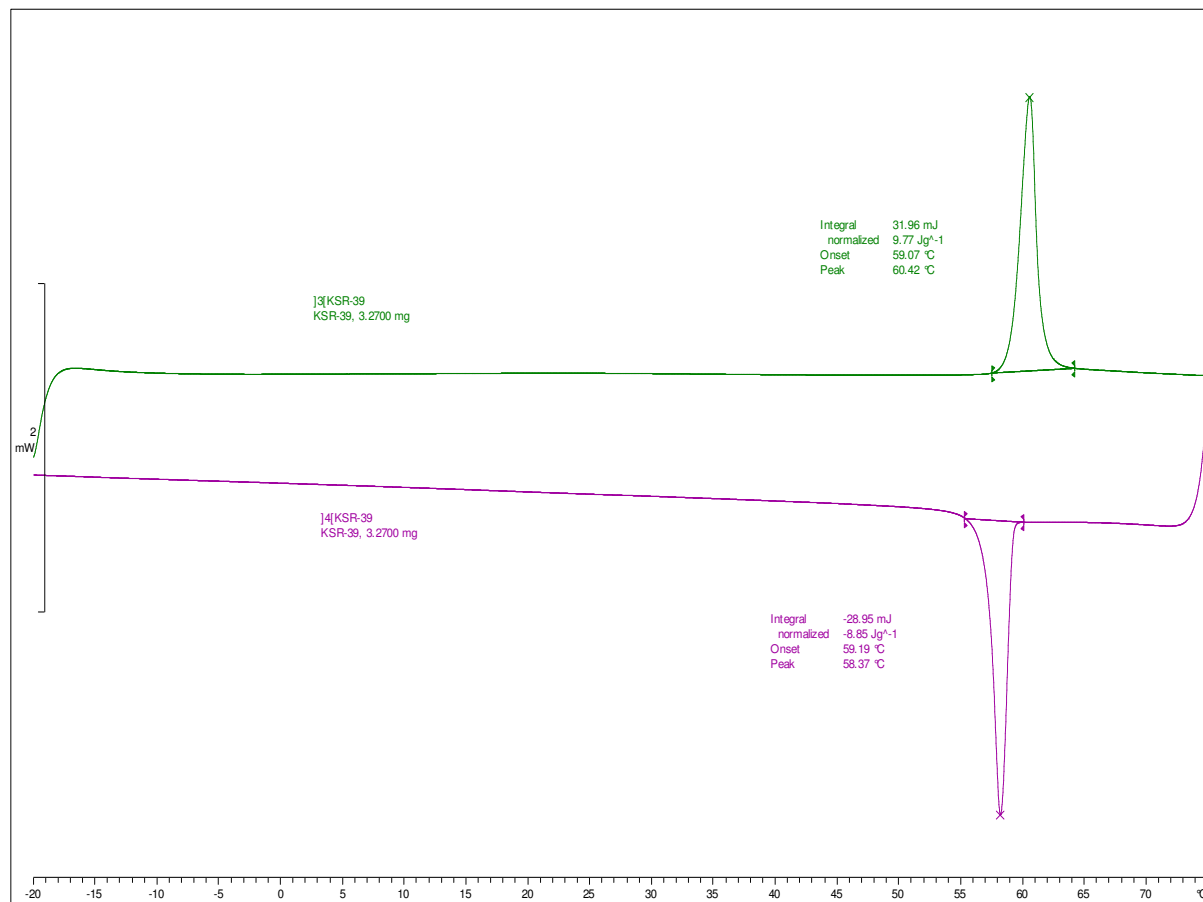
Hull Liquid Crystal Group: METTLER   **STAR**e **SW 8.10**

DSC thermograph of the compound **34c** (KSR-40):

^endo

Integral 133.29 mJ
normalized 43.99 Jg^-1
Onset 45.84 ℃
Peak 47.34 ℃

Integral 19.79 mJ
normalized 6.53 Jg^-1
Onset 56.37 ℃
Peak 58.70 ℃

]3[KSR-40
KSR-40, 3.0300 mg

5
mW

]4[KSR-40
KSR-40, 3.0300 mg

Integral -113.87 mJ
normalized -37.58 Jg^-1
Onset 28.98 ℃
Peak 26.98 ℃

Integral -17.58 mJ
normalized -5.80 Jg^-1
Onset 56.67 ℃
Peak 55.14 ℃
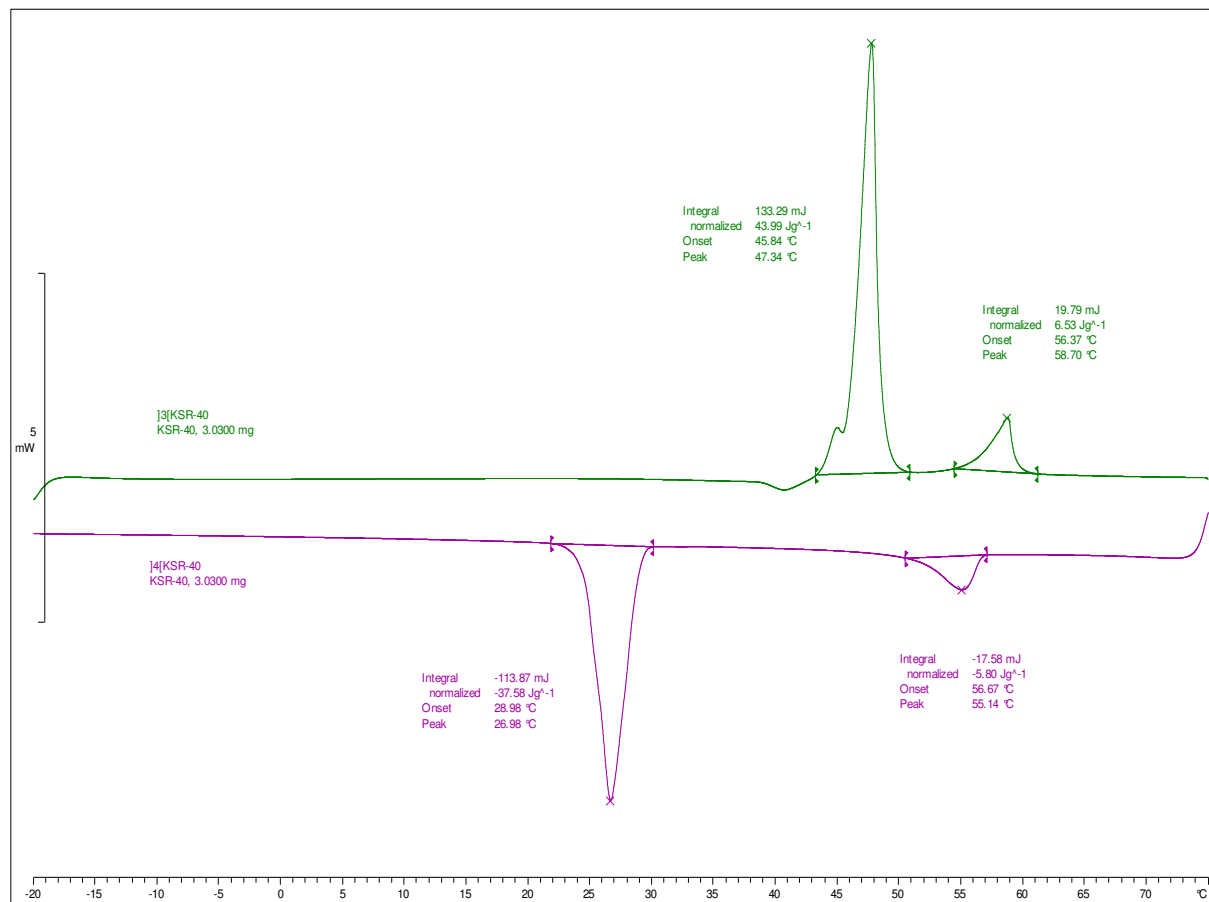
Hull Liquid Crystal Group: METTLER   **STAR^e SW 8.10**

DSC thermograph of the compound **34d** (KSR-41):

^endo

]3[KSR-41
KSR-41, 3.6000 mg

Integral   119.11 mJ
normalized   33.09 Jg^-1
Onset   26.53 ℃
Peak   28.78 ℃

Integral   27.39 mJ
normalized   7.61 Jg^-1
Onset   33.52 ℃
Peak   34.92 ℃

5
mW

]2[KSR-41
KSR-41, 3.6000 mg

Integral   -92.30 mJ
normalized   -25.64 Jg^-1
Onset   -5.00 ℃
Peak   -5.84 ℃

Integral   -25.45 mJ
normalized   -7.07 Jg^-1
Onset   33.72 ℃
Peak   33.03 ℃

-25 -20 -15 -10 -5 0 5 10 15 20 25 30 35 40 45 50 55 ℃
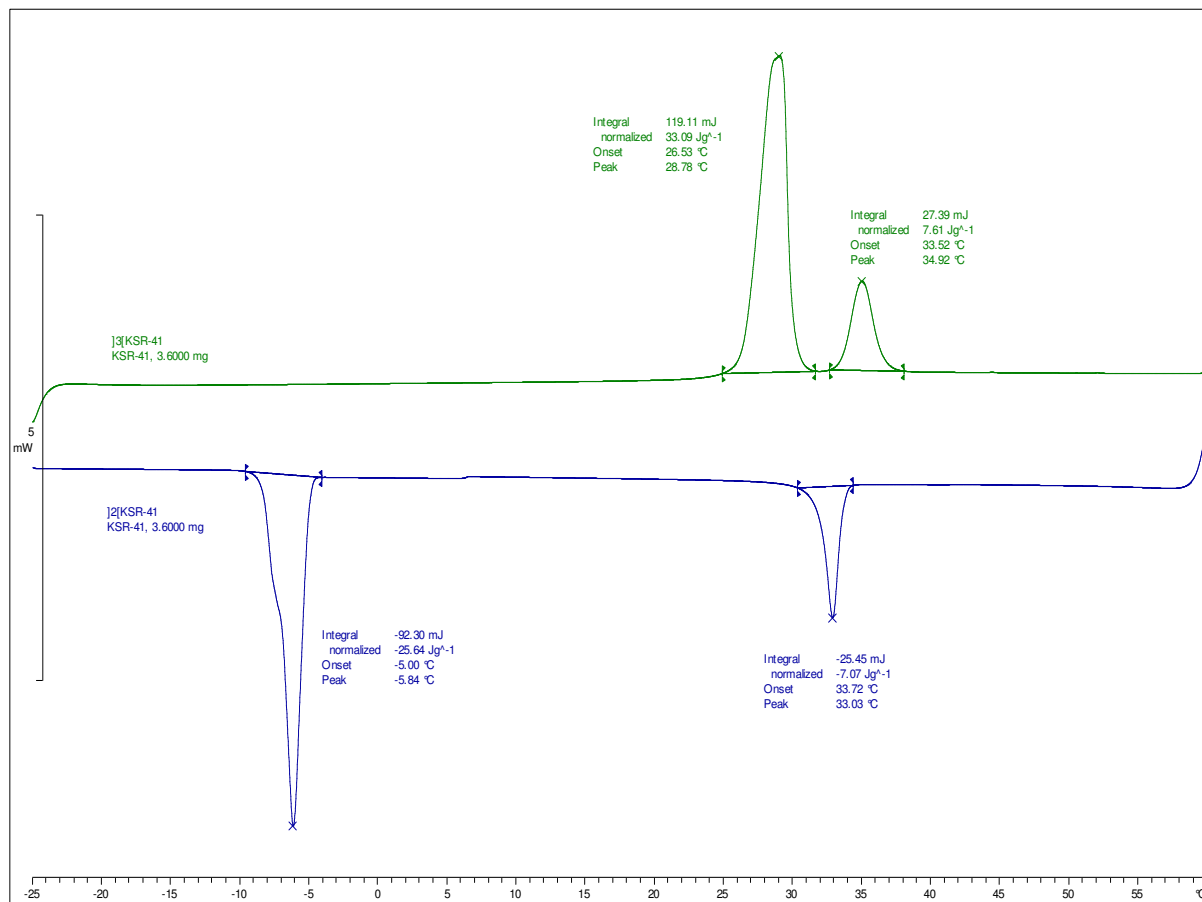
Hull Liquid Crystal Group: METTLER   *STAR^e SW 8.10*

DSC thermograph of the compound **34e** (KSR-42):

^endo

Integral 84.60 mJ
normalized 24.81 Jg^-1
Onset 9.36 °C
Peak 10.08 °C

Integral 29.82 mJ
normalized 8.74 Jg^-1
Onset 44.23 °C
Peak 45.17 °C

]3[KSR-42
KSR-42, 3.4100 mg

2 mW

]4[KSR-42
KSR-42, 3.4100 mg

Integral -28.87 mJ
normalized -8.47 Jg^-1
Onset 44.04 °C
Peak 43.52 °C

-25 -20 -15 -10 -5 0 5 10 15 20 25 30 35 40 45 50 55 °C
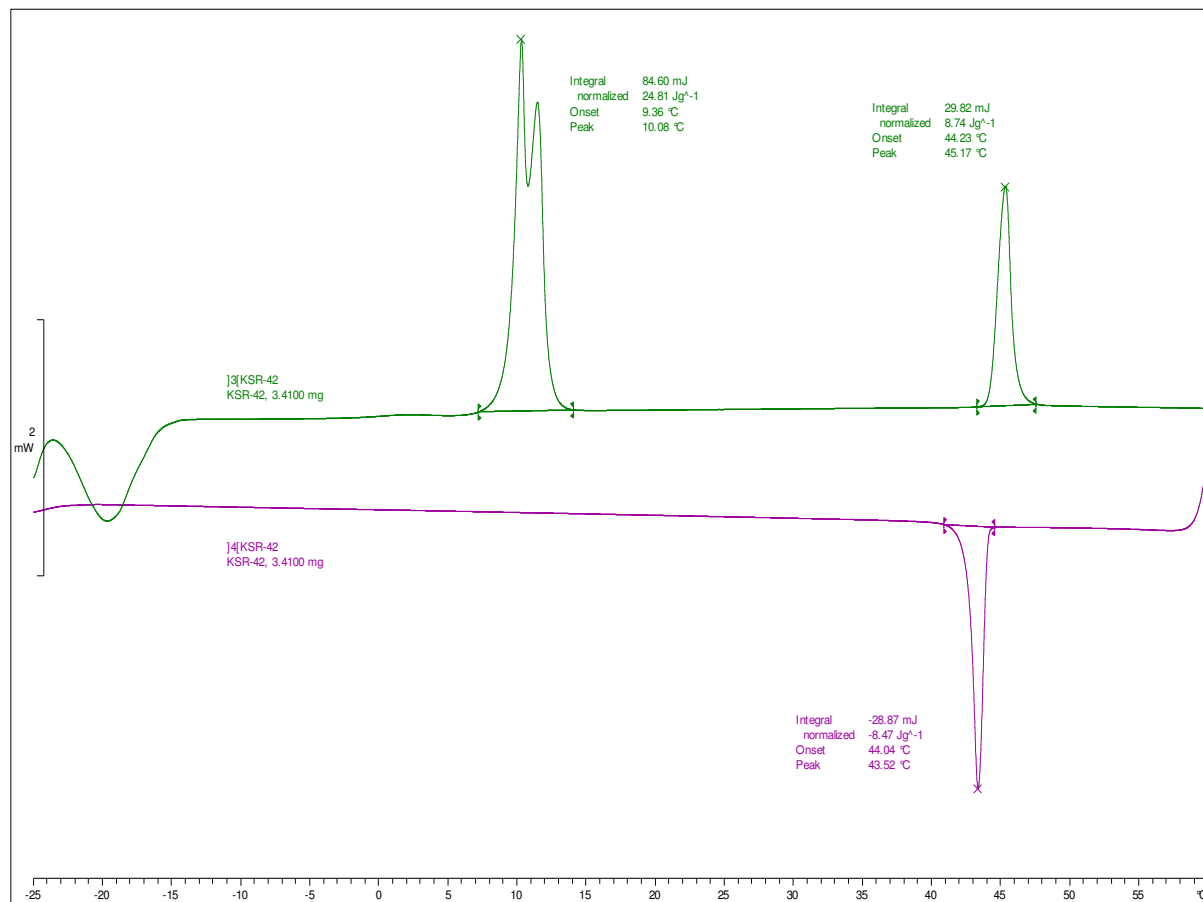
Hull Liquid Crystal Group: METTLER   **STAR^e SW 8.10**

DSC thermograph of the compound **34f** (KSR-43):

^endo

Integral   88.56 mJ
normalized   28.75 Jg^-1
Onset   23.37 ℃
Peak   25.09 ℃

Integral   24.36 mJ
normalized   7.91 Jg^-1
Onset   41.48 ℃
Peak   42.64 ℃

]3[KSR-43
KSR-43, 3.0800 mg

2
mW

]4[KSR-43
KSR-43, 3.0800 mg

Integral   -23.51 mJ
normalized   -7.63 Jg^-1
Onset   41.56 ℃
Peak   41.06 ℃

Integral   -76.22 mJ
normalized   -24.75 Jg^-1
Onset   3.67 ℃
Peak   2.27 ℃
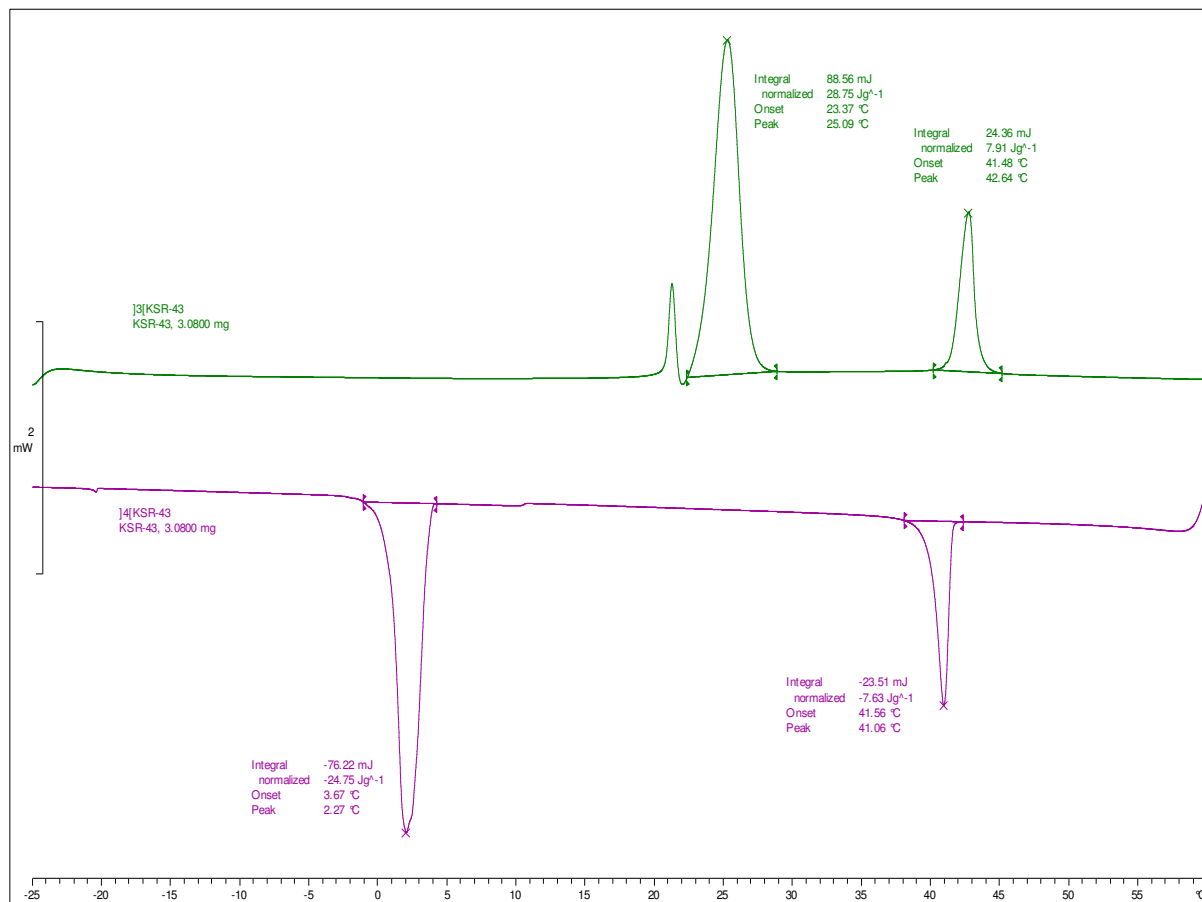
Hull Liquid Crystal Group: METTLER   **STAR^e SW 8.10**

DSC thermograph of the compound **37a** (KSR-50):

^endo

Integral	9.64 mJ	
normalized	2.58 Jg^-1	
Onset	15.36 ℃	
Peak	16.90 ℃	

Integral	5.52 mJ
normalized	1.48 Jg^-1
Onset	48.21 ℃
Peak	49.72 ℃

Integral	29.81 mJ
normalized	7.99 Jg^-1
Onset	94.49 ℃
Peak	98.99 ℃

]3[KSR-50
KSR-50, 3.7300 mg

]4[KSR-50
KSR-50, 3.7300 mg

2 mW

Integral	-10.93 mJ
normalized	-2.93 Jg^-1
Onset	12.48 ℃
Peak	11.35 ℃

Integral	-4.28 mJ
normalized	-1.15 Jg^-1
Onset	50.00 ℃
Peak	48.08 ℃

Integral	-27.40 mJ
normalized	-7.35 Jg^-1
Onset	98.26 ℃
Peak	96.53 ℃
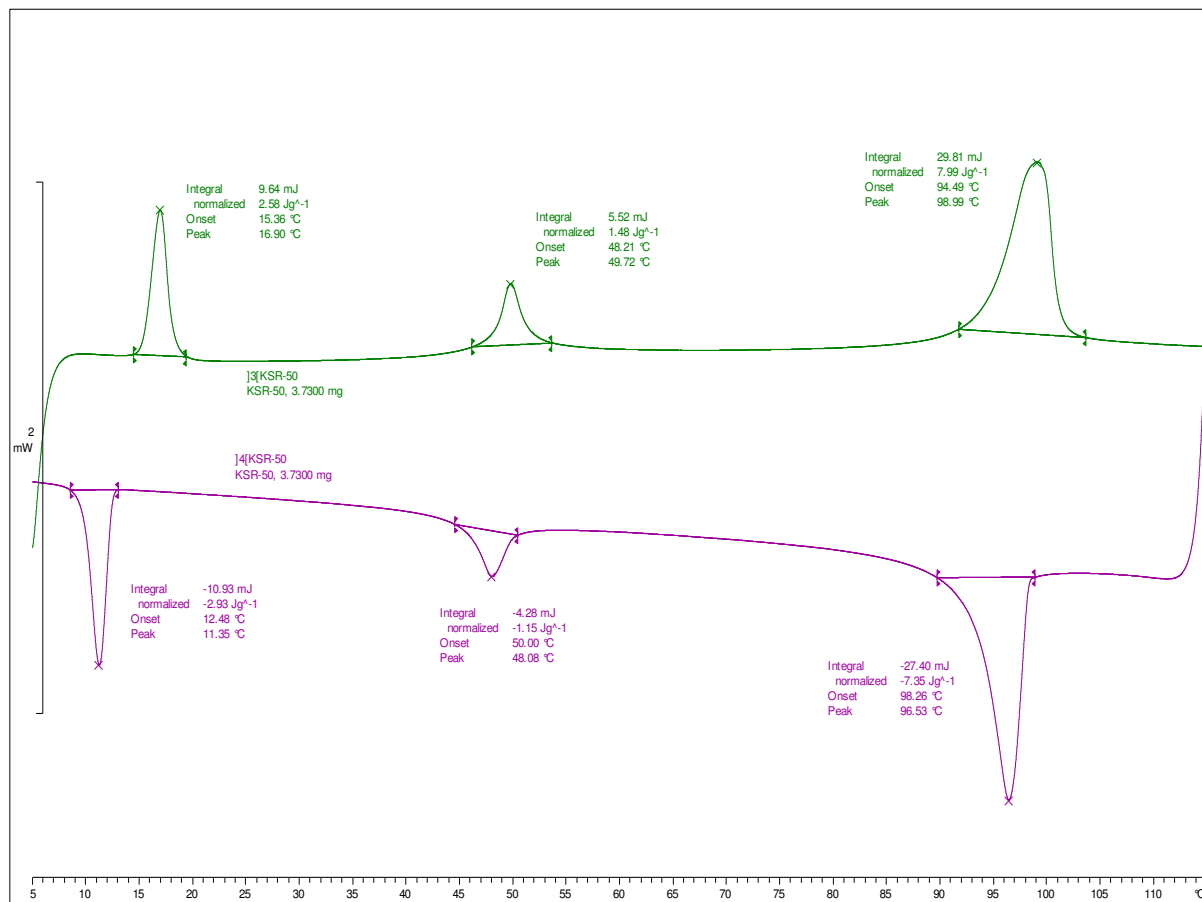
Hull Liquid Crystal Group: METTLER   **STAR^e SW 8.10**

DSC thermograph of the compound **37b** (KSR-51):

^endo

Integral   3.97 mJ
  normalized   1.10 Jg^-1
Onset   52.29 °C
Peak   53.62 °C

Integral   42.07 mJ
  normalized   11.62 Jg^-1
Onset   118.59 °C
Peak   121.72 °C

]3[KSR-51
KSR-51, 3.6200 mg

]4[KSR-51
KSR-51, 3.6200 mg

2
mW

Integral   -3.37 mJ
  normalized   -0.93 Jg^-1
Onset   53.34 °C
Peak   50.98 °C

Integral   -41.53 mJ
  normalized   -11.47 Jg^-1
Onset   121.15 °C
Peak   119.39 °C

10   20   30   40   50   60   70   80   90   100   110   120   130   °C
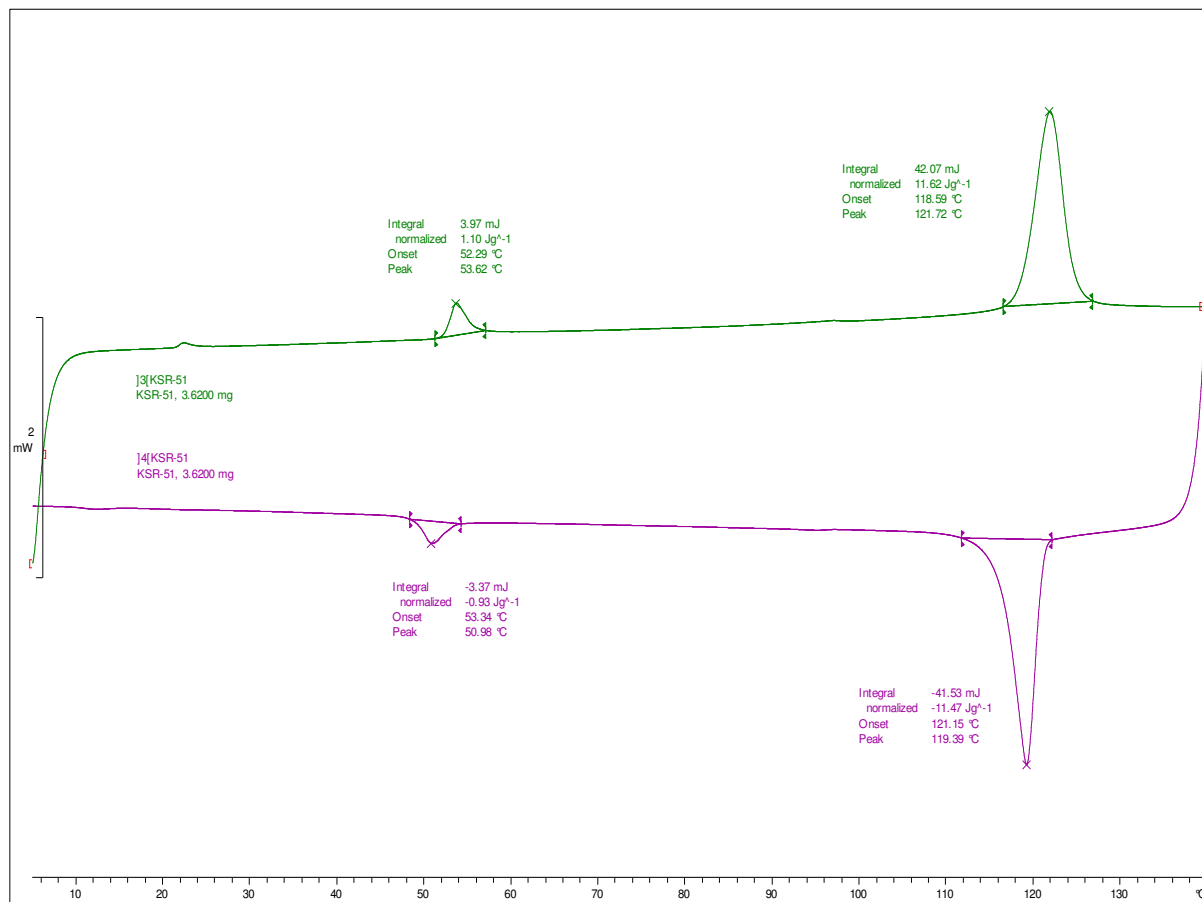
Hull Liquid Crystal Group: METTLER   **STAR^e SW 8.10**

DSC thermograph of the compound **41a** (KSR-57):

Integral 18.38 mJ
normalized 5.83 Jg^-1
Onset 75.01 ℃
Peak 76.60 ℃

Integral 50.37 mJ
normalized 15.99 Jg^-1
Onset 136.01 ℃
Peak 138.57 ℃

Integral 1.59 mJ
normalized 0.50 Jg^-1
Onset 84.92 ℃
Peak 88.55 ℃

]3[KSR-57
KSR-57, 3.1500 mg

5/
mW

]4[KSR-57
KSR-57, 3.1500 mg

Integral -1.55 mJ
normalized -0.49 Jg^-1
Onset 88.49 ℃
Peak 86.20 ℃

Integral -17.25 mJ
normalized -5.48 Jg^-1
Onset 75.53 ℃
Peak 74.09 ℃

Integral -45.17 mJ
normalized -14.34 Jg^-1
Onset 137.35 ℃
Peak 135.12 ℃

20 30 40 50 60 70 80 90 100 110 120 130 140 ℃
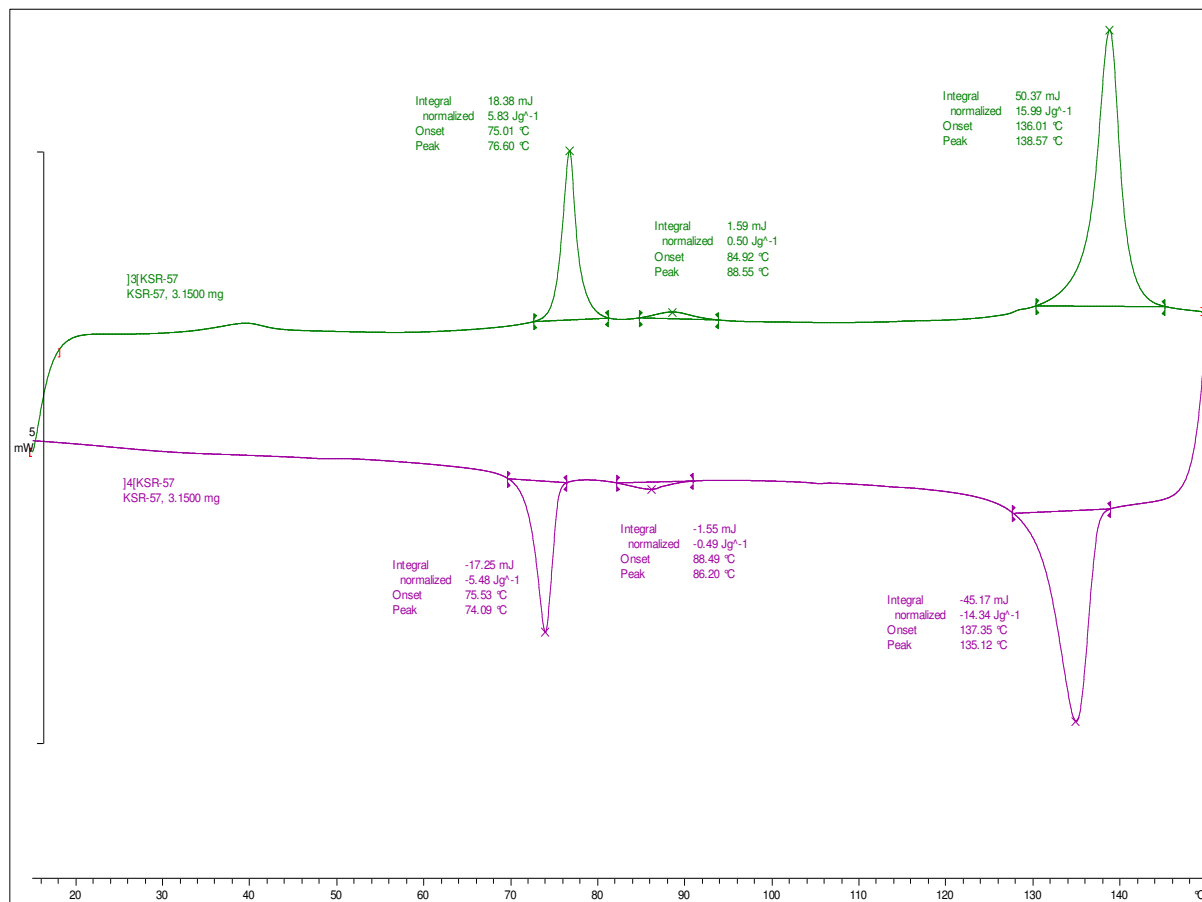
Hull Liquid Crystal Group: METTLER   **STAR^e SW 8.10**

DSC thermograph of the compound **41b** (KSR-58):

^endo

Integral 26.50 mJ
normalized 7.66 Jg^-1
Onset 88.81 ℃
Peak 89.25 ℃

Integral 62.52 mJ
normalized 18.07 Jg^-1
Onset 141.70 ℃
Peak 142.59 ℃

]3[KSR-58
KSR-58, 3.4600 mg

10
mW

]4[KSR-58
KSR-58, 3.4600 mg

Integral -26.01 mJ
normalized -7.52 Jg^-1
Onset 87.81 ℃
Peak 87.46 ℃

Integral -57.87 mJ
normalized -16.73 Jg^-1
Onset 141.33 ℃
Peak 140.57 ℃

20 30 40 50 60 70 80 90 100 110 120 130 140 150 ℃
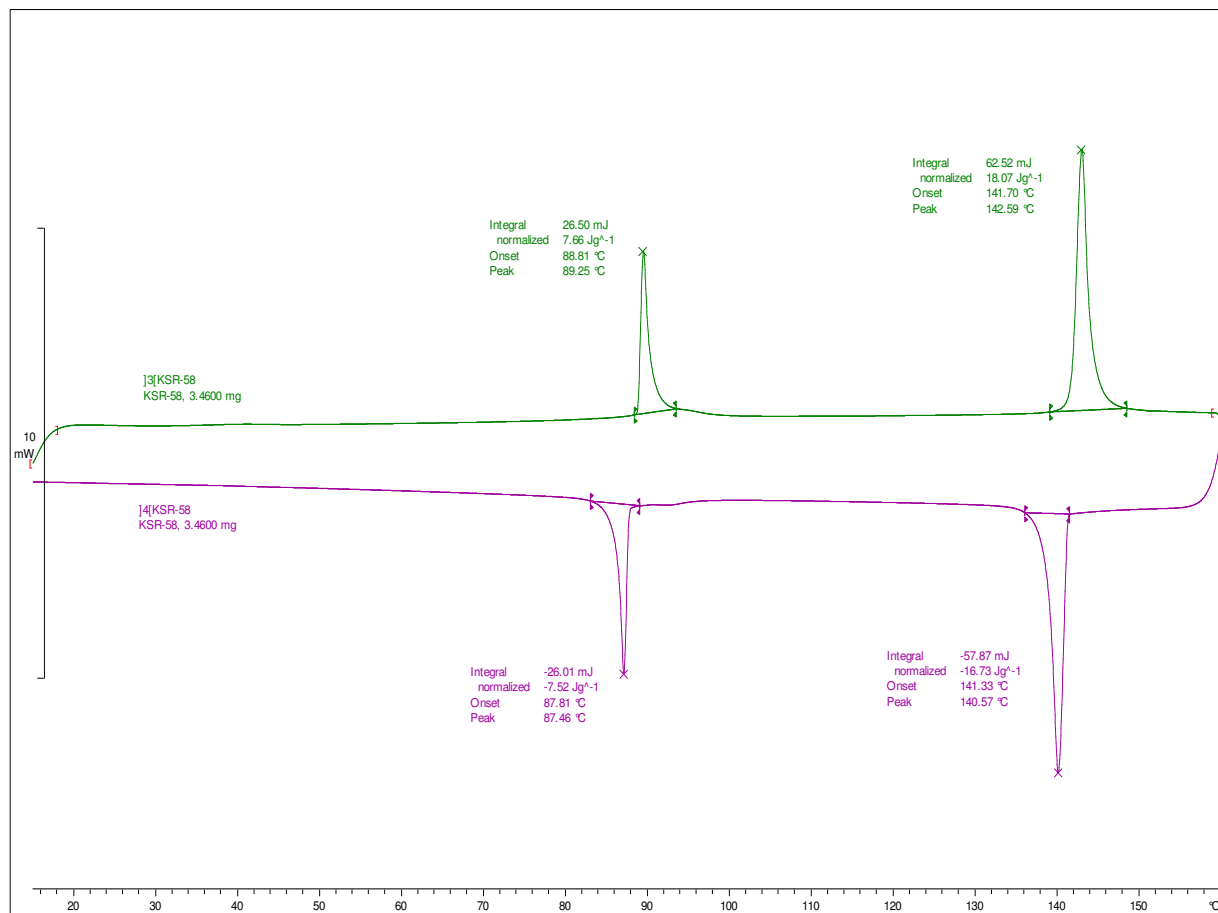
Hull Liquid Crystal Group: METTLER   **STAR^e SW 8.10**

DSC thermograph of the compound **39** (KSR-59):

^endo   KSR-59   05.12.2014 15:11:00

Integral   51.48 mJ
normalized   13.69 Jg^-1
Onset   114.50 ℃
Peak   116.15 ℃

Integral   0.50 mJ
normalized   0.13 Jg^-1
Onset   55.42 ℃
Peak   58.91 ℃

]3[KSR-59
KSR-59, 3.7600 mg

5
mW

]4[KSR-59
KSR-59, 3.7600 mg

Integral   -0.51 mJ
normalized   -0.14 Jg^-1
Onset   59.38 ℃
Peak   56.20 ℃

Integral   -51.47 mJ
normalized   -13.69 Jg^-1
Onset   115.19 ℃
Peak   113.33 ℃

10   20   30   40   50   60   70   80   90   100   110   120   130   ℃
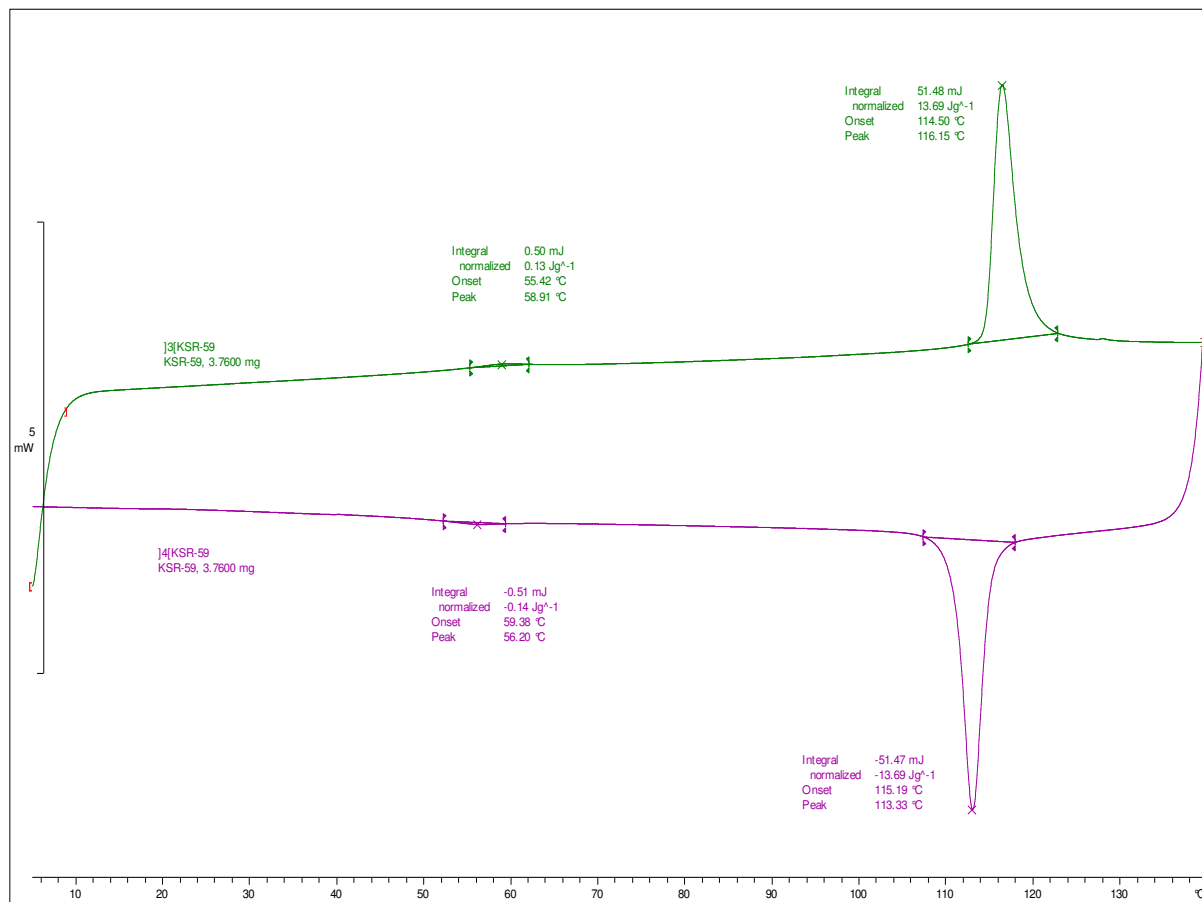
Hull Liquid Crystal Group: METTLER   **STAR^e SW 8.10**

DSC thermographs for 50% mixtures of final compounds:

DSC thermograph of 50 % Mixrure of compound **30a** (KSR-20) and KC1020:

^endo

Integral	141.22 mJ
normalized	35.57 Jg^-1
Onset	24.19 ℃
Peak	26.77 ℃

Integral	25.88 mJ
normalized	6.52 Jg^-1
Onset	96.80 ℃
Peak	97.78 ℃

Integral	50.30 mJ
normalized	12.67 Jg^-1
Onset	10.91 ℃
Peak	16.59 ℃

Integral	0.86 mJ
normalized	0.22 Jg^-1
Onset	57.27 ℃
Peak	59.39 ℃

2 mW

]1[50 % KSR-20 + KC1020
50 % KSR-20 + KC1020, 3.9700 mg

Integral	0.18 mJ
normalized	46.21e-03 Jg^-1
Onset	27.72 ℃
Peak	24.35 ℃

Integral	-0.13 mJ
normalized	-31.97e-03 Jg^-1
Onset	50.57 ℃
Peak	49.91 ℃

Integral	-30.67e-03 mJ
normalized	-7.72e-03 Jg^-1
Onset	84.71 ℃
Peak	84.11 ℃

Integral	-25.18 mJ
normalized	-6.34 Jg^-1
Onset	97.43 ℃
Peak	96.89 ℃

Hull Liquid Crystal Group: chsjah   **STAR^e SW 8.10**

DSC thermograph of 50 % mixture of compound **34a**(KSR-38) and KC1020:

^endo

Integral 11.57 mJ
normalized 2.69 Jg^-1
Onset 78.05 °C
Peak 79.13 °C

Integral 2.95 mJ
normalized 0.69 Jg^-1
Onset 63.08 °C
Peak 63.56 °C

]3[50% of KSR-38 + KC1020
50% of KSR-38 + KC1020, 4.3000 mg

1 mW

]4[50% of KSR-38 + KC1020
50% of KSR-38 + KC1020, 4.3000 mg

Integral -2.72 mJ
normalized -0.63 Jg^-1
Onset 62.84 °C
Peak 62.53 °C

Integral -11.09 mJ
normalized -2.58 Jg^-1
Onset 78.94 °C
Peak 78.18 °C

Hull Liquid Crystal Group: chsjah

STAR^e SW 8.10
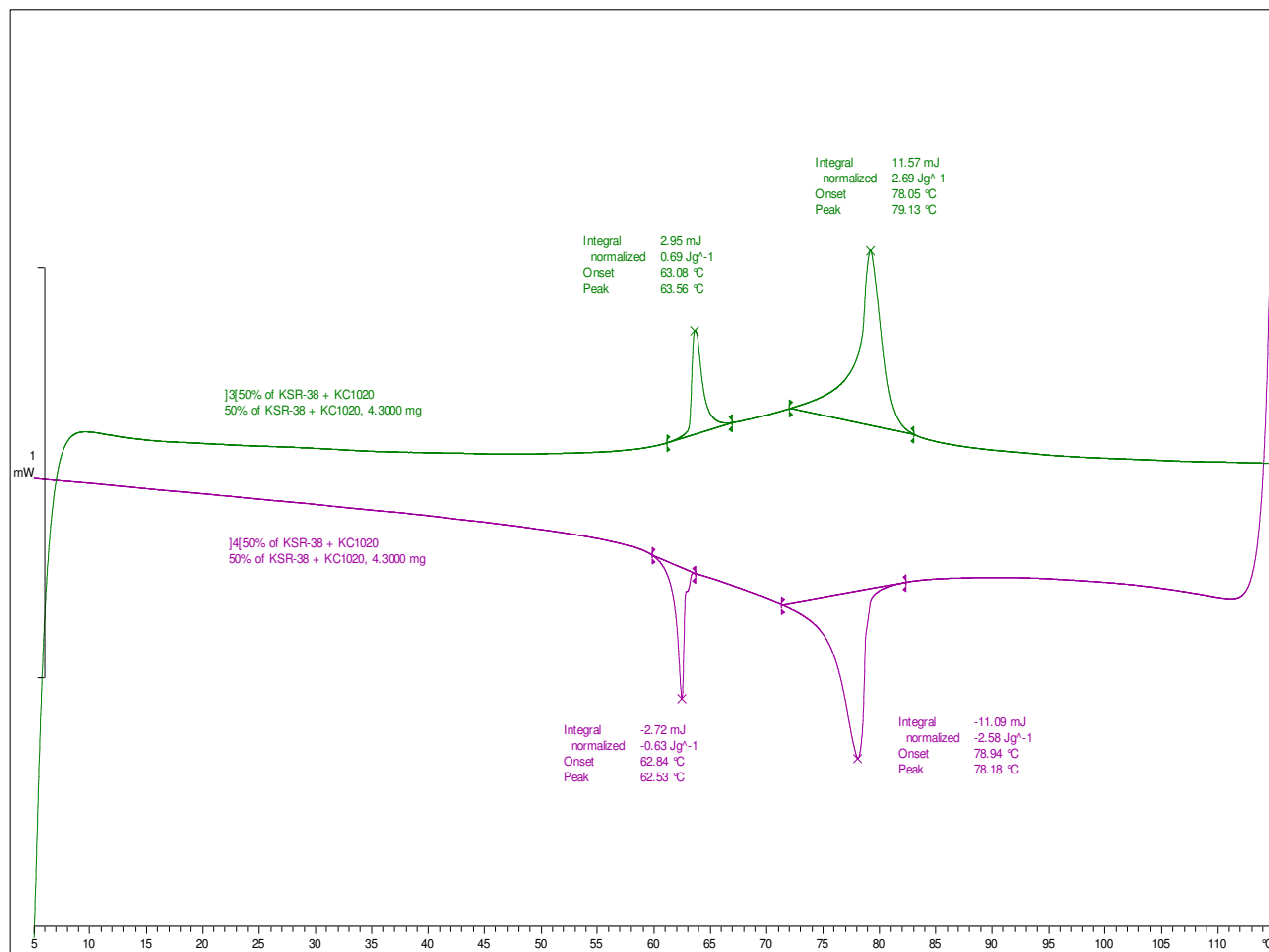
DSC thermograph of 50 % mixture of compound **37a**(KSR-50) and KC1020:

^**endo**

Integral   3.18 mJ
normalized   0.89 Jg^-1
Onset   -3.13 °C
Peak   -1.46 °C

]3[50% of KSR-50 + KC1020
50% of KSR-50 + KC1020, 3.5600 mg

Integral   18.28e-03 mJ
normalized   5.14e-03 Jg^-1
Onset   60.18 °C
Peak   60.89 °C

Integral   0.71 mJ
normalized   0.20 Jg^-1
Onset   77.94 °C
Peak   78.86 °C

Integral   6.06 mJ
normalized   1.70 Jg^-1
Onset   101.15 °C
Peak   101.76 °C

1
mW

Integral   -7.97e-03 mJ
normalized   -2.24e-03 Jg^-1
Onset   60.25 °C
Peak   59.93 °C

Integral   -0.21 mJ
normalized   -58.64e-03 Jg^-1
Onset   78.45 °C
Peak   77.83 °C

]4[50% of KSR-50 + KC1020
50% of KSR-50 + KC1020, 3.5600 mg

Integral   -7.00 mJ
normalized   -1.97 Jg^-1
Onset   101.20 °C
Peak   100.74 °C

Hull Liquid Crystal Group: chsjah   ***STAR**e* **SW 8.10**

DSC thermograph of 50 % mixture of compound **41b** (KSR-58) and **KC1020**:

^endo

Integral   93.24 mJ
  normalized   29.60 Jg^-1
Onset   28.98 ℃
Peak   30.87 ℃

]1[50% of KSR-58 +KC1020
50% of KSR-58 +KC1020, 3.1500 mg

Integral   7.78 mJ
  normalized   2.47 Jg^-1
Onset   121.92 ℃
Peak   122.26 ℃

Integral   5.15e-03 mJ
  normalized   1.63e-03 Jg^-1
Onset   78.73 ℃
Peak   78.98 ℃

2
mW

Integral   -5.64 mJ
  normalized   -1.79 Jg^-1
Onset   9.99 ℃
Peak   9.00 ℃

Integral   -38.11e-03 mJ
  normalized   -12.10e-03 Jg^-1
Onset   59.19 ℃
Peak   59.00 ℃

]2[50% of KSR-58 +KC1020
50% of KSR-58 +KC1020, 3.1500 mg

Integral   -9.62 mJ
  normalized   -3.05 Jg^-1
Onset   121.74 ℃
Peak   121.44 ℃

10   20   30   40   50   60   70   80   90   100   110   120   130   ℃

Hull Liquid Crystal Group: chsjah   **STAR^e SW 8.10**

DSC thermograph of 50 % mixture of compound **39** (KSR-58) and KC1020:

^endo

Integral   8.12 mJ
normalized   1.81 Jg^-1
Onset   109.24 ℃
Peak   109.51 ℃

Integral   0.28 mJ
normalized   62.59e-03 Jg^-1
Onset   96.19 ℃
Peak   96.64 ℃

Integral   77.95e-03 mJ
normalized   17.32e-03 Jg^-1
Onset   88.28 ℃
Peak   89.28 ℃

]3[50% of KSR-59+KC1020
50% of KSR-59+KC1020, 4.5000 mg

1
mW

]4[50% of KSR-59+KC1020
50% of KSR-59+KC1020, 4.5000 mg

Integral   -0.15 mJ
normalized   -33.97e-03 Jg^-1
Onset   88.93 ℃
Peak   88.28 ℃

Integral   -0.43 mJ
normalized   -94.94e-03 Jg^-1
Onset   96.49 ℃
Peak   95.87 ℃

Integral   -9.94 mJ
normalized   -2.21 Jg^-1
Onset   109.03 ℃
Peak   108.79 ℃

0   10   20   30   40   50   60   70   80   90   100   110   120   ℃

Hull Liquid Crystal Group: chsjah   **STAR**^{e} **SW 8.10**